

AD-A059 046

NATIONAL BUREAU OF STANDARDS BOULDER COLO CRYOGENICS DIV F/G 7/2
HELIUM HEAT TRANSFER, (U)

JUN 72 V ARP, E R BALLINGER, P J GIARRATANO

N00014-76-C-0706

UNCLASSIFIED

NBS-10753

NL

1 OF 2
AD
A059046



LEVEL

P

NBS REPORT

14 NBS-10753

15 N00014-76-C-0706

6 HELIUM HEAT TRANSFER

DDC
RECEIVED
SEP 22 1978
F

AD A059046

DDC FILE COPY

10

V./Arp, E. R./Ballinger, P. J./Giarratano, R. C./Hess, M. C./Jones

K. Mittag, N. S. Snyder, W. G. Steward, and G. H. Wallace

NBS

11 30 Jun 72

12 181p.

This document has been approved
for public release and sale; its
distribution is unlimited.

78 09 06 005

U. S. DEPARTMENT OF COMMERCE
NATIONAL BUREAU OF STANDARDS

BOULDER LABORATORIES
Boulder, Colorado

400992

~~78 08 02 006~~

JUB

Memorandum

DATE: 473:MKE:1cb
5 September 1978

FROM ONR, Code 473

TO DDC-TCA, Mr. J. E. Cundiff

SUBJ Your request of 29 August 1978

1. With reference to your request (enclosed), use contract No. N00014-76-C-0706 and the following distribution instructions:

Approved for public release; distribution unlimited.

Reproduction in whole or in part is permitted for any purpose of the United States Government.

M. Keith Ellingsworth
M. KEITH ELLINGSWORTH

78 00 000

NATIONAL BUREAU OF STANDARDS

The National Bureau of Standards¹ was established by an act of Congress March 3, 1901. The Bureau's overall goal is to strengthen and advance the Nation's science and technology and facilitate their effective application for public benefit. To this end, the Bureau conducts research and provides: (1) a basis for the Nation's physical measurement system, (2) scientific and technological services for industry and government, (3) a technical basis for equity in trade, and (4) technical services to promote public safety. The Bureau consists of the Institute for Basic Standards, the Institute for Materials Research, the Institute for Applied Technology, the Center for Computer Sciences and Technology, and the Office for Information Programs.

THE INSTITUTE FOR BASIC STANDARDS provides the central basis within the United States of a complete and consistent system of physical measurement; coordinates that system with measurement systems of other nations; and furnishes essential services leading to accurate and uniform physical measurements throughout the Nation's scientific community, industry, and commerce. The Institute consists of a Center for Radiation Research, an Office of Measurement Services and the following divisions:

Applied Mathematics—Electricity—Heat—Mechanics—Optical Physics—Linac Radiation²—Nuclear Radiation²—Applied Radiation²—Quantum Electronics³—Electromagnetics³—Time and Frequency³—Laboratory Astrophysics³—Cryogenics³.

THE INSTITUTE FOR MATERIALS RESEARCH conducts materials research leading to improved methods of measurement, standards, and data on the properties of well-characterized materials needed by industry, commerce, educational institutions, and Government; provides advisory and research services to other Government agencies; and develops, produces, and distributes standard reference materials. The Institute consists of the Office of Standard Reference Materials and the following divisions:

Analytical Chemistry—Polymers—Metallurgy—Inorganic Materials—Reactor Radiation—Physical Chemistry.

THE INSTITUTE FOR APPLIED TECHNOLOGY provides technical services to promote the use of available technology and to facilitate technological innovation in industry and Government; cooperates with public and private organizations leading to the development of technological standards (including mandatory safety standards), codes and methods of test; and provides technical advice and services to Government agencies upon request. The Institute also monitors NBS engineering standards activities and provides liaison between NBS and national and international engineering standards bodies.* The Institute consists of the following divisions and offices:

Engineering Standards Services—Weights and Measures—Invention and Innovation—Product Evaluation Technology—Building Research—Electronic Technology—Technical Analysis—Measurement Engineering—Office of Fire Programs.

THE CENTER FOR COMPUTER SCIENCES AND TECHNOLOGY conducts research and provides technical services designed to aid Government agencies in improving cost effectiveness in the conduct of their programs through the selection, acquisition, and effective utilization of automatic data processing equipment; and serves as the principal focus within the executive branch for the development of Federal standards for automatic data processing equipment, techniques, and computer languages. The Center consists of the following offices and divisions:

Information Processing Standards—Computer Information—Computer Services—Systems Development—Information Processing Technology.

THE OFFICE FOR INFORMATION PROGRAMS promotes optimum dissemination and accessibility of scientific information generated within NBS and other agencies of the Federal Government; promotes the development of the National Standard Reference Data System and a system of information analysis centers dealing with the broader aspects of the National Measurement System; provides appropriate services to ensure that the NBS staff has optimum accessibility to the scientific information of the world, and directs the public information activities of the Bureau. The Office consists of the following organizational units:

Office of Standard Reference Data—Office of Technical Information and Publications—Library—Office of International Relations.

¹ Headquarters and Laboratories at Gaithersburg, Maryland, unless otherwise noted; mailing address Washington, D.C. 20234.

² Part of the Center for Radiation Research.

³ Located at Boulder, Colorado 80302.

78 08 02 006

NATIONAL BUREAU OF STANDARDS REPORT

NBS PROJECT

NBS REPORT

2750476

June 30, 1972

10 753

HELIUM HEAT TRANSFER

V. Arp, E. R. Ballinger, P. J. Giarratano, R. C. Hess, M. C. Jones,
K. Mittag, N. S. Snyder, W. G. Steward, and G. H. Wallace

Cryogenics Division
Institute for Basic Standards
National Bureau of Standards
Boulder, Colorado 80302

IMPORTANT NOTICE

NATIONAL BUREAU OF STANDARDS REPORTS are usually preliminary or progress accounting documents intended for use within the Government. Before material in the reports is formally published it is subjected to additional evaluation and review. For this reason, the publication, reprinting, reproduction, or open-literature listing of this Report, either in whole or in part, is not authorized unless permission is obtained in writing from the Office of the Director, National Bureau of Standards, Washington, D.C. 20234. Such permission is not needed, however, by the Government agency for which the Report has been specifically prepared if that agency wishes to reproduce additional copies for its own use.



U.S. DEPARTMENT OF COMMERCE
NATIONAL BUREAU OF STANDARDS

TABLE OF CONTENTS

List of Figures	vi
List of Tables	ix
Abstract.	x
1. Introduction	1
1.1 Published Work	2
1.2 Work in Progress for the Coming Year	4
2. Helium I Heat Transfer	7
2.1 Pool Boiling - Review	7
2.1.1 References	10
2.2 Forced Flow Two Phase Heat Transfer - Status Report	13
2.2.1 References	14
2.3 Forced Flow Single Phase Heat Transfer - Synopsis	16
2.3.1 Introduction	16
2.3.2 Summary of Supercritical Helium Heat Transfer Study	16
2.3.3 Nomenclature	19
2.3.4 References	19
2.4 Thermal Oscillations and Instabilities - Review. .	22
2.4.1 Introduction	22
2.4.2 Operational Instabilities and Oscillations	24
2.4.3 Analyses.	26
2.4.4 Cooldown Transients and Oscillations . .	27
2.4.5 Application to Superconducting Systems .	29

TABLE OF CONTENTS (con't)

2.4.6	Conclusions	31
2.4.7	References	33
2.5	Helium Refrigeration Systems and Cooling Loops- Discussion of the Problem	39
2.5.1	References	42
2.6	Stability of Force - Cooled Superconducting Magnets - Analysis	47
2.6.1	Introduction	47
2.6.2	Cryogenic Stabilization	48
2.6.3	Pool Boiling Stabilization	49
2.6.4	Forced Flow Cooling of Superconductors	52
2.6.5	Thermal Runaway Limit	54
2.6.6	Warming of the Helium in the Flow Channel	59
2.6.7	Boundry Layer Development	62
2.6.8	Exact Solution to Forced-Flow Cooling of a Normal Region	64
2.6.9	Nomenclature	68
2.6.10	References.	70
2.7	Critical Two Phase Flow - Status Report	80
3.	Helium II Heat Transfer.	81
3.1	Thermal Gradients in Helium II - Synopsis	81
3.1.1	References	82
3.2	Kapitza Conductance - Status Report.	86
3.2.1	Bachground	86
3.2.2	Experimental Program	87
3.2.3	Current Status - Results to Date	89
3.2.4	References	89

TABLE OF CONTENTS (con't)

3.3	Kapitza Conductance and Thermal Conductivity of Cu, Nb, and Al in the Range from 1.3 to 2.1 K - Engineering Measurements	93
	Abstract - Kapitza Conductance and Thermal Conductivity of Copper, Niobium and Aluminum in the Range from 1.3 to 2.1K	94
1.	Experimental Procedure	96
2.	Sample Preparation and Experimental Results .	99
3.	Discussion	103
4.	Conclusions	108
4.	Properties Summary and Related Work at NBS	118
4.1	New Equation of State	118
4.1.1	References	119
4.2	Summary of Useful Transport and Thermo- dynamic Properties - Tables	131
4.2.1	References	132

LIST OF FIGURES

Figure 1.1	Helium heat transfer and properties programs at NBS Cryogenics Division	6
Figure 2.1.1	Pool boiling heat transfer to liquid helium I.	12
Figure 2.2.1	Schematic view of boiling heat transfer flow loop . .	15
Figure 2.3.1	Experimental and predicted heat transfer results using equation 2.3.1	21
Figure 2.5.1	Basic liquid refrigerator	45
Figure 2.5.3	Three arrangements of the cable as the refrigerator load	46
Figure 2.6.1	Representation of magnet stability analysis by pool boiling as given by Maddock, James, and Norris (1969). The solid and dotted lines give the heat transfer rate, while the dashed lines (a, b, c) give the heat generation rate as a function of temperature of the superconductor. The curves (a, b, c) are for successively higher values of current and/or stability parameter.	72
Figure 2.6.2	Comparison of pool boiling and forced convection heat transfer to helium at 4.2 K. The forced convection curves are for supercritical helium at pressures within the range 0.3 to 1.0 MN/m ² (3 to 10 atmospheres), arbitrarily assuming a channel diameter of 0.2 cm	73
Figure 2.6.3	Evaluation of the Cold End Recovery Critical Current for forced supercritical flow. The heat transfer characteristic is taken from Giarratano, Arp, and Smith (1971). In this plot the generating line is drawn assuming a current equal to 86% of the short	

LIST OF FIGURES (con't)


- sample critical current, and a transition temperature (in ambient magnetic field) of 11.2 K. Equality of the crosshatched areas predicts stable magnet performance for $\alpha \leq 1.2$ in this case 74
- Figure 2.6.4 Film boiling heat transfer characteristic. Figures 2.6.4 through 2.6.7 are all drawn to the same logarithmic scale 75
- Figure 2.6.5 Forced convection heat transfer characteristic for helium at 4.2 K and pressures within the range 0.3 to 1.0 MN/m² (3 to 10 atmospheres). Figures 2.6.4 through 2.6.7 are all drawn to the same logarithmic scale 76
- Figure 2.6.6 The resistivity of three different purities of copper as a function of temperature. RRR is the residual resistivity ratio, equal to the resistivity at 273 K divided by the resistivity at 4 K. Figures 2.6.4 through 2.6.7 are all drawn to the same logarithmic scale 77
- Figure 2.6.7 The resistivity of five different purities of aluminum as a function of temperature. RRR is the residual resistivity ratio, equal to the resistivity at 273 K divided by the resistivity at 4 K. Figures 2.6.4 through 2.6.7 are all drawn to the same logarithmic scale 78
- Figure 2.6.8 Forced convection heat transfer as a function of helium temperature for two wall temperatures, 7.2 K and 11.2 K, and two pressures, 3 atmospheres (solid lines) and 10 atmospheres (dashed lines). The arrows indicate the pseudocritical temperatures at these two pressures 79

LIST OF FIGURES (con't)

Figure 3. 1. 1	Helium II thermal gradient as a function of thermal flux at 1.5 K	83
Figure 3. 1. 2	Helium II thermal gradient as a function of thermal flux at 1.9 K	84
Figure 3. 1. 3	Limiting thermal flux in helium II above which vapor formation may occur	85
Figure 3. 2. 1	Closeup view of the chamber in which the sample surface is prepared under UHV	91
Figure 3. 2. 2	Overall view of the vacuum system	92
Figure 1:	Schematic drawing of the lower inner part of the cryostat	113
Figure 2:	Thermal conductivity of OFHC-copper and of the aluminum alloy Al 6061	114
Figure 3:	Kapitza conductance of OFHC-copper and niobium	115
Figure 4:	Thermal conductivity of niobium	116
Figure 5:	Kapitza conductance of high purity aluminum and of the aluminum alloy Al 6061	117

LIST OF TABLES

Table 2.4.1	Operational Instabilities and Oscillations	37
Table 2.5.1	Comparison of Selected 1 kW Plants	44
Table 2.5.2	Approximate values of the mass flow and pressure drop for the different systems with normal and standby operation	44
Table 2.6.1	Thermal Runaway Cooling Limits for Conductors in Helium Film Boiling	57
Table 1	111
Table 4.2.1	Helium ⁴ thermal conductivity, K , mW/cm-K	133
Table 4.2.2	Helium ⁴ viscosity, μ , μ g/cm-s	137
Table 4.2.3	Helium ⁴ density, ρ , mg/cm ³	141
Table 4.2.4	Helium ⁴ specific heat at constant pressure, c_p , J/g-K	145
Table 4.2.5	Helium ⁴ specific heat at constant volume c_v , J/k-K	149
Table 4.2.6	$(P/T) (\partial T / \partial P)_h$. This is the dimensionless quantity, Joule Thomson coefficient times pressure divided by temperature	153
Table 4.2.7	Helium ⁴ Prandtl number, $c_p \mu / K$	157
Table 4.2.8	$(P/\rho) (\partial \rho / \partial P)_T$. This is the dimensionless quantity, pressure times isothermal compressibility	161
Table 4.2.9	$-(T/\rho) (\partial \rho / \partial T)_P$. This is the dimensionless quantity, temperature times bulk expansivity	165



ABSTRACT

Publications of the NBS Cryogenic Division relating to helium heat transfer are summarized, and new results from this past year are given in full. In this latter category are included the following: (1) comprehensive review of thermal oscillations and instabilities, including recommendations for needed direction of study, (2) brief summary of the combination of refrigeration systems and cooling loops, (3) analytical study of superconductor stability under forced flow conditions, analogous to previous studies for pool boiling, (4) Kapitza conductance and thermal conductivity measurements on copper, niobium, and aluminum, and (5) tabular data on a variety of helium properties of importance to the cryogenic engineer. In addition, a brief outline is given of work in progress and/or planned for next year, including forced two-phase flow experiments, further Kapitza conductance measurements, possible superfluid forced flow studies, helium pump survey and evaluation, and thermal stability studies on a cryogenic power transmission line.

This report collects and summarizes work carried out under the separate sponsorship of AEC, ONR, NASA, and NBS.

Key Words: Critical Flow; Fluid Flow; Heat Transfer; Helium I; Helium II; Kapitza Conductance Properties; Refrigeration; Stability; Summary; Superconductivity.

1. INTRODUCTION

The past few years have witnessed the development of reliable high field superconductors, whose use as current conductors at low temperatures leads to new technological systems of increased performance and efficiency. Examples of working systems include superconducting magnets for beam control in high energy physics and for plasma containment in controlled thermonuclear reaction studies. Serious consideration is being given to superconducting motors, generators, transmission lines, magnetic levitation systems for high speed ground transport, and magnetic ore filtration techniques.

Helium technology must keep pace with this materials development. For relatively small laboratory systems, it is common to simply immerse the conductor in a container supplied with liquid helium vented at atmospheric pressures, and thus maintained at 4 K. However, as the system size, cost, and complexity increases, it is important to take a closer look at the means for maintaining the low temperature environment. In brief summary, the selection of an optimum system requires comparison of the merits of (1) the common pool boiling heat transfer mode, (2) cooling by forced flow of supercritical or boiling helium through flow channels, (3) the use of superfluid helium, below 2.17 K, and (4) operation of the device in conjunction with its own closed cycle refrigeration system, especially as the size increases.

The purpose of this study has been to provide the reliable data on helium properties and helium heat transfer which are necessary for serious engineering studies of superconducting systems. At the start of this work, in 1968, such information was seriously lacking. Our work to date has, we feel, been effective in filling in broad areas of relevant knowledge on helium heat transfer and properties. The total

program outline from 1968 through the work planned for FY 1973 is shown graphically in figure 1.1. Component programs are discussed in the following sections.

1.1 PUBLISHED WORK

The following completed works have been (or soon will be) published in the open literature. Brief technical synopses of the major results are given in later sections of this report.

HELIUM HEAT TRANSFER

Review papers with design recommendations

"Review of heat transfer to helium I," R. V. Smith, Cryogenics 9, No. 1, 11-19 (Feb. 1969) and Proceedings of the 1968 summer study on superconducting devices and accelerations, Part K, BNL 50155 (C-55) 249-92, Brookhaven Natl. Lab., Upton, N. Y. (April, 1969).

"The influence of surface characteristics on the boiling of cryogenic fluids, R. V. Smith, ASME J. of Engr. for Industry (Nov. 1969).

"Survey of heat transfer to near critical fluids," R. C. Hendricks and R. J. Simoneau, NASA Lewis Research Center, and R. V. Smith, National Bureau of Standards, Institute for Basic Standards, Boulder, Colorado, NASA TMX - 5612 (1969), to be published in Advances in Cryogenic Engineering, 15 (1970) and NASA-TND-5886.

Experimental and Analytical Paper

"Forced convection heat transfer to supercritical helium," P. J. Giarratano, V. D. Arp, and R. V. Smith, Cryogenics 11, 385 (1971).

Analytical Paper

"Forced flow single phase helium cooling systems," V. Arp, to appear in Advances in Cryogenic Engineering, 17.

HELIUM PUMPING AND ELECTRICAL COMPONENTS

"A miniature centrifugal helium pump," Sixsmith and P. J. Giarratano, Rev. of Sci. Inst., 41, No. 11, 1570-73, (Nov. 1970).

"A digital technique for generating variable frequency multiple-phase waveforms," J. E. Cruz and J. C. Jellison. Rev. of Sci. Inst. 7, 1099 (1970).

KAPITZA CONDUCTANCE

"Thermal conductance at the interface of a solid and helium II," N. S. Snyder, NBS Tech.Note 385 (1969), in a shorter form under the title, "Heat transfer to helium II: Kapitza conductance." Cryogenics, 10, No. 2, 89-95, (1970).

"Kapitza conductance and thermal conductivity of copper, niobium, and aluminum in the range from 1.3 to 2.1 K," K. Mittag, to appear in Cryogenics.

HE II CONDUCTANCE

"Heat transport through He II," V. D. Arp, Cryogenics, 10, No. 2, (1970).

HELIUM PROPERTIES

"Interim values for the viscosity and thermal conductivity coefficients of fluid He⁴ between 2 and 50 K," H. J. M. Hanley and G. E. Childs, Cryogenics 9, No. 2, 106-111 (April 1969).

"Helium⁴ Viscosity Measurements - 4 to 20 K, 0 to 10 MN/m²", W. G. Steward and G. H. Wallace, NBS Report 10 704 (1971).

"Thermophysical properties of helium-4 from 4 to 3000 R with pressures to 15000 psia," R. D. McCarty, to appear (estimated July 1972) as an NBS Tech. Note. A future edition will appear using SI units. This Tech. Note supercedes NBS Report 9762 "Provisional thermodynamic functions for helium-4 for temperatures from 2 to 1500 K with pressures to 100 MN/m^2 (1000 atmospheres)", by R. D. McCarty (1970).

1.2 WORK IN PROGRESS FOR THE COMING YEAR

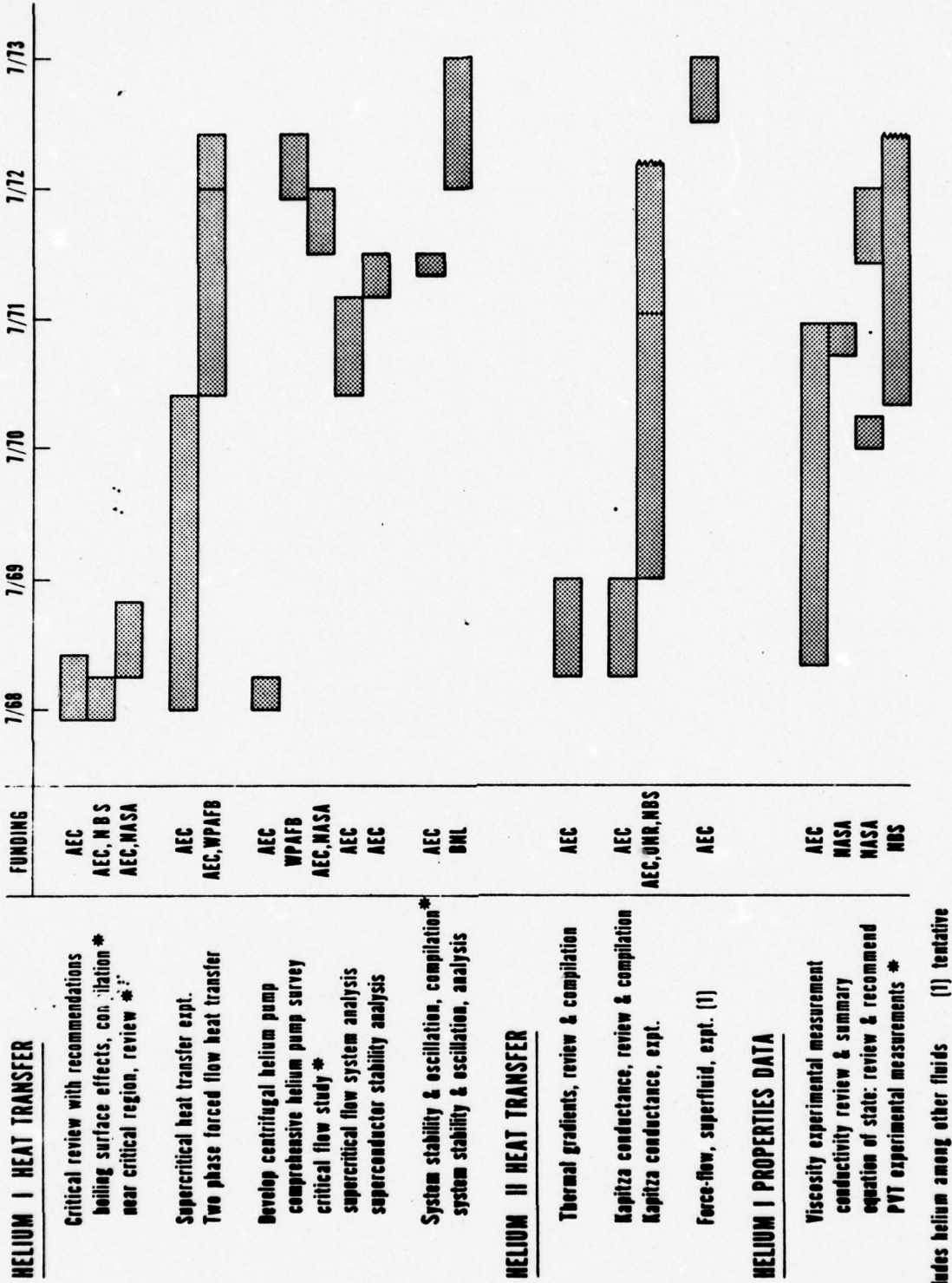
Major work in progress at this time utilizes our helium flow loop to study forced flow heat transfer with boiling helium, nominally at 4 K. The loop is modified somewhat from that described in Giarratano, Arp, and Smith [1971], and is illustrated in figure 2.2.1. Our original plans had been to obtain results for this report, but experimental problems make it necessary to postpone the report until the next fiscal year. We further plan in the coming year to try operating the loop below the lamda point (2.17 K), to test whether a conventional centrifugal pump can be used to obtain net mass flow of helium II. We believe that the results will be positive, and potentially useful, due to vorticity formation at the pump impeller.

Study of Kapitza conductance is continuing, as described in section 3. The broad plan here is to do definitive conductance measurements on a copper specimen with an atomically clean and ordered surface.

We are setting up an analytical study of the thermal stability of a force-cooled superconducting transmission line, following the concepts developed in section 2.2 of this report. This work will be directly in support of the superconducting power line work at Brookhaven National Laboratory.

We are starting on a survey of available helium pumps as would be required for various forced-flow cooling loops. Also, we are planning performance tests of at least one representative, commercially available pump.

• We are starting some analytical studies on the combination of forced flow cooling and helium refrigeration systems, wherein the forced flow is maintained by the room temperature compressors.



* includes helium among other fluids (1) tentative

Figure 1.1 Helium heat transfer and properties programs at NBS Cryogenics Division.

2. HELIUM I HEAT TRANSFER

2.1 POOL BOILING - REVIEW - M. C. Jones

Considerable experimental data exist for pool boiling to liquid helium I in both nucleate and film regimes. A general characteristic of all boiling systems, particularly in nucleate boiling, is the poor reproducibility between results of different workers and also in the data of a single worker. Part of the latter may be attributed to the well known hysteresis effect, namely, that a larger heat flux will often be transferred for a given temperature difference when the heat flux is being reduced than when increased. Contributing factors also appear to be associated with variations in surface chemistry (as it affects inhomogeneous nucleation and activation of nucleation sites), with surface roughness, and with substrate effects. The latter are characterized by the factor $k\rho C_p$ and affect more the critical points in the q vs. ΔT curve. (Here, k is the thermal conductivity, ρ the density, C_p the heat capacity, q the heat flux and ΔT is the difference between boiling surface temperature and the bulk liquid temperature.) In short, we do not yet know how to completely specify a solid surface and its preparation so that an accurate and precise heat transfer coefficient may be predicted in the same way that, for example, a purely convective or hydrodynamically determined heat transfer coefficient may be. In pool boiling the hydrodynamics are coupled to surface effects.

Nevertheless, hydrodynamics does play a role and average or probable behavior of an arbitrary surface may be inferred by looking at data for other surfaces and, in particular, by using correlations based on hydrodynamics in which is incorporated a degree of empiricism for real surfaces. Thus, we reproduce in figure 2.1.1 a representation of boiling heat transfer data to liquid helium I from Smith (1968). Super-

imposed on the same graph is the correlation of Kutateladze for nucleate boiling and that of Breen and Westwater for film boiling. Also shown is the prediction of the maximum nucleate boiling flux given by another correlation of Kutateladze. These correlations are all given by Smith. For any real surface they are good to an order of magnitude only.

Since the paper of Smith was published some additional results have become available (not shown on the figure). In a study of heat transfer to helium II Goodling and Irey [1969] included some results for boiling heat transfer to helium I from horizontal copper and platinum cylinders. Both nucleate and film boiling were studied at 3.27 and 2.51 K and the results were represented with typical accuracy by the above-mentioned correlations. No hysteresis was observed in this study. Holdredge and McFadden [1971] performed a similar study using a horizontal glass cylinder coated with a Fe-Ni vapor-deposited film which served as a heating element. Again the above-mentioned correlations were tested with similar outcome. Hysteresis was observed as it was also in the results of Dinaburg [1970] who investigated only the nucleate boiling regime of vertical cylinders of copper and aluminum. The curves for the copper and aluminum were distinct in this study. Purdy, et al., [1971] studied nucleate boiling of helium I from gallium single crystals between 2.5 and 4.2 K. Hysteresis was clearly evident and the maximum heat flux was adequately represented by the Kutateladze correlation. These authors argue from the basis of fluid superheat and critical bubble radii for a nucleation mechanism based on desorption of atoms from the boiling surface, apparently, unique to helium. The above papers do not appear to have added much to what was already known at the time of Smith's review.

James, et al., studied the critical points for pool boiling in small parallel rectangular channels. Critical fluxes for vertical channels were not greatly reduced from open surface values, but were much less than for horizontal channels unless circulation was induced. Opposite faces of a channel could both be heated with little drop in the critical fluxes from the case where only one side was heated and, finally, the latter were hardly affected by extra vapor in the liquid. This might occur in a solenoid, for example, where vapor could be produced from lower turns.

In summary, accurate predictions of pool boiling heat transfer cannot be made, but the review of Smith indicates order of magnitude predictability. Some more recent papers have opened up the possibility of large shifts in the critical heat fluxes and it would seem, from the point of view of cooling superconductors, that attention might be profitably focussed upon substrate physical properties and flow configuration.

2.1.1 References

- Butler, A. P., James, G. B., Maddock, B. J., and Norris, W. T., "Improved pool boiling heat transfer to helium from treated surfaces and its application to superconducting magnets," *Int. J. Heat Mass Transfer* 13, 105-115 (1970).
- Dinaburg, L. B., "Experimental study of boiling heat transfer in liquid helium," *Cryogenics* 9, 238-239 (1971).
- Epstein, M., "Heat transfer to liquid helium," Dissertation, University of California, Berkeley (1970).
- Goodling, J. S., and Irey, R. K., "Non-boiling and film boiling heat transfer to a saturated bath of liquid helium," *Advances in Cryogenic Engineering*, 14, (Plenum Press, New York, 1969) pp. 159-169.

Holdredge, R. M., and McFadden, P. W., "Heat transfer from horizontal cylinders to a saturated helium I bath," *Advances in Cryogenic Engineering*, 16, (Plenum Press, New York, 1971) pp. 352-358.

James, G. B., Lewis, K. G., and Maddock, B. J., "Critical heat fluxes for liquid helium boiling in small channels," *Cryogenics* 11, 480-485 (1970).

Purdy, V., Linnet, C., and Frederking, T. H. K., "Nucleate boiling of liquid helium on gallium single crystals," *Advances in Cryogenic Engineering*, 12 (Plenum Press, New York, 1971) pp. 359-367.

Smith, R. V., "Review of heat transfer to helium I," *Cryogenics* 9, 11-19 (1968).

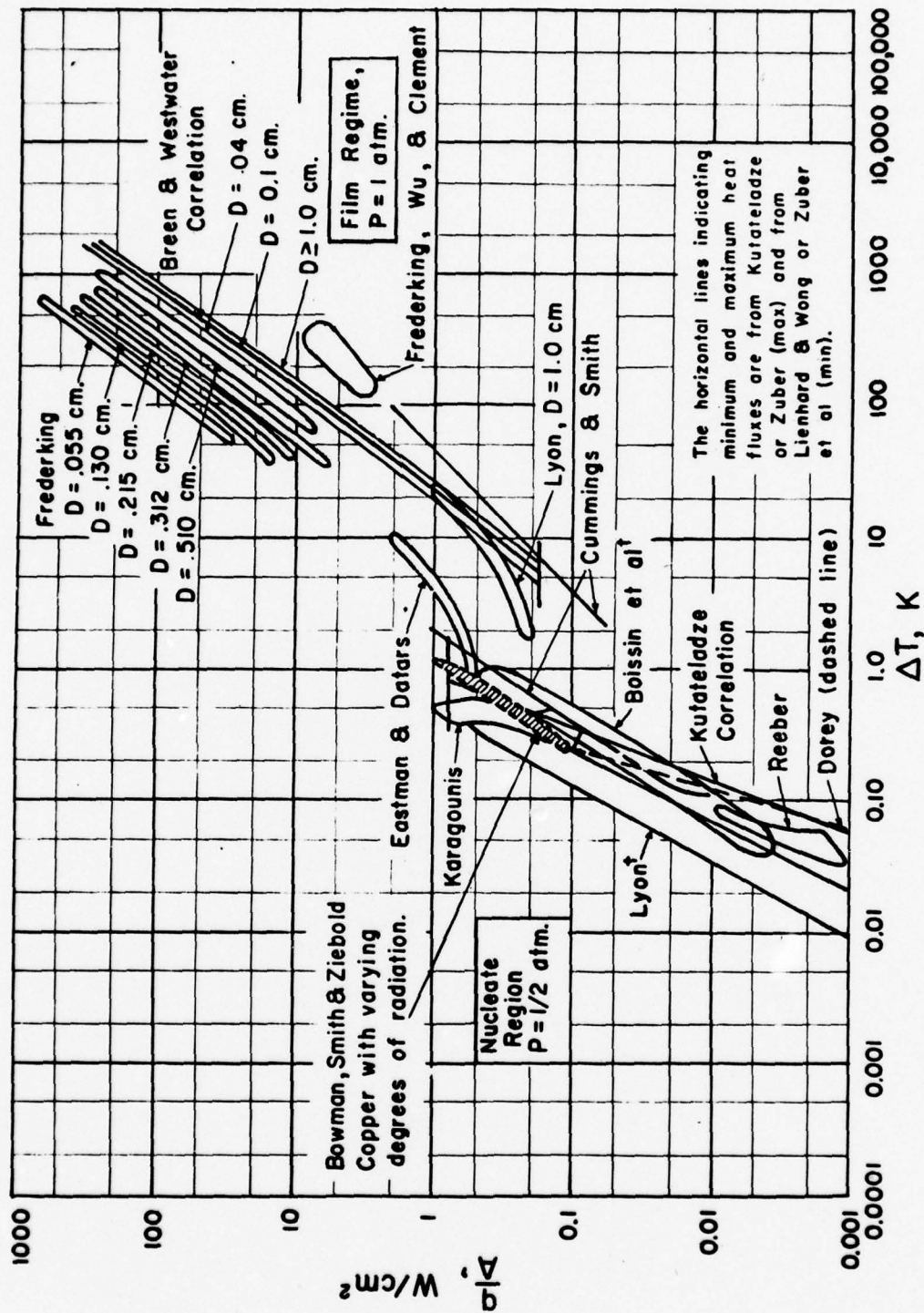


Figure 2.1.1.1 Pool boiling heat transfer to liquid helium I.

2.2 FORCED FLOW TWO PHASE HEAT TRANSFER - STATUS REPORT - M. C. Jones and P. J. Giarratano

In this study our goals are twofold. First, and most obviously, we wish to measure the heat transfer coefficient to liquid helium under forced convection in straight uniformly heated tubes. Insofar as our apparatus permits, we shall vary the operating pressure, the enthalpy of the stream at inlet, (i. e., the amount of vapor or degree of sub-cooling) and the velocity of flow. For each condition the relationship of wall heat flux to wall temperature will be determined. Boiling will take place under some conditions and, by appropriate instrumentation along the tube, we shall attempt to identify the transition from nucleate to film boiling. Results for both upward and downward flow will be investigated in vertical tubes and, if possible, we shall also investigate horizontal tubes.

The second goal is to effect these measurements in a closed flow loop using a centrifugal pump to circulate the liquid, rather than use a blow-down system. In fact, the flow loop is quite similar to that which was described earlier (Giarratano, Arp, and Smith 1971) for the single-phase helium measurements summarized in the next section. Figure 2.2.1 is a schematic diagram of the flow loop which has been built. The main differences with respect to the single phase loop are in the heat exchangers, which are now combined in a single reservoir of saturated liquid helium at atmospheric pressure. The heat exchange capacity is now much larger and the condition of the fluid in the flow loop should not be susceptible to fluctuations in coolant supply, as was experienced in the single phase experiments. It should also be possible in this apparatus to repeat some of the single phase data for purposes of confirmation.

To date this apparatus has been operated several times. We have experienced operating difficulties which have necessitated some modifications in the design and these modifications are under way at this time. A complete report on this study will be issued later.

2.2.1 References

Giarratano, P. J., Arp, V. D., and Smith, R. V., "Forced convection heat transfer to supercritical helium," Cryogenics 11, 385 (1971).

2.3 FORCED FLOW SINGLE PHASE HEAT TRANSFER - SYNOPSIS, by P. J. Giarratano

2.3.1 Introduction

Predictive correlations for heat transfer during turbulent forced convection of a single phase fluid have been well established, e.g., the correlations of Dittus-Boelter [1930], Colburn [1933] and Sieder and Tate [1936]. These equations are applicable for moderate ΔT situations where there is negligible property variation across the boundary layer. However, for heat transfer with large ΔT 's or for heat transfer in the near critical region where fluid properties may change significantly with small changes in temperature, the above correlations are inadequate. Many correlations have been developed for predicting heat transfer coefficients for fluids with widely ranging properties and generally are a modification of the classical constant property equations noted above. Typical modification to the correlation may involve any combination of the following:

1. Selection of some temperature other than bulk temperature for properties evaluation.
2. Inclusion of a T_w/T_b and/or L/D parameter or some function of these parameters.

Examples of the variable property correlations are given by Taylor [1968].

2.3.2 Summary of Supercritical Helium Heat Transfer Study

A complete description of this study is given in NBS Report 10 703 and by Giarratano, Arp, and Smith [1971] in the open literature.

Heat transfer coefficients have been measured for supercritical helium, circulated around a closed flow loop by a miniature centrifugal pump (Sixsmith, and Giarratano, 1967). Reynolds numbers in the 0.21 cm i.d. by 10 cm long stainless steel test section ranged from 1×10^4 to 3.8×10^5 with pressures 3 to 20 atm (0.3 to 2 MN/m^2) and fluid temperatures 4.4 to 30 K. Wall-to-bulk temperature ratios varied from approximately 1.03 to 3.0.

The experimental data are presented graphically in figure 2.3.1, where $(hD^{0.2}/G^{0.8})(T_W/T_b)^{0.716}$ is plotted versus T_b/T_{tc} for the range of pressures covered in the experimental measurements. T_{tc} is the transposed critical (or pseudocritical) temperature defined as the temperature at which the specific heat, C_p , is a maximum for the given pressure. The ordinate for figure 2.3.1 is suggested from the following correlation, determined by a least-squares-fit technique, which best represents the supercritical helium experimental heat transfer data. (Std. deviation 8.5%)

$$\frac{hD^{0.2}}{G^{0.8}} \left(\frac{T_W}{T_b} \right)^{0.716} = 0.0259 \frac{k^{0.6} C_p^{0.4}}{\mu^{0.4}} \quad (2.3.1)$$

It is worth noting here that the Dittus-Boelter constant property correlation was found to represent the data to within 15%.

It has often been reported that system oscillations may appear during heat transfer to near critical fluids (Cornelius [1965], Thurston [1965], Goldman [1961], McCarthy and Wolf [1960], Hines and Wolf [1962], and Knapp and Sabersky [1966]). An apparent criterion for the onset of oscillations (judging from the above noted references) is the presence of vastly differing density states of the fluid within the system. This situation can be encountered in the near critical region, where large changes in density occur with small changes in temperature,

or in the region away from the critical under high heat flux or high wall-to-bulk temperature ratio conditions.

Low frequency oscillations occasionally appeared during these helium heat transfer studies. The frequency of the oscillations varied from about 0.05 to 0.1 Hz, with amplitude in temperature varying from about 0.01 to 1 K and amplitude in pressure generally less than 0.03 MN/m^2 . The conditions necessary for the inception and maintenance of oscillations have not been well established here. The apparatus was not completely instrumented for an oscillations study; however, there is some evidence that they are at least partially induced and sustained by instabilities in the heat exchanger cooling system and are not necessarily dependent upon the thermodynamic state of the fluid in the flow-loop (oscillations were observed at high pressures as well as near critical pressures). The oscillations could be eliminated by an increased flow rate through the heat exchanger. Further investigation is required to understand the nature and cause of the oscillations observed in this system. See section 2.4.

To summarize, the heat transfer coefficients, predicted by the classical Dittus-Boelter correlation (if the 0.023 constant is replaced by 0.022), agree reasonably well with the experimentally determined heat transfer coefficients over the range of operating conditions of this investigation. The standard deviation for this correlation is 14.8%. Modification of this correlation to include a wall-to-bulk temperature ratio (eq. 2.3.1) substantially improves the predictive quality resulting in a standard deviation of 8.5%.

2.3.3 Nomenclature

C_p	= specific heat at constant pressure
D	= diameter
h	= heat transfer coefficient
G	= maximum flow rate per unit area
k	= thermal conductivity
L	= length
P	= pressure
T	= temperature
T_b	= temperature of the bulk stream
T_{tc}	= transposed critical temperature
T_w	= wall temperature
ΔT	= temperature difference $T_w - T_b$
μ	= viscosity

2.3.4 References

- Colburn, A. P., "A method of correlating forced convection heat transfer data and a comparison with fluid friction," Trans. A.I.Ch.E., 29, 174-210 (1933).
- Cornelius, A. J., "An investigation of instabilities encountered during heat transfer to a supercritical fluid," Argonne National Laboratory Report ANL-7032 (1965).
- Dittus, F. W. and Boelter, L. M., "Heat transfer in automobile radiators of the tubular type," Univ. of Calif. Pubs Eng. 2, 443 (1930).
- Giarratano, P. J., Arp, V. D. and Smith, R. V., "Forced convection heat transfer to supercritical helium," Cryogenics, 11, 385-393 (1971).

- Goldman, K., "Heat transfer to supercritical water at 5000 psi flowing at high mass flow rates through round tubes," Int. Developments in Heat Transfer, Part III, 561-568 (1961).
- Hines, W. W. and Wolf, H., "Pressure oscillations associated with heat transfer to hydrocarbon fluids at supercritical pressures and temperatures," ARS J., 32, 361-366 (1962).
- Knapp, K. K. and Sabersky, R. H., "Free convection heat transfer to carbon dioxide near the critical point," Int. J. Heat and Mass Trans., 9, 41-51 (1966).
- McCarthy, J. R. and Wolf, H., "The heat transfer characteristics of gaseous hydrogen and helium," Rocketdyne Research Report RR-60-12 (1960).
- Sieder, E. N. and Tate, G. E., "Heat transfer and pressure drop of liquids in tubes," Ind. Eng. Chem., 28, 1429-1435 (1936).
- Sixsmith, H. and Giarratano, P. J., "A miniature centrifugal pump," Rev. Sci. Inst. 41, 1570-1573 (1967).
- Taylor, M. F., "Correlation of local heat transfer coefficients for single phase turbulent flow of hydrogen in tubes with temperature ratios to 23," NASA TND-4332 (1968).
- Thurston, R. S., "Probing experiments on pressure oscillations in two-phase and supercritical hydrogen with forced convection heat transfer," Advances in Cryogenic Engineering, 10, 305-312 (Plenum, N. Y., 1965).

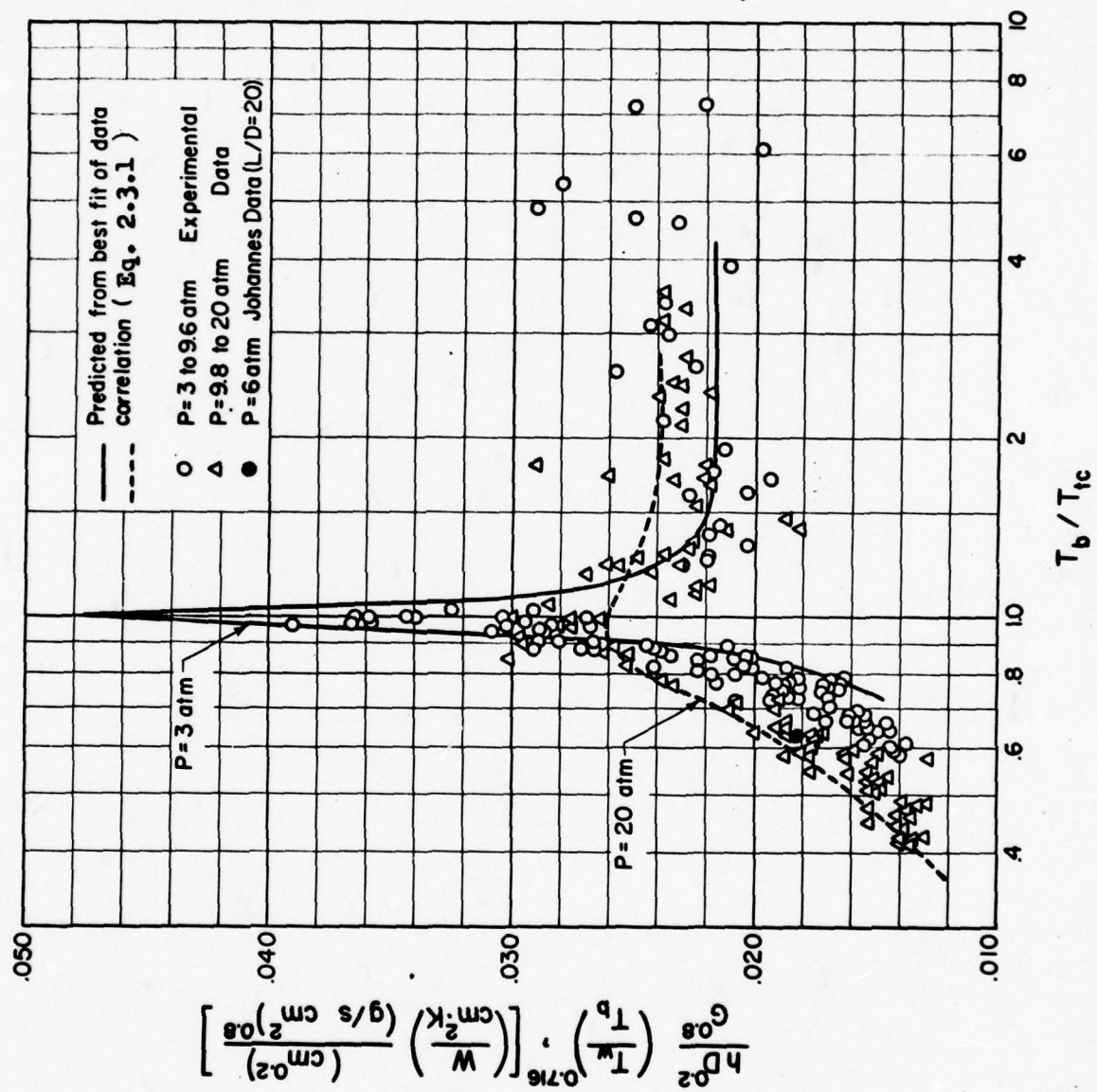


Figure 2.3.1 Experimental and predicted heat transfer results using equation 2.3.1.

2.4 THERMAL OSCILLATIONS AND INSTABILITIES - REVIEW

W. G. Steward

2.4.1 Introduction

The rise of a new technology centered around helium cooled superconducting devices has made obvious the need for accurate helium properties and design data. One aspect of design still often neglected, however, is analysis of system stability and oscillations. The importance of these considerations becomes apparent when one reviews the many operational problems caused by instabilities.

Very few studies have been devoted specifically to helium system stability, with the exception of the thermal oscillations which occur in closed tubes leading to a warm environment ("thistle tubes"). Closed tube oscillations are an example of phenomena which, though present in other fluids, are most strongly evident in helium near 4 K. They are troublesome sources of heat transfer from the environment into helium systems through pressure sensing tubes and other external connections.

General conclusions which have been drawn from various analyses lead one to expect that some of the oscillations and instabilities observed in other fluids would be at least as severe in helium. Some examples of destabilizing factors are: (1) large ratio of density change to heat addition, (2) high compressibility, (3) low effective inertia of the fluid (in some cases), (4) low frictional damping, (5) low nucleate boiling critical heat flux, and (6) low heat capacity for the solid materials. These are all factors which suggest possible stability problems in future helium cooled systems. In addition to these characteristics special problems may be created by unavoidable design features of some of the currently planned devices; extremely

long coolant passages as in superconducting transmission lines, parallel passages in superconducting magnets and generator windings, etc.

Actual examples of helium stability problems can be cited: Runaway pressure oscillations during cooldown of a pumped supercritical flow loop at CERL in England (Heron and Cairns, 1970) forced a manual venting to protect the system. In the same system oscillations occurred when the loop was immersed in liquid helium without the pump motor running. Other oscillations appeared when the flow was started, which were correlatable to operation near the "transposed critical" line. An attempt to operate a helium flow loop at MIT (Smith, 1968) resulted in oscillations which prevented the taking of heat transfer data. Low frequency oscillations were also reported by Arp, et al., [1971] at the NBS Cryogenics Division in a supercritical helium heat transfer flow loop under some operating conditions.

The purpose of this preliminary work is to review the current state of knowledge concerning instabilities and oscillations, and to appraise the possibilities of stability problems in helium cooled superconducting devices. Finally, we wish to outline some appropriate investigations needed for design of helium-cooled systems.

We classify stability problems according to two major areas: (1) operational instabilities and oscillations, and (2) cooldown transients and oscillations. In the following sections we summarize the recently reviewed literature in these areas along with the related research performed at this laboratory, discuss the various analyses, and present our conclusions.

2.4.2 Operational Instabilities and Oscillations

Pump work or heat transferred to a flowing fluid may be partly converted to vibrational energy. Heat transfer plus an unfavorable combination of pump characteristic and system pressure drop may give rise to temperature, pressure, and flow rate excursions. Periodic oscillations or erratic fluctuations may also occur when a system is operated near any of the various heat transfer or flow regime transitions. Transitions may be nucleate-to-film boiling, laminar to turbulent flow or two phase slug-to-annular flow. Still another class of instability can result from interaction between heat exchangers and automatic control systems or pumps. Many of these instabilities are reviewed in some detail in a recent paper by Bouré, Bergles, and Tong [1971].

Some general qualitative conclusions may be drawn regarding conditions which tend to produce instabilities. Five of these which relate particularly to helium properties were listed earlier. The following is a list of operating conditions which tend to promote instabilities :

- (1) pressure below the critical
- (2) high heat flux
- (3) low heat capacity of the solid material
- (4) low heat transfer film coefficient
- (5) flow rates on the borderline between laminar and turbulent flow
- (6) large overall density ratio
- (7) restricted outlet of heated section. (An inlet restriction tends to stabilize the system.)
- (8) subcooling of inlet liquid for most kinds of oscillations

- (9) decreased subcooling in pressure drop oscillations
- (10) low velocity
- (11) small tube diameter
- (12) small bypass parallel to heated section
- (13) highly compressible medium
- (14) unobstructed closed tubes leading to a warm environment.
(Expansion chambers or restrictions may help damp closed tube oscillations.)
- (15) heat transfer coefficient which decreases with increasing flow rate as in some two phase flow situations
- (16) long heated length
- (17) heated section pressure drop which increases with decreasing flow rate
- (18) condition (17) combined with pump operating characteristic having relatively small pressure rise for a given flow decrease
- (19) large time delay in control system response
- (20) control based on downstream conditions.

This list is referred to by number in table 2.4.1.

There is no question that operation in the two phase region promotes stability problems. However, it should be pointed out that a pseudo-two phase behavior can extend to pressures two or three times the critical pressures. For example, Thurston has observed thermal-acoustic oscillations in liquid hydrogen at pressures up to 2.8 MN/m^2 (400 psia), about twice the critical pressure. This pseudo-two phase region is not sharply defined but exists near the temperatures determined by the locus of specific heat maxima, or transposed critical temperatures. A discussion of the pseudo-two phase region may be found in Hendricks, Simoneau, and Smith [1969].

Oscillations have been reported in highly subcooled systems as well. Oscillations in a slush hydrogen flow loop at the NBS Cryogenics Division (Daney, Ludtke, Sindt, and Chelton, 1967) produced heat transfer rates sufficient to condense air on the warm end of a ventpipe. A checkvalve at the slush hydrogen end solved this problem. Other oscillations were observed in a hollow stirring vane shaft, and in instrument lines.

The enhancement of heat transfer coefficient and the low coolant pressures and temperatures in two-phase and pseudo-two phase fluid may make the risk of stability problems worthwhile in some applications. Furthermore, this region may be unavoidable in systems with large pressure drops. For these reasons consideration of the two phase stability is important.

Operational instabilities and oscillations are summarized in table 2.4.1. It should be pointed out that the distinct separation of the various instabilities in table 2.4.1 is an analytical convenience but not highly accurate since the phenomena occurring in real systems may result from combinations of several effects.

2.4.3 Analyses

Analyses fall into three broad categories:

- (1) Computer solutions of the conservation equations in the time domain, e.g., Cornelius [1965]; Arp [1971]; Steward, Smith, and Brennan [1969]. These solutions yield greater amounts of information than other analyses, including amplitudes, wave forms, and detailed outputs of all the variables as functions of location and time. Generalized solutions have not been obtained so that each system must be treated

individually and solved for each desired operating condition. Computational time can be quite significant in solutions in which flow rate is considered to be a dependent variable.

(2) Stability criteria developed from nonlinear equations or linearized equations. These have been used successfully to develop stability threshold lines and surfaces (Bhatt and Hsu, [1965]; Wallis and Heasley, [1961]; Zuber, [1966]; Bouré, [1966]) for various fluids, but have not as yet been applied to helium. These studies have been very useful in establishing the qualitative effects of the property and system parameters, but have been less successful in predicting amplitudes.

(3) Correlations developed from highly simplified models in addition to experimental data, e.g., Thurston [1966]. Analyses are also summarized in table 2.4.1.

2.4.4 Cooldown Transients and Oscillations

During the cooldown of cryogenic equipment the heat transferred from the warm solid parts into the cooling medium supplied the driving energy for oscillations. Liquid alternately flows into the warm system, and then is expelled by the pressure built up when vapor forms faster than it can escape through the discharge. Pressure peaks in transfer lines of at least four times the inlet supply pressure and reverse volume flow rates of fifteen times the forward flow have been reported by Burke, Byrnes, and Post [1958]; Steward, Smith and Brennan [1969]. The surges at the beginning cooldown are the largest in amplitude and depend on the way in which the inlet valve is opened and other starting conditions. After the initial spasms, however, oscillations continue with smaller amplitude until a stable operating temperature is achieved, and as already discussed, various oscillations may be

encountered thereafter. These later oscillations do not depend on the start-up procedure. A mathematical modeling of the cooldown process which takes into account the start-up procedure as well as the changing wall temperature distribution, liquid location, and heat transfer modes is given by Steward, Smith and Brennan [1969].

Cooldown time and total consumption of liquid is another matter of concern. The methods for prediction of cooldown time consider only the longer term transients in wall temperatures and liquid location and not the oscillations. Thus, mathematical models can be considerably simplified. Cooldown time predictions tend to be bracketed by two extreme cases: the first of these, "gas flow limited cooldown," is characteristic of long narrow passages such as transfer lines or cryogenically cooled electrical transmission lines. In these the rate of cooling is limited primarily by the rate at which the warm gas can escape. A. D. Little [1959]; and Steward, Smith and Brennan [1967] use cooldown time predictive methods based on the gas-flow-limited model.

The second extreme case is characteristic of an apparatus which contains very short flow passages or is immersed in a cooling bath. Cooldown of such apparatus could be termed "heat transfer limited." Under the condition of negligible internal thermal resistance (Newtonian cooling) and constant film coefficient the time constant for temperature change is proportional to the heat capacity and mass and inversely proportional to heat transfer film coefficient and surface area (Schneider, 1957). Variable film coefficient and non-negligible internal thermal resistance somewhat complicate the problem, but standard methods of solution are applicable.

Large diameter transfer lines constructed of low thermal conductivity material could conceivably warp due to uneven cooling of the top and bottom parts of the pipe. Warping was actually observed by Bronson, et al., [1962] when liquid hydrogen was fed into a system slowly enough to allow liquid to lie along the bottom of the pipe with vapor above. Higher flow rate may eliminate this problem while aggravating the oscillation problem.

2.4.5 Application to Superconducting Systems

Certainly not all of the many possible oscillations and instabilities need concern designers of helium cooled devices, but some should not be ignored.

The cooldown oscillations have the greatest reported pressure amplitudes; however, these may be tolerable since no attempt is made to operate in a superconducting mode during cooldown. The handling of boil-off gas and cooldown time may be of more immediate concern. The volume flow of gas evolved may exceed the capacity of the refrigeration system. Some gas would be wasted or would have to be compressed and stored. Intermediate venting and compressor stations and precooling with another fluid may be advisable. Thermal contraction problems should be considered. An estimation of cooldown time would depend greatly on the configuration of the apparatus.

After cooldown, a number of significant oscillations could remain. Some of these which are strictly associated with forced flow systems and two phase flow, such as flow pattern transitions, appear avoidable by employing sufficient pressure to the system. Other phenomena extend into the supercritical or pseudo-two phase region. The "thermal acoustic" oscillations reported by Thurston are of significant amplitude and have been observed at pressures up to at least

twice critical. Thermal acoustic oscillations are associated with very high heat fluxes, however, and with film boiling temperature differences. These conditions probably would not exist in the normal, steady operation of superconducting devices. A study of the effect of heat pulses or off-design operation might consider these phenomena.

In forced flow through channels of extremely large length to diameter (L/D) ratio, as would be the case with helium cooled superconducting electrical transmission lines, the propagation of density waves would appear to be potentially one of the most significant problems. Even though the entire length of a line might operate at supercritical pressure if the flow were steady, the actual flow may be unsteady, with density and pressure rarefaction waves below critical pressures. A small density perturbation toward lower density can cause a slight increase in the local pressure drop. This pressure drop tends to propagate the density perturbation downstream and the amplitude may be either attenuated or amplified depending on the fluid and solid thermal properties and flow rates (Bouré, 1966). It is conceivable that density perturbation could develop into a warm low density pocket which, combined with the very small heat capacity of metals at helium temperature, could allow a section of the transmission line to become normal. An analysis of this problem should include a calculation of wall temperature fluctuations which have been ignored in previous studies.

Apparatus such as magnet coils or motor windings cooled either by forced or natural convection (including pool boiling) may experience oscillations such as those investigated by Blumenkrantz and Taborek [1971]. The Bouré [1966] model was used successfully by these authors to predict the onset of oscillations. These apparatus

often employ parallel coolant passages. Bouré [1966] and others have concluded that a small number of parallel passages tend to be highly unstable and result in maldistribution of flow and Ledinne [1954] type temperature and flow excursions. In a large number of parallel passages, the effect of a perturbation in any one has less influence on the others and thus the system is more stable.

2.4.6 Conclusions

This preliminary investigation indicates very few studies have been directed specifically toward instabilities in helium systems. General conclusions based on other fluids warn of possible stability problems and, in fact, troublesome oscillations have been encountered in helium heat transfer loops. These problems begin with the cooldown and continue in a wide variety of forms after the operational conditions have been reached. The mathematical analyses may be classed into three broad categories; stepwise computer solutions of the governing equations in the time domain, development of stability criteria from linearized or nonlinear equations, and correlations involving dimensionless parameters and based on experimental data.

Some of the instabilities, though significant under certain conditions, appear avoidable, tolerable, or not very relevant to the problem of helium cooling of superconductors. Other instabilities could constitute serious problems, or are important design considerations: during cooldown, allowance must be made for the large, spasmodic expulsion of gas which undoubtedly would exceed the capacity of a system refrigerator. The transient conditions and cooldown time are also important questions. Two limiting cases of gas flow limited

cooldown and heat transfer limited cooldown require different treatments. Prediction of, and allowance for thermal contraction, though not a stability problem, is an important consideration associated with cooldown.

Of the various oscillations and instabilities which could remain after the operation conditions have been reached, the density wave oscillations appear to be potentially one of the most serious problems. Low density, warm fluid pockets might develop either in very long systems such as superconducting transmission lines or in natural convection heat exchangers, such as are common in motor coils or magnets. This could lead to temperature rise and loss of superconductivity. Stability criteria type analyses should be useful in predicting the onset of this phenomenon; the stepwise computer solutions would be required for more detailed predictions.

The stability problems summarized here warrant further investigation. Applicable computer analyses have been developed within this Division and studies are currently being undertaken for Brookhaven National Laboratories in collaboration with NSF. These studies should provide valuable design information for future helium cooled superconducting systems.

The references noted in this review and listed below are some of those we consider to be the more pertinent papers dealing with instabilities and oscillations. A very large number of studies in this area have appeared, (exclusive of specific helium studies) particularly in the past six years. A much more extensive list of references, consisting of 110 on cooldown and 127 on stability and oscillations, has been compiled by the Cryogenic Data Center and is available on request.

2.4.7 References

- Arp, V. D., "Forced flow single phase helium cooling systems," to appear in Advances in Cryogenic Engineering (Plenum Press, New York, 1972).
- Arp, V., Ballinger, E. R., Giarratano, P. J., Roder, H. M., Smith, R. V., Snyder, N. S., Steward, W. G., and Wallace, G. H., "Helium heat transfer," NBS Report 10 703 (1971).
- Bergles, A. E., Goldberg, P., and Maubetsch, J. S., "Acoustic oscillations in a high pressure single channel boiling system," EURATOM Report, Proceedings of the Symposium on Two Phase Flow Dynamics at Eindhoven (1967).
- Bhatt, S. J., and Hsu, C. S., "Stability criteria for second order dynamical systems with time lag," ASME paper 65-APMW-11 presented at the Western Conference of the ASME Appl. Mech. Div. (Sept. 1, 1965).
- Blumenkeatz, A., and Taborek, J., "Application of stability analysis for design of natural circulation boiling systems and comparison with experimental data," AIChE Paper 13 presented at ASME-AIChE Heat Transfer Conference, Tulsa, Oklahoma (August 15-18, 1971).
- Bouré, J. A., "The oscillatory behavior of heated channels," EURATOM Report, Proceedings of the Symposium on Two-Phase Flow Dynamics, Eindhoven (1967).
- Bouré, J. A., Bergles, A. E., and Tong, L. S., "Review of two-phase flow instability," ASME paper 71-HT-42 presented at the ASME-AIChE Heat Transfer Conference, Tulsa, Oklahoma (August 15-18, 1971).

- Bronson, J. C., Edeskuty, F. J., Fretwell, J. H., Hammel, E. F., Keller, W. E., Meier, K. L., Schuch, A. G., and Willis, W. L., "Problems in cooldown of cryogenic systems," Advances in Cryogenic Engineering, 7 (Plenum Press Inc., New York, 1962).
- Burke, J. C., Byrnes, W. R., Post, A. H., and Ruccia, F. E., "Pressurized cooldown of cryogenic transfer lines," Advances in Cryogenic Engineering, 4 (Plenum Press Inc., New York, 1960).
- Cornelius, A. J., "An investigation of instabilities encountered during heat transfer to a supercritical fluid," Argonne National Laboratory Report ANL-7032 (April 1965).
- Daney, D. E., Ludtke, P. R., Sindt, C. F., and Chelton, D. B., "Slush hydrogen fluid characterization and instrumentation analysis," NBS Report 9701 (1967).
- Ellerbrock, H. H., Livingood, N. B., and Straight, D. M., "Fluid flow and heat-transfer problems in nuclear rockets," Nuclear Rocket Propulsion, NASA SP-20, NASA, Washington, D.C. (December 1962).
- Friedly, J. C., and Krishnan, V. S., "Prediction of nonlinear flow oscillations in boiling channels," AIChE paper 14 presented at the ASME-AIChE Heat Transfer Conference, Tulsa, Oklahoma (August 15-18, 1971).
- Friedly, J. C., Manganaro, J. L., and Kroeger, P. G., "Two-phase flow stability," General Electric Technical Information Series No. 68-C-078, available from Distribution Unit, Bldg. 5, room 345, Research and Development Center, P.O. Box 8, Schenectady, New York 12301 (1968).

- Hendricks, R. C., Simoneau, R. J., and Smith, R. V., "Survey of heat transfer to near-critical fluids," Advances in Cryogenic Engineering, 15 (Plenum Press Inc., New York, 1970).
- Heron, K., and Cairns, D. N. K., "Experiments on a pumped supercritical helium test loop," Central Electricity Research Laboratories Lab Note No. RD/L/N 190/70 (Job No. VB 341) (December 1, 1970).
- Koshilev, I. I., Surnov, A. V., and Nikitina, L. V., "Inception of pulsations using a model of vertical water wall tubes," Heat Transfer, Soviet Research, 2, 3 (1970).
- Ledinegg, M., "Instability of flow during natural and forced circulation," Die Warme, 61, No. 8, (1938); AEC-tr 1861 (1954).
- A. D. Little Co., "Pressurized cooldown of cryogenic transfer lines," Special Report No. 106 (October 1, 1959).
- Maulbetsch, J. S., and Griffith, P., "A study of system-induced instabilities in forced convection flows with subcooled boiling," MIT Engineering Projects Lab Report 5283-35 (1965).
- Maulbetsch, J. S., and Griffith, P., "Prediction of the onset of system induced instabilities in subcooled boiling," EURATOM Report, Proceedings of the Symposium on Two Phase Flow Dynamics, Eindhoven (1967).
- Norton, M. T., and Muhlenhaupt, R. C., "Computer solutions for thermal-acoustical oscillations in gas-filled tubes," NBS Technical Note 363 (November 30, 1967).
- Rubin, S., "Longitudinal instability of liquid rockets due to propulsion feedback (POGO)," Journal of Spacecraft and Rockets, 3, No. 8, (August 1966).
- Schneider, P. J., Conduction Heat Transfer (Addison-Wesley Publishing Co. Inc., Reading, Mass., 1957).

- Smith, Joseph, MIT, private communication (1968).
- Stenning, A. H., and Veziroglu, T. N., "Flow oscillation modes in forced convection boiling," Proc. 1965 Heat Transfer and Fluid Mechanics Institute (Stanford University Press, Stanford, Calif., 1965).
- Stenning, A. H., Veziroglu, T. N., and Callahan, G. M., "Pressure drop oscillations in forced convection flow with boiling," EURATOM Report, Proceedings of the Symposium on Two Phase Flow Dynamics, Eindhoven (1967).
- Steward, W. G., Smith, R. V., and Brennan, J. A., "Transient flow of cryogenic fluids," NBS Report 9702 (1968).
- Thullen, P., and Smith, J. L., Jr., "Model for thermally sustained pressure oscillations associated with liquid helium," Advances in Cryogenic Engineering, 13 (Plenum Press Inc., New York, 1968).
- Thurston, R. S., "Thermal acoustic oscillations induced by forced convection heating of dense hydrogen," Advances in Cryogenic Engineering, 11 (Plenum Press Inc., New York, 1966).
- Wallis, G. B., and Heasley, J. H., "Oscillations in two-phase flow systems," ASME Journal of Heat Transfer, Series C 83 (August 1961).
- Zuber, N., "An analysis of thermally induced flow oscillations in the near-critical and super-critical thermodynamic region," Final Report NAS8-11422, prepared for Marshall Space Flight Center, NASA Huntsville, Alabama (May 25, 1966).

TABLE 2.4.1 OPERATIONAL INSTABILITIES AND OSCILLATIONS

Type of instability and where observed	Mechanism and Characteristics	Relative Amplitude	Frequency	Destabilizing Conditions (numbers refer to previous list)	Analyses
Flow pattern transition, 2 phase flow only	When bubbly slug flow exists an increase in the bubble content may change the flow pattern to annular flow which has characteristically lower pres. drop. The flow rate then tends to increase which reduces the vapor generated per unit volume, whence the flow pattern may revert to the bubbly slug flow, etc.	no large amplitudes observed	not necessarily periodic $0 < f < 1$ Hz	1, 2, 3, 4	Bergles, Goldberg, and Maulbetsch (1967) (descriptive only)
Laminar-turbulent transitions, single phase, forced or natural convection systems	This instability has been observed at very low forced flow or in natural convection systems operating near the transition. A momentary flow reduction may result in a transition from turbulent to laminar, which in turn causes a reduction in friction factor and tends to increase the flow again	small	$1 < f < 10$ Hz	5	Ellerbrock, Livingood, and Straight (1962) (descriptive only)
Thermal acoustic or film boiling osc. H ₂ rocket engines-nuclear reactors	Thurston (1966) attributes oscillations to variations in film boiling coefficient, h; increase in pressure increases h, generates thicker film, reduces h etc.	20-30% of driving pressures	4 to 38 Hz (Thurston-Helmholtz mode, 50 to 150 Hz - 1st pipe mode - 10 ¹ sect. (geometry dependent))	6, 7, 8	Thurston (1966) correlated frequency with Helmholtz and organ pipe modes, amplitudes with boiling number Friedly, Mangano, Kroeger (1968) by means of linearised anal. (perturbation eq., Laplace transforms, transfer function, Nyquist criterion) produced stability maps
Pressure drop-compressible volume oscillations	Compressible pockets may act as springs. These oscillations have been observed to cause large reductions in critical heat flux (CHF).	Δ pressure 50% of inlet P	0 (excursion to CHF) for tubes of low thermal cap. Low freq. (0.02 - 0.1 Hz) - higher thermal cap.	3, 7, 9, 10, 11	Maulbetsch and Griffith (1965, '67) lumped parameters, perturbation technique and stability criterion. Also Stenning, Veziroglu, and Callahan (1967) similar
Parallel channel oscillations coils, boilers	Interaction between channels	flow reversals of large amplitude essentially constant ΔP	"manometer" mode possible (0.2 to 2 Hz)	12	manometer dynamics Koshelev, Surnov, and Nikitina (1970)
Acoustic oscillation	Pressure wave propagation		acoustical frequency	7, 13	Bergles, Goldberg and Maulbetsch (1967) perturbation techniques

TABLE 2.4.1 OPERATIONAL INSTABILITIES AND OSCILLATIONS (cont'd)

Type of instability and where observed	Mechanism and Characteristics	Relative Amplitude	Frequency	Destabilizing Conditions (numbers refer to previous list)	Analyses
Thermal acoustic-"phistie tube" or closed tube	Heat transfer driven due to large temperature gradient along closed tubes	produces extreme heat transfer in some cases	related to geometry	7, 14	Norton, Mühlenhaupt (1965) simplified wave eq. Taitien and Smith (1967) - non-linear lumped parameter
Density wave oscillations, forced or natural convection heat exchangers	Wave of large density change (as in phase change) travels through heated section	Stenning (1965) reports flow reversals of 1/3 forward flow rate	period about equal to 1 or 2 times residence time of fluid in heated zone, $f = 0.1$ to 1 Hz	1, 2, 6, 7, 8, 15, 16	Friedly (1971)-Poincaré non-linear analysis neglecting velocity derivatives and w. constant heat flux Stenning and Vezirglu (1965) experimental stability maps Bouré (1966) linearized, stability criterion
Ledinegg flow excursion	Decrease in flow increases enthalpy rise and vapor content leads to higher ΔP and further decrease in flow, etc.	peak temperature limited by system or burn-out (CHF)	0	7, 18	Flow instability boundary for Density Wave Oscillations From Bouré (1966)† Cornelius (1965) and Steward, Smith, Brennan (1969) time domain computer solutions Zuber (1966) perturbation technique Ledinegg (1954)
Parallel channel Ledinegg excursion	Each channel sees essentially constant pressure drop, no stable operation is possible when decreasing flow results in increasing pressure drop				Maulbeth and Griffith (1965)
Control system or time delay oscillations outstanding example is "POGO" in liquid fueled rockets	Delayed response of heat exchangers to automatically controlled flow changes particularly when the control is based on downstream conditions. POGO is caused by coupling between engine thrust structural members, fuel control.	have been observed to CHF or in POGO, premature shutdown or destruction of vehicle	depends on delay characteristics	1, 2, 3, 4, 7, 8, 19, 20	Friedly (1967) stability criterion Rubin (1966) instabilities in liquid rockets

† u^* , h^* are reduced velocity and subcooling parameters.

2.5 HELIUM REFRIGERATION SYSTEMS AND COOLING LOOPS - DISCUSSION OF THE PROBLEM - W. G. Steward

NBS Cryogenics Division has contributed significantly to the analysis and design of helium cooled superconducting equipment through fundamental studies in helium transport and thermodynamic properties, heat transfer, flow, and pumping. This laboratory is currently conducting further studies in normal and superfluid helium pumping and thermal and fluid dynamical stability. Important considerations which should also be included in future studies are the interactions between refrigerators and the varying heat loads and flow resistance in cooling loops and superconducting machines.

Requirements of refrigerators vary widely according to the applications. In superconducting transmission lines, the emphasis will be on economy of operation, reliability, and ability to tolerate fault currents. Cairns, et al., [1969] have analyzed possible modes of operation for typical systems to supply 1 kW of refrigeration at 4.2 to 5.8 K for a niobium transmission line. System variables are outlined in tables 2.5.1 and 2.5.2 and the refrigerator-load arrangements are shown in figures 2.5.1, 2.5.2 and 2.5.3 taken from that paper. As may be seen in table 2.5.1, three conditions--supercritical, liquid, and gaseous helium--were analyzed for three basic refrigeration-load arrangements designated as A, B, and C in figure 2.5.3. Wide variations in the required inlet temperature mass flow rates, pressure drops, and total power consumption of the refrigerators were found, due to the variations in specific heat, density, and viscosity at the three assumed fluid conditions. These authors concluded that the best method for circulation of helium coolant will be with a low temperature pump which is independent of the refrigerator. This conclusion was based not only on the results shown in table 2.5.1 but on the

need for the additional flexibility afforded by the low temperature pump. Bogner and Schmidt [1970] reach the same conclusion for a superconducting transmission line.

The conclusions of Cairns, et al., [1969] were based on the use of niobium as the superconductor, thus limiting the system temperature to about 6.7 K. Work is being done with higher temperature superconductors such as Nb_3Sn (e.g., at Gulf General Atomic reported by Snowden [1972]). In these materials, the losses and current capacity at 10 to 12 K are comparable to those of niobium at 4.2 K. The savings in refrigeration capital cost and power would be extremely significant with operation at these higher temperatures. Furthermore, conclusions as to the optimum fluid condition and refrigerator-loading combinations may be considerably altered by such advances in superconductor technology.

Cooldown of the line is anticipated to be a troublesome operation which will add to the demands on the refrigeration system. Large pressure drops will be unavoidable, and the flow rate reduction will prolong the cooldown time. Since approximately 95 percent of the heat capacity in the solid materials is extracted above 77 K, precooling with liquid nitrogen may be a requirement. Such dual systems would undoubtedly create problems in helium contamination during transition. Kellner, et al., [1969] have studied the cooldown of these long passages under conditions of limited driving pressure. Cooldown rate may be limited either by the pumping ability, or the refrigeration capacity. In the latter case, an extra reservoir of liquid helium may be advisable to expedite cooldown.

For military applications such as Naval propulsion machinery (W. I. Levedahl, 1972), the emphasis will be on compactness, invulnerability to mechanical shock or gunfire, and ability to be maintained by unskilled or moderately skilled servicemen. Ship propulsion machinery is subject to sudden start-ups, maneuvering transients, and must have redundant components to enable operation even after sustaining damage. Military users are willing to sacrifice some degree of efficiency and economy for these performance features; however, efficiency and economy cannot be ignored as these factors ultimately affect the ship's operational range. To some degree, advantages in both efficiency and redundancy can be gained by dividing the load among several generators and motors. Then at low cruise speeds, smaller components can operate near design loads. For higher speeds, these can be combined, and in case of damage, there is a good probability of some units remaining operational. Dividing the refrigeration system into several smaller units of course means a sacrifice of peak efficiency since small refrigerators are inherently less efficient than larger ones.

In superconducting magnet coils, the coolant helium may be a liquid bath in which the coils are submerged. In such cases, a refrigerator merely replenishes the helium lost through heat absorption and no significant head production or circulating ability is required of the refrigerator. In other designs (Carter, et al., 1969) or the CERN "Omega" magnet (Morpurgo, 1970) gas or supercritical helium may be circulated. Considerable flow rate may be required to achieve adequate forced convection heat transfer coefficients, and many advantages already cited can be gained by maintaining pressures

above the critical. Thus, cold pumps or high flow and high pressure refrigerators are called for.

Many basic configurations and infinite variations of refrigerators combined with external circulation pumps, heat exchangers, and cooling loops are possible. Resulting pump powers, sizes, weights, and reliability vary greatly from one configuration to another, but no one system is universally preferable. Design requirements such as high acceleration loading, ability to operate under highly variable heat loading for brief or extended periods, and the need for redundancy will influence the design approach. Obviously these diverse requirements preclude a generalized solution of design problems, and there is no substitute for refrigeration cycle analysis of individual proposed systems. However, certain aspects of these analyses may be facilitated by generalized heat transfer, pressure drop and pumping computational programs. Such programs could prove particularly useful in feasibility studies and preliminary design. This is an area we feel should be explored.

2.5.1 References

- Bogner, G., and Schmidt, F., "Energietransport durch tiefgekühlte kabel," Naturwissenschaft (Feb 27, 1970).
- Cairns, D. N. H., Edney, K., Steel, A. J., and Swift, D. A., "Refrigeration and circulation of helium in superconducting power cables," Commission 1 of the IIR in conjunction with The British Cryogenics Council - Conference on Low Temperatures and Electric Power, London, England, March 24-26, 1969, pp. 24-31.

- Carter, C. N., Lewis, K. G., Maddock, B. J., and Noe, J. A.,
"Closed cycle refrigeration of a superconducting magnet,"
Commission 1 of the IIR in conjunction with The British
Cryogenics Council - Conference on Low Temperatures
and Electric Power, London, England, March 24-26, 1969,
pp. 8-18.
- Kellner, K., Morton, I. P., Saldanha, S., and Seurlock, R. G.,
"The cooldown of long ducts," Commission 1 of the IIR
in conjunction with The British Cryogenics Council-
Conference on Low Temperatures and Electric Power,
London, England, March 24-26, 1969, pp. 77-80.
- Levedahl, W. J., "Superconductive naval propulsion systems,"
Paper B-1, Applied Superconductivity Conference, Annapolis,
Maryland (May 1-3, 1972).
- Morgpurgo, M., "The design of a superconducting magnet for the
'Omega' project," Particle Accelerators 1, pp 255-263
(1970) (Glasgow, Scotland).
- Snowden, D. P., "Superconductors for power transmission,"
Scientific American, 226, No. 4, 84-91 (April 1972).

Table 2. 5. 1:* Comparison of Selected 1 kW Plants

System	Supercritical			Liquid			Gaseous
	A	B	C	A	B	C	
Loading Arrangement	A	B	C	A	B	C	C
Circulator ¹	MC	MC	LT, P	MC	MC	LT, P	LT, P
Number of Turbines	2	3	2	2	2	2	2
Joule-Thomson Valves	-	-	-	2	3	1	1
Cable Inlet Temp. K	5.6	5.4	5.8	4.2	3.8	4.6	4.6
Cable Outlet Temp. K	6.5	6.5	6.7	5.0	5.0	5.0	6.5
Cable Operating Pressure MN m ⁻²	0.37	0.37	≈0.6- 0.3	0.3	0.3	≈0.4- 0.3	1.0
Cable Flow kg s ⁻¹	.09	.07	.09	.27	.19	.40	.12
Total Compressor Flow kg s ⁻¹	.11	.12	.11	.33	.29	.16	.16
Total Power Consumption kW	220	240	220	830	700	260	260
Carnot Efficiency	22.0	21.0	21.0	8.0	10.0	24.0	20.0

Note 1. MC = main compressor

LT, P = low temperature pump

2. No pressure drop in the load has been allowed.

3. The LN₂ refrigeration is not included but is represented by 5-10% increase in compressor power.

Table 2. 5. 2:* Approximate values of the mass flow and pressure drop for the different systems with normal and standby operation

		Liquid	Gaseous	Supercritical	
Normal Operation	Mass Flow	.25	.35	.23	kg s ⁻¹
	Pressure Drop	.005	.03	.03	MN m ⁻²
Standby	Mass Flow	.40	.80	.45	kg s ⁻¹
	Pressure Drop	.02	.27	.3	MN m ⁻²

* From Cairns, et al. (1969)

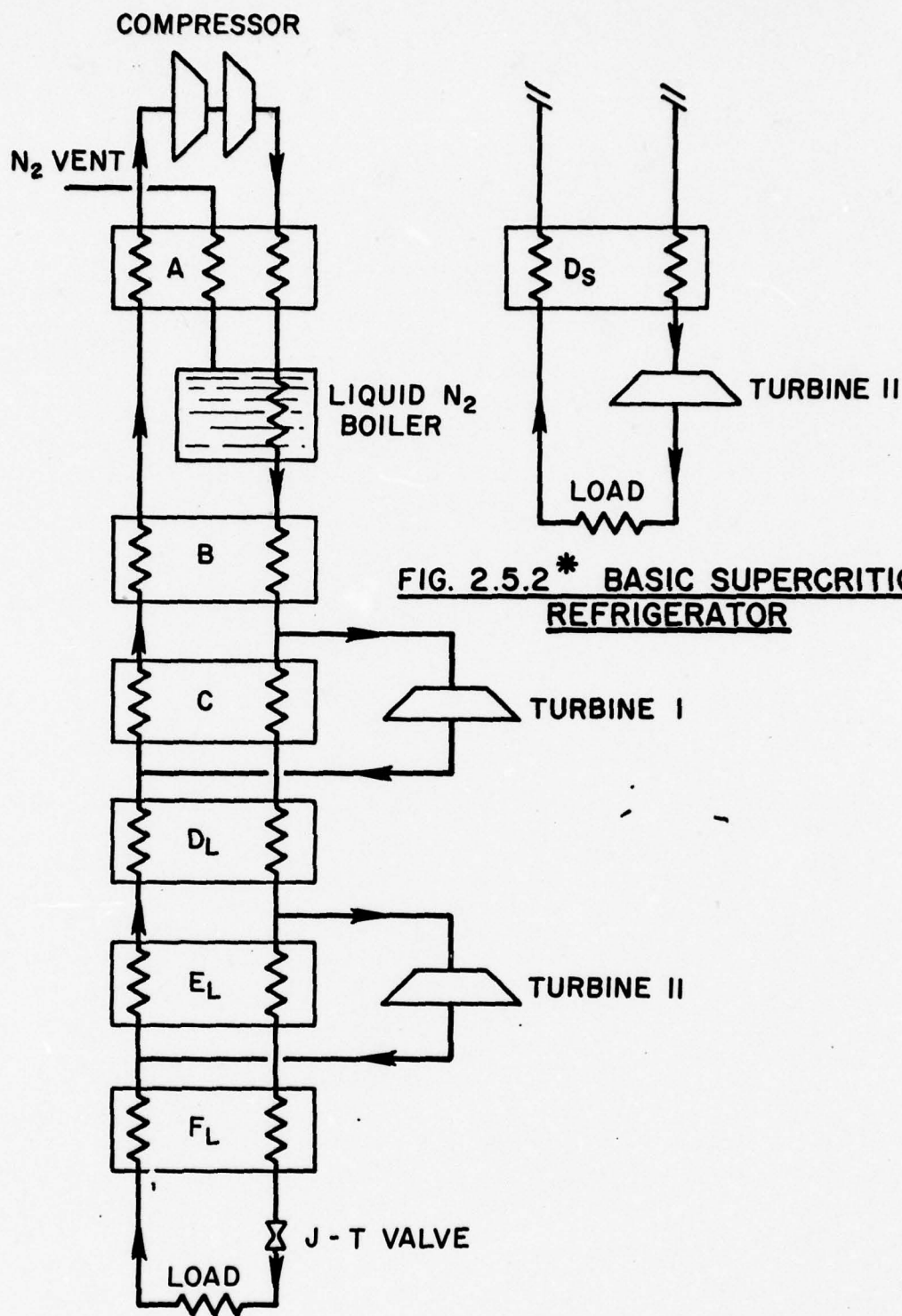


FIG. 2.5.2 * BASIC SUPERCRITICAL REFRIGERATOR

FIG. 2.5.1 * BASIC LIQUID REFRIGERATOR

* From Cairns, et al. (1969)

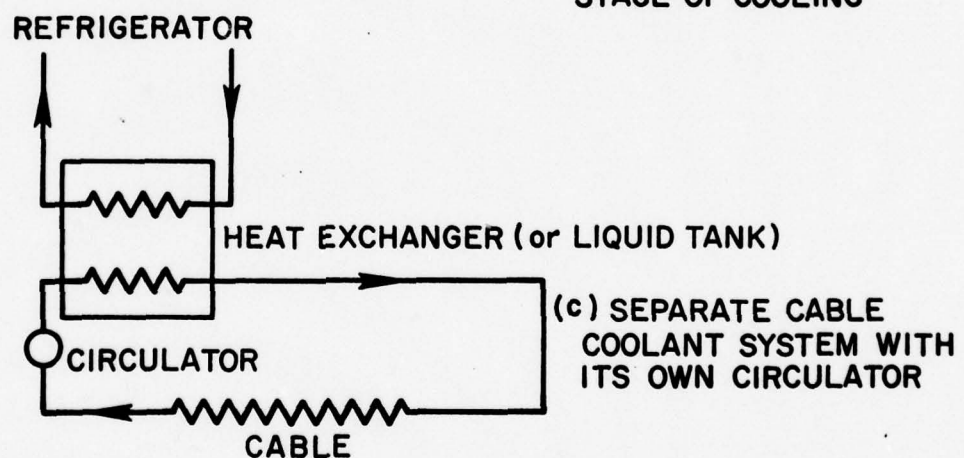
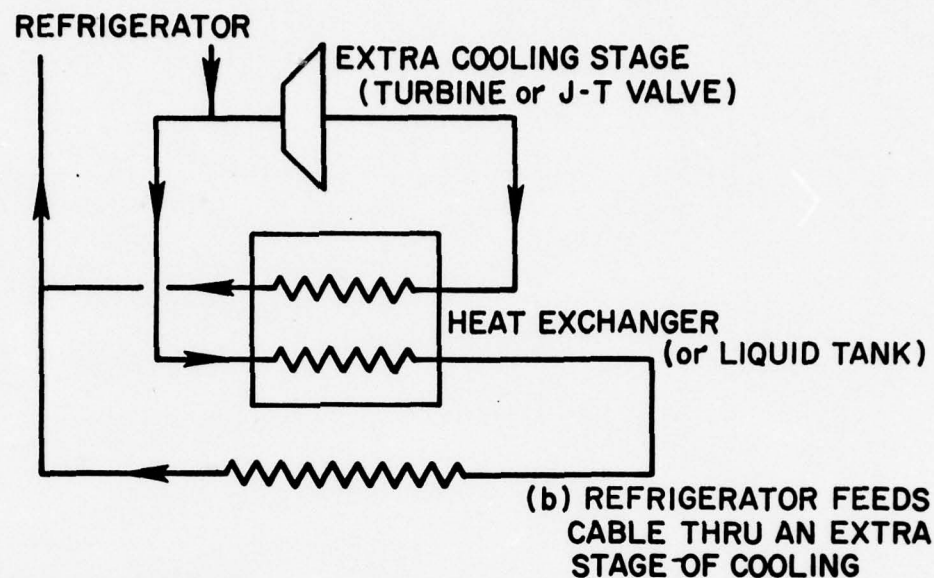
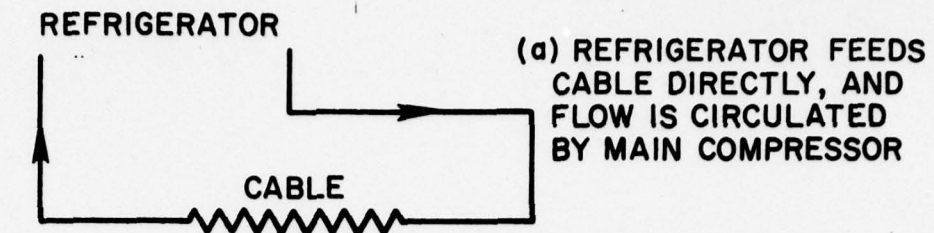


FIG. 2.5.3* THREE ARRANGEMENTS OF THE CABLE AS THE REFRIGERATOR LOAD

* From Cairns, et al, (1969)

2.6 STABILITY OF FORCE-COOLED SUPERCONDUCTING MAGNETS - ANALYSIS - V. D. Arp

2.6.1 Introduction

In the decade which has passed since the first attempt to produce high field superconducting magnets, the factors which tend to cause the magnets to quench at current less than that predicted from short sample measurements have been thoroughly studied. Basically, these are related to (1) pinning and sudden motion of magnetic flux within the superconducting wire, and (2) small mechanical motions of the wires relative to each other. Performance of modern stabilized magnets at the short sample level comes from careful attention to both these factors.

Three approaches to stabilization of magnets in the face of magnetic flux jumps have been recognized and applied (Mulhall and Hutton, 1971). The earliest may be termed cryogenic stabilization, wherein heat transfer from a copper (or aluminum) substrate is sufficient to maintain superconducting temperatures even when it carries the full transport current. Somewhat different is dynamic stabilization, wherein the thermal diffusivity is so much greater than the magnetic diffusivity that, provided an adequate heat sink is somewhere available, the energy dissipated during flux motion is removed from the superconductor as fast as it appears. The most effective, when it can be achieved, is adiabatic stabilization, and leads to small superconductor diameters or thickness ($\approx 20\mu\text{m}$) twisted in a normal matrix, relying on their own heat capacity to insure stable flux penetration. Twisted multifilament niobium-titanium wires in a copper matrix have become commercially available in the past year or so, and have been used almost exclusively for magnets in the past

year or so; they now are used almost exclusively for magnets of up to 6 or 7 tesla, at least in small size.

Even with the twisted multifilament superconductor, however, different makers will assign different weights to the opposing demands for heat transfer area and for maximum mechanical stability. Small coils tend to be impregnated for maximum mechanical stability, with heat transfer a more minor consideration. However, very large magnets, e.g., those for the 12 ft. ANL and 15 ft. NAL bubble chambers are designed for full cryogenic stability, and at the present time it seems that no one is willing to give up the assurance of a cryogenically stable design where large sums of money ride on a single large magnet. Alternatively, adiabatically stable (i.e., twisted multifilament) Nb_3Sn wire is not available at this time, so that magnets for fields exceeding about 8 tesla are forced to rely upon one of the other forms of stabilization.

At this time, then, it appears that cryogenic stabilization of superconducting coils is still an important consideration in some systems. This section is concerned with cryogenic stabilization using the forced flow of supercritical helium.

2.6.2 Cryogenic Stabilization

The importance of heat transfer from the superconductor to the helium bath was first stated by Stekly and Zar [1965], with a later publication (Stekly, Thome, and Strauss, 1969) giving much more detail. They introduced a stability parameter, α , which is the ratio of Joule heating when the normal metal carries the critical current to the heat transfer rate when the sample is at the superconducting transition temperature (it is probably better called an instability parameter since the magnet instability grows as α increases):

$$\alpha = \frac{\rho_r I_c^2}{A \phi q_m} \quad (2.6.1)$$

When $\alpha < 1$ the heat generated by any localized flux jump is quickly removed by the helium, with the result that propagation of the normal region, leading to quenching of the magnet, generally does not occur. Other factors which influence the stability when examined in more detail are (1) the finite thermal conductivity of both the superconductor and the substrate, (2) the temperature dependence of the resistivity of the substrate, (3) the boundary (Kapitza) thermal resistance between the superconductor and the substrate, and (4) thermal contact between adjacent turns of the superconductor, including the effect of insulating layers. However, they do not have a major effect on the analysis in this paper, except that (2) provides an important design limit.

2.6.3 Pool Boiling Stabilization

The early studies considered just the nucleate boiling heat transfer characteristic, or simplified generalizations of this, in evaluating the stability of superconducting coils. Kremlev, et al., [1968] used the combined nucleate and film boiling characteristic, but it remained for Maddock, James, and Norris [1969] to emphasize the importance of the total curve, including the relatively unstable heat transfer for ΔT 's between the peak nucleate boiling and the minimum film boiling points. Their work basically outlines the recovery of superconductivity in a coil where a localized region has been driven to high temperature, as from a flux jump, including the effect of heat transport along the wire from the heated region to a cold end.

The several types of critical currents which have been recognized can be conveniently explained using their analytical techniques, and for our present analysis it is appropriate to briefly recapitulate them here.

Figure 2.6.1 illustrates the graphical analysis used by Maddock, James, and Norris. The solid and dotted lines give the heat transfer per unit surface area as a function of the sample temperature, with the dotted line indicating the relatively undefined portion of the curve. The dashed lines give the heat generation per unit surface area as a function of the sample temperature (which determines what fraction of the applied current flows through the substrate). The generating line (a) corresponds to a low current and/or a low α . The full recovery critical current is defined by such a line which just touches but does not cross the heat transfer characteristic. Because of the rather flat heat transfer characteristic in the 7 to 11 K range, generally bracketing the critical temperature of high field superconductors in ambient magnetic fields, this full recovery critical current may be calculated from equation 2.6.1 with $q \approx 0.18 \text{ W/cm}^2$ and $\alpha = 1$.

The generating line (b) corresponds to a higher current and/or α . The major contribution of Maddock, James, and Norris was to show that recovery from localized heat generation will occur when the current is less than that for which the cross-hatched areas are equal, provided that portions of the wire on either side of the heated length remain fully superconducting. (For quantitative calculations, because the thermal conductivity of metals is proportional to temperature in the helium region, the abscissa should be the square of the temperature difference between the wire and the helium).

From integration over the pool boiling characteristic, including the relatively uncertain region between the peak nucleate boiling and minimum film boiling points, their calculations show that this cold-end-recovery critical current can be obtained from equation 2.6.1 with $\alpha \approx 2$ (and $q = 0.18 \text{ W/cm}^2$, for the reasons cited above), depending somewhat on the superconductor transition temperature. This is equivalent to designing for a heat flux of 2×0.18 or about 0.3 to 0.4 W/cm^2 at the transition temperature, as has become more or less standard practice for cryogenic stabilization.

Curve (c) corresponds to high current and/or a high value of the stability parameter α . The curvature of the line at high ΔT 's is due to temperature dependent resistivity of the substrate, and can lead to thermal runaway if the line fails to intersect the film boiling heat transfer line. They estimate that this limit is reached when the heat flux at the transition temperature is of the order of 0.6 W/cm^2 for copper of nominal purity, and 0.4 W/cm^2 for aluminum having a resistivity ratio of 1000. This provides a stringent limitation of magnet stability with pool boiling.

The crossing of the nucleate boiling curve by curve (c) at small ΔT 's illustrates a further problem with high currents or high α 's. Recovery from a thermal transient can be to a stable nucleate boiling state, depending on the relative sizes of the two small areas enclosed between curve (c) and the nucleate boiling curve. This possibility is particularly sensitive to the finite thermal conductivity of the substrate.

2.6.4. Forced Flow Cooling of Superconductors

We consider a locally heated section of a flow passage, as would exist following a flux jump. The analysis of the recovery of superconductivity is quite simple if we neglect the temperature rise in the flowing helium. This is done in the following section, with close comparison to the pool boiling analysis of the previous section. The effect of heating the flowing helium is discussed in the subsequent section, where we see that in many cases it may not be an important factor with respect to recovery from a flux jump.

Data for forced convection heat transfer to supercritical He have recently been reported by Giarratano, Arp, and Smith [1971]. At a helium temperature of 4.2 K, for pressures from 3 to 10 atm, their data fit the equation

$$q(W/cm^2) \approx \frac{0.048}{D(cm)} \left(\frac{Re}{10^5} \right)^{0.8} \left(\frac{4.2}{T_W} \right)^{0.72} (T_W - 4.2) \quad (2.6.2)$$

within a few percent. Arbitrarily setting the channel diameter D to 0.2 cm, this correlation is plotted in figure 2.6.2 with the Reynolds number as a parameter. Also shown in this figure is the pool boiling heat transfer characteristic (Brentari, Giarratano, and Smith, 1965), combining the nucleate boiling curve, the relatively unstable transition region (dotted), and the film boiling region.

Several facts may be noted. First, within the framework of the Maddock, James and Norris equal-area analysis, recovery from a thermal overload can be predicted with greater certainty for forced flow cooling than for pool boiling, since the latter depends upon integrals over the rather uncertain dotted portion of the curve. Secondly,

inasmuch as recovery involves temperature differences of several degrees (perhaps 3 K for NbTi and 7 K for Nb₃Sn in high fields), very high thermal fluxes may be available for recovery using forced flow, as compared to the pool boiling case. Finally, the pool boiling "catastrophic" limit of 0.4 to 0.6 W/cm², above which a warm section of winding will heat up until the current falls off, can be somewhat higher with forced supercritical flow. It is useful to put these in more quantitative terms.

Figure 2.6.3 shows the construction for calculating the cold end recovery current for forced supercritical flow. The cold end recovery flux is that for which the two cross-hatched areas are equal. The ratio of this flux, q_e , to the full recovery flux, q_r , depends on the values of the superconductor critical temperature in the applied field at zero current, T_c , and the ratio of actual current to short-sample critical current. Graphical integration, not shown here, leads to the conclusion that the ratio q_e/q_r is in fact only weakly dependent on these parameters, and is generally less than 1.2 when the magnet current is more than half of the short sample current. Further, the finite thermal conductivity of the substrate tends to bow the load line to the left, as illustrated in curve c of figure 2.6.1, reducing the ratio q_e/q_r towards its limiting value of 1.0. We conclude that the cold end recovery current will be insignificantly greater than the full recovery current, for which $\alpha = 1$. If this latter is the magnet design current, the coil will be fully stable in the sense that the heat transfer from any transiently normal region is sufficient to restore superconductivity, without recourse to heat transfer along the conductor to a cold end. If the magnet current exceeds this full recovery current, then for practical purposes any small normal region

will propagate to drive the whole coil normal at a temperature above T_c , and recovery will take place only when the current is dropped below the critical current defined by $\alpha = 1$. This contrasts poorly at first sight with the pool boiling case where stability can be obtained with $\alpha > 1$ due to the cold end recovery effect and the large nucleate boiling peak. However, this restriction on α for forced flow will generally be more than offset by the much higher values of q'_m which can be obtained. As a consequence it will generally be possible to obtain stable magnet operation for smaller values of the product $A\phi$ for forced flow cooling than for pool boiling, leading to easier design or higher current densities.

2.6.5 Thermal Runaway Limit

In designs requiring a high current density, or with limited heat transfer, it may be possible for the magnet design current to exceed the full recovery current if well-stabilized wire is used so that a fully normal region is not likely to occur. Generally this requires a twisted multifilament NbTi wire with appropriate copper or aluminum cladding, though of course the cladding tends to reduce the overall current density. In this situation the basic design approach must be to avoid a catastrophic temperature rise and burnout of the coil in the off-chance of a transiently normal region where, due to coil inductance, it is not possible to reduce the current quickly to a low value. To accomplish this, one must consider the temperature-dependent resistivity of the cladding material which carries essentially the full current once the superconductor is normal. If the resistivity is independent of temperature, then a small increase in temperature will increase the heat transfer rate but not the joule heating, so that an equilibrium temperature will be reached where these two rates

are equal, hopefully not much higher than 20 or 30 K. However, if the resistivity increases rapidly with temperature, then a further small temperature rise may increase the heat transfer less than it does the joule heating, with the result that the temperature will rise until limited by some less controlled factor, such as possible burnout. Clearly, such an equilibrium temperature can be stable only if

$$\frac{1}{\rho_r} \frac{d\rho_r}{dT_W} < \frac{1}{q} \frac{dq}{dT_B}$$

or

$$\frac{d(\log \rho_r)}{d(\log T_W)} < \frac{d(\log q)}{d(\log T_W)} \quad (2.6.3)$$

This last inequality provides a handy means for graphical determination of the maximum heat flux at which a stable normal-state temperature is possible. Figure 2.6.4 is a plot of a quantity proportional to heat flux, given by equation 2.6.2 as a function of conductor temperature, assuming the fluid temperature is 4.2 K. Figure 2.6.5 is the film boiling curve of the Breen and Westwater correlation as given by Brentari, Giarratano, and Smith [1965]. Figure 2.6.6 is a plot of the resistivity of three different purities of copper as a function of temperature, calculated from Hall [1968] for zero applied magnetic field. Figure 2.6.7 is an analogous plot for aluminum, using the data of Corruccini [1964] and Fickett [1971], for zero magnetic field; the magnetoresistance of high purity aluminum in a field of more than a tesla is approximately saturated at three times the zero field value, so that its effect can be approximated by using the curve corresponding to a three times less pure sample. The parameter which separates the curves of various purity is the residual resistance

ratio (rrr), defined as the resistance at 273 K divided by the resistance at 4 K. These are all drawn on the same logarithmic graph paper, so that the temperature at which the inequality of equation 2.6.3 ceases to hold can be found simply by sliding a resistivity curve in the y-direction over a heat transfer curve (on a light table) so as to locate a common tangent. Results are shown in table 2.6.1.

In this table are listed two values of q_{\max} , or a quantity proportional to q_{\max} , for each metal and cooling mode. The unprimed q is that determined by the graphical method described above, and is the actual heat flux when the coil is driven to the point that the inequality of equation 2.6.3 is no longer correct. The primed q is this latter quantity multiplied by the factor $\rho(4\text{ K})/\rho(T_m)$, and is more convenient for design purposes since it is the normal state heat flux which is easily calculated using just the residual resistance ratio of the cladding material without adding the effect of the temperature dependent resistivity. These results are obtained from the zero-field resistivity curves. In practice, magnetoresistance will tend to increase T_{\max} , but only by a few degrees, which is within the uncertainty of the broad engineering design factors considered here.

Maddock, James, and Norris have done an analysis of this type for film boiling, though they give no details. They give q'_{\max} equal to 0.59 W/cm^2 for 200-ratio copper in a 5 T field, and 0.36 W/cm^2 for 1000-ratio aluminum in the same field; these numbers are lower than the corresponding results from table 2.6.1, presumably because of a slight difference in the assumed film boiling curve. The forced flow calculations are less subject to uncertainties of this type, since they are much less dependent on properties of the heat transfer surface.

Table 2.6.1
Thermal Runaway Cooling Limits for Conductors in Helium

Metal, rrr	Film Boiling			Forced Flow		
	T_m [K]	q_m [W/cm ²]	q'_m [W/cm ²]	T_m [K]	$q_m D \left(\frac{Re}{10} \right)^{0.8}$ [W/cm]	$q'_m D \left(\frac{Re}{10} \right)^{0.8}$ [W/cm]
Cu, 30	42	2.0	1.2	28	0.28	0.27
Cu, 100	29	1.15	0.9	22	0.26	0.25
Cu, 300	24	0.90	0.64	17	0.23	0.21
Al, 300	25	0.95	0.77	20	0.25	0.23
Al, 1 000	22	0.80	0.57	18	0.23	0.20
Al, 3 000	18	0.62	0.39	14	0.20	0.16
Al, 10 000	12.5	0.40	0.24	10.5	0.16	0.11
Al, 30 000	9	0.27	0.17	9	0.13	0.08

Several features can be seen from inspection of table 2.6.1. First, the limiting thermal flux, above which thermal runaway occurs, is noticeably less dependent on material and purity with forced-flow cooling than with pool boiling. For all but the purest aluminum, the forced-flow cooling limit is within about 20% of the value determined by

$$q'_m D \left(\frac{Re}{10^5} \right)^{0.8} \approx 0.2 \text{ W/cm.} \quad (2.6.4)$$

For our nominal 0.2 cm channel, with $Re = 10^5$, this gives $q'_m \approx 1 \text{ W/cm}^2$, which is about twice as high as the corresponding pool boiling situation. Further, an additional factor of 6 or so can be gained simply by increasing the flow rate. In practice, it is the energizing of the coil in the high field limit which is the sensitive operational stage in using a coil whose design current exceeds the critical recovery current at the design cooling rate. During this operation a boost in the flow rate may be all that is necessary to give the required stability. On the other hand, at these high heat fluxes, heating of the helium must be considered if any extended region along the flow channel were to reach the temperatures indicated in table 2.6.1. This is discussed in more detail in section 2.6.6.

It is seen that q_{\max} or q'_{\max} decreases with increasing sample purity. However, using table 2.6.1 as a basis for the selection of an optimum cladding material, the figure of merit which most reasonably measures the advantage of a given cross-sectional area of cladding material applied to the superconductor is $q'_{\max}/\rho(4 \text{ K})$. This factor indeed increases with increasing purity. For a given residual resistance ratio, copper holds a slight edge over aluminum, but aluminum is commercially available in much higher purity (higher ratio).

2.6.6 Warming of the Helium in the Flow Channel

The discussion up to this point has been concerned with the restoration of superconductivity within a length of conductor which is heated locally to its superconducting transition temperature, nominally above 7 K. The stability analysis which was used implicitly assumes that this heated region continues to be cooled with helium at a fixed temperature of about 4.2 K, whereas with a single-phase forced flow system the helium temperature will rise as it traverses the heated section.

This brings up two rather basic questions: to what extent will this temperature rise invalidate the stability analysis used above? What effect does the warmed helium have upon possible subsequent lengths of flow passage (superconductor) which were otherwise unaffected by the flux jump? In this section we consider the first question, and show that in fact the stability analysis is insensitive to small fluid temperature changes.

As explained earlier, the parameter α is essentially the ratio of heat generation rate to heat transfer rate with the superconductor at its transition temperature. The heat transfer rate for forced flow of single phase helium has been given by Giarratano, et al., [1971] as

$$q = 0.026 \frac{\lambda}{D} (\text{Pr})^{0.4} (\text{Re})^{0.8} \left(\frac{T_B}{T_W} \right)^{0.72} (T_W - T_B). \quad (2.6.5)$$

Equation 2.6.2 of this paper is in fact just this equation evaluated for a fixed fluid temperature, T_B , of 4.2 K and averaged over pressures from 3 to 10 atmospheres (0.3 to 1.0 MN/m²). In this section, on the

other hand, we assume one or more fixed wall temperatures corresponding to reasonable superconducting transition temperatures in an ambient magnetic field, and investigate the dependence of the heat flux q upon the fluid temperature. Following the example of Maddock, James, and Norris, we assume (a) a T_c of 7.2 K appropriate for a typical NbTi wire in a magnetic field of 4 to 5 T, and (b) a T_c of 11.2 K, appropriate for Nb₃Sn wire in a field of about 10 T.

Numerical evaluation of equation 2.6.5 leads to figure 2.6.8 for the heat flux q as a function of the fluid temperature T_b for fixed wall temperatures of 7.2 K and 11.2 K. The sharp peaks in the curves occur at the transposed critical or pseudo-critical temperature for the given pressure, and generally should be avoided for heat transfer work because of associated thermal instabilities. The important fact, however, is that the rate of heat removal from the superconductor in the normal state, q , is more or less independent of fluid temperature in the range from 4 to 5 or 6 K, and in fact tends to increase with temperature for superconductors of high transition temperature due to the non-linear heat transfer correlation. This means that the stability parameter is correspondingly independent of, or even decreased by, rising helium temperature, and hence that the stability predictions of the previous section are quite general.

We must point out, though, that this conclusion applied to the initial stage of recovery from a flux jump, i.e., it determines whether or not recovery begins, but the detailed temperature-time characteristic will differ from the pool boiling case because of the helium temperature rise.

It is instructive to calculate the helium temperature rise ΔT which would occur due to generation of heat in a length l of conductor at its transition temperature. For this approximate calculation, it is reasonable to neglect heat generation within or axial heat flow into the transition region between superconducting and normal resistance at either end of the length l . Simple energy balance gives the equation

$$\pi q D \frac{l}{v} = \frac{\pi}{4} D^2 \rho C_p \Delta T$$

where v is the average flow velocity, i. e., $v = \eta \text{ Re}/(\rho D)$. Combining terms, we find that

$$\Delta T = 40. \frac{q l}{C_p (10^{-5} \text{ Re}) (10^6 \eta)} .$$

The thermal flux q into the helium can be estimated from the analysis of section 2.6.2 where it was shown that in order to avoid thermal runaway, the coil design and operation must be limited by equation 2.6.4. Using this result and $10^6 \eta \approx 40 \mu\text{g}/\text{cm}\cdot\text{s}$ and $C_p \approx 4 \text{ J/g}\cdot\text{K}$ in the range of 3 to 10 atmospheres at 4 K, the temperature rise through a normal section of length l is approximately

$$\Delta T \leq 0.05 \frac{l}{(10^{-5} \text{ Re})^{1.8} D} .$$

Flux jumps or other instabilities in superconducting windings are commonly associated with some sort of localized imperfections in the conductor, or with poorly made electrical joints; in either case, the heated region will be localized to within a few centimeters of the conductor, and Reynolds numbers of 10^5 or above are sufficient to keep the ΔT to 1 K or less at any one such imperfection. We conclude that

warming of the helium due to the usual localized magnet instabilities will not seriously perturb the operational stability obtainable with forced-flow cooling.

2.6.7 Boundary Layer Development

It is important to note that transient heat transfer, as occurs in the recovery of superconductivity following a localized flux jump, may exceed the rates predicted from equation 2.6.5 by a significant factor. As can be found from the original work of Giarratano, et al., [1971], equation 2.6.5 predicts heat transfer rates with reasonable accuracy some 20 diameters or so downstream from the beginning of the heated section, where the thermal boundary layer within the fluid stream is essentially fully developed. Near the beginning of the heated section, thermal gradients in the fluid near the wall are very high, as is the heat transfer rate. Several authors have studied models in which there is either a step increase in wall temperature at one point along the flow stream or the stepwise appearance of a constant heat flux along the flow stream, with no axial heat flow through the heated wall material. Classic papers on this topic are those of Deissler [1955], Sleicher and Tribus [1956], and Sparrow, Hallman, and Seigel [1957]. Deissler uses a boundary layer analytical technique of less generality than the others. Sleicher and Tribus investigate the constant surface temperature case, and Sparrow, et al., investigate the constant heat flux case. In general, the analyses show that the effective heat transfer rate can be from 20% to factors of 2 higher in the first one or two channel diameters than far downstream where a full boundary layer has developed; actually they predict an ever increasing heat transfer rate as one approaches the point of discontinuous change in wall temperature or heat flux from the downstream side, and

additional analysis must be used to estimate saturation of the enhancement factors. This result is in qualitative accord an effect which can be deduced from the empirical correlation given by Taylor [1968] for forced flow heat transfer with supercritical hydrogen:

$$Nu = 0.023 Re^{-.8} Pr^{0.4} (T_W/T_B)^{-0.57 + 1.59/(L/D)}.$$

The factor $(T_W/T_B)^{-0.57}$ (cf. equation 2.6.5 for helium where the exponent is -0.72) causes a nonlinear reduction in the heat transfer rate over that which would be obtained with a constant heat transfer coefficient, obtained for large values of L/D . Though this correlation was never tested or intended to be used in the limit of small values of L/D , it is interesting to note that it does predict a nonlinear enhancement of heat transfer rate for L/D values less than about 2.8, i. e., within 2.8 diameters of the beginning of the heated section. This type of analysis has never been done allowing for axial thermal flux along the wall material. This axial heat flux will cause saturation of the enhancement curves which otherwise diverge on approaching the singular point. One can make a plausible argument that this saturation will occur at an L/D value over which the axial temperature gradient between heated and unheated wall sections produces an axial thermal flux comparable with the radial heat transfer to the fluid. This in effect suggests a small enhancement factor for wall material of high cross-section or high conductivity, and vice versa.

The timewise sudden appearance of a heated wall section, e. g., from a localized transient instability in the superconductor, puts cold fluid in direct contact with the wall for a short time interval, just as occurs in the analyses of Deissler and others close to the point of discontinuous temperature change. The correspondingly enhanced

heat transfer will decrease to its steady state value in a time determined by: (1) the time required to establish an axial thermal gradient in the wall material, and (2) the time required to build up a thermal boundary layer as a function of distance along this axial thermal gradient. Inasmuch as the position of the axial thermal gradient along the wall may in itself tend to move depending on the ratio of heat generation to heat transfer, advanced analysis of the problem would entail a major research effort; portions of it might make an interesting thesis study.

This enhanced heat transfer, though its magnitude is uncertain and temporary, can only improve the stability of force-cooled magnets over that given by the analysis of the previous sections.

2.6.8 Exact Solution to Forced-Flow Cooling of a Normal Region

We consider that at time $t = 0$ the temperature profile along the conductor is perturbed as would occur following a localized flux jump. The temperature profile in the helium is not perturbed at this instant. Neglecting temperature gradients perpendicular to the conductor and flow axis, the complete time and position dependent equations governing these temperature profiles are

$$\frac{d}{dz} (\lambda A \frac{dT_W}{dz}) = h\theta (T_W - T_B) - Q + \rho C_p A \frac{dT_W}{dt} \quad (2.6.6)$$

and

$$h\theta (T_W - T_B) = G\alpha (C_p - v^2 \beta) \frac{dT_B}{dz} + G\alpha (-\psi C_p - v^2 K) \frac{dP}{dz} \quad (2.6.7)$$

where

$$\frac{dP}{dz} \approx \frac{G^2 f \theta}{2 \rho A} \quad (2.6.8)$$

The coupling between these two differential equations is provided by the heat transfer coefficient h . In the simplest analysis it is just dependent on the helium temperature, T_B , but a more exact expression, equation 2.6.5, makes it a nonlinear function of both T_B and T_W . From consideration of the formation of a thermal boundary layer next to the surface, h is probably also dependent on past history, or on dT_B/dt and dT_W/dt , but we have little idea of what form this dependence should take. It is consistent with the other approximations to assume just that h is a constant, provided that the fluid does not warm more than a few percent in the region of interest.

For the heat generation term, Q , it is common to assume that the short-sample critical current varies linearly with temperature between the desired operating temperature T_O and the superconducting transition temperature T_C (Stekly, Thome, and Strauss, 1969; Maddock, James, and Norris, 1969). Then if the operating current divided by the short sample critical current is the fraction X , Q is given by

$$\begin{aligned}
 Q &= 0 & \text{for} & & T < T_C - X(T_C - T_O) \\
 &= \rho_r \frac{A}{\phi} J_C^2(T_O) \left(X - \frac{T_C - T}{T_C - T_O} \right)^2 & & & T_C - X(T_C - T_O) \leq T \leq T_C \\
 &= \rho_r \frac{A}{\phi} J_C^2(T_O) X^2 & & & T_C \leq T.
 \end{aligned}$$

Two rather similar analyses of these equations have been made (Greene and Saibel, 1969; and Bald, 1971). Both of these make an important assumption: that the solution to these equations corresponds to movement of the normally conducting zone along the conductor generally in the direction of helium flow, shrinking or expanding in length as it moves. The shape of both the leading and trailing temperature profiles (in the conductor) are assumed constant. The velocities

of these temperature profiles would generally both be different than the helium flow velocity. Both authors assume a discontinuous appearance or disappearance of I^2R heating at a temperature T_c rather than the linear approximation above. This could have a measurable influence on the shape of the profile. Likewise, both neglect all but the first term on the right-hand side of equation 2.6.7. Greene and Saibel conclude that there is a critical length of normal region below which the region shrinks as it moves, and vice versa. The critical length depends upon the velocity of propagation, and appears to peak at roughly 1.5 meters for a profile velocity of about 5 meters per second, for one representative conductor. However, the profile velocity appears implicitly in the calculation, and it is not at all obvious from this work how one would calculate it. Bald concludes that "...the velocity of propagation is unknown for any given design concept." Neither paper explores the validity of the initial assumption that the normal zone moves along the conductor.

Maddock, James, and Norris [1969] have essentially set up these equations for the pool boiling case and explored the character of the solutions. Using a change of variable $\lambda dT/dZ = S$, they show that the temperature profile, once developed, will propagate without change of shape only if the heat generation line crosses the heat transfer line at a point of stable equilibrium (the intersection of curve (b) with the film boiling line in figure 2.6.1). Further, they give an iterative analytical scheme for calculating this velocity. However, we have concluded earlier that for forced flow cooling the heat flux at which this "cold end recovery" process will be obtained is only 10 to 20% above that for which full recovery is obtained; i.e., without depending on axial heat transfer. Because of the small margin

of difference between these two recovery modes, coil design should generally be based on the lower full recovery heat transfer mode. In this latter mode, the height of the temperature profile decreases with time, and the axial movement of the temperature profile, if it occurs at all, would not be at a uniform velocity since there is no point of thermal equilibrium at the center of the heated section.

We have not been able to obtain detailed solutions to those general equations for the full recovery mode. It is possible to determine, however, that near the beginning of the recovery, where the heat transfer to the helium is much larger than the axial heat flux in the copper, movement of the normal zone along the conductor will be negligible compared to the general decrease in the zone temperature. This means that the rather simple stability analyses of the previous section would be valid. It is very possible, though, that the location of the normal zone will have become smeared out and displaced downstream by the time the recovery process is nearly complete. This certainly will happen when the helium temperature rises above the transition temperature at the operating current, i. e., above $T_c - X(T_c - T_o)$. But by this time, the recovery will be far along, and though the details may be obscure, there is no means by which the recovery could fail to move to completion.

2.6.9 Nomenclature

Symbol	Meaning
A	x-sectional area of stabilizing metal (e.g., copper) in the superconductor
a	x-sectional area of flow channel
C_p	heat capacity at constant pressure
D	channel diameter
f	friction factor for fluid flow
G	mass flow rate/unit area
h	heat transfer coefficient
I_c	critical current
J_c	critical current density, I_c/A
K	$(1/\rho) (\partial \rho / \partial P)_T$
P	pressure
θ	wetted perimeter of flow channel
Pr	Prandtl number
Q	heat generation
q	thermal flux
Re	Reynolds number
T_B	helium temperature, averaged over flow cross-section where appropriate
T_c	transition temperature of superconductor in the limit of zero current. A function of the ambient magnetic field
T_o	operating temperature
T_w	wall or surface temperature of the superconductor
v	velocity (of flow)
X	ratio of operating current to short circuit current
Z	distance along the cooling channel, in direction of flow

Symbol	Meaning
α	stability parameter
β	$(1/\rho)(\partial\rho/\partial T)_P$
λ	thermal conductivity
ρ_d or ρ	density
ρ_r	resistivity
ψ	$(\partial P/\partial T)_H$; the Joule-Thomson coefficient

2.6.10 References

- Bald, W. B., "Supercritical helium cooling of hollow superconductors," BNL Report No. 15805, (1970).
- Brentari, E. G., Giarratano, P. J., and Smith, R. V., "Boiling heat Transfer for oxygen, nitrogen, hydrogen, and helium," NBS Tech.Note 317, (1965).
- Corruccini, R. J., "The electrical properties of aluminum for cryogenic electromagnets," NBS Tech.Note 218, (1964).
- Deissler, R. G., "Turbulent heat transfer and friction in the entrance regions of smooth passages," Transactions of the ASME, 1221, (1955).
- Fickett, F. R., "A review of resistive mechanisms in aluminum," Cryogenics 11, 349, (1971).
- Giarratano, P. J., Arp, V., Smith, R. V., "Forced convection heat transfer to supercritical helium," Cryogenics 11, 385, (1971).
- Greene, W. J., and Saibel, E., "Stability of internally cooled superconductors," Advances in Cryogenic Engineering 14, 138, (1968).
- Hall, L. A., "Survey of electrical resistivity measurements on 16 pure metals in the temperature range from 0 to 273 K," NBS Tech. Note 365, (1968).
- Kremlev, M. G., Zenkevitch, V. B., Altov, V. A., "Concerning the influence of nucleate to film boiling transition on the stability of composite conductors," Cryogenics 8, 173, (1968).
- Maddock, B. J., James, G. B., and Norris, W. T., "Superconductive composites: Heat transfer and steady state stabilization," Cryogenics 9, 261, (1969).

- Mylhall, B. E., and Hutton, W., "Stabilizing superconductors - modern methods and present problems," (Report of Meeting of Low Temperature Group of the Institute of Physics), Cryogenics 11, 319, (1971).
- Sleicher, C. A., and Tribus, M., Heat Transfer Fluid Mech. Inst., Stanford, California, p. 59, (1956); reported and summarized in "Convective heat and mass transfer," W. M. Kays, (McGraw-Hill, 1966).
- Sparrow, E. M., Hallman, T. M., and Seigel, R., Applied Science Research, Ser A, 7, pp. 37-52, (1957); reported and summarized in "Convective heat and mass transfer," W. M. Kays (McGraw-Hill, 1966).
- Stekly, Z. J. J., Thome, R., and Strauss, B., "Principles of stability in cooled superconducting magnets," Proceedings of the 1968 Summer Study on Superconducting Devices and Accelerators, p. 748, (1969).
- Stekly, Z. J. J. and Zar, J. L., "Stable superconducting coils," IEEE Trans. Nuclear Science, NS-12, 367, (1965).
- Taylor, M. F., "Correlation of local heat-transfer coefficients for single-phase turbulent flow of hydrogen in tubes with temperature ratios to 23," NASA TN D-4332, (1968).

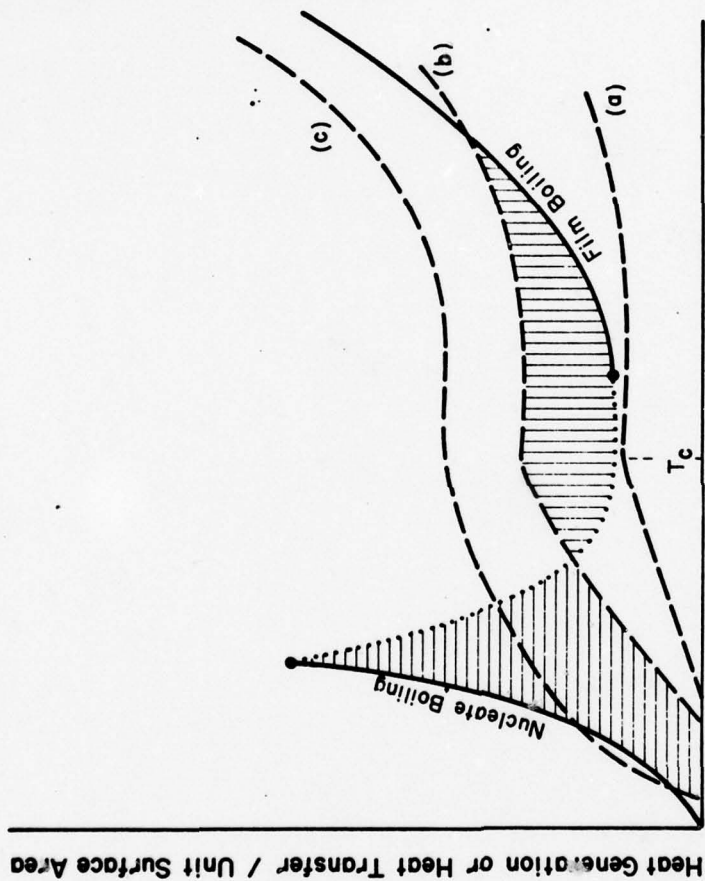


Figure 2.6.1 Representation of magnet stability analysis by pool boiling as given by Maddock, James, and Norris (1969). The solid and dotted lines give the heat transfer rate, while the dashed lines (a, b, c) give the heat generation rate as a function of temperature of the superconductor. The curves (a, b, c) are for successively higher values of current and/or stability parameter.

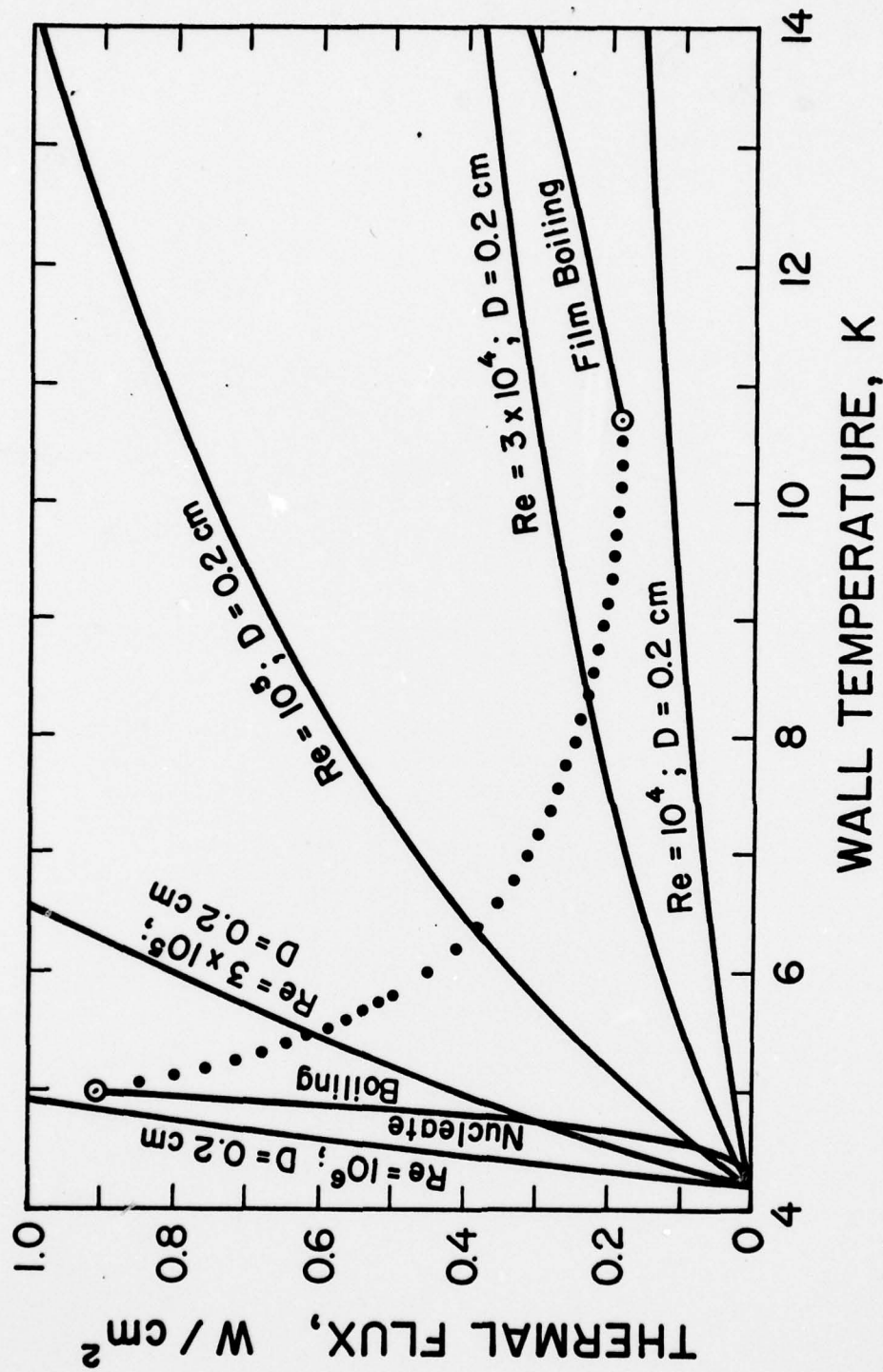


Figure 2.6.2 Comparison of pool boiling and forced convection heat transfer to helium at 4.2 K. The forced convection curves are for supercritical helium at pressures within the range 0.3 to 1.0 MN/m² (3 to 10 atmospheres), arbitrarily assuming a channel diameter of 0.2 cm.

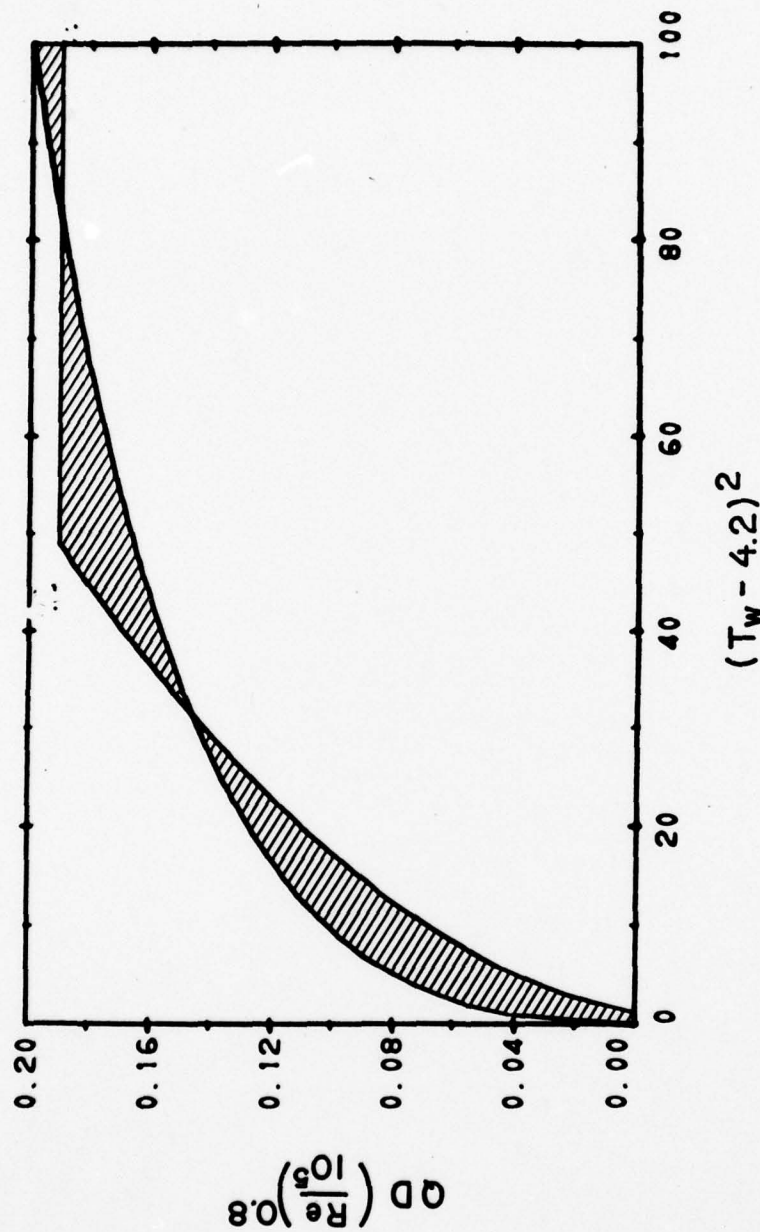


Figure 2.6.3 Evaluation of the Cold End Recovery Critical Current for forced supercritical flow. The heat transfer characteristic is taken from Giarratano, Arp, and Smith (1971). In this plot the generating line is drawn assuming a current equal to 86% of the short sample critical current, and a transition temperature (in ambient magnetic field) of 11.2 K. Equality of the crosshatched areas predicts stable magnet performance for $\alpha \leq 1.2$ in this case.

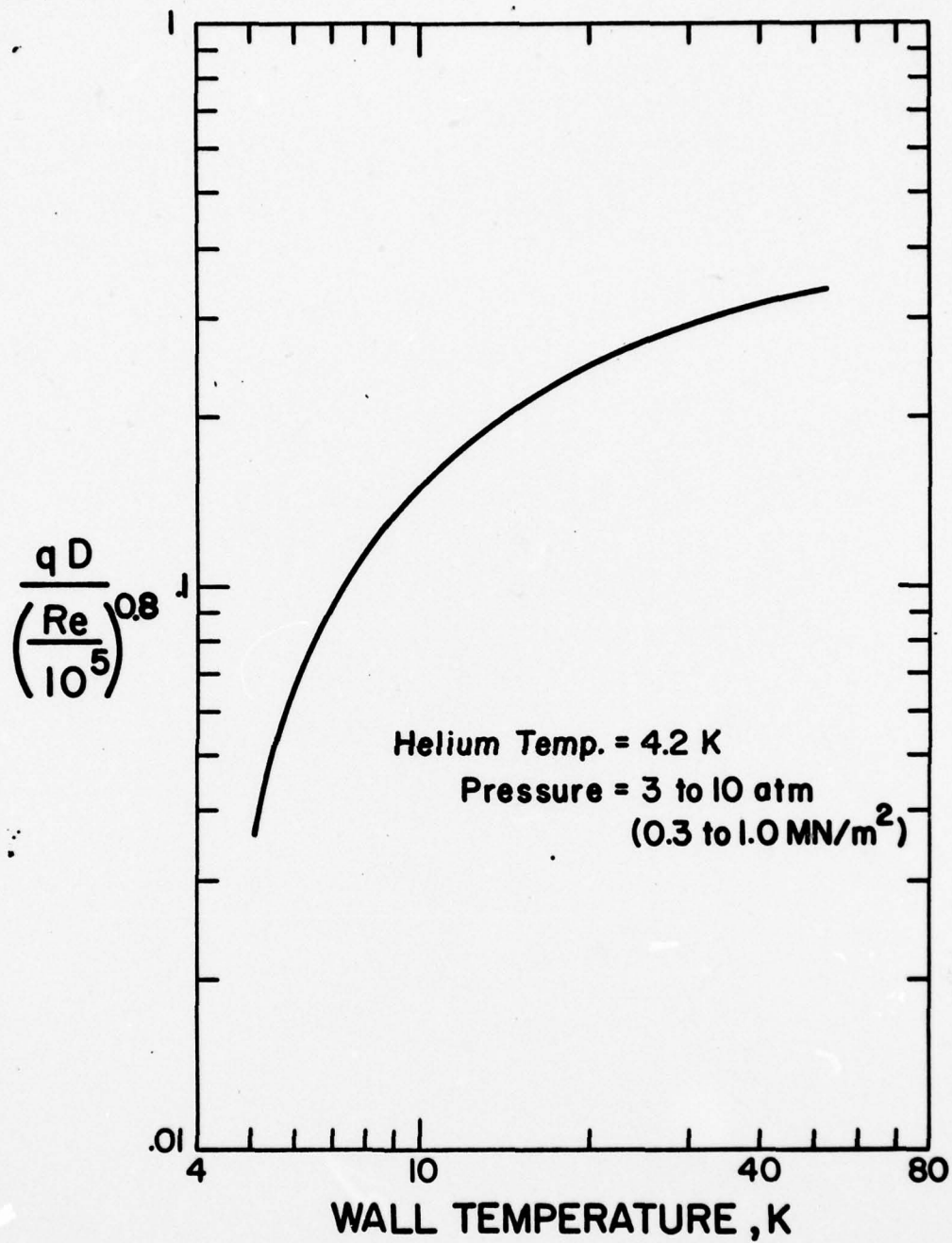


Figure 2.6.4 Film boiling heat transfer characteristic. Figures 2.6.4 through 2.6.7 are all drawn to the same logarithmic scale.

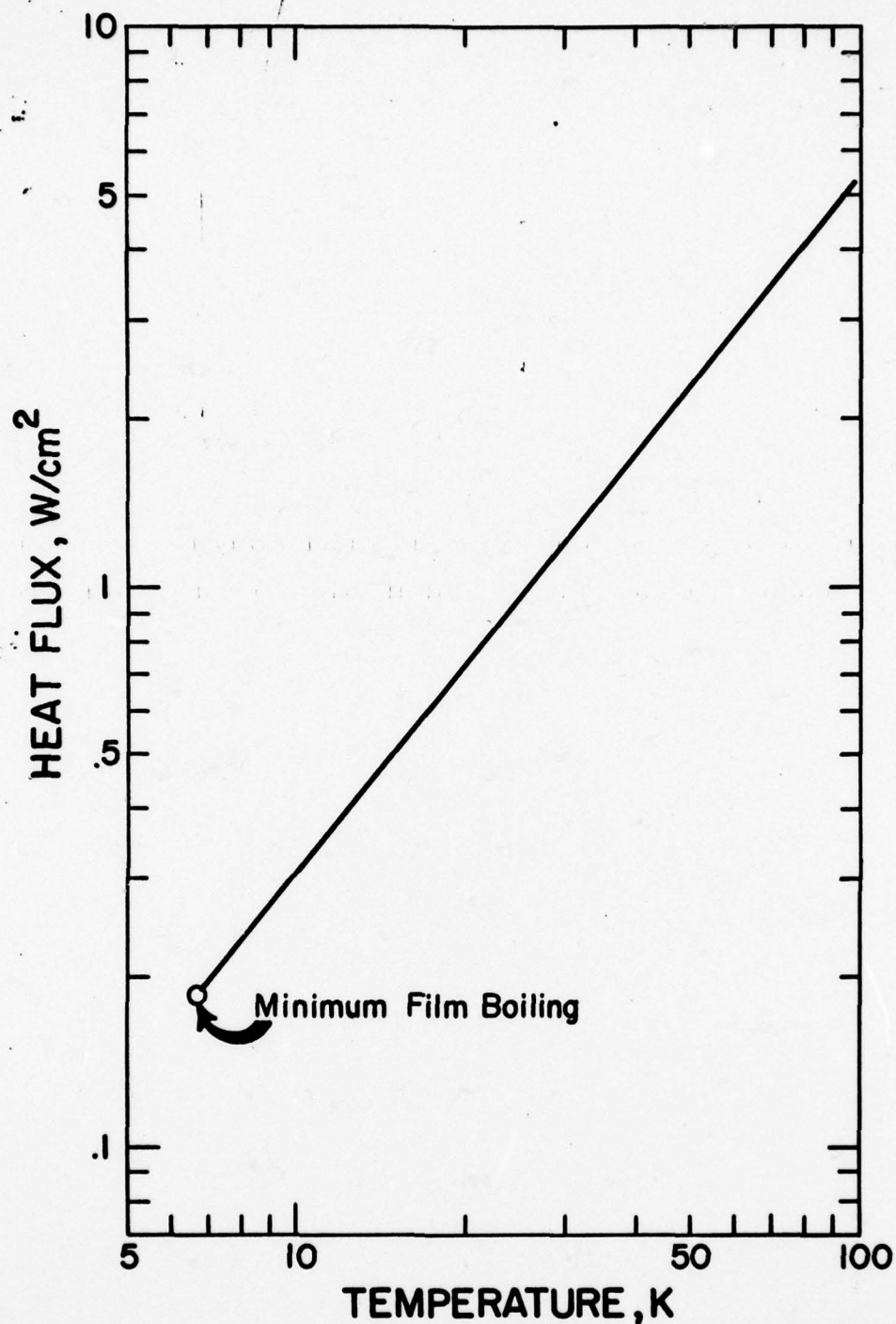


Figure 2.6.5 Forced convection heat transfer characteristic for helium at 4.2 K and pressures within the range 0.3 to 1.0 MN/m² (3 to 10 atmospheres). Figures 2.6.4 through 2.6.7 are all drawn to the same logarithmic scale.

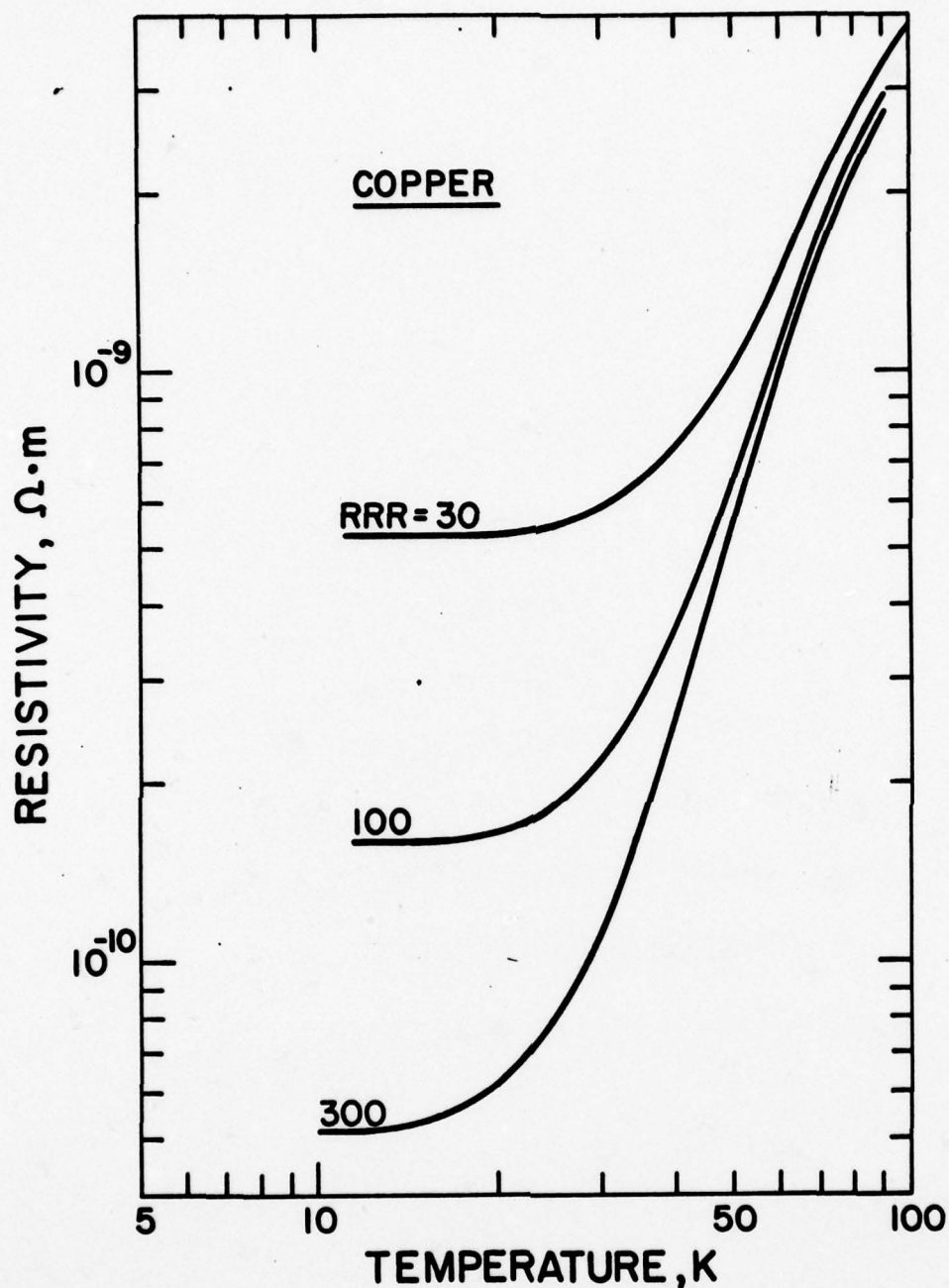


Figure 2.6.6 The resistivity of three different purities of copper as a function of temperature. RRR is the residual resistivity ratio, equal to the resistivity at 273 K divided by the resistivity at 4K. Figures 2.6.4 through 2.6.7 are all drawn to the same logarithmic scale.

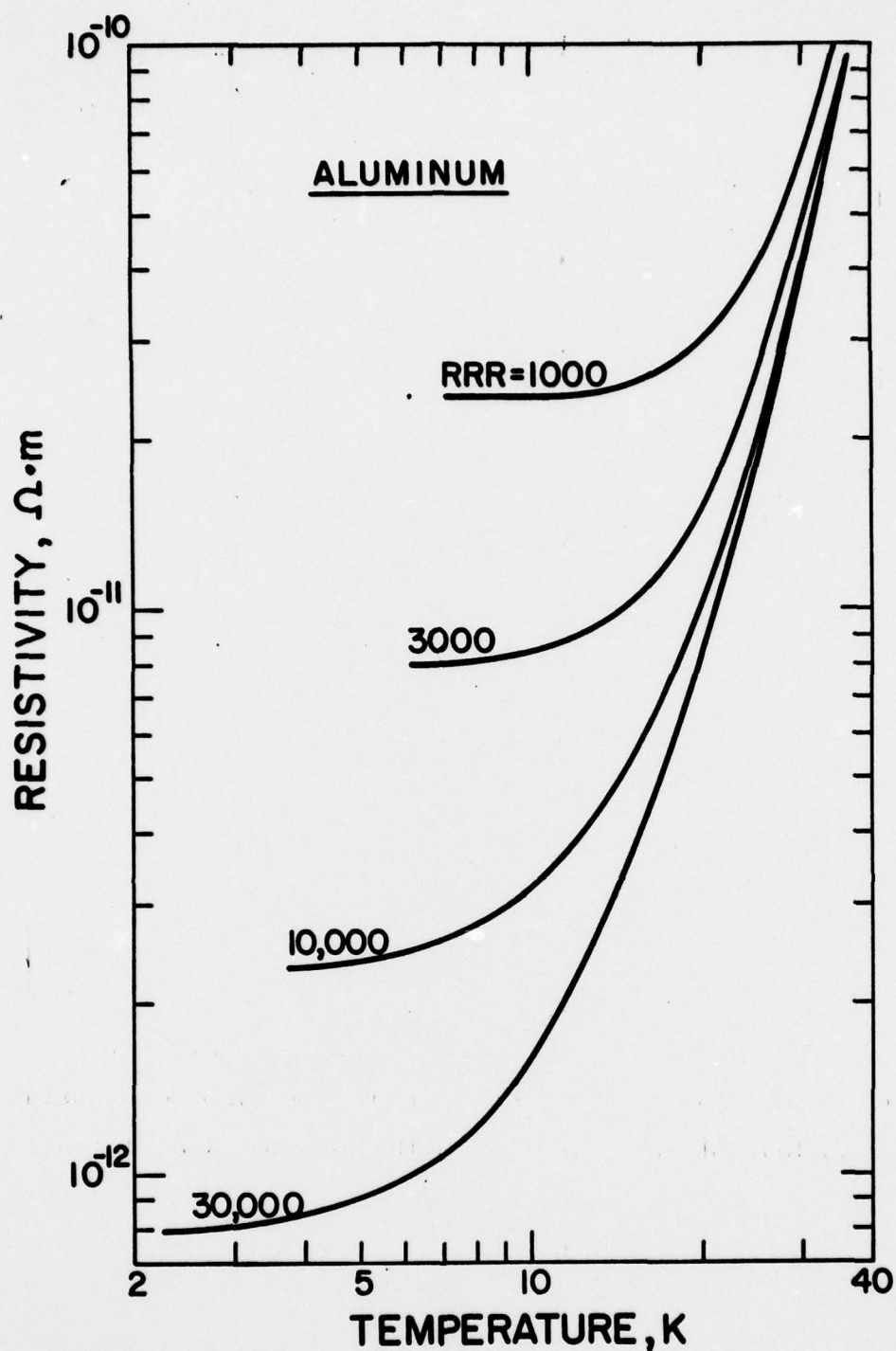


Figure 2.6.7 The resistivity of five different purities of aluminum as a function of temperature. RRR is the residual resistivity ratio, equal to the resistivity at 273 K divided by the resistivity at 4K. Figures 2.6.4 through 2.6.7 are all drawn to the same logarithmic scale.

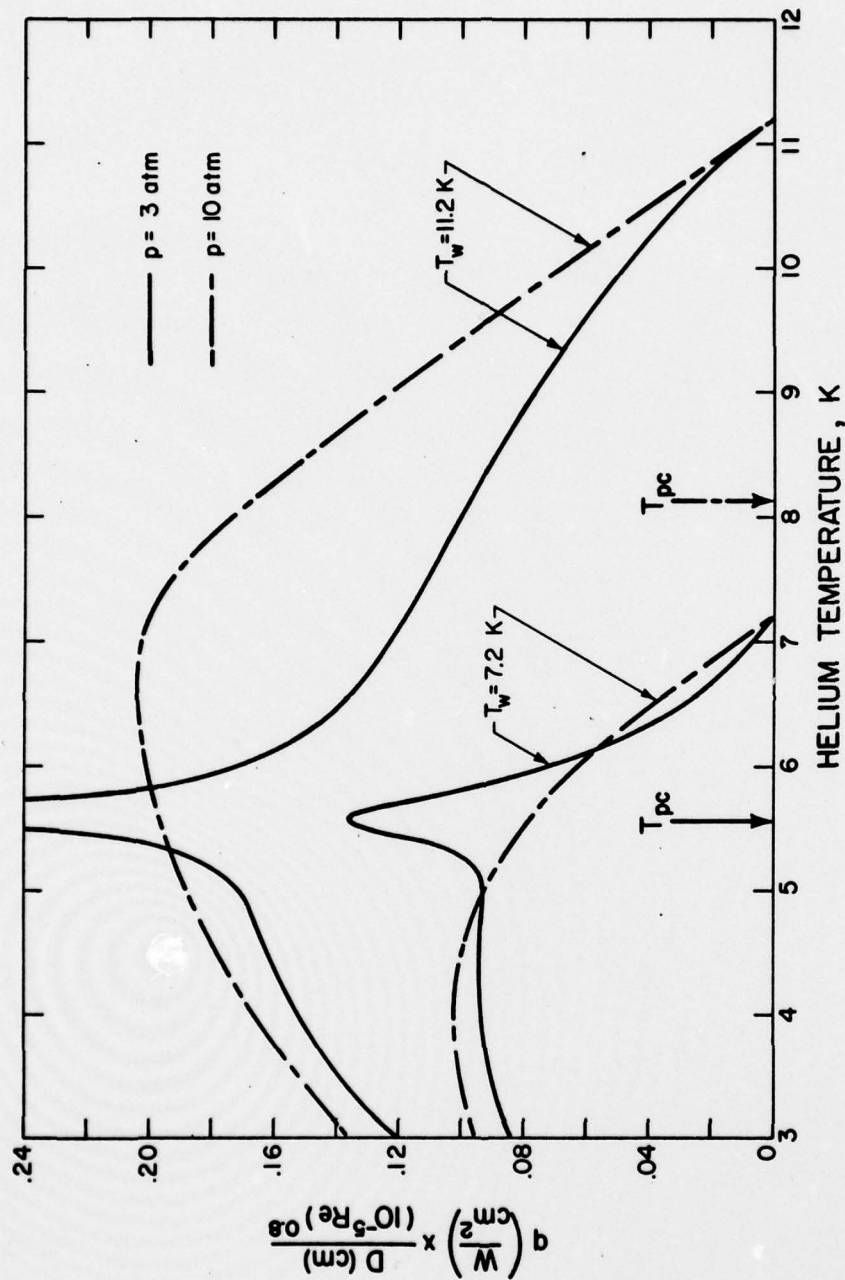


Figure 2.6.8 Forced convection heat transfer as a function of helium temperature for two wall temperatures, 7.2 K and 11.2 K, and two pressures, 3 atmospheres (solid lines) and 10 atmospheres (dashed lines). The arrows indicate the pseudocritical temperatures at these two pressures.

2.7 CRITICAL TWO PHASE FLOW - STATUS REPORT -

R. V. Smith

In cryogenic pumps, flow loops, jet pumps, refrigeration expanders and other devices, critical two phase flow during cooldown or steady operation may well be the limiting condition. A state-of-the-art survey of this subject with design recommendations is in progress. The work, which will appear in 1972 as an NBS Technical Note by R. V. Smith (presently of Wichita State University), will contain design charts, graphs, and other computational aids for helium as well as hydrogen and oxygen. Recommendations will be made as to the best predictive models and expressions.

3. HELIUM II HEAT TRANSFER

For some systems, the performance improves significantly by reducing the temperature below 2.17 K where heat transfer improves markedly due to superfluidity of the helium. The increased refrigeration cost may be compensated by the reduced power dissipation in the load. The removal of heat from a solid body by a helium II bath has two parts. First, a small temperature gradient is found along the length of the bulk fluid. Second, a thermal barrier known as the Kapitza resistance exists at the solid-liquid interface. In the temperature region near 1.9 K, where most large scale applications of helium II technology are currently anticipated, the Kapitza temperature drop across the interface is usually larger than the temperature drop across many meters of fluid; e.g., for heat inputs of 0.1 W/cm^2 , experimentally measured temperature differences across the interface range from about 0.02 to 10 K, whereas thermal gradients in the helium are in the neighborhood of 10^{-7} K/cm . These two factors are summarized separately in sections 3.1 and 3.2.

3.1 THERMAL GRADIENTS IN HELIUM II - SYNOPSIS - V. D. Arp

Thermal gradients in the helium bath have been summarized for engineering purposes by Arp [1970]. Figures 3.1.1 and 3.1.2 are taken from that paper, with some modifications for the sake of clarity, and show the thermal gradients as a function of the thermal flux, with channel diameters as a parameter. Three different regimes are evident: (1) a low flux regime where dT/dX is proportional to $(\text{diameter})^{-2}$, for a given flux, (2) an intermediate region which is poorly understood, and (3) a high flux region where the thermal gradient is (approximately) independent of the channel size, but restricted by the mutual friction between the superfluid and normal fluid. It is important to note that

there is a limiting thermal flux given by figure 3.1.3 above which vapor formation may occur within the helium bath, provided that it is in equilibrium with its vapor at some point in the system at that specified temperature. Pressurizing the helium II bath will raise the limiting thermal flux above that given by figure 3.1.3. The derivation of these curves, and detailed discussion, is given in Arp [1970]. Recent work on the limiting thermal flux has been reported by Eaton, Lee, and Agee [1972].

3.1.1 References

- Arp, V. D., "Heat transport through He II," *Cryogenics*, 10, No. 2 (1970).
- Eaton III, R., Lee, W. D., and Agee Jr., F. J., "High heat-flux regime cooling in vertical channels," *Phys. Rev.* A5, 1342 (1972).

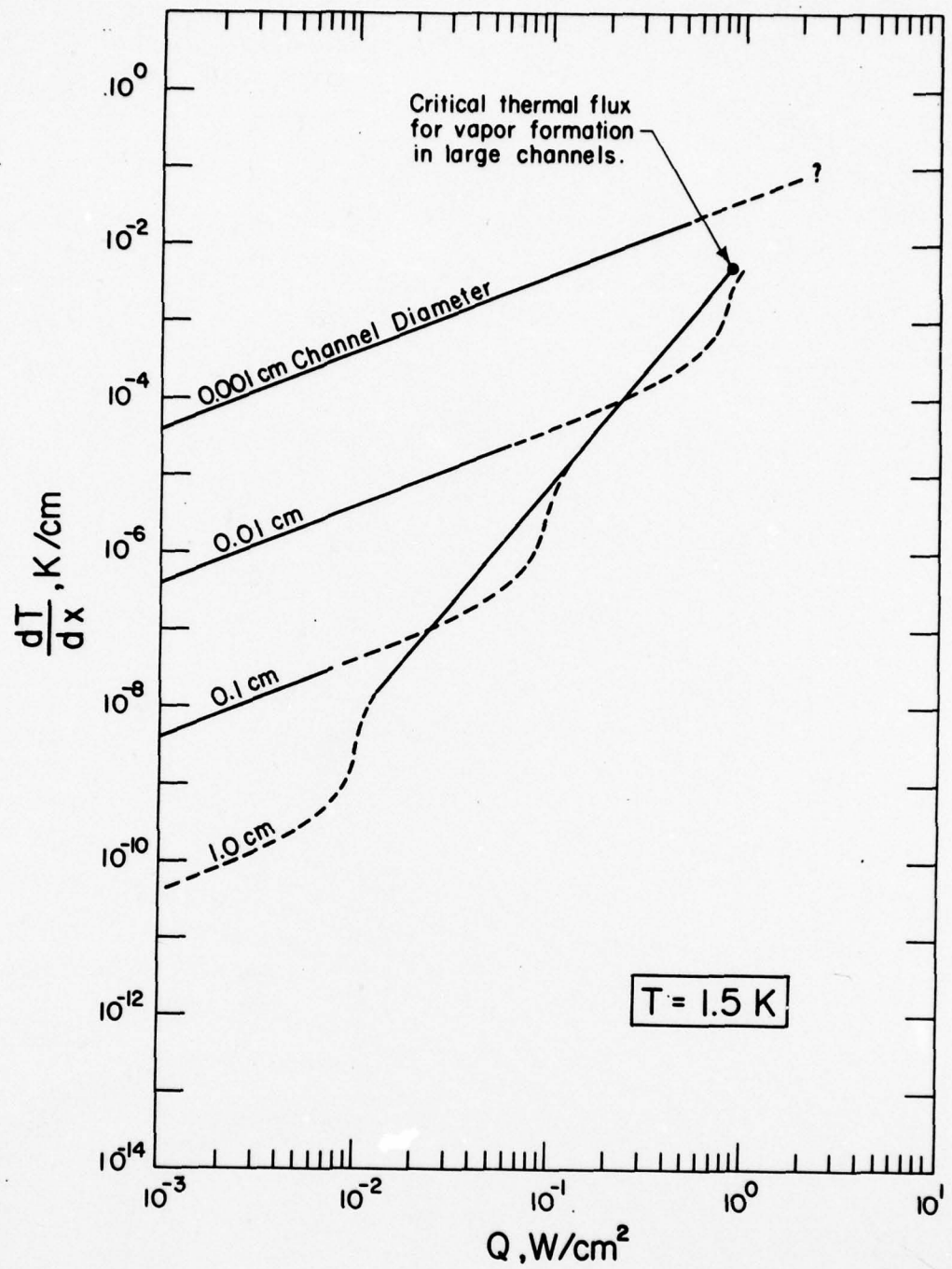


Figure 3.1.1 Helium II thermal gradient as a function of thermal flux at 1.5 K.

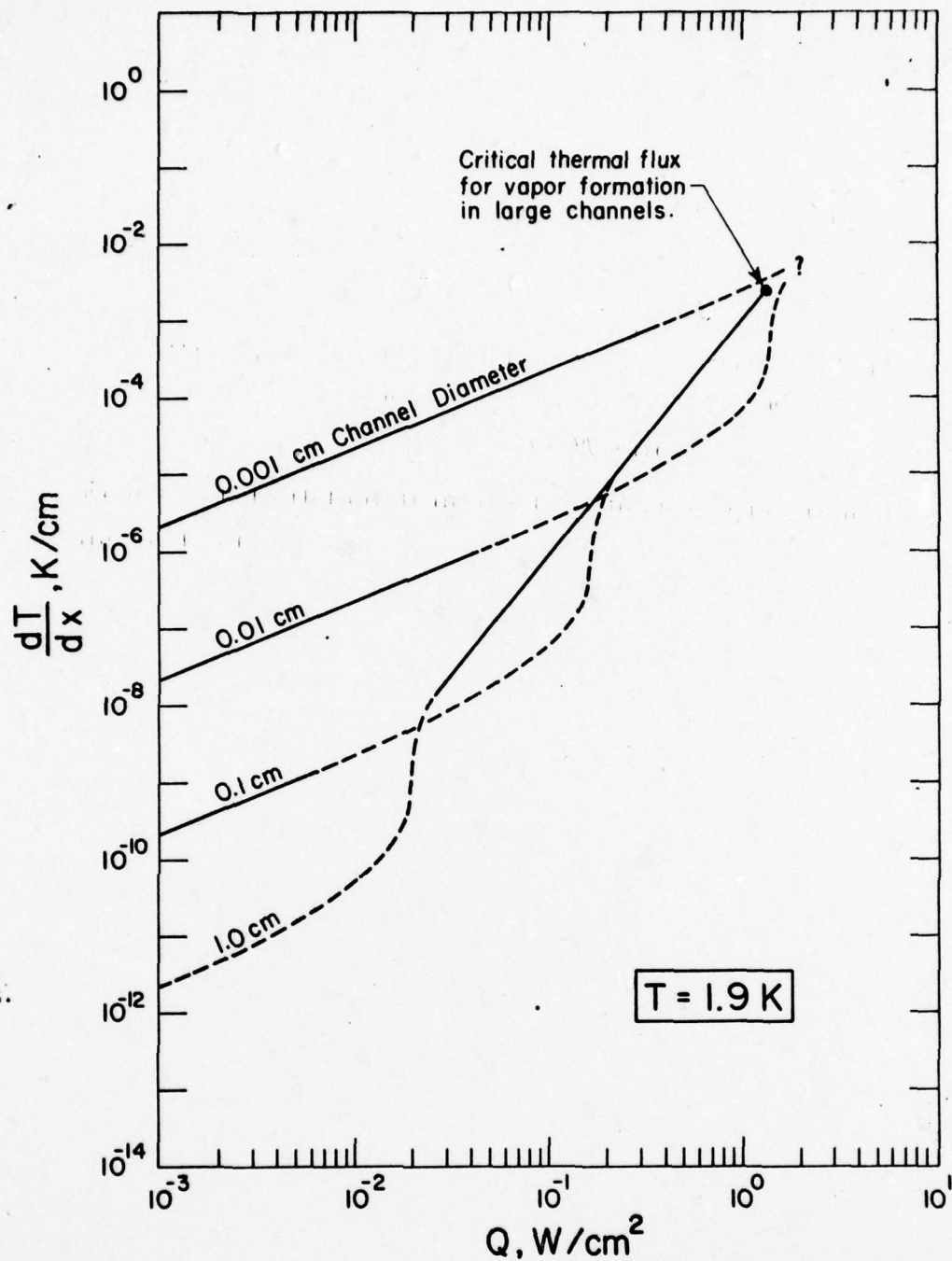


Figure 3.1.2 Helium II thermal gradient as a function of thermal flux at 1.9 K.

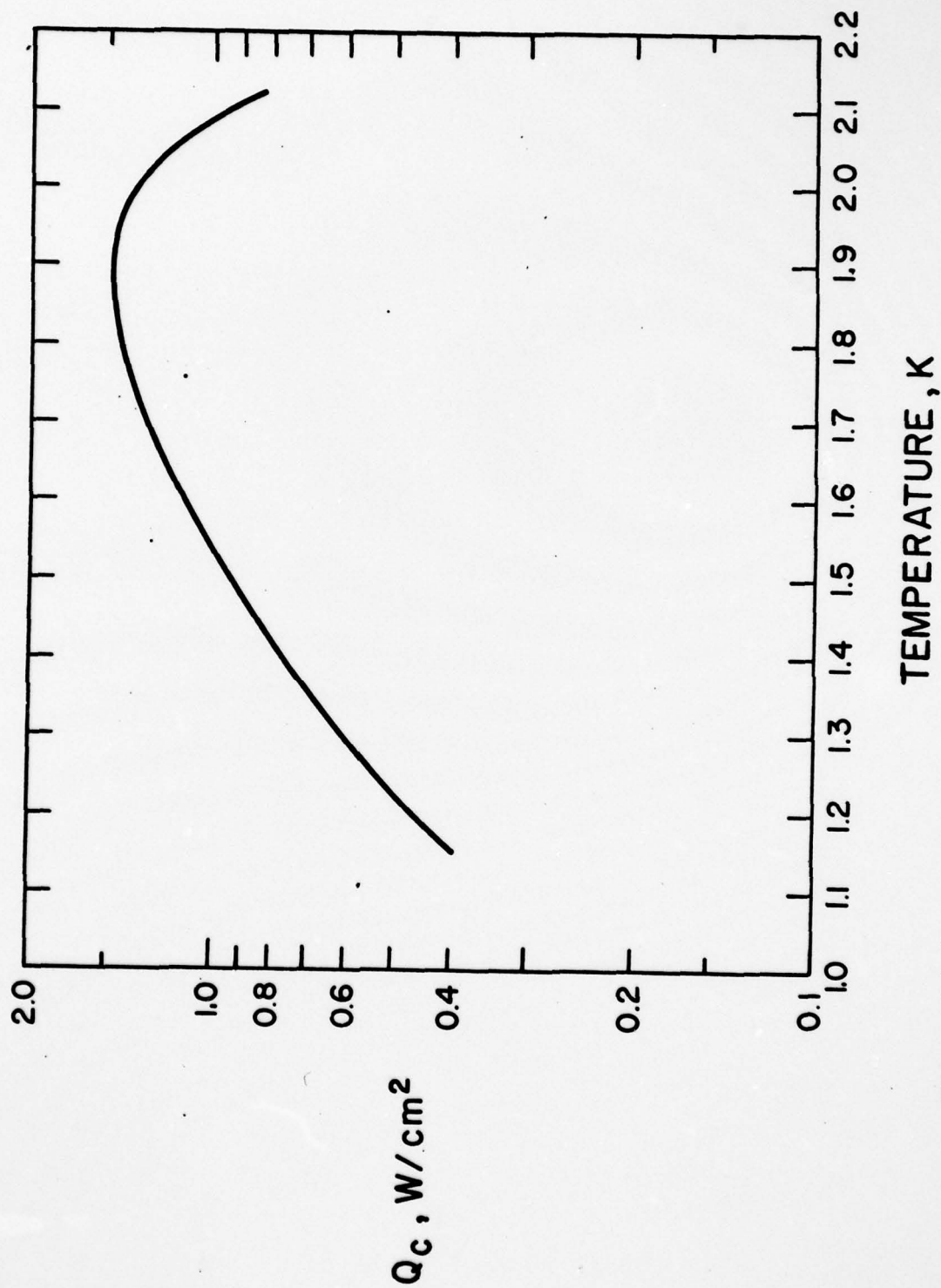


Figure 3.1.3 Limiting thermal flux in helium II above which vapor formation may occur.

AD-A059 046

NATIONAL BUREAU OF STANDARDS BOULDER COLO CRYOGENICS DIV F/G 7/2
HELIUM HEAT TRANSFER, (U)

JUN 72 V ARP, E R BALLINGER, P J GIARRATANO

N00014-76-C-0706

UNCLASSIFIED

NBS-10753

NL

2 OF 2
AD
A059 046

END
DATE
FILMED
11-78

DDC

3.2 KAPITZA CONDUCTANCE - STATUS REPORT - N. S. Snyder

3.2.1, Background

For a number of solids of technical interest, no measurements of Kapitza conductance exist. Even when measurements have been made, the results are difficult to apply in a design situation, because order-of-magnitude differences in conductance have been reported for samples of the same solid. A theoretical expression for the conductance, the Khalatnikov-acoustic mismatch equation (sec. 4.1, Snyder, 1969; Pollack, 1969) is at least an order of magnitude smaller than most of the conductances that have been reported, though it perhaps should apply only to an ideal interface that is atomically clean and structurally a "simple termination of the bulk," (Narnhofer, Thirring, and Sexl, 1969). On the other hand, much of the existing data suggest that a higher limit called the phonon radiation limit (Frederking, 1968; Snyder, 1969) may apply at such a surface. The phonon radiation limit is two or three orders of magnitude higher than the acoustic mismatch conductance. At this time, one can only conclude that the mechanism of energy interchange across the surface is not understood.

This situation results in the following design problems:

- A. If heat is dissipated in a given solid in helium II, the ΔT across the surface can't be predicted to better than one or two orders of magnitude.
- B. If there is some freedom in choosing the solid material to minimize the ΔT , there is very little basis on which to make the decision.
- C. Attempts to improve the conductance across a surface by etching, or adding coatings, etc., are likely to be tedious and unproductive in the absence of theoretical understanding.

If we learn the factors governing energy interchange at the surface, we should be able to improve the reliability of design data based on surface specifications, and to optimize the conductance by control of the surface conditions.

3.2.2 Experimental program

An apparatus to measure Kapitza conductance of an atomically clean, structurally undamaged copper surface is currently undergoing testing. Because of stringent requirements for doing this experiment (ion bombardment under ultra high vacuum, high temperature annealing, helium II tight seal for cooling to helium temperatures for the measurements), and limited funding and time, the equipment utilizes the sample preparation techniques developed by Low Energy Electron Diffraction (Leed) investigations, but does not incorporate devices for in situ surface characterization. It will be an order-of-magnitude advance in the preparation of well-defined surfaces for Kapitza measurements, and should provide a significant test of the two theories and a better understanding of the mechanism of thermal energy exchange at a copper surface.

The proposed program divides logically into two stages. The first is to extend the measurements to solids other than copper, for example, to solids with Debye temperatures which differ substantially from that of copper. The element niobium will be included because it is the best available superconductor for construction of extremely high Q resonant cavities (with possible applications ranging from frequency standards to linear accelerators). Selection and preparation of samples will be guided by the knowledge gained from our reviews of the subject (Snyder, 1969 and 1970). For example, it is desirable to avoid a cold-worked or otherwise damaged region just below the surface of the sample,

because such a layer may decrease the thermal conductance below that of the bulk sample, resulting in a spurious additional interface resistance. Contamination of the surface by foreign atoms will also be minimized.

These experiments will assist with design problem B above, as well as provide more information about which surface parameters are important, thus guiding work on the next stage. The next stage in the research program is to determine how surfaces can best be prepared to optimize Kapitza conductance, so that design uncertainties under A can be reduced to values of perhaps 20 to 30%. The procedure here is dependent upon the results of the first stage. If the acoustic mismatch theory holds for ideal surfaces, then coatings which have analogous acoustic properties to $1/4$ wavelength optical coatings should be tried first to reduce the mismatch (Whelan and Osborne, 1968). To avoid surface-to-coating contact problems, UHV evaporation may be used initially. The present apparatus can be readily modified for this.

However, if near-ideal surfaces have conductances substantially above the acoustic mismatch limit, then thinner coatings will probably be more efficient as stabilizers, since nonclassical phonon interaction across the surface (as in tunneling) will be a significant part of the heat transfer (Mitchell, 1970). The fact that some stabilization is essential is already evident from results on deterioration with time of Pb surfaces (Challis and Cheeke, 1965) and In surfaces (Neeper and Dillinger, 1964).

These approaches should provide guidance for design problems A and C by indicating quantitatively how surface parameters control Kapitza conductance. In addition, measurements that involve varying

the parameters for the types of surfaces that are presently in use have been undertaken to provide more such information. The results are reported in section 3.3. It is expected that all work will be done at temperatures near the lambda point.

3.2.3 Current status--results to date

The cryostat is necessarily more complex than is usual for Kapitza measurements, and it has some features which are novel. Hence, it was felt that it was necessary to test rather carefully whether the cryostat would work as designed to measure the Kapitza coefficient, and it was decided that it would be most expedient to carry out these tests before final cleaning and assembly of the cryostat into the UHV system. These tests were completed satisfactorily. Further work on cleaning and assembly of the UHV system followed. Testing of the UHV system is currently underway. Figure 3.2.1 shows a closeup photograph of the chamber in which the sample surface is prepared under UHV. An overall view of the vacuum system is shown in figure 3.2.2. The walls of the bakeout oven have been removed in the photograph. Clean helium gas is supplied from a storage dewar of liquid helium and further purified before being introduced into the system.

3.2.4 References

- Challis, L. J., and Cheeke, J. D. N., "The Kapitza conductance in lead," Prog. in Refrig. Sci. and Tech., 1, 227-230 (Pergamon Press, London), (1965).
- Frederking, T. H. K., "Thermal transport phenomena at liquid helium II temperatures," Chem. Eng. Prog. Symp. Series 64, No. 87, 21-55, (1968).

- Mitchell, W., private communication. (Statistical Physics Div.,
Institute for Basic Standards, NBS, Washington), (1970).
- Narnhófer, H., Thirring, W., and Sexl, R., "On the theory of
interfacial conductivity," *Thermal Conductivity--Proceedings
of the Eighth Conference*, 161 (Plenum Press, New York),
(1969).
- Neeper, D. A., and Dillinger, J. R., "Thermal resistance at
indium-sapphire boundaries between 1.1 and 2.1 K," *Phys.
Rev.* 135, No. 4A, A1028-A1033, (1964).
- Pollack, G. L., "Kapitza resistance," *Rev. Mod. Phys.* 41, No. 1,
48-81, (1969).
- Snyder, N. S., "Thermal conductance at the interface of a solid
and helium II (Kapitza Conductance)," NBS Technical Note 385,
(1969).
- Snyder, N. S., "Heat transport through helium II: Kapitza conduc-
tance," *Cryogenics* 10, No. 2, 89-95, (1970).
- Whelan, M. F., and Osborne, D. V., "The modification of the
Kapitza resistance due to a surface film," *Proc. 11th Intern.
Conf. on Low Temperature Physics*, 1, 575-578 (University of
St. Andrews Printing Dept., St. Andrews, Scotland), (1969).

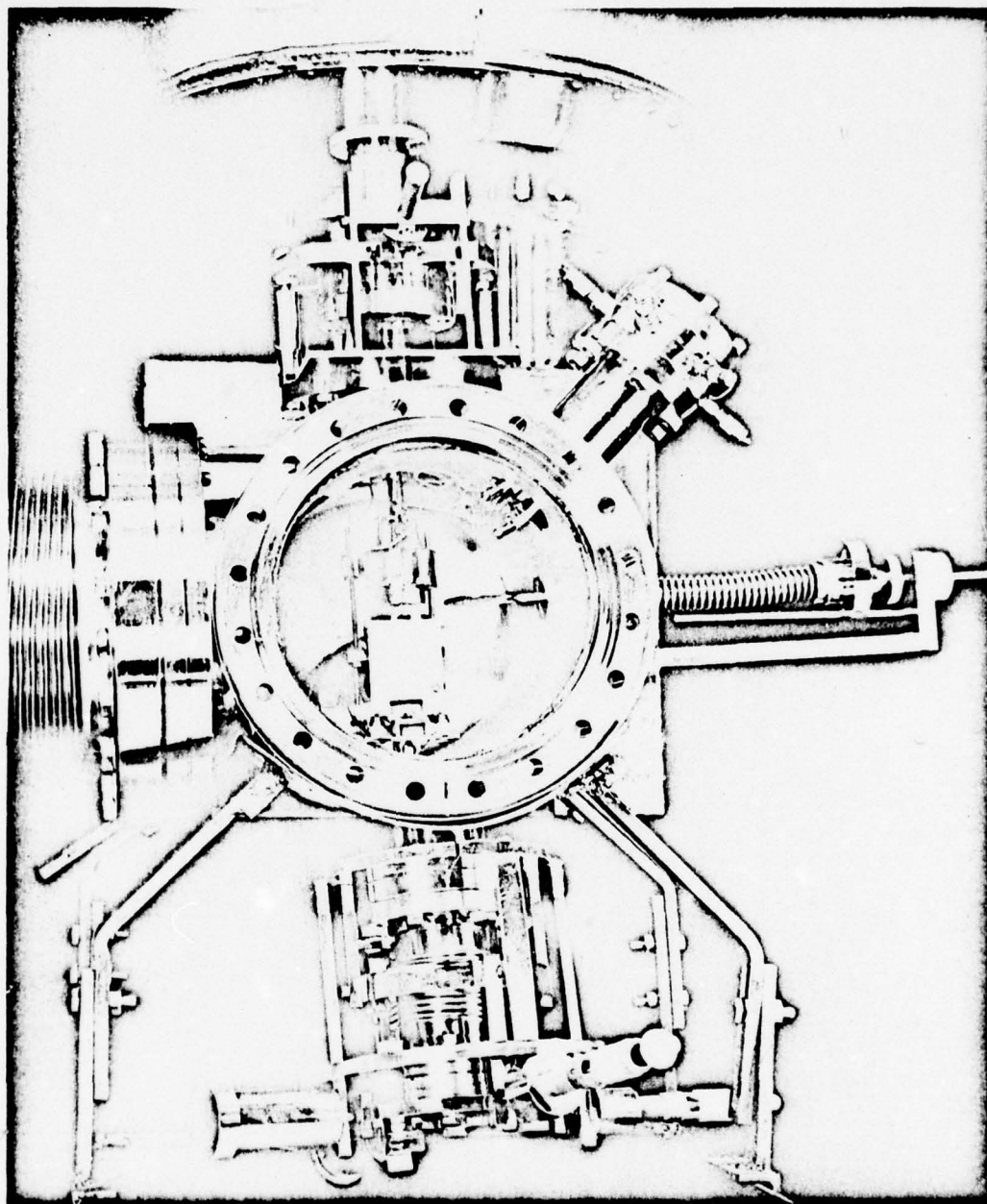


Figure 3.2.1 Closeup view of the chamber in which the sample surface is prepared under UHV.

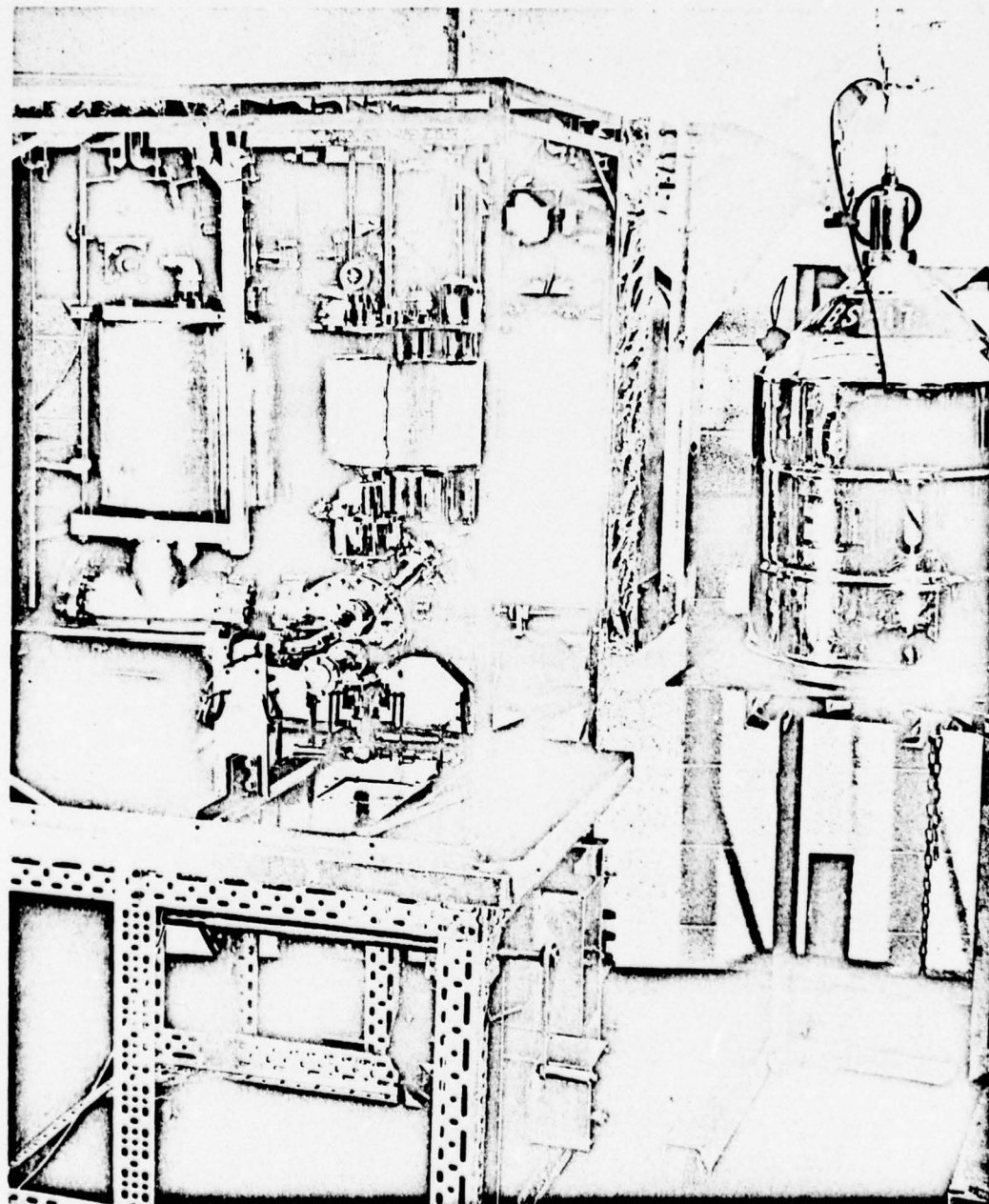


Figure 3.2, 2 Overall view of the vacuum system.

3.3 KAPITZA CONDUCTANCE AND THERMAL CONDUCTIVITY OF Cu, Nb, AND Al IN THE RANGE FROM 1.3 TO 2.1 K - ENGINEERING MEASUREMENTS - K. Mittag

Kapitza conductance and thermal conductivity have been measured at this laboratory for samples of Cu, Nb, and Al in which the surface preparation was typical of cryogenic engineering applications. A report covering this work has been written and is now awaiting publication in "Cryogenics." Although this experimental program was not funded by AEC the results are of practical interest and compliment the Kapitza conductance studies for well defined surfaces in progress; therefore, the report is included here in its original form.

KAPITZA CONDUCTANCE AND THERMAL CONDUCTIVITY OF
COPPER, NIOBIUM AND ALUMINUM IN THE RANGE FROM
1.3 to 2.1 K*

K. Mittag†
Cryogenics Division
NBS - Institute for Basic Standards
Boulder, Colorado

and
Kernforschungszentrum
Karlsruhe, Germany

ABSTRACT

The Kapitza conductance and the thermal conductivity of OFHC-copper,[‡] niobium, ultra high purity aluminum, and of the aluminum alloy 6061 Al have been measured in the temperature range from 1.3 to 2.1 K, yielding both quantities in the same steady state experiment. The temperature dependence of the Kapitza conductance, h_0 , was between $T^{3.3}$ and $T^{4.6}$ for the different samples, which is higher than the most often observed T^3 dependence. The magnitude of h_0 for both OFHC-copper and aluminum agrees well at 1.9 K with an empirical prediction, but for niobium it is a factor of two to four lower than the value predicted. At 1.9 K, h_0 is higher by a factor of two for

* Contribution of the National Bureau of Standards, not subject to copyright.

† Max Kade Foundation Fellow.

‡ Certain commercial materials and manufacturers are identified in this paper in order to adequately specify the experimental procedure. In no case does such identification imply recommendation or endorsement by the National Bureau of Standards, nor does it imply that the material or manufacturer identified is necessarily the best available for the purpose.

an annealed and chemically polished niobium sample than for an untreated sample. The thermal conductivity measured for OFHC-copper and 6061 Al is in good agreement with the value calculated from the resistivity of these materials and the Wiedemann-Franz law. The measured thermal conductivity obtained for an annealed niobium sample is a factor of 2.8 higher than the highest published value.

Key Words: Aluminum; copper; heat transfer; Kapitza conductance; niobium; superfluid helium; thermal conductivity.

The Kapitza conductance h_0 is a limiting factor in removing heat from a metal into helium II near 1.9 K, the operating temperature of superconducting particle accelerators, built with rf structures made of niobium. But up to now no experimentally determined values for h_0 of niobium have been published, and available theoretical predictions are uncertain by factors of 10. Another material of interest in cryogenic technology is aluminum for which only an experimental value obtained by second sound heat transfer has been reported.¹ It was this lack of information which led to setting up a straightforward experiment in which the temperature drop across a solid body-helium II interface for a given constant heat flux could be measured for temperatures between 1.3 K and 2.1 K. Measuring the temperature gradient along the sample in order to extrapolate to the sample surface temperature yielded the thermal conductivity λ in the same experiment. As pointed out in nearly every publication on Kapitza conductance the sample and especially its surface preparation affects h_0 crucially

with factors of 2 difference being not unusual. Sample preparations were chosen to be typical for cryogenic engineering applications.

As extensive review articles have appeared recently covering both theoretical and experimental aspects on the subject^{2, 3, 4, 5}, a review will be omitted in this paper.

1. Experimental procedure

Fig. 1 shows a schematic drawing of the lower inner part of the cryostat which is quite similar to the one used by Johnson and Little⁶. The samples were cylinders of 2.5 cm in both length and diameter. The He-sample chamber was sealed against the insulation vacuum by having an indium O-ring of about 0.7 mm diameter between the sample and the stainless steel flange. The force by which the spring pressed the sample against the flange gave rise to a stress on the sample surface in the sealing region of about 4 MN/m^2 .

The heater wire inside the heater element was coiled evenly over the entire cross section in order to deliver a homogeneous heat flux Q into the sample. The helium bath temperature T_B in the He-sample chamber was electronically stabilized and was measured by a Ge-resistance thermometer. Although measured a few cm away from the sample surface, T_B was taken to be the temperature in the helium at the sample surface, giving rise to an error of less than 0.1% of the temperature drop ΔT across the interface. The temperature distribution along the sample was measured by three carbon-resistance thermometers called C1 to C3 in fig. 1, which were attached to copper clamps. The axial length of the clamp in contact with the sample was 0.5 mm, and the distance between C1 and the surface was 2 mm.

Both the resistance R of the thermometers and the power delivered to the heater element were determined using four-lead dc circuitry. Voltages were recorded with a digital voltmeter (resolution $0.1 \mu\text{V}$), and thermal voltages were eliminated by measuring both current polarities.

All resistance thermometers used were calibrated in situ for $Q = 0$ by measuring the vapor pressure in the He-sample chamber and applying the 1958 temperature scale⁷. A least squares fit yielded the coefficients of the expansion $\ln T = \sum_0^n a_n (\ln R)^n$. A three term fit was sufficient to make the overall accuracy of these calculated T -values less than 0.1% and of dT/dR less than 0.7% in the temperature range from 1.3 to 2.2 K. The changes in calibration of the C-resistors between different experiments were smaller than these errors.

With the set-up assembled, the He-sample chamber--separated from the main helium bath--was flushed several times with He-gas and pumped at room temperature to at least 10^{-4} Torr (1.3×10^{-2} N/m²) before starting the cooldown of the cryostat. Helium gas, cleaned by flowing through a liquid nitrogen cooled length of copper tubing, was condensed into the He-sample chamber.

A typical cycle for measuring both h_0 and λ at a given temperature consisted in measuring all temperatures and the heater power for $Q = 0$ and three values of Q between 1 mW/cm² and 40 mW/cm², resulting in ΔT values between 5 mK and 140 mK, depending on T and the sample used. The sample surface temperature (T_S) was calculated by extrapolating the temperature gradient between C1 and C2 linearly towards the interface. This procedure is correct only if λ is independent of temperature. The error introduced by this assumption turned out to be negligible compared to the error of locating the

thermometer position on the sample (± 0.25 mm). The temperature difference between the sample surface and helium bath was calculated by comparing the thermometer readings with their values for $Q = 0$: $\Delta T = T_S(Q) - T_B(Q) - (T_S(0) - T_B(0))$, thereby minimizing the error from residual calibration inaccuracies or possible calibration shifts between the calibration run and the experiment. The same method was applied to evaluate the temperature gradient between a given pair of thermometers on the sample. The power dissipated in the thermometer resistors (about 1 nW) was kept constant between the $Q = 0$ and $Q \neq 0$ data taking, so that the error introduced by the self-heating effect (0.4 mK/nW for the C-resistors) was negligible. Heat leaks along spring and heater-element current wires were found to be below 0.1% by measuring temperature gradients along them. Heat leaks along the thermometer leads were calculated to be negligible, too. On the other hand, corrections had to be made for heat leaks along the stainless steel sample support (depending on sample between 2% and 10%) and by the indium fin protruding from the indium O-ring seal into the helium⁸ (between 1% and 17%).

The amount of macroscopic geometrical sample surface area contributing directly to heat transfer between sample and He II (about 4.2 cm^2) could be determined to within 1% by investigating both sample surface and In O-ring under a traveling microscope after the experiment. No unanimous agreement exists in the literature on the effect of surface roughness on the He II-solid heat transfer. Little⁹ suggests that both an increased heat flow and temperature dependence would occur if the "amplitude of the roughness" is comparable to the phonon mean free path in the solid. For the case that the roughness is comparable with the phonon wavelength he predicts a small decrease in heat transfer¹⁰. In a recent paper Adamenko and Fuks¹¹ contradict

these results and point out that the important parameter governing this question is the phonon wavelength in the helium (about $4 \cdot 10^{-6} T^{-1}$ K mm), the heat transfer being ruled by the microscopic rough surface area if the phonon wavelength is much smaller than the dimension of asperities. Discussions of the effect of surface roughness on phonon scattering by Ziman¹² support the latter viewpoint. Accepting this, the geometrical macroscopic surface area was multiplied by a roughness factor r defined as rough surface area divided by macroscopic surface area. To determine r , after each experiment the surface roughness was measured by the stylus method, the width of the stylus at the tip being 2.5μ (2.5×10^{-6} m). By this the influence of asperities being larger than 0.025μ in height and at least 2.5μ apart could be corrected for. Microscopic asperities from this size down to the size of the phonon wavelength were taken into account.

The error bars shown in the figures originate from all possible sources of errors which were discussed in this section. They include in particular the estimated uncertainties in the area and Kapitza conductance of the protruding indium fin, the Kapitza conductance and thermal conductivity of the stainless steel sample support, and the uncertainty of determining the area factor r .

2. Sample Preparation and Experimental Results

Several authors^{3, 4, 13} have shown that the Kapitza conductance h_0 in the limit of zero temperature drop across the interface can be calculated from the conductance $Q/\Delta T$ by

$$h_0(T_B) = Q/(\Delta T f) \text{ with } f = 1 + \frac{3}{2} \frac{\Delta T}{T_B} + \left(\frac{\Delta T}{T_B} \right)^2 + \frac{1}{4} \left(\frac{\Delta T}{T_B} \right)^3.$$

They show that this reduction agrees with heat transfer experiments as long as $Q < 0.1 \text{ W/cm}^{13}$ and T_S is smaller than the superfluid transition temperature⁴. This result emerges from theoretical considerations based on the assumption that Q is proportional to the difference in phonon energy densities between helium and sample which is proportional to $T_S^4 - T_B^4$. Most theories and experimental data on H_0 are in favor of h_0 varying as T^3 in the temperature range from 1.3 to 2.1 K; the experimental results on the Kapitza conductance are displayed in fig. 3 and fig. 5 as $Q/(\Delta T f T_B^3) = h_0(T_B)/T_B^3$ for varying T_S . T_S was chosen as the independent variable because deviations from a T^3 -dependence of h_0 probably originate more from sample surface properties than from He II bulk properties. This assumption is true, for instance, if the heat transfer is enhanced by single particle excitation in the helium layers adjacent to the interface^{14, 15}.

a) OFHC-copper

Measurements on OFHC-copper served mainly as a method for testing the reliability and accuracy of the experiments.

Sample OFHC-Cu1 was turned on a lathe, vapor degreased, rinsed with ethanol, then remained in contact with air for several hours before pumping was started in the cryostat; $r = 1.27 \pm 0.10$.

Sample OFHC-Cu2 was turned on a lathe; vapor degreased; rinsed with ethanol; chemically polished¹⁶ 1 min in a solution of 50 ml H_3PO_4 (86%), 20 ml HNO_3 (70%), and 25 ml CH_3COOH (99.7%) at 70°C; and electroplished¹⁶ 6 min in a solution of 77 ml H_3PO_4 (86%) and 28 ml H_2O at 20°C and a current density of 0.025 A/cm^2 ; it was then rinsed in ethanol, remaining in air 1 hour before pumping was started in the cryostat; $r = 1.0004 \pm 0.0003$. From measurements using the eddy current decay method¹⁷ at 4 K the residual resistivity

ratio (RRR) came out to be 59 and the resistivity $23.3 \text{ n}\Omega\text{cm} \pm 10\%$. For these low temperatures and the relatively impure material, the Wiedemann-Franz law can be used to calculate the thermal conductivity¹⁸, resulting in $0.93 \text{ T W}/(\text{cm K}^2) \pm 10\%$. This value is in good agreement with the measured conductivity of $1.03 \text{ T W}/(\text{cm K}^2) \pm 10\%$ of OFHC-Cu1 and OFHC-Cu2 obtained in the Kapitza experiments (fig. 2 and tab. 1). This agreement gives confidence for all the following results of Kapitza conductances and thermal conductivities. The experimental values for h_o of OFHC-Cu1 and OFHC-Cu2 are shown in fig. 3.

b) Niobium

The measurements on the niobium samples were done in the superconducting state for zero fields. This is the information which is needed, e.g., for the design of superconducting particle accelerators, in which the helium-niobium interface is not subject to electromagnetic fields.

Sample Nb1, which was 99.9% pure, electron beam melted, and microcrystalline reactor grade material, was delivered by Fansteel Co.[‡] containing less than 500 ppm Ta. It was turned on a lathe with a 0.3 mm cut depth, remained 5 months in air, then was rinsed with toluene, acetone, and ethanol; $r = 1.003 \pm 0.002$.

Sample Nb2, which was electron beam melted, reactor grade material, and microcrystalline, containing about 100 ppm Ta, was delivered by Wah Chang Co.[‡], and chemically polished 3 min in a solution of 60 ml HNO_3 (70%) and 40 ml HF (40%) between 0 and 6°C ; it was then

high vacuum and high temperature annealed (heated from 23°C to 1850°C in 4 h in better than $5 \cdot 10^{-7}$ Torr, lowered to 1750°C in 0.5 h, held at 1750°C for 4 h at $3 \cdot 10^{-8}$ Torr, cooled down to 23°C and $9 \cdot 10^{-8}$ Torr in 24 h), heating at 190°C for 18 h in a clean vacuum container designed for sample shipment with an end vacuum of $8 \cdot 10^{-8}$ Torr remaining in this container for 6 days at 20°C. Next, a few soft solder spherical deposits from the 190°C heat treatment were mechanically removed, and the sample was chemically polished for 6 min at -10°C, then rinsed with ethanol, remaining in air 15 min before pumping was started in the cryostat; $r = 1.0007 \pm 0.0004$.

The thermal conductivities evaluated from temperature gradients between thermometers C1 - C2 and C2 - C3, respectively (see fig. 1), are shown in fig. 4 for both niobium samples. No simple analytic expression can be given for the temperature dependences. The Kapitza conductances for the two samples are displayed in fig. 3.

c) Aluminum

Two samples with large differences in both purity and sample treatment were chosen.

Sample Al(RRR = 13000) which was ultra pure aluminum was vacuum melted, annealed for 1 h at 450°C in air, cooled down to 20°C in 24 h, turned on a lathe, surface ground with number 500 emery paper, vapor degreased, chemically polished for 3.5 min in a solution of 25 ml H_2SO_4 (98%) and 70 ml H_3PO_4 (98) = 10 ml HNO_3 (63%) at the boiling point¹⁶, then rinsed with ethanol, remaining 1 h in air before pumping was started in the cryostat; $r = 1.0004 \pm 0.0004$, RRR = $13000 \pm 10\%$.

Sample Al 6061, which was aluminum alloy type 6061 with a T6 temper, was turned on a lathe, vapor degreased, then rinsed with ethanol, remaining 1 h in air before pumping was started in the cryostat; $r = 1.004 \pm 0.002$.

The Kapitza conductances for both samples are shown in fig. 5 and the thermal conductivity of Al 6061 in fig. 2. The thermal conductivity for Al(RRR = 13000) was estimated, using measured resistivity at 4 K and the Wiedemann-Franz law, to be in the order of $130 \text{ T W}/(\text{cm K}^2)$ in the normal conducting state. This estimate is uncertain to not more than 20% because of applying the Wiedemann-Franz law to such a high purity material in the temperature range of interest here¹⁸. Because of the small temperature gradients developed in such a high conductivity sample even for the highest heat fluxes applied, no reliable information on λ could be deduced from them, although no contradiction to the $130 \text{ T W}/(\text{cm K}^2)$ value was observed.

The results from fig. 2 to fig. 5 and the thermal conductivities emerging from resistivities (λ_ρ) together with the Kapitza conductance calculated from an empirical relation (h_o , empirical) are summarized in tab. 1.

3. Discussion

At first glance the most striking of the experimental results on Kapitza-conductance seems to be their temperature dependence. It varies for different samples, even for the same material, well outside experimental errors and is in most cases higher than the T^3 dependence most often reported by other authors. The most apparent explanation is differences in sample preparation, which

can have their origin in one or more parameters of the following list: material impurity density, dislocation density, surface damage, stress, grain size of crystals, surface roughness, impurity and oxide layers on the surface. As often pointed out, experimentalists have great difficulties in defining the state of their samples by exact values for these parameters, and the task for theoreticians to weave all of them into a common net seems to be nearly impossible. A temperature dependence stronger than T^3 is predicted by theoretical approaches, which either take into account the improved acoustic mismatch by a dense helium layer at the surface or the independent particle excitations of helium atoms out of this layer^{2, 4, 5, 14, 15}. Because of the basically simple experimental set-up, described in this paper, the information available on the state of the sample, especially its surface, during the time of the experiment is not complete. Especially uncertain is the thickness and structure of oxide and impurity layers on the surface, which necessarily were present during all experiments due to mounting procedure. Furthermore, it is not known how the sample crystal structure was disturbed by applying a stress of 4 MN/m^2 on the sealing circumference. A Laue-backscattering analysis²⁰ on the very soft high purity aluminum sample after the experiment showed disturbances in crystal structure on the sealing surface but not in the center of the sample surface.

a) OFHC-Cu

It seems worthwhile to point out again the good agreement for the thermal conductivities of the two samples measured with that deduced from resistivity of the same material and the Wiedemann-Franz law. The κ_0 values for both samples lie in the upper range of values reported by other authors^{2, 3, 4, 5} although the surface damage

layer resulting from turning on a lathe was not removed for OFHC-Cu1. The only difference in sample preparation between OFHC-Cu1 and OFHC-Cu2 is the, at least, partial removal of surface damage and the smoothing of the surface by chemical means and electropolishing. As the large error introduced by the surface roughness of OFHC-Cu1 is taken care of in the error bars (fig. 3), the result indicates that for copper a surface damage enhances the Kapitza-conductance at least below 1.6 K. This statement agrees with recent observations of W. L. Johnson and A. C. Anderson^{14, 21} and disagrees with conclusions drawn by N. S. Snyder in a review article².

b) Niobium

The thermal conductivity for niobium in the superconducting state well below the transition temperature of 9.1 K is predominantly due to phonon energy transport. The values for λ presented here are higher by factors of 1.2 and 2.8, for the unannealed sample Nb1 and the annealed sample Nb2, respectively, compared to the highest values reported so far²², which were obtained for a zone refined single crystal. The tendency of shifting of the maximum of thermal conductivity to lower temperatures for the higher purity samples²² (fig. 4) is continued in the results presented here. As also indicated by unpublished measurements at Stanford University²³, the magnitude of λ for Nb2 is probably due to the high vacuum, high temperature annealing process giving rise to lower dislocation densities combined with growing of the crystal size in the material (between 1 mm and 2 mm for Nb2). This hypothesis is reinforced by the different results for λ obtained between different pairs of thermometers, the pair C1 - C2 giving lower values than C2 - C3 (fig. 1) for temperatures below 2 K. This is the temperature region in which the dislocation density in the sample influences the

energy transport by phonons most²⁴, and the region measured by C1 - C2 probably has a higher dislocation density than the one between C2 - C3 due to stress in the vicinity of the seal. This fact complicates the evaluation for h_0 since the extrapolation of the temperature gradient to the surface becomes uncertain, because the dependence of dislocation density on the distance from the surface is unknown. Assuming that λ decreases linearly towards the surface with a gradient determined by the difference between $\lambda(C1 - C2)$ and $\lambda(C2 - C3)$, and evaluating h_0 from the temperature of C2 and the value of λ at the surface, a correction of only +3% has to be applied to h_0 at 1.4 K for Nb2, where the effect is largest.

As pointed out before^{25, 26} the temperature extrapolation is also uncertain if the mean free path l of the phonons is no longer microscopic. Using the equation $\lambda = Cv l$ (C = specific heat, v = mean phonon velocity), which is well established for heat transport by phonons only, and the Debye-approximation for C and v , it turns out that $l = \frac{1.463 \lambda}{T^3} \text{ cm}^2 \text{ K}^4 / \text{W}$. For Nb2 this gives $l = 2.5 \text{ mm}$ at 1.4 K and 0.6 mm at 2.1 K, which is not negligible compared to the distance C1-surface. The correction method used by Neeper and Dillinger²⁶, for measurements on sapphire, is only applicable if l is limited by the dimensions of the sample, which is not the case here. The highest correction possible results when one assumes that the sample temperature is constant within a distance l of the surface. Again for Nb2, this assumption results in a correction to h_0 of 5% at 1.4 K, -7% at 0.9 K and -8% at 2.2 K. Taking both corrections together, the uncertainty for the values of h_0 for Nb should therefore be not much larger than indicated by the error bars (fig. 2).

c) Aluminum

Until now, h_0 for aluminum has only been measured by the second sound method by Sherlock and Challis¹, and these authors report $h_0 = 0.058 \cdot T^{4.0}$ for an aluminum foil measured in the as-received conditions. As no other specifications are given by these authors, a comparison with the data presented here in fig. 5 for Al(RRR = 13000) and Al 6061 is not very promising. Although the thermal conductivity for Al 6061 gave reasonable values (tab. 1 fig. 2), especially concerning the linear temperature dependence, the measurement of h_0 showed a systematic dependence on heat flux-- h_0 decreasing, with heat flux increasing (fig. 5) which was not understood. The error introduced by the temperature extrapolation towards the surface for this poor heat conducting material was much larger, however.

d) Comparison of h_0 with empirical relation

Well established theoretical predictions for the Kapitza-conductance are, up to now, only the ones by Khalatnikov^{2, 3, 4, 5} and the phonon radiation limit^{2, 3, 4}. They predict lower and upper limits, respectively, for h_0 of a real sample-He II interface. The data presented in tab. 1 lie well within these limits. Up to now, the effect of a real sample-He II interface on h_0 seems to be best represented by empirical relations, as given in some papers^{2, 3}. The one chosen for comparison² in tab. 1 is $h_0 = 79.5 \left(\frac{K}{\theta}\right)^{0.8} \text{ W}/(\text{cm}^2 \text{ K})$ at 1.9 K*. According to the reviewer, this dependence may be representative

* (θ = Debye temperature)

for surfaces etched or otherwise treated to remove oxidized and cold worked layers with an accuracy of perhaps a factor of 2. The agreement is good for OFHC-Cu2 and Al(RRR = 13000) and fair for Nb2. These were the samples which met the surface treatment specifications.

4. Conclusions

The Kapitza-conductance of niobium is higher for a sample which has been annealed and chemically polished, than for a sample which was only machined. The treatment used is nearly the same one applied on superconducting accelerator cavities^{27,28}. The results presented indicate that at 1.9 K--about the operating temperature of these devices--the thermal conductivity is approximately proportional to T^{-4} whereas the Kapitza-conductance is about proportional to T^4 . From this it follows that for an accelerator structure wall thickness smaller than 1.2 cm the total thermal resistance between the location of heat creation and the He II will decrease with rising temperature. This may have an important stabilizing effect on the operation of such a device.

Acknowledgements

I wish to thank V. D. Arp for many valuable discussions, which were particularly helpful in improving the design of the apparatus; and to N. S. Snyder for providing the essential parts of the hardware. For help in preparing the samples, I thank E. R. Ballinger, NBS Boulder; P. Bendt, Los Alamos (Nb2); M. B. Kasen, NBS Boulder (Al, 13000); and J. E. Vetter, Karlsruhe (Nb1). I would also like to acknowledge the contribution by J. C. Hust who made the RRR measurements.

This work was sponsored by a grant of the Max Kade Foundation, Inc., New York, for which I would like to express my gratitude. The opportunity of working at NBS Boulder is greatly appreciated.

REFERENCES

1. L. J. Challis, R. A. Sherlock, J. Phys. C: Solid St. Phys. 3, 1193 (1970)
2. N. S. Snyder, Cryogenics 10, 89 (1970)
3. N. Snyder, NBS Technical Note No. 385 (1969)
4. T. H. K. Frederking, Chem. Eng. Prog. Symp. 64, No. 87, 21 (1968)
5. G. L. Pollack, Rev. Mod. Phys. 41, 48 (1969)
6. R. C. Johnson and W. A. Little, Phys. Rev. 130, 596 (1963)
7. F. G. Brickwedde et al., J. Research NBS, 64A (Physics and Chemistry), 1 (1960)
8. T. H. K. Frederking, private communication
9. W. A. Little, Can. J. Phys. 37, 334 (1959)
10. W. A. Little, Phys. Rev. 123, 1909 (1961)
11. I. N. Adamenko, I. M. Fuks, Sov. Phys. JETP 32, 1123 (1971)
12. J. M. Ziman, Electrons and Phonons, Oxford at the Clarendon Press (1962)
13. J. S. Goodling and R. K. Irey, Advances in Cryogenic Engineering 14, 159 (Plenum Press, New York, 1969)
14. A. C. Anderson, W. L. Johnson, to be published
15. G. A. Toombs, L. J. Challis, J. Phys. C: Solid St. Phys. 4, 1085 (1971)
16. W. J. Tegart, The Electrolytic and Chemical Polishing of Metals, Pergamon Press (1959)

17. A. F. Clark, V. A. Deason, J. G. Hust, R. L. Powell, NBS Special Publication 260-XX (1972), to be published
18. J. G. Hust, A. F. Clark, Materials Research and Standards 11, No. 8, 22 (1971)
19. A. F. Clark, G. E. Childs, G. H. Wallace, Cryogenics 10, 295 (1970)
20. B. D. Cullity, X-Ray Diffraction, Addison-Wesley Publ. Co. (1967)
21. W. L. Johnson, A. C. Anderson, Phys. Lett., 37A, 101 (1971)
22. G. E. Childs, L. J. Ericks, R. L. Powell, NBS Monograph (1972), to be published
23. H. Brechna, Stanford University, Office Memorandum (1969); M. Rabinowitz, private communication
24. H. M. Rosenberg, Low Temperature Solid State Physics, Oxford at the Clarendon Press (1963)
25. J. D. N. Cheeke, Cryogenics 10, 463 (1970)
26. D. A. Neeper, J. R. Dillinger, Phys. Rev. 135, 4A, A1028 (1964)
27. J. P. Turneaure, IEEE Trans. Nucl. Science, NS18, No. 3 166 (1971)
28. P. Kneisel, O. Stoltz, J. Halbritter, IEEE Trans. Nucl. Science, NS18, No. 3 (1971)

Table 1.

Sample	h_o $W/(cm^2 K)$	Δn	$h_o(1.9 K)$ $W/(cm^2 K)$	h_o , empirical $W/(cm^2 K)$	λ/T $W/(cm K^2)$	λ_o/T $W/(cm K^2)$
OFHC-Cu 1	$(0.085 \pm 0.008) T^{3.34}$	± 0.27	0.73 ± 0.07	--	1.03 ± 0.10	0.93 ± 0.10
OFHC-Cu 2	$(0.048 \pm 0.004) T^{4.11}$	± 0.27	0.67 ± 0.06	0.74	1.03 ± 0.10	0.93 ± 0.10
Nb 1	$(0.017 \pm 0.002) T^{3.62}$	± 0.32	0.18 ± 0.03	--	--	--
Nb 2	$(0.020 \pm 0.003) T^{4.65}$	± 0.28	0.40 ± 0.05	0.88	--	--
Al(RRR = 13000)	$(0.035 \pm 0.002) T^{4.21}$	± 0.28	0.52 ± 0.03	0.63	--	135 ± 20
Al 6061	$(0.09 \pm 0.03) T^3$	± 0.4	0.6 ± 0.2	--	0.027 ± 0.002	0.018

Δn is the possible uncertainty in the exponent of the temperature dependence of h_o . " h_o , empirical" is an approximate empirical estimate from reference 2.

The values quoted for h_o and λ/T are average values of the experimental data.

The value $\lambda_o(Al 6061)^{19}$ was not obtained from resistivity measurements on the material used in this experiment. The deviation between λ/T and λ_o/T may well have its origin in different composition of the alloy.

Figure Captions

- fig. 1: Schematic drawing of the lower inner part of the cryostat
- fig. 2: Thermal conductivity of OFHC-copper and of the aluminum alloy Al 6061
- fig. 3: Kapitza conductance of OFHC-copper and niobium
- fig. 4: Thermal conductivity of niobium
- fig. 5: Kapitza conductance of high purity aluminum and of the aluminum alloy Al 6061

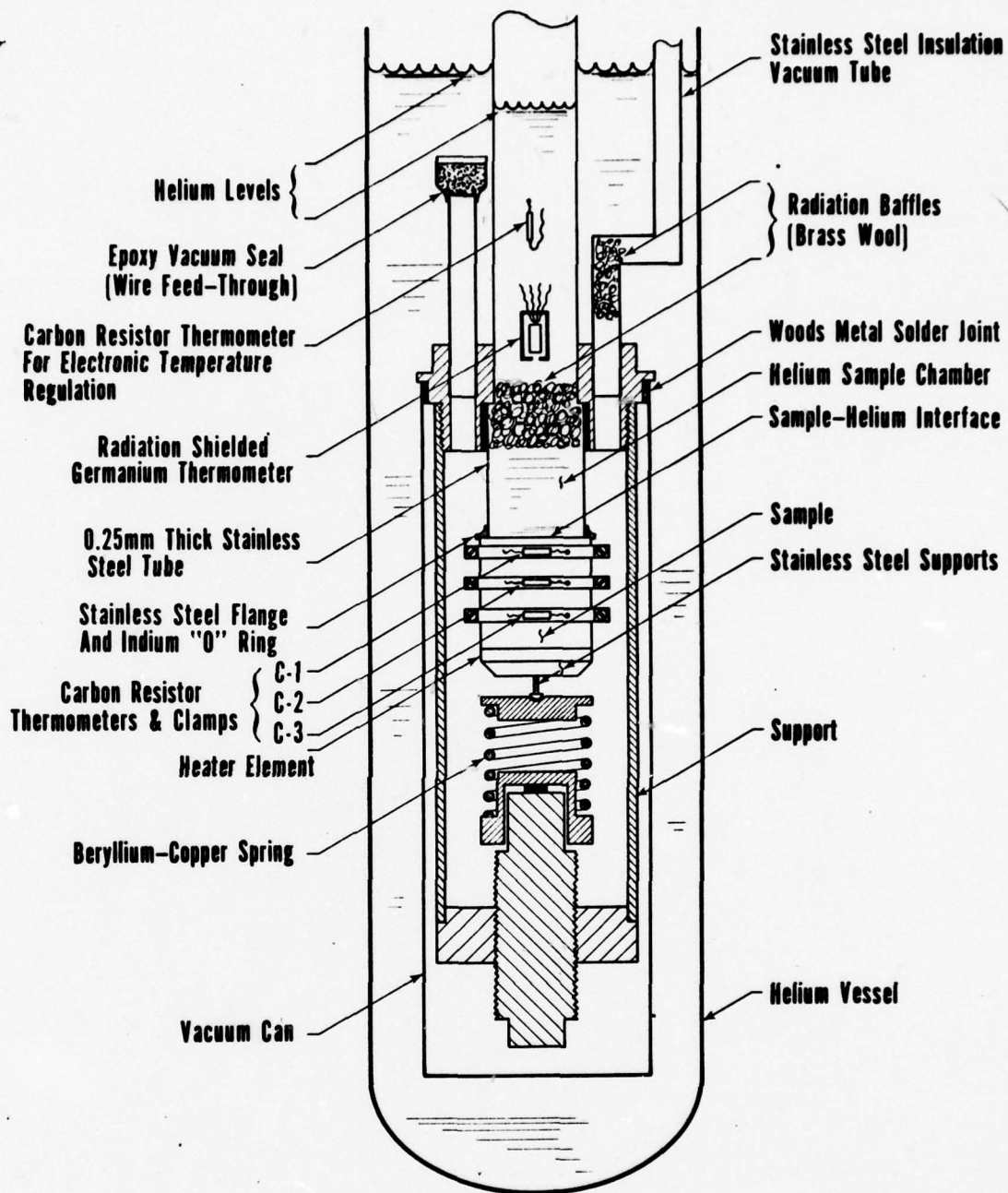


Figure 1: Schematic drawing of the lower inner part of the cryostat.

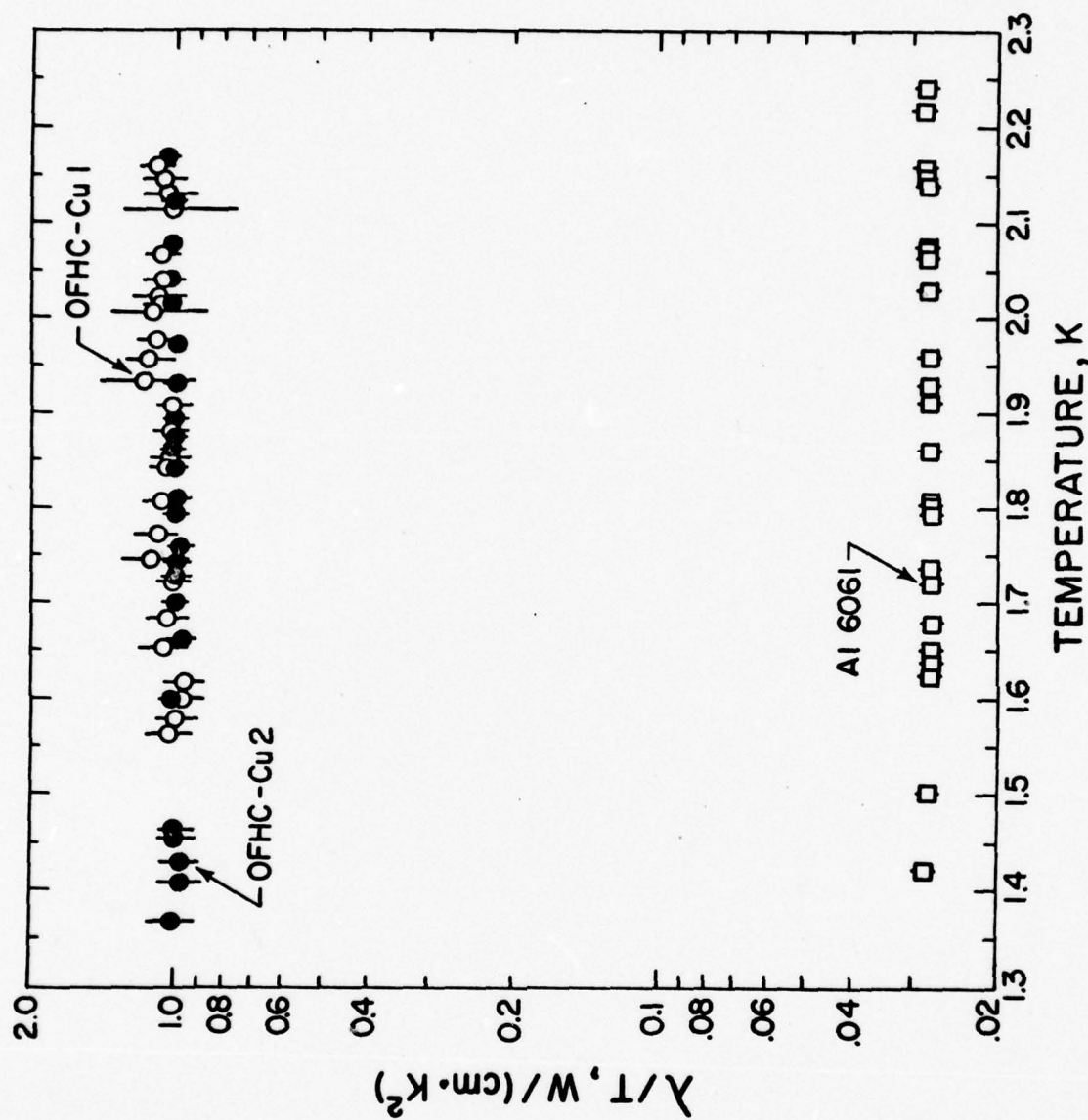


Figure 2: Thermal conductivity of OFHC-copper and of the aluminum alloy Al 6061.

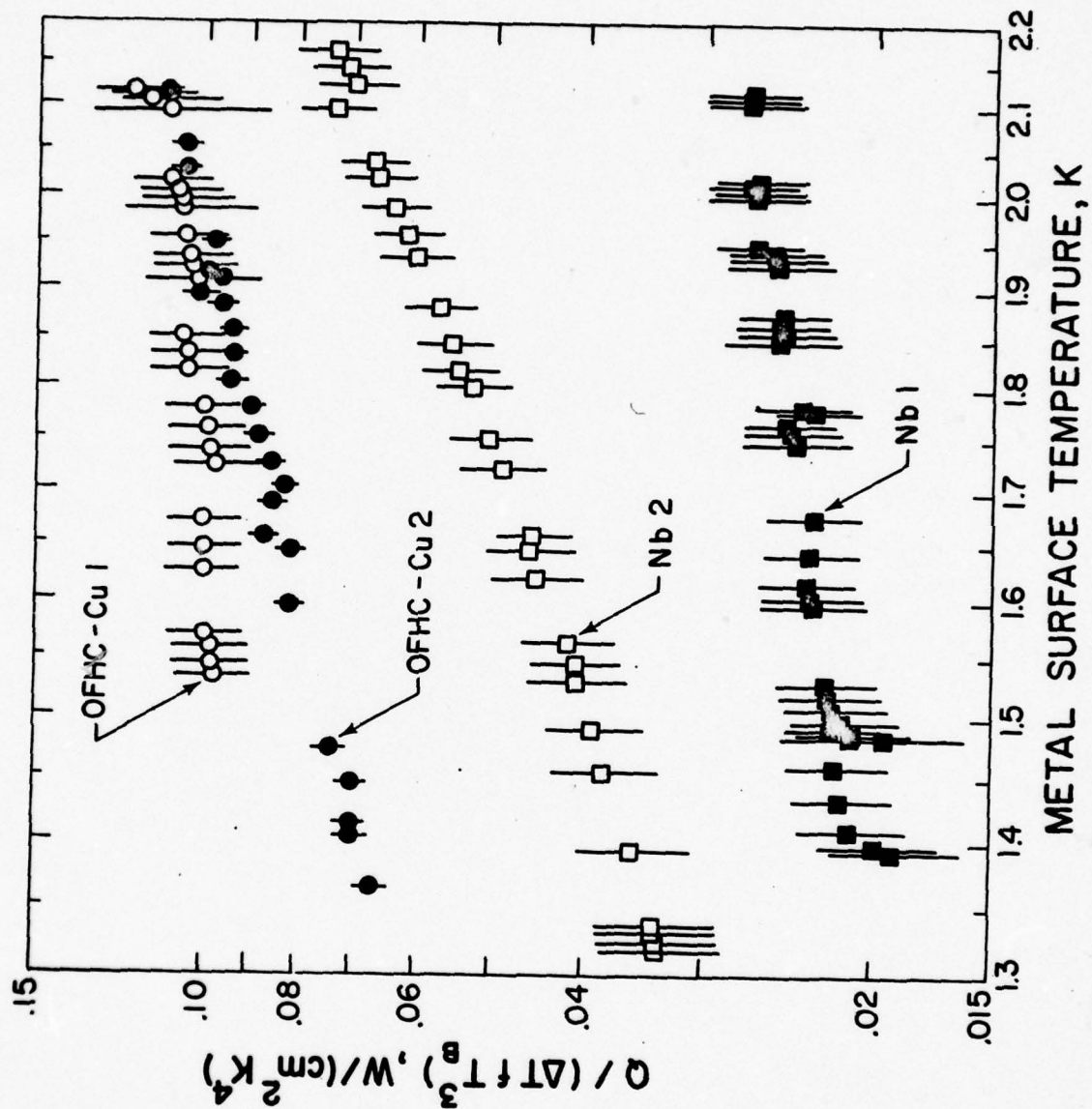


Figure 3: Kapitza conductance of OFHC-copper and niobium.

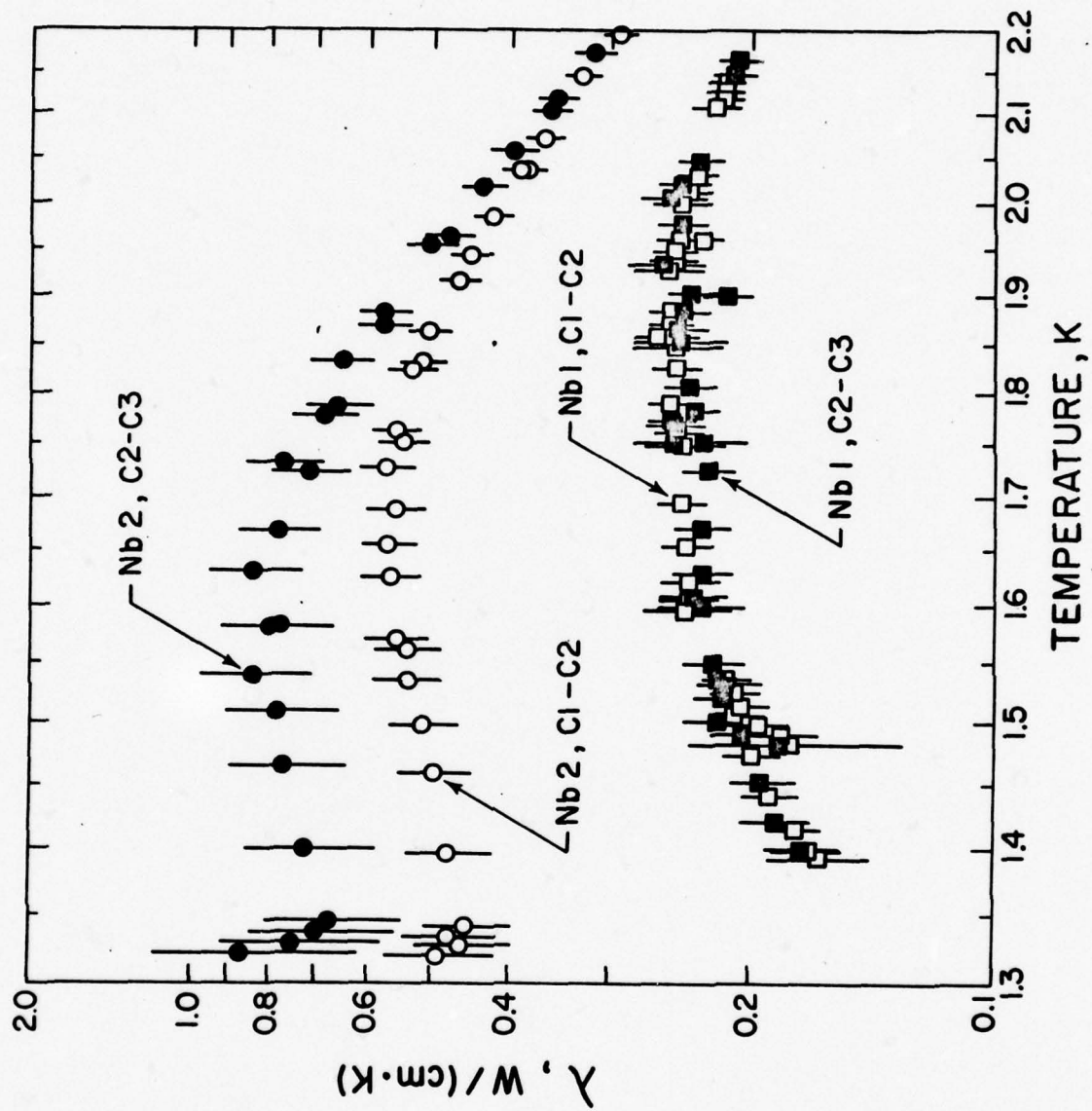


Figure 4: Thermal conductivity of niobium.

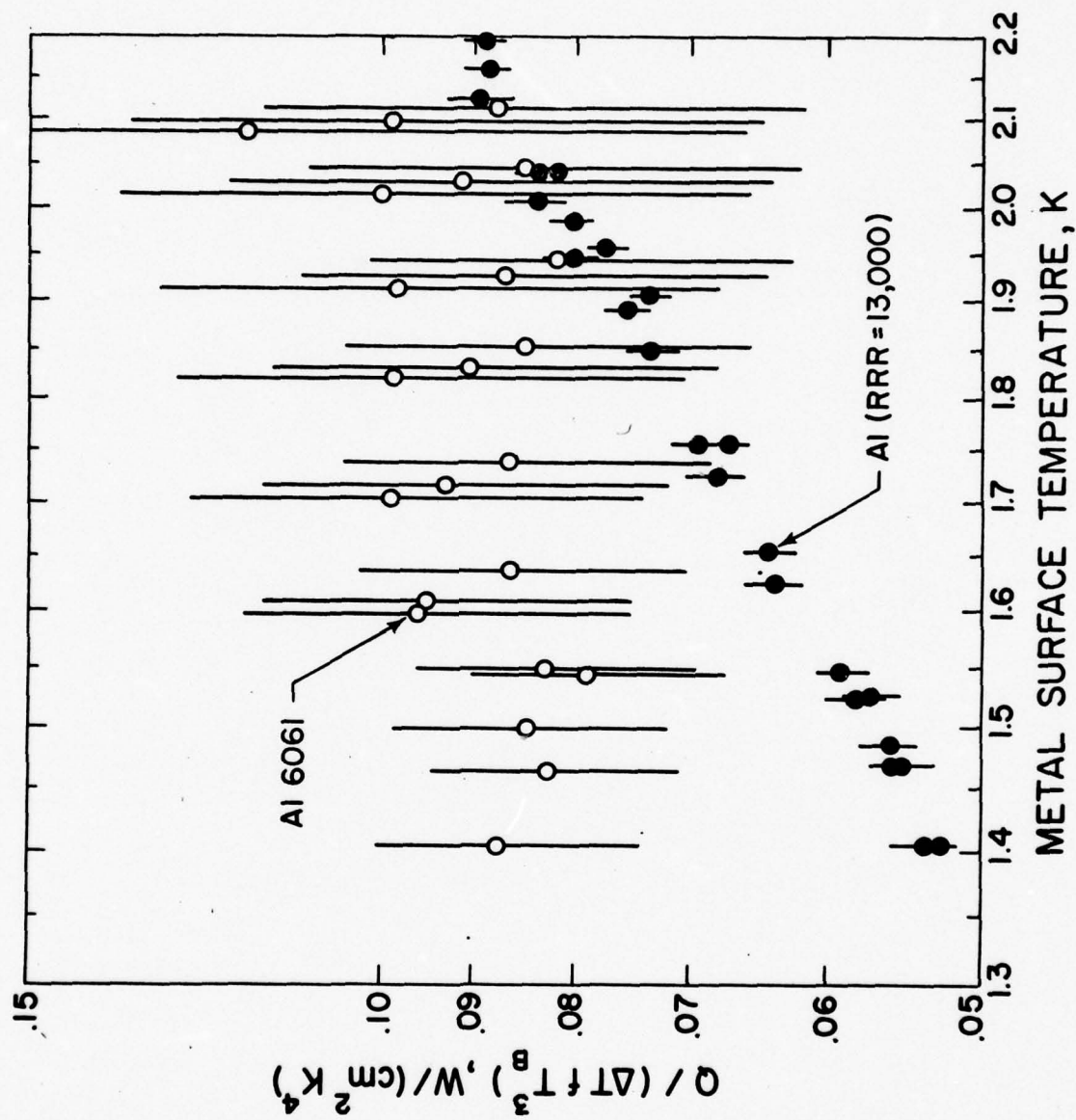


Figure 5: Kapitza conductance of high purity aluminum and of the aluminum alloy Al 6061.

4. PROPERTIES SUMMARY AND RELATED WORK AT NBS

4.1 NEW EQUATION OF STATE - R. D. McCarty

Tables of properties and parameters presented in the previous report (Arp, et al., 1971) were based on an interim equation of state by R. D. McCarty [1970]. The values tabulated in section 4.2 of this report reflect revisions and improvements in that equation. The new equation (McCarty 1972) differs from the previous interim equation primarily in the computation of properties and property derivatives in the critical region. Tabulated values of density vary from those of the previous report by no more than four percent and generally less than one half percent. However, in a few instances, the properties and parameters which depend upon derivatives of the properties are changed by as much as thirty percent. It should be pointed out that these large changes are restricted to a small region near the critical, in which experimental uncertainties are equally large. In all regions, the new equation represents the experimental data more closely than the previous interim equation. Following is a FORTRAN listing of the new equation of state including subprograms which return properties as follows: (Pressure, temperature, and density arguments have the units atmospheres, degrees K, and moles per liter, respectively).

FINDD (P, T, D) returns density, mols/l (D is a first approximation of density)

DPDTVP (T) returns the derivative $\partial P/\partial T$, atm/K, along the vapor pressure curve

VPTEMP (P) returns saturation temperature, K

VPN (T) returns saturation pressure, atm

DSATV (T) returns saturated vapor density, g/mol

DPDD (D, T) returns the derivative $(\partial P / \partial \rho)_T$, atm · l/mol
 CP (D, T) returns specific heat at constant pressure, J/mol · K
 CV (D, T) returns specific heat at constant volume, J/mol · K
 ENTROP (D, T) returns entropy, J/mol · K
 ENTHAL (D, T) returns enthalpy, J/mol.
 SOUND (D, T) returns speed of sound, m/s

4.1.1 References

- Arp, V. D., Ballinger, E. R., Giarratano, P. J., Roder, H. M.,
 Smith, R. V., Snyder, N. S., Steward, W. G., and Wallace,
 G. H., "Helium heat transfer," NBS Report 10 703 (Jul 1, 1971).
 McCarty, R. D., "Thermodynamic properties of helium⁴ for tempera-
 tures from 4 to 3000°R with pressures to 15,000 psia," to
 appear (estimated Jul 1972) as an NBS Tech. Note. A future
 edition will appear using SI units.
 McCarty, R. D., "Provisional thermodynamic functions for helium⁴
 for temperatures from 2 to 1500 K with pressures to
 100 MN/m² (1000 atmospheres)," NBS Report 9762 (1970)
 (superseded by preceding reference).

```

FUNCTION D2DBDT2(T)
  DIMENSION A(9)
  DATA(A=-5.0815710041E-7,-1.1168680862E-4,1.1652480354E-2,
1 7.4474587998E-2,-5.3143174768E-1,-9.5759219306E-1,
2 3.9374414843,-5.1370239224,2.0804456338)
C   THIS SUB PROGRAM CALCULATES THE SECOND VIRIAL COEFFICIENT FOR
C   HELIUM. THE RANGE IS FROM 2 TO 1500 DEG K. INPUT IS TEMPERATURE
C   IN DEGREES KELVIN AND IUSE, IF IUSE IS 0 OR NEGATIVE THE ROUTINE
C   CALCULATES B FOR THE EQUATION PV=RT(1+BD+...., FOR OTHER VALUES OF
C   IUSE, THE ROUTINE CALCULATES THE VARIANCE OF B AT THE INPUT TEMP
C   UNITS ARE ATM, DEG KELVIN, AND MOLES/LITER, 5/28/70-1630, R.D. MCCARTY
1 B=0
  DO 5 I=1,9
    FI=I
5 B=B+T**(.5-FI/2.-1.)*(1.5-FI/2.)*(1.5-FI/2.)*A(I)
  D2DBDT2=B
  RETURN
  END

```

```

FUNCTION FINDD(PI, TI, DI)
  T=TI
  P=PI
  D=DI
7 DO 10 I=1,50
  P2=DTPRESS(D,T)
  IF(ABS(P-P2)-1.E-7)*P)20,20,8
8 DP=DPDD(D,T)
  CORR=(P2-P)/DP
  IF(ABS(CORR)-1.E-7)*D)20,20,10
10 D=D-CORR
  FIND D=D
  RETURN
20 FIND D=D
  RETURN
  END

```

```

FUNCTION VPN(TT)
  DIMENSION C(12), D(14)
  DATA(C=-3.9394635287,141.27497598,-1640.7741565,11974.557102,
1 -55283.309818,166219.56504,-325212.82840,398843.22750,
2 -277718.06992,83395.204183)
  DATA(D=-49.510540356,651.9236417,-3707.5430856,12880.673491,
1 -30048.545554,49532.267436,-59337.558548,52311.296025,
2 -33950.233134,16028.674003,-5354.1038967,1199.0301906,
3 -161.46362959,9.8811553386)
  T=TT
  P=0
  IF(T-2.1720)10,10,1
1 DO 5 I=1,10
5 P=P+C(I)*T**(2-I)
  VP=EXP(P)
  RETURN
10 DO 15 I=1,14
15 P=P+D(I)*T**(2-I)
  VPN=EXP(P)
  RETURN
  END

```



```

      A(N)=(D4*D)/5.      $ N=N+1
      A(N)=(D4*D/5.)*(2./T)      $ N=N+1
      DO 402 I=1,6
      FI=I
      A(N)=(D4/4.)*(T**(.75-FI/4.)-T**(.75-FI/4.)*(.75-FI/4.))
402  N=N+1
      DO 403 I=1,4
      FI=I
      A(N)=(D3/3.)*(T**(1.5-FI)-T**(1.5-FI)*(1.5-FI))
403  N=N+1
      DO 401 I=1,8
      FI=I
      A(N)=(D2/2.)*(T**(1.5-FI/2.)-T**(1.5-FI/2.)*(1.5-FI/2.))
401  N=N+1
      DO 404 I=1,3
      FI=I
      A(N)=(EX/(2.*GAMMA))*(T**(1.-FI)-T**(1.-FI)*(1.-FI))
404  N=N+1
      DO 405 I=1,3
      FI=I
      A(N)=(D2*EX/(2.*GAMMA)-EX/(2.*GAMMA**2))*(T**(1.-FI)-T**(1.-FI)
      1*(1.-FI))
405  N=N+1
      N=N-1
      HINT=R*T*T*D*DBDT(T) *(-1.)
      DO 406 I=1,N
406  HINT=HINT+B(I,M)*A(I)
      N=21
      D2=0
      EX=1.
      DO 410 I=1,3
      FI=I
      A(N)=(EX/(2.*GAMMA))*(T**(1.-FI)-T**(1.-FI)*(1.-FI))
410  N=N+1
      DO 411 I=1,3
      FI=I
      A(N)=(D2*EX/(2.*GAMMA)-EX/(2.*GAMMA**2))*(T**(1.-FI)-T**(1.-FI)
      1*(1.-FI))
411  N=N+1
      N=N-1
      DO 412 I=21,N
412  HINT=HINT-B(I,M)*A(I)
      P=36.5582+5.193043*(T-4.2144)+25.31469*(HINT+PP/D-R*T)
      P=P*4.0026
      I=M
      GO TO(50,50,30,40)K
500  D2=D*D
      D3=D2*D
      D4=D3*D
      N=1
      R=.0820558
      M=1
      GAMMA=R(27,M)
      EX=EXP(D2*GAMMA)
      SINT=T*D*R*(2.*DBDT(T)+D2DBDT2(T)*T)
      A(N)=0.0 $ N=N+1
      A(N)=(D4*D/5.)*T**(-2.)*(-1.)*(-2.) $ N=N+1
      DO 502 I=1,6
      FI=I
      A(N)=(D4/4.)*T**(.75-FI/4.-1.)*(.75-FI/4.)*(.75-FI/4.-1.)
502  N=N+1
      DO 503 I=1,4
      FI=I

```

```

      A(N)=(D3/3.)* T**((1.5-FI-1.)*(1.5-FI)*(1.5-FI-1.))
503 N=N+1
      DO 501 I=1,3
      FI=I
      A(N)=(D2/2.)*T**((1.5-FI/2.-1.)*(1.5-FI/2.)*(1.5-FI/2.-1.))
501 N=N+1
      DO 504 I=1,3
      FI=I
      A(N)=(EX/(2.*GAMMA))*T**((1.-FI-1.)*(1.-FI)*(1.-FI-1.))
504 N=N+1
      DO 505 I=1,3
      FI=I
      A(N)=(D2*EX/(2.*GAMMA)-EX/(2.*GAMMA**2))*
      T**((1.-FI-1.)*(1.-FI)*(1.-FI-1.))
505 N=N+1
      N=N-1
      DO 506 I=1,N
506 SINT=SINT+B(I,M)*A(I)
      P=SINT
      EX=1.
      D2=0
      N=21
      DO 510 I=1,3
      FI=I
      A(N)=(EX/(2.*GAMMA))*T**((1.-FI-1.)*(1.-FI)*(1.-FI-1.))
510 N=N+1
      DO 511 I=1,3
      FI=I
      A(N)=(D2*EX/(2.*GAMMA)-EX/(2.*GAMMA**2))*
      T**((1.-FI-1.)*(1.-FI)*(1.-FI-1.))
511 N=N+1
      N=N-1
      DO 512 I=21,N
512 P=P-B(I,M)*A(I)
      P=5.193043*(3./5.)*4.0026-P*101.3278
      I=M
      GO TO(50,50,30,40)K
20 K=2
      I=3
      T=TT
      D=DD
      GO TO 8
30 K=3
      GO TO(33,34,35)KK
33 D=DD
      T=TT
      KK=2
      IF(DD.GT.17.3987)GO TO 40
      I=1
      GO TO 8
34 PTI=P
      I=3
      KK=3
      T=TT
      D=DD
      GO TO 8
35 PTIII=P
38 F=(15.-T)/5.
      P=F*PTI+(1.-F)*PTIII
      IF(KH.LT.1)GO TO 413
      DTPRESS=P
      RETURN

```

```

40 IF(K.EQ.3)K1=3
   GO TO(41,42,43,44)K4
41 K=4
   I=2
   K4=2
   D=DD
   IF(K1.EQ.0)T=TT
   GO TO 8
42 PIID=P
   D=17.3987
   IF(T.LT.5.2014)D=DSATL(T)*1000./4.0026
   K4=3
   GO TO 8
43 PIIDC=P
   I=1
   K4=4
   GO TO 8
44 PIDC=P
   P=PIDC+(PIID-PIIDC)
   K4=1
   IF(K1.EQ.3)GO TO 30
   DTPRESS=P
   RETURN
50 DTPRESS=P
   RETURN
   END

```

```

FUNCTION CP(D,T)
CP=CV(D,T)+(T*(DPDT(D,T)**2)/((D**2)*DPDD(D,T)))*101.3278
RETURN
END

```

```

FUNCTION SOUND(D,T)
SOUND=((CP(D,T)/CV(D,T))*(DPDD(D,T)*25311.))**.5
RETURN
END

```

```

C FUNCTION P MELT(TT)
TEMPORARY EQUATION, NOT ACCURATE FOR LOW TEMPS
T=TT
PMELT=-17.80+17.31457*T**1.555414
PMELT=PMELT*.98066/1.01325
RETURN
END

```

```

FUNCTION DSATV(TT)
DIMENSION GV(6),GL(6)
DATA(GL=.12874326484,-.43128217346,1.7851911824,-3.3509624489,
1 3.0344215824,-1.0981289602)
DATA(GV=-.069267495322,-.1292532553,.29347470712,-.40806658212,
1 .35809505624,-.11315580397)
DATA(DC=.06964)
DATA(TC=5.2014)
T=TT
DCAL=DC
R=(1.-T/TC)

```



```

DO 1 I=1,6
FI=I
1 DCAL=DCAL+GV(I)*R**(FI/3.)
DSATV=DCAL
RETURN
ENTRY DSATL
T=TT
DCAL=DC
R=(1.-T/TC)
DO 2 I=1,6
FI=I
2 DCAL=DCAL+GL(I)*R**(FI/3.)
DSATV=DCAL
RETURN
END

```

```

FUNCTION VIRB(T)
DIMENSION A(9),V(45)
DATA(A=-5.0815710041E-7,-1.1168680862E-4,1.1652480354E-2,
1 7.4474587998E-2,-5.3143174768E-1,-9.5759219306E-1,
2 3.9374414843,-5.1370239224,2.0804456338)
C COEFFICIENTS FROM PROGRAM 5/28/70-1630
C THIS SUB PROGRAM CALCULATES THE SECOND VIRIAL COEFFICIENT FOR
C HELIUM. THE RANGE IS FROM 2 TO 1500 DEG K. INPUT IS TEMPERATURE
C IN DEGREES KELVIN AND IUSE, IF IUSE IS 0 OR NEGATIVE THE ROUTINE
C CALCULATES B FOR THE EQUATION PV=RT(1+BD+...., FOR OTHER VALUES OF
C IUSE, THE ROUTINE CALCULATES THE VARIANC OF B AT THE INPUT TEMP
C UNITS ARE ATM, DEG KELVIN, AND MOLES/LITER,4/3/69-1253,R.D.MCCARTY
C REVISED 2/12/70-925
1 B=0
DO 5 I=1,9
FI=I
5 B=B+T**((1.5-FI/2.)*A(I))
VIRB=B
RETURN
END

```

```

FUNCTION DBDT (T)
DIMENSION A(9),V(45)
C THIS SUB PROGRAM CALCULATES THE SECOND VIRIAL COEFFICIENT FOR
C HELIUM. THE RANGE IS FROM 2 TO 1500 DEG K. INPUT IS TEMPERATURE
C IN DEGREES KELVIN AND IUSE, IF IUSE IS 0 OR NEGATIVE THE ROUTINE
C CALCULATES B FOR THE EQUATION PV=RT(1+BD+...., FOR OTHER VALUES OF
C IUSE, THE ROUTINE CALCULATES THE VARIANC OF B AT THE INPUT TEMP
DATA(A=-5.0815710041E-7,-1.1168680862E-4,1.1652480354E-2,
1 7.4474587998E-2,-5.3143174768E-1,-9.5759219306E-1,
2 3.9374414843,-5.1370239224,2.0804456338)
C UNITS ARE ATM, DEG KELVIN, AND MOLES/LITER,5/28/70-1630,R.D.MCCARTY
1 B=0
DO 5 I=1,9
FI=I
5 B=B+T**((.5-FI/2.)*A(I))*(1.5-FI/2.)
DBDT=B
RETURN
END

```

```
FUNCTION DELT(TT)
T=TT
DELT=.001+.002*T
RETURN
END
```

THIS PAGE IS BEST QUALITY PRACTICABLE
FROM COPY FURNISHED TO DDG

```

FUNCTION DPDTVP(TT)
  DIMENSION C(12),D(14)
  DATA(C=-3.9394635287,141.27497598,-1640.7741565,11974.557102,
1-55283.309818,166219.56504,-325212.82840,398843.22750,
2-277718.06992,83395.204183)
  DATA(D=-49.510540356,651.9236417,-3707.5430856,12880.673491,
1 -30048.545554,49532.267436,-59337.558548,52311.296025,
2-33950.233134,16028.674003,-5354.1038967,1199.0301906,
3 -161.46362959,9.8811553386)
  P=0
  T=TT-DELT(TT)
  IF(T-2.1720)10,10,1
1 DO 5 I=1,10
5 P=P+C(I)*T**((1-I)*(2-I))
  DPDTVP=P*VPN(T)
  RETURN
10 DO 15 I=1,14
15 P=P+D(I)*T**((1-I)*(2-I))
  DPDTVP=P*VPN(T)
  RETURN
END

```

```

FUNCTION VPTEMP(PP)
  P=PP
  IF(P.LT.6.4E+5) GOTO 12
  T=5.0
  PCAL=VPN(T)
  GO TO 13
12 PCAL=37800.
  IF(ABS(P-PCAL)-.0000001*PP)11,11,1
1 T=2.1720
13 DO 10 I=1,50
  DP=DPDTVP(T)
  DEL=(PCAL-P)/DP
  T=T-DEL
  PCAL=VPN(T)
  IF(ABS(P-PCAL)-.0000001*P)11,11,2
2 IF(ABS(DEL)-.0000001*T)11,11,10
10 CONTINUE
  PRINT 100,T
11 VPTEMP=T
  RETURN
100 FORMAT(* TEMPERATURE ITERATION FAILED AT T=*,E14.7)
END

```



```

FUNCTION DTPRESS(DD,TT)
DIMENSION A(26),R(27,3)
COMMON/COEFF/R
DATA((B(I),I=55,81))=-1.4802195348E-8,4.1721791119E-7,-2.3326553271
1E-7,4.085511088E-7,1.0900567964E-5,-5.0060952775E-5,1.1312765043
2E-4,-1.2539843287E-4,1.9661380688E-6,1.7122932666E-4,2.3051000563
3E-4,-9.65647391E-4,-3.6027 735292E-5,1.6079946555E-3,-2.7441763615
4E-2,.14739506957,-.43559344838,1.3447956078,-1.7040375125,.9026267
54040,5.6875644111E-3,-1.4438146625E-1,3.3768874851E-3,1.0754201218
6E-6,-4.5264622308E-5,3.8597388864E-5,-.0005)
DATA((B(I),I=28,54))=-4.2287454626E-8,4.4529354413E-7,-1.0246150954
1E-5,8.5254608956E-5,-2.5163069255E-4,3.2877709285E-4,-1.060195758
2E-4,-1.0687738074E-4,-3.2120950632E-5,1.415901897E-4,1.4725630701
4E-3,-2.618354941E-3,2.0461501117E-5,1.2746996288E-3,-2.0272929583
5E-2,7.4648036615E-2,-.17217966521,.51053439738,-.40178202697,
6.26829864632,7.906601204E-3,-8.9393485656E-2,-.15076580053,
72.6882494327E-6,-3.3794316835E-5,-2.4495951195E-5,-.0005)
DATA((B(I),I=1,27))=
A      -1.5096862619E-7,6.4640898904E-7,4.1362357367E-5,
1-3.7910190353E-4,1.3806454049E-3,-2.5085412058E-3,2.3697560398E-3
2,-9.5726461066E-4,3.7405931828E-5,-6.4103220333E-4,
31.8579366177E-3,7.4007986606E-4,1.4792568148E-4,-3.2531355477E-3,
41.9518739286E-2,-.10571817135,.33164944449,-.51130022535,
53.9940004906E-1,-.15555244471,4.906264031E-3,-2.6148004377E-2,
63.4221685545E-2,5.4159662622E-6,-1.0687806777E-5,-8.9484651869E-6,
7,-.0025)
KP=1
GO TO 10
ENTRY DPDT
KP=2
GO TO 10
ENTRY DPDD
KP=3
GO TO 10
ENTRY ENTROP
KP=4
GO TO 10
ENTRY ENTHAL
KP=5
GO TO 10
ENTRY CV
KP=6
10 K1=0
KH=1
K=1
KK=1
K4=1
IF(TT.GE.15)GO TO 20
IF(TT.GT.10)GO TO 30
IF(DD.GT.17.3987)GO TO 40
11 I=1
T=TT
D=DD
8 GO TO (9,100,200,300,400,500)KP
9 D2=D*D
D3=D2*D
D4=D3*D
D5=D4*D
GAMMA=R(27,I)
EX=EXP(-D2/GAMMA)
EXD3=EX*D3
EXD5=EX*D5

```

```

M=I
N=1
A(N)=D5*D $ N=N+1
A(N)=A(N-1)/T $ N=N+1
DO 2 I=1,6
FI=I
A(N)=D5*T**(.75-FI/4.)
2 N=N+1
DO 3 I=1,4
FI=I
A(N)=D4*T**(1.5-FI)
3 N=N+1
DO 1 I=1,8
FI=I
A(N)=D3*T**(1.5-FI/2.)
N=N+1
1 CONTINUE
DO 4 I=1,3
FI=I
A(N)=EXD3*T**(1.-FI)
4 N=N+1
DO 5 I=1,3
FI=I
A(N)=EXD5*T**(1.-FI)
5 N=N+1
N=N-1
I=M
7 P=0
DO 15 J=1,N
15 P=P+B(J,I)*A(J)
P=P+.0820558*D*T*(1.+VIRB(T)*D)
IF(KH.LT.1)GO TO 413
GO TO(50,50,30,40)K
100 D2=D*D
D3=D**3
D4=D3*D
D5=D4*D
D6=D5*D
T2=T*T
T3=T2*T
T4=T**4
M=I
GAMMA=B(27,M)
EX=EXP(D2*GAMMA)
N=1
R=.0820558
A(N)=0.0 $ N=N+1
A(N)=(-1.)*D6/T2 $ N=N+1
DO 102 I=1,6
FI=I
A(N)=D5*T**(.75-FI/4.-1.)*(.75-FI/4.)
102 N=N+1
DO 103 I=1,4
FI=I
A(N)=D4*T**(1.5-FI/1.-1.)*(1.5-FI)
103 N=N+1
DO 101 I=1,8
FI=I
A(N)=D3*T**(1.5-FI/2.-1.)*(1.5-FI/2.)
101 N=N+1

```

```

DO 104 I=1,3
FI=I
A(N)=EX*D3*T**((1.-FI-1.)*(1.-FI))
104 N=N+1
DO 105 I=1,3
FI=I
A(N)=EX*D5*T**((1.-FI-1.)*(1.-FI))
105 N=N+1
N=N-1
P=0
DO 115 J=1,N
115 P=P+A(J)*B(J,M)
P=P+R*D*(1.+VIRB(T)*D)+R*D*T*DBDT(T)*D
I=M
GO TO(50,50,30,40)K
200 D2=D*D
D3=D2*D
D4=D3*D
D5=D4*D
M=I
GAMMA=R(27,M)
FX=FXPF(D2*GAMMA)
DEX=GAMMA*2.*D*EX
N=1
R=.0820558
A(N)=6.*D5 $ N=N+1
A(N)=A(N-1)/T $ N=N+1
DO 202 I=1,6
FI=I
A(N)=5.*D4*T**(.75-FI/4.)
202 N=N+1
DO 203 I=1,4
FI=I
A(N)=D3*4.*T**((1.5-FI))
203 N=N+1
DO 201 I=1,8
FI=I
A(N)=D2*3.*T**((1.5-FI/2.))
201 N=N+1
DO 204 I=1,3
FI=I
A(N)=(DEX*D3+3.*D2*FX)*T**((1.-FI))
204 N=N+1
DO 205 I=1,3
FI=I
A(N)=(DEX*D5+5.*D4*FX)*T**((1.-FI))
205 N=N+1
N=N-1
P=0
DO 215 J=1,N
215 P=P+A(J)*B(J,M)
I=M
P=P+R*T*(1.+2.*D*VIRB(T))
GO TO(50,50,30,40)K
300 D2=D*D
D3=D2*D
D4=D3*D
N=1
R=.0820558
M=I

```



```

      GAMMA=B(27,M)
      EX=EXP(D2*GAMMA)
      A(N)=0.0      S N=N+1
      A(N)=(D4*D/5.)*T**(-2.)*(-1.) S N=N+1
      DO 302 I=1,6
      FI=I
      A(N)=(D4/4.)*T**(.75-FI/4.-1.)*(0.75-FI/4.)
302 N=N+1
      DO 303 I=1,4
      FI=I
      A(N)=(D3/3.)* T**(1.5-FI-1.)*(1.5-FI)
303 N=N+1
      DO 301 I=1,8
      FI=I
      A(N)=(D2/2.)*T**(1.5-FI/2.-1.)*(1.5-FI/2.)
301 N=N+1
      DO 304 I=1,3
      FI=I
      A(N)=(EX/(2.*GAMMA))*T**(1.-FI-1.)*(1.-FI)
304 N=N+1
      DO 305 I=1,3
      FI=I
      A(N)=(D2*EX/(2.*GAMMA)-EX/(2.*GAMMA**2))*
      1T**(1.-FI-1.)*(1.-FI)
305 N=N+1
      N=N-1
      SINT=D*R*(VIRB(T)+T*DBDT(T))
      DO 306 I=1,N
306 SINT=SINT+B(I,M)*A(I)
      N=21
      EX=1.
      D2=0
      DO 310 I=1,3
      FI=I
      A(N)=(EX/(2.*GAMMA))*T**(1.-FI-1.)*(1.-FI)
310 N=N+1
      DO 311 I=1,3
      FI=I
      A(N)=(D2*EX/(2.*GAMMA)-EX/(2.*GAMMA**2))*
      1T**(1.-FI-1.)*(1.-FI)
311 N=N+1
      N=N-1
      DO 312 I=21,N
312 SINT=SINT-B(I,M)*A(I)
      P=(9.2609+5.193043*LOGF(T/4.2144)-25.31469*(SINT+R*LOGF(R*T*D)))
      P=P*4.0026
      I=M
      GO TO(50,50,30,40)K
400 KH=0
      GO TO 9
413 PP=P
      KH=1
      D2=D*D
      D3=D*D2
      D4=D3*D
      N=1
      R=.0820558
      M=I
      GAMMA=B(27,M)
      EX=EXP(D2*GAMMA)

```

4.2 SUMMARY OF USEFUL TRANSPORT AND THERMODYNAMIC PROPERTIES - TABLES - W. G. Steward

The tables of properties and parameters in this section supersede those presented in the previous report of Arp, et al., [1971]. The new tables not only reflect the revisions in the equation of state, but are more extensive and are presented in a uniform format. The properties which have been added are density, specific heat at constant pressure, specific heat at constant volume, and the Joule-Thomson coefficient.

In the following tables, the increments of the pressure and temperature arguments vary with the region being tabulated. Relatively small increments are taken in the range $0.01 < P < 0.7$ MN/m² and $3 < T < 10$ K, since this is a region of rapid, non-linear change in the properties, as well as a region of particular interest. A wide range, $0.7 < P < 10$ MN/m² and $11 < T < 300$ K, is covered in succeeding parts of the tables. In these wide range tables, the increments are increased, consistent with the more gradual and more linear changes in the properties.

Viscosity is computed from the equation of Steward (Arp, et al., 1971) and all of the thermodynamic properties and thermal conductivity are computed from the helium properties computational package of McCarty (see section 4.1). The tables are arranged as follows:

- Table 4.2.1 Helium⁴ Thermal Conductivity, mW/cm·K
- Table 4.2.2 Helium⁴ Viscosity, μ g/cm·s
- Table 4.2.3 Helium⁴ Density, mg/cm³
- Table 4.2.4 Helium⁴ Specific Heat at Constant Pressure, J/g·K
- Table 4.2.5 Helium⁴ Specific Heat at Constant Volume, J/g·K

Table 4.2.6 $(P/T)(\partial T/\partial P)_h$ for Helium⁴

Table 4.2.7 Helium⁴ Prandtl Number

Table 4.2.8 $(P/\rho)(\partial \rho/\partial P)_T$ for Helium⁴

Table 4.2.9 Helium⁴ Bulk Expansivity

In tables 4.2.1 through 4.2.9, no more than three digits are significant. Excess digits appear in some parts of the tables as a result of retaining at least three in other parts.

4.2.1 References

Arp, V. D., Ballinger, E. E., Giarratano, P. J., Roder, H. M.,
Smith, R. V., Snyder, N. S., Steward, W. G., and Wallace,
G. H., "Helium heat transfer," NBS Report 10 703 (Jul 1, 1971).

Table 4.2.1 Helium⁴ thermal conductivity, K, mW/cm-K.

PHES MM/M ² ATM	0.010	0.051	0.101	0.152	0.182	0.193	0.203	0.213	0.223	0.233	0.243	0.253
TEMP. K	0.100	0.500	1.000	1.500	1.800	1.900	2.000	2.100	2.200	2.300	2.400	2.500
3.0	0.065	0.179	0.182	0.184	0.185	0.185	0.185	0.186	0.186	0.187	0.187	0.187
3.5	0.075	0.188	0.191	0.194	0.195	0.196	0.196	0.196	0.197	0.197	0.198	0.198
4.0	0.085	0.092	0.196	0.200	0.202	0.203	0.204	0.204	0.205	0.205	0.206	0.207
4.2	0.088	0.094	0.197	0.201	0.204	0.204	0.205	0.206	0.207	0.207	0.208	0.209
4.4	0.092	0.097	0.113	0.201	0.204	0.205	0.206	0.207	0.207	0.208	0.209	0.210
4.6	0.096	0.100	0.112	0.204	0.202	0.203	0.204	0.206	0.207	0.208	0.209	0.210
4.8	0.099	0.103	0.112	0.141	0.212	0.211	0.210	0.210	0.210	0.210	0.210	0.211
5.0	0.103	0.106	0.114	0.131	0.169	0.224	0.239	0.228	0.222	0.219	0.217	0.216
5.1	0.104	0.108	0.115	0.129	0.153	0.172	0.217	0.316	0.254	0.235	0.227	0.223
5.2	0.106	0.109	0.116	0.128	0.145	0.156	0.173	0.210	0.366	0.348	0.259	0.238
5.3	0.107	0.111	0.117	0.128	0.141	0.148	0.158	0.174	0.203	0.277	0.696	0.340
5.4	0.109	0.112	0.118	0.128	0.139	0.144	0.151	0.160	0.174	0.197	0.241	0.346
5.5	0.111	0.114	0.119	0.128	0.137	0.141	0.146	0.153	0.162	0.174	0.192	0.222
5.6	0.112	0.115	0.121	0.129	0.136	0.140	0.144	0.149	0.155	0.163	0.174	0.188
5.7	0.114	0.117	0.122	0.129	0.136	0.139	0.142	0.146	0.151	0.157	0.164	0.173
5.8	0.115	0.118	0.123	0.130	0.136	0.138	0.141	0.145	0.148	0.153	0.158	0.165
5.9	0.117	0.120	0.124	0.131	0.136	0.138	0.141	0.144	0.147	0.150	0.155	0.160
6.0	0.119	0.121	0.126	0.132	0.137	0.139	0.141	0.143	0.146	0.149	0.152	0.156
6.2	0.122	0.124	0.128	0.134	0.138	0.139	0.141	0.143	0.145	0.148	0.150	0.153
6.4	0.125	0.127	0.131	0.136	0.139	0.141	0.142	0.144	0.146	0.147	0.149	0.152
6.6	0.128	0.130	0.134	0.138	0.141	0.142	0.144	0.145	0.147	0.148	0.149	0.152
6.8	0.130	0.133	0.136	0.140	0.143	0.144	0.145	0.147	0.148	0.149	0.151	0.152
7.0	0.133	0.135	0.139	0.143	0.145	0.146	0.147	0.148	0.150	0.151	0.152	0.153
7.5	0.140	0.142	0.145	0.148	0.151	0.152	0.152	0.153	0.154	0.155	0.156	0.157
8.0	0.147	0.149	0.151	0.154	0.156	0.157	0.158	0.159	0.159	0.160	0.161	0.162
8.5	0.153	0.155	0.157	0.160	0.162	0.163	0.163	0.164	0.165	0.165	0.166	0.167
9.0	0.159	0.161	0.163	0.166	0.168	0.168	0.169	0.169	0.170	0.171	0.171	0.172
9.5	0.165	0.167	0.169	0.172	0.173	0.174	0.174	0.175	0.175	0.176	0.176	0.177
10.0	0.171	0.173	0.175	0.177	0.178	0.179	0.179	0.180	0.180	0.181	0.182	0.182
11.0	0.182	0.184	0.186	0.188	0.189	0.189	0.190	0.190	0.191	0.191	0.192	0.192
12.0	0.193	0.194	0.196	0.198	0.199	0.200	0.200	0.200	0.201	0.201	0.202	0.202
13.0	0.203	0.204	0.206	0.208	0.209	0.209	0.210	0.210	0.211	0.211	0.211	0.212
14.0	0.212	0.214	0.216	0.217	0.218	0.219	0.219	0.220	0.220	0.220	0.221	0.221
15.0	0.222	0.223	0.225	0.227	0.228	0.228	0.228	0.229	0.229	0.229	0.230	0.230
16.0	0.231	0.232	0.234	0.235	0.236	0.237	0.237	0.237	0.238	0.238	0.239	0.239
17.0	0.240	0.241	0.242	0.244	0.245	0.245	0.246	0.246	0.246	0.247	0.247	0.247
18.0	0.248	0.249	0.251	0.253	0.253	0.254	0.254	0.254	0.255	0.255	0.255	0.256
19.0	0.257	0.258	0.259	0.261	0.262	0.262	0.262	0.263	0.263	0.263	0.264	0.264
20.0	0.265	0.266	0.267	0.269	0.270	0.270	0.270	0.271	0.271	0.271	0.272	0.272
25.0	0.301	0.304	0.306	0.307	0.308	0.308	0.308	0.309	0.309	0.309	0.309	0.310
30.0	0.339	0.340	0.341	0.342	0.343	0.343	0.343	0.344	0.344	0.344	0.344	0.345
35.0	0.373	0.374	0.375	0.376	0.376	0.377	0.377	0.377	0.377	0.377	0.378	0.378
40.0	0.405	0.406	0.407	0.408	0.408	0.409	0.409	0.409	0.409	0.409	0.410	0.410
45.0	0.436	0.437	0.438	0.439	0.439	0.439	0.440	0.440	0.440	0.440	0.440	0.440
50.0	0.466	0.467	0.468	0.469	0.469	0.469	0.469	0.470	0.470	0.470	0.470	0.470
60.0	0.524	0.525	0.525	0.526	0.527	0.527	0.527	0.527	0.527	0.527	0.528	0.528
80.0	0.633	0.633	0.634	0.634	0.635	0.635	0.635	0.635	0.635	0.635	0.636	0.636
100.0	0.735	0.735	0.736	0.736	0.736	0.737	0.737	0.737	0.737	0.737	0.737	0.737
120.0	0.831	0.832	0.832	0.833	0.833	0.833	0.833	0.833	0.833	0.833	0.834	0.834
140.0	0.923	0.924	0.924	0.925	0.925	0.925	0.925	0.925	0.925	0.925	0.926	0.926
160.0	1.012	1.012	1.013	1.013	1.013	1.014	1.014	1.014	1.014	1.014	1.014	1.014
180.0	1.097	1.097	1.098	1.098	1.098	1.098	1.099	1.099	1.099	1.099	1.099	1.099
200.0	1.179	1.179	1.180	1.180	1.180	1.180	1.180	1.180	1.180	1.180	1.181	1.181
220.0	1.258	1.258	1.258	1.259	1.259	1.259	1.259	1.259	1.259	1.259	1.259	1.259
240.0	1.334	1.334	1.334	1.335	1.335	1.335	1.335	1.335	1.335	1.335	1.335	1.335
260.0	1.407	1.408	1.408	1.408	1.408	1.408	1.408	1.409	1.409	1.409	1.409	1.409
280.0	1.478	1.479	1.479	1.479	1.479	1.479	1.479	1.479	1.479	1.480	1.480	1.480
300.0	1.547	1.547	1.547	1.548	1.548	1.548	1.548	1.548	1.548	1.548	1.548	1.548

Table 4.2.1 Helium⁴ thermal conductivity, K, mW/cm-K (continued).

PHES MM/M ² ATM TEMP, K	0.263 2.600	0.274 2.700	0.284 2.800	0.294 2.900	0.304 3.000	0.355 3.500	0.405 4.000	0.456 4.500	0.507 5.000	0.557 5.500	0.608 6.000	0.659 6.500
3.0	0.188	0.188	0.188	0.189	0.189	0.191	0.192	0.194	0.195	0.197	0.198	0.200
3.5	0.199	0.199	0.200	0.200	0.200	0.202	0.204	0.206	0.208	0.210	0.211	0.213
4.0	0.207	0.208	0.208	0.209	0.209	0.212	0.215	0.217	0.219	0.221	0.223	0.225
4.2	0.209	0.210	0.211	0.211	0.212	0.215	0.218	0.220	0.223	0.225	0.227	0.229
4.4	0.211	0.211	0.212	0.213	0.214	0.217	0.220	0.223	0.226	0.228	0.231	0.233
4.6	0.211	0.212	0.213	0.213	0.214	0.218	0.222	0.225	0.228	0.231	0.234	0.236
4.8	0.209	0.210	0.211	0.212	0.213	0.218	0.222	0.226	0.230	0.233	0.236	0.239
5.0	0.215	0.215	0.215	0.215	0.216	0.216	0.222	0.226	0.230	0.234	0.237	0.240
5.1	0.220	0.219	0.218	0.217	0.217	0.219	0.221	0.226	0.230	0.234	0.238	0.241
5.2	0.228	0.223	0.221	0.219	0.219	0.219	0.222	0.225	0.229	0.234	0.238	0.241
5.3	0.264	0.241	0.231	0.226	0.223	0.220	0.222	0.225	0.229	0.234	0.238	0.242
5.4	0.460	0.321	0.266	0.245	0.234	0.222	0.223	0.226	0.228	0.233	0.238	0.242
5.5	0.272	0.338	0.354	0.299	0.264	0.226	0.224	0.226	0.230	0.233	0.238	0.242
5.6	0.210	0.240	0.277	0.306	0.306	0.233	0.226	0.227	0.230	0.234	0.237	0.242
5.7	0.185	0.201	0.222	0.246	0.267	0.245	0.228	0.228	0.231	0.234	0.238	0.241
5.8	0.173	0.183	0.196	0.211	0.227	0.257	0.232	0.229	0.231	0.234	0.238	0.241
5.9	0.166	0.173	0.181	0.191	0.203	0.252	0.237	0.231	0.231	0.234	0.238	0.242
6.0	0.161	0.166	0.173	0.180	0.188	0.234	0.241	0.232	0.232	0.235	0.238	0.242
6.2	0.156	0.160	0.164	0.168	0.173	0.204	0.230	0.235	0.235	0.238	0.242	0.242
6.4	0.154	0.157	0.159	0.163	0.166	0.187	0.211	0.228	0.233	0.235	0.238	0.241
6.6	0.153	0.156	0.158	0.160	0.163	0.178	0.197	0.215	0.227	0.233	0.237	0.240
6.8	0.154	0.155	0.157	0.159	0.161	0.173	0.188	0.204	0.218	0.228	0.234	0.239
7.0	0.155	0.156	0.158	0.159	0.161	0.171	0.183	0.196	0.209	0.220	0.229	0.236
7.5	0.158	0.159	0.160	0.161	0.163	0.169	0.177	0.186	0.196	0.206	0.215	0.224
8.0	0.163	0.163	0.164	0.165	0.166	0.171	0.177	0.184	0.191	0.199	0.207	0.214
8.5	0.167	0.168	0.169	0.170	0.170	0.175	0.179	0.185	0.190	0.197	0.203	0.209
9.0	0.172	0.173	0.174	0.174	0.175	0.179	0.183	0.187	0.192	0.197	0.202	0.208
9.5	0.177	0.178	0.179	0.179	0.180	0.183	0.187	0.190	0.195	0.199	0.203	0.208
10.0	0.183	0.183	0.184	0.184	0.185	0.188	0.191	0.194	0.198	0.202	0.206	0.210
11.0	0.193	0.193	0.194	0.194	0.195	0.197	0.200	0.203	0.206	0.209	0.212	0.215
12.0	0.203	0.203	0.203	0.204	0.204	0.207	0.209	0.211	0.214	0.217	0.219	0.222
13.0	0.212	0.213	0.213	0.213	0.214	0.216	0.218	0.220	0.223	0.225	0.228	0.230
14.0	0.221	0.222	0.222	0.223	0.223	0.225	0.227	0.229	0.231	0.234	0.236	0.238
15.0	0.230	0.231	0.231	0.232	0.232	0.234	0.236	0.238	0.240	0.242	0.244	0.246
16.0	0.239	0.240	0.240	0.240	0.241	0.242	0.244	0.246	0.248	0.250	0.252	0.254
17.0	0.248	0.248	0.248	0.249	0.249	0.251	0.253	0.254	0.256	0.258	0.260	0.262
18.0	0.256	0.256	0.257	0.257	0.257	0.259	0.261	0.262	0.264	0.266	0.268	0.270
19.0	0.264	0.265	0.265	0.265	0.265	0.267	0.269	0.270	0.272	0.274	0.275	0.277
20.0	0.272	0.272	0.273	0.273	0.273	0.275	0.276	0.278	0.280	0.281	0.283	0.285
25.0	0.310	0.310	0.310	0.311	0.311	0.312	0.314	0.315	0.316	0.318	0.319	0.320
30.0	0.345	0.345	0.345	0.346	0.346	0.347	0.348	0.349	0.351	0.352	0.353	0.354
35.0	0.378	0.378	0.379	0.379	0.379	0.380	0.381	0.382	0.383	0.384	0.385	0.387
40.0	0.410	0.410	0.410	0.411	0.411	0.412	0.413	0.414	0.415	0.416	0.417	0.418
45.0	0.441	0.441	0.441	0.441	0.441	0.442	0.443	0.444	0.445	0.446	0.447	0.448
50.0	0.470	0.471	0.471	0.471	0.471	0.472	0.473	0.474	0.475	0.475	0.476	0.477
60.0	0.529	0.528	0.528	0.528	0.528	0.529	0.530	0.531	0.532	0.532	0.533	0.534
80.0	0.636	0.636	0.636	0.636	0.636	0.637	0.638	0.638	0.639	0.640	0.640	0.641
100.0	0.737	0.738	0.738	0.738	0.738	0.738	0.739	0.740	0.740	0.741	0.741	0.742
120.0	0.834	0.834	0.834	0.834	0.834	0.835	0.835	0.836	0.836	0.837	0.837	0.838
140.0	0.926	0.926	0.926	0.926	0.926	0.927	0.927	0.928	0.928	0.929	0.929	0.930
160.0	1.014	1.014	1.014	1.014	1.014	1.015	1.015	1.016	1.016	1.017	1.017	1.018
180.0	1.099	1.099	1.099	1.099	1.099	1.100	1.100	1.101	1.101	1.101	1.102	1.102
200.0	1.181	1.181	1.181	1.181	1.181	1.181	1.182	1.182	1.183	1.183	1.183	1.184
220.0	1.259	1.260	1.260	1.260	1.260	1.260	1.261	1.261	1.261	1.261	1.262	1.262
240.0	1.335	1.336	1.336	1.336	1.336	1.336	1.336	1.337	1.337	1.337	1.338	1.338
260.0	1.409	1.409	1.409	1.409	1.409	1.409	1.410	1.410	1.410	1.411	1.411	1.411
280.0	1.480	1.480	1.480	1.480	1.480	1.480	1.480	1.481	1.481	1.481	1.482	1.482
300.0	1.548	1.548	1.548	1.548	1.548	1.549	1.549	1.549	1.549	1.550	1.550	1.550

Table 4.2.1 Helium⁴ thermal conductivity, K, mW/cm-K (continued).

PRES MM/HG ATM TEMP, K	0.608 6.000	0.709 7.000	0.811 8.000	0.912 9.000	1.013 10.000	1.520 15.000	2.126 20.000	2.533 25.000	3.040 30.000	3.546 35.000	4.053 40.000	4.560 45.000
3.0	0.198	0.201	0.203	0.206	0.208	0.219	0.229	0.238	0.246	0.254	0.261	0.269
3.5	0.211	0.215	0.218	0.221	0.223	0.236	0.246	0.256	0.265	0.274	0.282	0.289
4.0	0.223	0.227	0.231	0.234	0.237	0.251	0.263	0.274	0.284	0.293	0.302	0.311
4.2	0.227	0.231	0.235	0.239	0.242	0.257	0.270	0.281	0.292	0.301	0.310	0.319
4.4	0.231	0.235	0.239	0.243	0.247	0.263	0.276	0.288	0.299	0.309	0.319	0.328
4.6	0.234	0.239	0.243	0.247	0.251	0.268	0.282	0.295	0.306	0.317	0.327	0.336
4.8	0.236	0.241	0.246	0.251	0.255	0.273	0.288	0.301	0.313	0.324	0.334	0.344
5.0	0.237	0.243	0.249	0.254	0.258	0.278	0.294	0.307	0.320	0.331	0.342	0.352
5.1	0.238	0.244	0.250	0.255	0.260	0.280	0.296	0.310	0.323	0.334	0.345	0.356
5.2	0.238	0.245	0.251	0.256	0.261	0.282	0.299	0.313	0.326	0.338	0.349	0.359
5.3	0.238	0.245	0.252	0.257	0.262	0.284	0.301	0.316	0.329	0.341	0.352	0.363
5.4	0.238	0.246	0.252	0.258	0.264	0.286	0.304	0.319	0.332	0.344	0.356	0.367
5.5	0.238	0.246	0.253	0.259	0.265	0.288	0.306	0.321	0.335	0.348	0.359	0.370
5.6	0.237	0.246	0.253	0.260	0.266	0.290	0.308	0.324	0.338	0.351	0.363	0.374
5.7	0.238	0.246	0.254	0.260	0.267	0.291	0.310	0.326	0.341	0.354	0.366	0.377
5.8	0.238	0.245	0.254	0.261	0.267	0.293	0.312	0.329	0.343	0.357	0.369	0.381
5.9	0.238	0.245	0.254	0.261	0.268	0.294	0.314	0.331	0.346	0.360	0.372	0.384
6.0	0.238	0.245	0.253	0.261	0.268	0.295	0.316	0.333	0.348	0.362	0.375	0.387
6.2	0.238	0.245	0.253	0.261	0.269	0.298	0.319	0.337	0.353	0.368	0.381	0.393
6.4	0.238	0.245	0.253	0.260	0.269	0.300	0.322	0.341	0.358	0.373	0.386	0.399
6.6	0.237	0.244	0.253	0.260	0.268	0.301	0.325	0.345	0.362	0.377	0.391	0.405
6.8	0.234	0.243	0.252	0.260	0.268	0.302	0.327	0.348	0.365	0.381	0.396	0.410
7.0	0.229	0.241	0.250	0.259	0.267	0.303	0.329	0.351	0.369	0.385	0.400	0.414
7.5	0.215	0.232	0.245	0.255	0.265	0.303	0.333	0.356	0.376	0.394	0.410	0.425
8.0	0.207	0.222	0.236	0.249	0.260	0.302	0.334	0.360	0.381	0.400	0.418	0.434
8.5	0.203	0.216	0.229	0.242	0.254	0.300	0.334	0.362	0.385	0.405	0.423	0.440
9.0	0.202	0.213	0.225	0.236	0.248	0.297	0.333	0.362	0.387	0.409	0.428	0.446
9.5	0.203	0.213	0.223	0.234	0.244	0.293	0.331	0.362	0.388	0.411	0.431	0.450
10.0	0.206	0.214	0.223	0.232	0.242	0.289	0.328	0.360	0.388	0.412	0.433	0.452
11.0	0.212	0.219	0.226	0.234	0.241	0.282	0.322	0.356	0.385	0.411	0.434	0.455
12.0	0.219	0.225	0.231	0.238	0.244	0.280	0.316	0.350	0.381	0.406	0.432	0.454
13.0	0.228	0.233	0.238	0.244	0.250	0.282	0.314	0.347	0.377	0.404	0.429	0.452
14.0	0.236	0.241	0.246	0.251	0.256	0.285	0.315	0.345	0.373	0.400	0.426	0.449
15.0	0.244	0.248	0.253	0.258	0.263	0.289	0.317	0.345	0.372	0.398	0.423	0.446
16.0	0.252	0.256	0.260	0.265	0.269	0.293	0.319	0.345	0.371	0.396	0.420	0.443
17.0	0.260	0.264	0.268	0.272	0.276	0.298	0.322	0.347	0.371	0.395	0.418	0.441
18.0	0.268	0.271	0.275	0.279	0.283	0.304	0.326	0.349	0.372	0.395	0.417	0.439
19.0	0.275	0.279	0.282	0.286	0.290	0.309	0.330	0.352	0.374	0.396	0.417	0.438
20.0	0.283	0.286	0.290	0.293	0.297	0.315	0.335	0.355	0.376	0.397	0.417	0.437
25.0	0.319	0.322	0.325	0.327	0.330	0.345	0.361	0.377	0.393	0.410	0.427	0.443
30.0	0.353	0.355	0.358	0.360	0.363	0.376	0.389	0.402	0.416	0.430	0.444	0.458
35.0	0.385	0.388	0.390	0.392	0.394	0.406	0.417	0.429	0.441	0.453	0.465	0.477
40.0	0.417	0.419	0.421	0.423	0.425	0.435	0.445	0.456	0.467	0.477	0.488	0.499
45.0	0.447	0.449	0.451	0.453	0.454	0.464	0.473	0.483	0.493	0.502	0.512	0.522
50.0	0.476	0.478	0.480	0.482	0.483	0.492	0.501	0.510	0.519	0.528	0.537	0.546
60.0	0.533	0.535	0.536	0.538	0.539	0.547	0.555	0.563	0.571	0.579	0.587	0.595
80.0	0.640	0.642	0.643	0.644	0.646	0.652	0.659	0.665	0.672	0.679	0.685	0.692
100.0	0.741	0.743	0.744	0.745	0.746	0.752	0.758	0.763	0.769	0.775	0.781	0.786
120.0	0.837	0.838	0.839	0.840	0.842	0.847	0.852	0.857	0.862	0.868	0.873	0.878
140.0	0.929	0.930	0.931	0.932	0.933	0.938	0.942	0.947	0.952	0.957	0.961	0.966
160.0	1.017	1.018	1.019	1.020	1.021	1.025	1.029	1.034	1.038	1.043	1.047	1.051
180.0	1.102	1.103	1.103	1.104	1.105	1.109	1.113	1.117	1.121	1.125	1.129	1.133
200.0	1.183	1.184	1.185	1.186	1.186	1.190	1.194	1.198	1.201	1.205	1.209	1.212
220.0	1.262	1.263	1.263	1.264	1.265	1.268	1.272	1.275	1.279	1.282	1.285	1.289
240.0	1.338	1.338	1.339	1.340	1.340	1.343	1.347	1.350	1.353	1.356	1.359	1.363
260.0	1.411	1.411	1.412	1.413	1.413	1.416	1.419	1.422	1.425	1.428	1.431	1.434
280.0	1.482	1.482	1.483	1.483	1.484	1.487	1.489	1.492	1.495	1.497	1.500	1.503
300.0	1.550	1.550	1.551	1.551	1.552	1.554	1.557	1.560	1.562	1.565	1.567	1.570

Table 4.2.1 Helium⁴ thermal conductivity, K, mW/cm-K (continued).

PRES MM/HG ATM	5.066 50.000	5.573 55.000	6.079 60.000	6.586 65.000	7.093 70.000	7.599 75.000	8.106 80.000	8.613 85.000	9.119 90.000	9.626 95.000	10.133 100.000	10.639 105.000
TEMP, K												
3.0	0.276	0.283	0.290	0.297	0.303	0.310						
3.5	0.297	0.304	0.311	0.319	0.325	0.332	0.339	0.346	0.352	0.359	0.366	
4.0	0.319	0.326	0.334	0.342	0.349	0.356	0.363	0.370	0.377	0.384	0.390	0.397
4.2	0.327	0.336	0.343	0.351	0.358	0.366	0.373	0.380	0.387	0.394	0.401	0.408
4.4	0.336	0.345	0.353	0.361	0.368	0.376	0.383	0.390	0.398	0.405	0.412	0.419
4.6	0.345	0.353	0.362	0.370	0.378	0.386	0.393	0.401	0.408	0.415	0.423	0.430
4.8	0.353	0.362	0.371	0.379	0.387	0.395	0.403	0.411	0.419	0.426	0.433	0.441
5.0	0.361	0.371	0.380	0.388	0.397	0.405	0.413	0.421	0.429	0.436	0.444	0.451
5.1	0.365	0.375	0.384	0.393	0.401	0.410	0.418	0.426	0.434	0.442	0.449	0.457
5.2	0.369	0.379	0.388	0.397	0.406	0.414	0.423	0.431	0.439	0.447	0.455	0.462
5.3	0.373	0.383	0.392	0.402	0.410	0.419	0.427	0.436	0.444	0.452	0.460	0.468
5.4	0.377	0.387	0.397	0.406	0.415	0.424	0.432	0.441	0.449	0.457	0.465	0.473
5.5	0.381	0.391	0.401	0.410	0.419	0.428	0.437	0.445	0.454	0.462	0.470	0.478
5.6	0.385	0.395	0.405	0.414	0.424	0.433	0.441	0.450	0.459	0.467	0.475	0.483
5.7	0.388	0.399	0.409	0.418	0.428	0.437	0.446	0.455	0.463	0.472	0.480	0.488
5.8	0.392	0.402	0.413	0.422	0.432	0.441	0.450	0.459	0.468	0.477	0.485	0.493
5.9	0.395	0.406	0.416	0.426	0.436	0.445	0.455	0.464	0.473	0.481	0.490	0.498
6.0	0.399	0.410	0.420	0.430	0.440	0.450	0.459	0.468	0.477	0.486	0.494	0.503
6.2	0.405	0.416	0.427	0.438	0.448	0.458	0.467	0.477	0.486	0.495	0.504	0.512
6.4	0.411	0.423	0.434	0.445	0.455	0.465	0.475	0.485	0.494	0.503	0.512	0.521
6.6	0.417	0.429	0.440	0.451	0.462	0.473	0.483	0.492	0.502	0.512	0.521	0.530
6.8	0.423	0.435	0.447	0.458	0.469	0.479	0.490	0.500	0.510	0.519	0.529	0.538
7.0	0.428	0.440	0.452	0.464	0.475	0.486	0.497	0.507	0.517	0.527	0.537	0.546
7.5	0.439	0.452	0.465	0.478	0.489	0.501	0.512	0.523	0.534	0.544	0.554	0.564
8.0	0.448	0.463	0.476	0.489	0.502	0.514	0.525	0.537	0.548	0.559	0.570	0.580
8.5	0.456	0.471	0.485	0.499	0.512	0.525	0.537	0.549	0.560	0.572	0.583	0.594
9.0	0.462	0.478	0.493	0.507	0.521	0.534	0.547	0.559	0.571	0.583	0.594	0.606
9.5	0.467	0.483	0.499	0.513	0.528	0.541	0.554	0.567	0.580	0.592	0.604	0.616
10.0	0.470	0.487	0.503	0.519	0.533	0.547	0.561	0.574	0.587	0.600	0.612	0.624
11.0	0.474	0.492	0.509	0.525	0.541	0.556	0.570	0.584	0.598	0.611	0.624	0.636
12.0	0.475	0.494	0.512	0.529	0.545	0.561	0.576	0.590	0.604	0.618	0.631	0.643
13.0	0.473	0.493	0.512	0.530	0.547	0.563	0.578	0.593	0.608	0.622	0.636	0.650
14.0	0.471	0.491	0.511	0.529	0.546	0.563	0.579	0.595	0.610	0.624	0.638	0.652
15.0	0.468	0.489	0.508	0.527	0.545	0.562	0.578	0.594	0.609	0.623	0.637	0.651
16.0	0.465	0.486	0.505	0.524	0.542	0.560	0.576	0.592	0.608	0.623	0.638	0.652
17.0	0.462	0.483	0.502	0.521	0.539	0.557	0.573	0.590	0.605	0.621	0.635	0.650
18.0	0.460	0.480	0.499	0.518	0.536	0.554	0.570	0.587	0.602	0.618	0.633	0.647
19.0	0.453	0.478	0.497	0.515	0.533	0.551	0.567	0.584	0.599	0.615	0.630	0.644
20.0	0.457	0.476	0.495	0.513	0.531	0.548	0.564	0.581	0.596	0.611	0.626	0.641
25.0	0.460	0.476	0.492	0.508	0.524	0.539	0.555	0.569	0.584	0.598	0.613	0.628
30.0	0.472	0.486	0.500	0.514	0.527	0.541	0.554	0.568	0.581	0.594	0.607	0.619
35.0	0.489	0.502	0.514	0.526	0.538	0.550	0.562	0.574	0.586	0.598	0.609	0.621
40.0	0.510	0.521	0.532	0.543	0.553	0.564	0.575	0.586	0.596	0.607	0.618	0.628
45.0	0.532	0.542	0.552	0.562	0.572	0.581	0.591	0.601	0.611	0.620	0.630	0.640
50.0	0.555	0.564	0.573	0.582	0.591	0.601	0.610	0.619	0.628	0.637	0.646	0.654
60.0	0.603	0.610	0.618	0.626	0.634	0.642	0.650	0.658	0.666	0.674	0.682	0.690
80.0	0.698	0.705	0.711	0.718	0.725	0.731	0.738	0.744	0.751	0.757	0.764	0.770
100.0	0.792	0.798	0.804	0.809	0.815	0.821	0.827	0.832	0.838	0.844	0.849	0.855
120.0	0.883	0.888	0.894	0.899	0.904	0.909	0.914	0.919	0.924	0.929	0.934	0.940
140.0	0.971	0.976	0.980	0.985	0.990	0.994	0.999	1.004	1.008	1.013	1.018	1.022
160.0	1.056	1.060	1.064	1.069	1.073	1.077	1.082	1.086	1.090	1.094	1.099	1.103
180.0	1.137	1.141	1.145	1.149	1.153	1.157	1.161	1.165	1.169	1.173	1.177	1.181
200.0	1.216	1.220	1.224	1.227	1.231	1.235	1.238	1.242	1.246	1.249	1.253	1.257
220.0	1.292	1.296	1.299	1.303	1.306	1.309	1.313	1.316	1.320	1.323	1.327	1.330
240.0	1.366	1.369	1.372	1.375	1.379	1.382	1.385	1.388	1.391	1.394	1.398	1.401
260.0	1.437	1.440	1.443	1.446	1.449	1.452	1.455	1.458	1.460	1.463	1.466	1.469
280.0	1.506	1.508	1.511	1.514	1.517	1.519	1.522	1.525	1.527	1.530	1.533	1.536
300.0	1.572	1.575	1.577	1.580	1.582	1.585	1.587	1.590	1.592	1.595	1.597	1.600

Table 4.2.2 Helium⁴ viscosity, μ , $\mu\text{g}/\text{cm}\cdot\text{s}$.

PRES MM/H ²	0.010	0.051	0.101	0.152	0.182	0.193	0.203	0.213	0.223	0.233	0.243	0.253
ATM	0.100	0.500	1.000	1.500	1.800	1.900	2.000	2.100	2.200	2.300	2.400	2.500
TEMP, K												
3.0	7.8	37.4	38.6	39.7	40.3	40.6	40.8	41.0	41.2	41.4	41.6	41.8
3.5	9.1	35.2	36.4	37.5	38.2	38.4	38.6	38.9	39.1	39.3	39.5	39.7
4.0	10.3	10.9	33.4	34.6	35.4	35.6	35.8	36.1	36.3	36.5	36.7	36.9
4.2	10.8	11.4	31.9	33.3	34.1	34.3	34.5	34.8	35.0	35.2	35.5	35.7
4.4	11.3	11.8	12.8	31.8	32.6	32.9	33.1	33.4	33.7	33.9	34.1	34.4
4.6	11.7	12.3	13.1	29.9	31.0	31.3	31.6	31.9	32.1	32.4	32.7	32.9
4.8	12.2	12.7	13.5	14.8	28.9	29.3	29.7	30.0	30.4	30.7	31.0	31.3
5.0	12.6	13.1	13.9	15.0	16.0	16.7	26.9	27.3	28.1	28.5	29.0	29.4
5.1	12.8	13.3	14.1	15.1	16.0	16.4	17.1	25.4	26.3	27.0	27.6	28.1
5.2	13.1	13.6	14.3	15.2	16.0	16.4	16.8	17.4	18.5	24.4	25.6	26.5
5.3	13.3	13.8	14.5	15.4	16.1	16.4	16.8	17.2	17.7	18.6	20.8	24.1
5.4	13.5	14.0	14.7	15.5	16.2	16.5	16.8	17.1	17.5	18.0	18.7	19.9
5.5	13.7	14.2	14.9	15.7	16.3	16.6	16.8	17.1	17.5	17.9	18.3	18.9
5.6	13.9	14.4	15.1	15.9	16.5	16.7	16.9	17.2	17.5	17.8	18.2	18.6
5.7	14.1	14.6	15.2	16.0	16.6	16.8	17.0	17.3	17.5	17.8	18.1	18.5
5.8	14.3	14.8	15.4	16.2	16.7	16.9	17.1	17.4	17.6	17.8	18.1	18.4
5.9	14.5	15.0	15.6	16.4	16.9	17.1	17.3	17.5	17.7	17.9	18.2	18.4
6.0	14.7	15.2	15.8	16.5	17.0	17.2	17.4	17.6	17.8	18.0	18.2	18.5
6.2	15.1	15.6	16.2	16.9	17.3	17.5	17.7	17.9	18.0	18.2	18.4	18.6
6.4	15.5	16.0	16.5	17.2	17.6	17.8	17.9	18.1	18.3	18.4	18.6	18.8
6.6	15.9	16.3	16.9	17.5	18.0	18.1	18.2	18.4	18.5	18.7	18.9	19.0
6.8	16.3	16.7	17.3	17.9	18.3	18.4	18.5	18.7	18.8	19.0	19.1	19.3
7.0	16.7	17.1	17.6	18.2	18.6	18.7	18.8	19.0	19.1	19.3	19.4	19.5
7.5	17.6	18.0	18.5	19.0	19.4	19.5	19.6	19.7	19.9	20.0	20.1	20.2
8.0	18.5	18.9	19.4	19.9	20.2	20.3	20.4	20.5	20.6	20.7	20.8	20.9
8.5	19.4	19.7	20.2	20.7	21.0	21.1	21.2	21.3	21.4	21.5	21.6	21.7
9.0	20.2	20.6	21.0	21.5	21.7	21.8	21.9	22.0	22.1	22.2	22.3	22.4
9.5	21.1	21.4	21.8	22.2	22.5	22.6	22.7	22.7	22.8	22.9	23.0	23.1
10.0	21.9	22.2	22.6	23.0	23.2	23.3	23.4	23.5	23.6	23.6	23.7	23.8
11.0	23.5	23.8	24.1	24.5	24.7	24.8	24.9	24.9	25.0	25.1	25.1	25.2
12.0	25.0	25.2	25.6	25.9	26.1	26.2	26.2	26.3	26.4	26.4	26.5	26.6
13.0	26.4	26.7	27.0	27.3	27.5	27.5	27.6	27.7	27.7	27.8	27.9	27.9
14.0	27.9	28.1	28.4	28.6	28.8	28.9	28.9	29.0	29.0	29.1	29.2	29.2
15.0	29.2	29.4	29.7	30.0	30.1	30.2	30.2	30.3	30.3	30.4	30.4	30.5
16.0	30.5	30.7	31.0	31.2	31.4	31.4	31.5	31.5	31.6	31.6	31.7	31.7
17.0	31.8	32.0	32.2	32.5	32.6	32.7	32.7	32.8	32.8	32.8	32.9	32.9
18.0	33.1	33.2	33.5	33.7	33.8	33.9	33.9	34.0	34.0	34.0	34.1	34.1
19.0	34.3	34.4	34.7	34.9	35.0	35.0	35.1	35.1	35.2	35.2	35.2	35.3
20.0	35.5	35.6	35.8	36.0	36.1	36.2	36.2	36.3	36.3	36.3	36.4	36.4
25.0	41.0	41.1	41.3	41.5	41.6	41.6	41.6	41.7	41.7	41.7	41.8	41.8
30.0	46.1	46.2	46.3	46.5	46.6	46.6	46.6	46.7	46.7	46.7	46.7	46.8
35.0	50.8	50.9	51.0	51.1	51.2	51.2	51.3	51.3	51.3	51.3	51.4	51.4
40.0	55.2	55.3	55.4	55.5	55.6	55.6	55.6	55.7	55.7	55.7	55.7	55.8
45.0	59.4	59.5	59.6	59.7	59.8	59.8	59.8	59.8	59.9	59.9	59.9	59.9
50.0	63.4	63.5	63.6	63.7	63.8	63.8	63.8	63.8	63.8	63.9	63.9	63.9
60.0	71.0	71.1	71.2	71.3	71.3	71.3	71.3	71.4	71.4	71.4	71.4	71.4
80.0	84.9	85.0	85.0	85.1	85.2	85.2	85.2	85.2	85.2	85.2	85.2	85.3
100.0	97.7	97.7	97.8	97.8	97.9	97.9	97.9	97.9	97.9	97.9	98.0	98.0
120.0	109.7	109.7	109.8	109.8	109.9	109.9	109.9	109.9	109.9	109.9	109.9	110.0
140.0	121.2	121.2	121.3	121.3	121.3	121.3	121.4	121.4	121.4	121.4	121.4	121.4
160.0	132.2	132.3	132.3	132.4	132.4	132.4	132.4	132.4	132.4	132.5	132.5	132.5
180.0	143.0	143.1	143.1	143.2	143.2	143.2	143.2	143.2	143.2	143.2	143.2	143.2
200.0	153.6	153.6	153.7	153.7	153.7	153.7	153.7	153.8	153.8	153.8	153.8	153.8
220.0	164.0	164.0	164.0	164.1	164.1	164.1	164.1	164.1	164.1	164.1	164.1	164.1
240.0	174.2	174.2	174.2	174.3	174.3	174.3	174.3	174.3	174.3	174.3	174.3	174.3
260.0	184.3	184.3	184.3	184.4	184.4	184.4	184.4	184.4	184.4	184.4	184.4	184.4
280.0	194.3	194.3	194.3	194.4	194.4	194.4	194.4	194.4	194.4	194.4	194.4	194.4
300.0	204.2	204.2	204.3	204.3	204.3	204.3	204.3	204.3	204.3	204.3	204.3	204.3

Table 4.2, 2 Helium⁴ viscosity, μ , $\mu\text{g}/\text{cm}\cdot\text{s}$ (continued).

PRES MM/H ² ATM	0.263 2.600	0.274 2.700	0.284 2.800	0.294 2.900	0.304 3.000	0.355 3.500	0.405 4.000	0.456 4.500	0.507 5.000	0.557 5.500	0.608 6.000	0.659 6.500
TEMP, K												
3.0	42.1	42.3	42.5	42.7	42.9	43.9	44.9	45.9	46.9	47.9	48.9	49.9
3.5	39.9	40.1	40.3	40.5	40.7	41.7	42.7	43.7	44.6	45.6	46.5	47.4
4.0	37.2	37.4	37.6	37.8	38.0	39.0	40.0	40.9	41.9	42.8	43.7	44.5
4.2	35.9	36.1	36.4	36.6	36.8	37.8	38.8	39.8	40.7	41.6	42.5	43.3
4.4	34.6	34.8	35.1	35.3	35.5	36.6	37.6	38.6	39.5	40.4	41.3	42.1
4.6	33.2	33.5	33.7	33.9	34.2	35.3	36.3	37.3	38.3	39.2	40.1	40.9
4.8	31.6	31.9	32.2	32.4	32.7	33.9	35.0	36.1	37.0	38.0	38.9	39.7
5.0	29.7	30.1	30.4	30.7	31.0	32.4	33.6	34.7	35.8	36.7	37.6	38.5
5.1	28.6	29.0	29.4	29.8	30.1	31.6	32.9	34.0	35.1	36.1	37.0	37.9
5.2	27.1	27.7	28.2	28.6	29.0	30.7	32.1	33.3	34.4	35.4	36.4	37.3
5.3	25.4	26.2	26.9	27.5	28.0	29.9	31.4	32.7	33.9	34.9	35.9	36.8
5.4	22.1	24.1	25.2	26.1	26.8	29.1	30.7	32.1	33.3	34.3	35.3	36.3
5.5	19.8	21.1	22.7	24.1	25.2	28.1	30.0	31.4	32.7	33.8	34.8	35.7
5.6	19.2	19.8	20.7	21.9	23.1	27.1	29.2	30.8	32.1	33.2	34.3	35.2
5.7	18.9	19.4	20.0	20.7	21.5	25.9	28.4	30.1	31.5	32.7	33.7	34.7
5.8	18.8	19.2	19.6	20.1	20.7	24.5	27.4	29.4	30.8	32.1	33.2	34.2
5.9	18.7	19.1	19.4	19.8	20.3	23.3	26.5	28.6	30.2	31.5	32.7	33.7
6.0	18.7	19.0	19.3	19.7	20.0	22.5	25.5	27.8	29.5	30.9	32.1	33.2
6.2	18.8	19.1	19.3	19.6	19.9	21.6	23.9	26.2	28.2	29.8	31.1	32.2
6.4	19.0	19.2	19.4	19.6	19.9	21.2	23.0	24.9	26.9	28.6	30.0	31.2
6.6	19.2	19.4	19.6	19.8	20.0	21.1	22.5	24.1	25.8	27.5	29.0	30.3
6.8	19.4	19.6	19.8	20.0	20.1	21.1	22.3	23.6	25.1	26.6	28.0	29.3
7.0	19.7	19.9	20.0	20.2	20.3	21.2	22.2	23.4	24.6	25.9	27.2	28.5
7.5	20.4	20.5	20.6	20.8	20.9	21.6	22.4	23.3	24.2	25.1	26.1	27.1
8.0	21.1	21.2	21.3	21.4	21.5	22.2	22.8	23.5	24.3	25.0	25.8	26.6
8.5	21.8	21.9	22.0	22.1	22.2	22.7	23.3	23.9	24.6	25.2	25.9	26.6
9.0	22.5	22.6	22.7	22.8	22.9	23.4	23.9	24.4	25.0	25.6	26.1	26.7
9.5	23.2	23.3	23.4	23.5	23.6	24.0	24.5	25.0	25.5	26.0	26.5	27.0
10.0	23.9	24.0	24.1	24.1	24.2	24.7	25.1	25.5	26.0	26.5	27.0	27.4
11.0	25.3	25.4	25.4	25.5	25.6	26.0	26.4	26.7	27.1	27.5	28.0	28.4
12.0	26.6	26.7	26.8	26.9	26.9	27.3	27.6	28.0	28.3	28.7	29.0	29.4
13.0	28.0	28.0	28.1	28.2	28.2	28.5	28.9	29.2	29.5	29.8	30.1	30.5
14.0	29.3	29.3	29.4	29.4	29.5	29.8	30.1	30.4	30.7	31.0	31.3	31.6
15.0	30.5	30.6	30.6	30.7	30.8	31.0	31.3	31.6	31.8	32.1	32.4	32.6
16.0	31.8	31.8	31.9	31.9	32.0	32.2	32.5	32.7	33.0	33.2	33.5	33.7
17.0	33.0	33.0	33.1	33.1	33.2	33.4	33.7	33.9	34.1	34.4	34.6	34.8
18.0	34.2	34.2	34.3	34.3	34.4	34.6	34.8	35.0	35.2	35.5	35.7	35.9
19.0	35.3	35.4	35.4	35.5	35.5	35.7	35.9	36.1	36.3	36.6	36.8	37.0
20.0	36.5	36.5	36.5	36.6	36.6	36.8	37.0	37.2	37.4	37.6	37.8	38.0
25.0	41.8	41.9	41.9	41.9	42.0	42.1	42.3	42.5	42.6	42.8	43.0	43.1
30.0	46.8	46.8	46.8	46.9	46.9	47.0	47.2	47.3	47.5	47.6	47.7	47.9
35.0	51.4	51.4	51.5	51.5	51.5	51.6	51.8	51.9	52.0	52.1	52.3	52.4
40.0	55.8	55.8	55.8	55.9	55.9	56.0	56.1	56.2	56.3	56.4	56.5	56.7
45.0	59.9	60.0	60.0	60.0	60.0	60.1	60.2	60.3	60.4	60.5	60.6	60.7
50.0	63.9	63.9	64.0	64.0	64.0	64.1	64.2	64.3	64.4	64.5	64.6	64.7
60.0	71.4	71.5	71.5	71.5	71.5	71.6	71.7	71.8	71.9	71.9	72.0	72.1
80.0	85.3	85.3	85.3	85.3	85.3	85.4	85.5	85.5	85.6	85.7	85.8	85.8
100.0	98.0	98.0	98.0	98.0	98.0	98.1	98.2	98.2	98.3	98.4	98.4	98.5
120.0	110.0	110.0	110.0	110.0	110.0	110.1	110.1	110.2	110.2	110.3	110.4	110.4
140.0	121.4	121.4	121.4	121.5	121.5	121.5	121.6	121.6	121.7	121.7	121.8	121.8
160.0	132.5	132.5	132.5	132.5	132.5	132.6	132.6	132.7	132.7	132.8	132.8	132.9
180.0	143.3	143.3	143.3	143.3	143.3	143.3	143.4	143.4	143.5	143.5	143.5	143.6
200.0	153.8	153.8	153.8	153.8	153.8	153.9	153.9	153.9	154.0	154.0	154.0	154.1
220.0	164.1	164.1	164.2	164.2	164.2	164.2	164.3	164.3	164.3	164.3	164.4	164.4
240.0	174.3	174.3	174.4	174.4	174.4	174.4	174.4	174.5	174.5	174.5	174.5	174.6
260.0	184.4	184.4	184.4	184.4	184.4	184.5	184.5	184.5	184.5	184.6	184.6	184.6
280.0	194.4	194.4	194.4	194.4	194.4	194.4	194.5	194.5	194.5	194.5	194.6	194.6
300.0	204.3	204.3	204.3	204.3	204.3	204.3	204.4	204.4	204.4	204.4	204.4	204.5

Table 4.2.2 Helium⁴ viscosity, μ , μ g/cm-s (continued).

PRES MM/HG ATM	0.608 6.000	0.709 7.000	0.811 8.000	0.912 9.000	1.013 10.000	1.520 15.000	2.026 20.000	2.533 25.000	3.040 30.000	3.546 35.000	4.053 40.000	4.560 45.000
TEMP. K												
3.0	46.9	50.8	52.8	54.7	56.6	66.1	75.9	86.1	96.8	108.3	120.5	133.6
3.5	46.5	48.3	50.1	51.9	53.6	62.3	71.0	79.9	89.2	98.9	109.2	120.0
4.0	43.7	45.4	47.1	48.7	50.4	58.3	66.1	73.9	82.0	90.4	99.1	108.2
4.2	42.5	44.2	45.8	47.5	49.0	56.7	64.2	71.7	79.4	87.3	95.5	104.0
4.4	41.3	43.0	44.6	46.2	47.8	55.2	62.4	69.6	76.9	84.4	92.2	100.2
4.6	40.1	41.8	43.4	45.0	46.5	53.7	60.7	67.6	74.6	81.7	89.0	96.6
4.8	38.9	40.6	42.2	43.7	45.3	52.3	59.0	65.7	72.4	79.2	86.1	93.3
5.0	37.6	39.4	41.0	42.5	44.0	51.0	57.5	63.9	70.3	76.8	83.4	90.2
5.1	37.0	38.8	40.4	41.9	43.4	50.3	56.7	63.0	69.3	75.7	82.1	88.6
5.2	36.4	38.2	39.8	41.4	42.8	49.7	56.0	62.2	68.3	74.6	80.9	87.4
5.3	35.9	37.7	39.3	40.9	42.3	49.1	55.4	61.4	67.5	73.6	79.8	86.1
5.4	35.3	37.1	38.8	40.4	41.8	48.6	54.7	60.7	66.6	72.6	78.7	84.9
5.5	34.8	36.6	38.3	39.9	41.4	48.0	54.1	60.0	65.8	71.7	77.6	83.7
5.6	34.3	36.1	37.8	39.4	40.9	47.5	53.5	59.3	65.1	70.8	76.6	82.6
5.7	33.7	35.7	37.4	38.9	40.4	47.0	53.0	58.7	64.3	70.0	75.7	81.5
5.8	33.2	35.2	36.9	38.5	40.0	46.5	52.4	58.1	63.6	69.2	74.8	80.4
5.9	32.7	34.7	36.4	38.0	39.5	46.1	51.9	57.5	62.9	68.4	73.9	79.4
6.0	32.1	34.2	36.0	37.6	39.1	45.6	51.4	56.9	62.3	67.6	73.0	78.5
6.2	31.1	33.3	35.1	36.7	38.3	44.7	50.4	55.8	61.0	66.2	71.4	76.6
6.4	30.0	32.3	34.2	35.9	37.5	43.9	49.5	54.7	59.8	64.8	69.9	75.0
6.6	29.0	31.4	33.4	35.1	36.7	43.1	48.6	53.8	58.7	63.6	68.5	73.4
6.8	28.0	30.5	32.6	34.4	36.0	42.4	47.8	52.9	57.7	62.4	67.2	71.9
7.0	27.2	29.7	31.8	33.6	35.3	41.7	47.1	52.0	56.7	61.4	65.9	70.6
7.5	26.1	28.2	30.2	32.0	33.7	40.2	45.4	50.1	54.6	58.9	63.2	67.5
8.0	25.8	27.5	29.1	30.8	32.4	38.8	44.0	48.5	52.8	56.9	61.0	65.0
8.5	25.9	27.3	28.6	30.1	31.5	37.7	42.7	47.1	51.2	55.2	59.0	62.8
9.0	26.1	27.3	28.5	29.7	31.0	36.8	41.7	46.0	49.9	53.7	57.3	60.9
9.5	26.5	27.6	28.6	29.7	30.8	36.1	40.8	45.0	48.8	52.4	55.9	59.3
10.0	27.0	27.9	28.9	29.9	30.8	35.6	40.1	44.2	47.8	51.3	54.7	58.0
11.0	28.0	28.8	29.6	30.4	31.2	35.2	39.2	42.9	46.3	49.6	52.7	55.7
12.0	29.0	29.7	30.5	31.2	31.9	35.4	38.8	42.2	45.3	48.4	51.3	54.1
13.0	30.1	30.8	31.4	32.1	32.7	35.9	38.9	41.9	44.8	47.6	50.3	53.0
14.0	31.3	31.8	32.4	33.0	33.6	36.5	39.3	42.0	44.6	47.2	49.7	52.2
15.0	32.4	32.9	33.5	34.0	34.5	37.2	39.8	42.3	44.7	47.1	49.4	51.7
16.0	33.5	34.0	34.5	35.0	35.5	38.0	40.4	42.7	45.0	47.2	49.4	51.5
17.0	34.6	35.1	35.5	36.0	36.5	38.8	41.0	43.2	45.3	47.4	49.5	51.5
18.0	35.7	36.1	36.6	37.0	37.5	39.6	41.6	43.8	45.8	47.8	49.7	51.6
19.0	36.8	37.2	37.6	38.0	38.4	40.5	42.5	44.5	46.4	48.2	50.1	51.9
20.0	37.8	38.2	38.6	39.0	39.4	41.4	43.3	45.2	47.0	48.8	50.5	52.2
25.0	43.0	43.3	43.6	43.9	44.2	45.8	47.4	48.9	50.4	51.9	53.3	54.6
30.0	47.7	48.0	48.3	48.6	48.8	50.2	51.6	52.9	54.2	55.5	56.7	57.9
35.0	52.3	52.5	52.8	53.0	53.2	54.4	55.6	56.8	58.0	59.1	60.2	61.4
40.0	56.5	56.8	57.0	57.2	57.4	58.5	59.6	60.7	61.7	62.8	63.8	64.8
45.0	60.6	60.8	61.1	61.3	61.5	62.5	63.5	64.5	65.4	66.4	67.4	68.3
50.0	64.6	64.8	65.0	65.1	65.3	66.3	67.2	68.1	69.1	70.0	70.8	71.7
60.0	72.0	72.2	72.4	72.5	72.7	73.6	74.4	75.2	76.0	76.9	77.7	78.4
80.0	85.8	85.9	86.1	86.2	86.3	87.1	87.8	88.5	89.2	89.9	90.5	91.2
100.0	98.4	98.6	98.7	98.8	98.9	99.6	100.2	100.8	101.4	102.0	102.6	103.2
120.0	110.4	110.5	110.6	110.7	110.8	111.4	111.9	112.5	113.1	113.6	114.1	114.7
140.0	121.8	121.9	122.0	122.1	122.2	122.7	123.2	123.7	124.2	124.7	125.2	125.7
160.0	132.8	132.9	133.0	133.1	133.2	133.6	134.1	134.5	135.0	135.4	135.9	136.3
180.0	143.5	143.6	143.7	143.8	143.9	144.3	144.7	145.1	145.5	145.9	146.3	146.7
200.0	154.0	154.1	154.2	154.3	154.3	154.7	155.1	155.4	155.8	156.2	156.5	156.9
220.0	164.4	164.4	164.5	164.6	164.6	165.0	165.3	165.6	165.9	166.2	166.6	166.9
240.0	174.5	174.6	174.7	174.7	174.8	175.1	175.3	175.6	175.9	176.2	176.5	176.7
260.0	184.6	184.6	184.7	184.7	184.8	185.0	185.3	185.5	185.8	186.0	186.3	186.5
280.0	194.6	194.6	194.6	194.7	194.7	194.9	195.1	195.4	195.6	195.8	196.0	196.2
300.0	204.4	204.5	204.5	204.5	204.6	204.8	204.9	205.1	205.3	205.4	205.6	205.8

Table 4.2.2 Helium⁴ viscosity, μ , $\mu\text{g/cm-s}$ (continued).

PRES MM/HG ATM	5.066 50.000	5.573 55.060	6.079 60.000	6.586 65.000	7.093 70.000	7.599 75.000	8.106 80.000	8.613 85.000	9.119 90.000	9.626 95.000	10.133 100.000	10.639 105.000
TEMP, K												
3.0	147.8	163.0	179.6	197.5	217.1	238.4						
3.5	131.5	143.7	156.6	170.5	185.2	201.0	217.9	236.0	255.5	276.3	298.7	
4.0	117.7	127.8	138.3	149.4	161.2	173.5	186.6	200.5	215.1	230.6	247.1	264.5
4.2	113.0	122.3	132.1	142.4	153.2	164.5	176.5	189.1	202.4	216.4	231.2	246.8
4.4	108.6	117.3	126.4	135.9	145.9	156.4	167.4	179.0	191.1	203.9	217.3	231.4
4.6	104.5	112.7	121.2	130.1	139.4	149.1	159.3	169.9	181.1	192.8	205.8	217.9
4.8	100.7	108.4	116.4	124.8	133.4	142.5	151.9	161.8	172.1	182.9	194.1	205.9
5.0	97.3	104.5	112.1	119.9	128.0	136.5	145.3	154.5	164.0	174.0	184.4	195.3
5.1	95.6	102.7	110.0	117.6	125.5	133.7	142.2	151.1	160.3	169.9	179.9	190.4
5.2	94.1	101.0	108.1	115.4	123.1	131.0	139.3	147.8	156.7	166.0	175.7	185.7
5.3	92.6	99.3	106.3	113.4	120.9	128.6	136.5	144.8	153.5	162.4	171.7	181.4
5.4	91.2	97.8	104.5	111.5	118.7	126.2	134.0	142.0	150.3	159.0	168.0	177.4
5.5	89.9	96.3	102.9	109.7	116.7	124.0	131.5	139.3	147.4	155.8	164.5	173.5
5.6	88.6	94.9	101.3	107.9	114.7	121.8	129.1	136.7	144.5	152.7	161.1	169.9
5.7	87.4	93.5	99.8	106.2	112.9	119.8	126.9	134.2	141.8	149.7	157.9	166.4
5.8	86.3	92.2	98.3	104.6	111.1	117.8	124.7	131.9	139.3	146.9	154.9	163.1
5.9	85.1	91.0	96.9	103.1	109.4	115.9	122.7	129.6	136.8	144.3	152.0	159.9
6.0	84.0	89.7	95.6	101.6	107.8	114.1	120.7	127.5	134.5	141.7	149.2	156.9
6.2	82.0	87.5	93.1	98.8	104.7	110.8	117.0	123.4	130.1	136.9	144.8	151.3
6.4	80.1	85.4	90.7	96.2	101.9	107.7	113.6	119.7	126.0	132.6	139.3	146.2
6.6	78.4	83.4	88.6	93.8	99.2	104.8	110.5	116.3	122.3	128.5	134.9	141.5
6.8	76.7	81.6	86.6	91.6	96.8	102.1	107.6	113.2	118.9	124.8	130.9	137.1
7.0	75.2	79.9	84.7	89.6	94.6	99.7	104.9	110.3	115.8	121.4	127.2	133.2
7.5	71.8	76.2	80.6	85.1	89.6	94.3	99.0	103.9	108.8	113.9	119.1	124.4
8.0	69.0	73.0	77.1	81.3	85.5	89.7	94.1	98.5	103.0	107.6	112.4	117.2
8.5	66.6	70.4	74.2	78.0	81.9	85.9	89.9	94.0	98.1	102.3	106.7	111.1
9.0	64.5	68.1	71.7	75.3	78.9	82.6	86.3	90.1	93.9	97.8	101.8	105.9
9.5	62.7	66.1	69.5	72.9	76.3	79.7	83.2	86.7	90.3	93.9	97.6	101.4
10.0	61.2	64.4	67.6	70.8	74.0	77.3	80.5	83.9	87.2	90.6	94.0	97.5
11.0	58.7	61.6	64.5	67.4	70.3	73.3	76.2	79.1	82.1	85.1	88.1	91.2
12.0	56.9	59.6	62.3	64.9	67.6	70.2	72.9	75.6	78.2	80.9	83.6	86.4
13.0	55.5	58.1	60.6	63.1	65.5	68.0	70.4	72.8	75.3	77.7	80.2	82.7
14.0	54.0	56.5	59.0	61.7	64.0	66.2	68.5	70.8	73.0	75.3	77.6	79.8
15.0	52.6	55.0	57.3	59.6	61.8	64.0	66.1	68.2	70.3	72.4	74.5	76.6
16.0	51.7	54.0	56.2	58.4	60.5	62.6	64.7	66.8	68.9	70.9	72.9	74.9
17.0	50.5	52.7	54.8	56.9	58.9	60.9	62.9	64.9	66.9	68.9	70.9	72.9
18.0	49.5	51.6	53.6	55.6	57.6	59.6	61.6	63.6	65.6	67.6	69.6	71.6
19.0	48.7	50.7	52.7	54.7	56.7	58.7	60.7	62.7	64.7	66.7	68.7	70.7
20.0	48.0	50.0	52.0	54.0	56.0	58.0	60.0	62.0	64.0	66.0	68.0	70.0
25.0	46.2	48.2	50.2	52.2	54.2	56.2	58.2	60.2	62.2	64.2	66.2	68.2
30.0	45.2	47.2	49.2	51.2	53.2	55.2	57.2	59.2	61.2	63.2	65.2	67.2
35.0	44.0	46.0	48.0	50.0	52.0	54.0	56.0	58.0	60.0	62.0	64.0	66.0
40.0	43.0	45.0	47.0	49.0	51.0	53.0	55.0	57.0	59.0	61.0	63.0	65.0
45.0	42.0	44.0	46.0	48.0	50.0	52.0	54.0	56.0	58.0	60.0	62.0	64.0
50.0	41.0	43.0	45.0	47.0	49.0	51.0	53.0	55.0	57.0	59.0	61.0	63.0
60.0	39.0	41.0	43.0	45.0	47.0	49.0	51.0	53.0	55.0	57.0	59.0	61.0
80.0	36.0	38.0	40.0	42.0	44.0	46.0	48.0	50.0	52.0	54.0	56.0	58.0
100.0	34.0	36.0	38.0	40.0	42.0	44.0	46.0	48.0	50.0	52.0	54.0	56.0
120.0	32.0	34.0	36.0	38.0	40.0	42.0	44.0	46.0	48.0	50.0	52.0	54.0
140.0	30.0	32.0	34.0	36.0	38.0	40.0	42.0	44.0	46.0	48.0	50.0	52.0
160.0	28.0	30.0	32.0	34.0	36.0	38.0	40.0	42.0	44.0	46.0	48.0	50.0
180.0	26.0	28.0	30.0	32.0	34.0	36.0	38.0	40.0	42.0	44.0	46.0	48.0
200.0	24.0	26.0	28.0	30.0	32.0	34.0	36.0	38.0	40.0	42.0	44.0	46.0
220.0	22.0	24.0	26.0	28.0	30.0	32.0	34.0	36.0	38.0	40.0	42.0	44.0
240.0	20.0	22.0	24.0	26.0	28.0	30.0	32.0	34.0	36.0	38.0	40.0	42.0
260.0	18.0	20.0	22.0	24.0	26.0	28.0	30.0	32.0	34.0	36.0	38.0	40.0
280.0	16.0	18.0	20.0	22.0	24.0	26.0	28.0	30.0	32.0	34.0	36.0	38.0
300.0	14.0	16.0	18.0	20.0	22.0	24.0	26.0	28.0	30.0	32.0	34.0	36.0

Table 4.2.3 Helium⁴ density, ρ , mg/cm³.

PRES MN/MM ATM	0.010	0.031	0.101	0.152	0.182	0.193	0.203	0.213	0.223	0.233	0.243	0.253
TEMP, K	0.100	0.500	1.000	1.500	1.800	1.900	2.000	2.100	2.200	2.300	2.400	2.500
3.0	1.716	141.913	143.305	144.588	145.316	145.552	145.786	145.916	146.244	146.469	146.691	146.911
3.5	1.446	136.166	138.004	139.655	140.573	140.869	141.160	141.446	141.728	142.005	142.278	142.548
4.0	1.253	7.175	130.061	132.473	133.759	134.166	134.563	134.950	135.329	135.700	136.063	136.418
4.2	1.190	6.688	125.602	128.010	130.170	130.655	131.125	131.582	132.026	132.458	132.879	133.290
4.4	1.133	6.275	15.240	123.837	125.819	126.424	127.006	127.566	128.107	128.629	129.135	129.626
4.6	1.081	5.917	13.888	117.466	120.276	121.096	121.870	122.604	123.302	123.970	124.609	125.222
4.8	1.034	5.604	12.807	24.157	112.406	113.730	114.926	116.020	117.031	117.972	118.853	119.693
5.0	0.991	5.327	11.944	21.282	30.826	36.656	103.214	105.611	107.577	109.260	110.739	112.065
5.1	0.971	5.193	11.567	20.225	28.157	32.020	37.548	45.173	49.461	102.428	104.754	106.632
5.2	0.952	5.078	11.220	19.321	26.237	29.285	33.059	38.213	47.585	88.591	95.017	98.826
5.3	0.933	4.964	10.896	18.532	24.728	27.305	30.307	33.956	38.730	45.009	63.631	85.704
5.4	0.916	4.854	10.599	17.832	23.484	25.746	28.291	31.226	34.726	39.127	45.171	54.818
5.5	0.898	4.750	10.313	17.204	22.425	24.457	26.695	29.137	32.048	35.385	39.441	44.630
5.6	0.882	4.651	10.057	16.635	21.503	23.360	25.373	27.578	30.024	32.781	35.952	39.694
5.7	0.866	4.556	9.810	16.115	20.688	22.405	24.245	26.232	28.336	30.779	33.435	36.441
5.8	0.851	4.466	9.577	15.637	19.959	21.560	23.262	25.080	27.035	29.152	31.465	34.017
5.9	0.836	4.379	9.358	15.195	19.299	20.804	22.391	24.074	25.842	27.783	29.849	32.081
6.0	0.822	4.295	9.144	14.784	18.697	20.119	21.611	23.182	24.842	26.603	28.481	30.491
6.2	0.794	4.138	8.763	14.042	17.635	18.922	20.261	21.657	23.116	24.645	26.251	27.943
6.4	0.769	3.993	8.413	13.388	16.719	17.901	19.122	20.387	21.698	23.061	24.478	25.957
6.6	0.745	3.859	8.094	12.804	15.918	17.013	18.141	19.302	20.499	21.735	23.013	24.336
6.8	0.723	3.733	7.800	12.278	15.208	16.231	17.281	18.356	19.453	20.600	21.769	22.972
7.0	0.702	3.616	7.530	11.801	14.571	15.534	16.518	17.525	18.555	19.610	20.691	21.799
7.5	0.654	3.355	6.936	10.778	13.228	14.071	14.929	15.831	16.698	17.591	18.510	19.440
8.0	0.613	3.133	6.435	9.938	12.145	12.899	13.664	14.439	15.224	16.020	16.827	17.645
8.5	0.576	2.935	6.007	9.232	11.246	11.932	12.624	13.325	14.032	14.748	15.471	16.203
9.0	0.544	2.763	5.636	8.628	10.485	11.115	11.750	12.391	13.037	13.689	14.347	15.011
9.5	0.515	2.613	5.310	8.105	9.830	10.413	11.001	11.593	12.189	12.789	13.395	14.004
10.0	0.484	2.474	5.021	7.645	9.258	9.802	10.350	10.901	11.455	12.013	12.574	13.139
11.0	0.444	2.242	4.533	6.876	8.308	8.790	9.273	9.759	10.248	10.738	11.231	11.726
12.0	0.407	2.049	4.134	6.254	7.544	7.977	8.411	8.847	9.284	9.723	10.164	10.606
13.0	0.376	1.888	3.801	5.739	6.914	7.308	7.703	8.099	8.496	8.894	9.293	9.693
14.0	0.349	1.751	3.519	5.305	6.386	6.747	7.109	7.472	7.836	8.201	8.566	8.932
15.0	0.325	1.632	3.277	4.934	5.935	6.269	6.604	6.940	7.276	7.612	7.949	8.287
16.0	0.305	1.529	3.066	4.613	5.545	5.856	6.168	6.480	6.793	7.106	7.419	7.732
17.0	0.287	1.438	2.882	4.332	5.205	5.496	5.788	6.080	6.372	6.665	6.958	7.251
18.0	0.271	1.357	2.718	4.084	4.905	5.179	5.454	5.728	6.003	6.277	6.552	6.828
19.0	0.257	1.285	2.573	3.863	4.639	4.898	5.157	5.416	5.675	5.934	6.193	6.453
20.0	0.244	1.220	2.442	3.666	4.401	4.646	4.891	5.136	5.382	5.627	5.873	6.118
25.0	0.195	0.975	1.949	2.923	3.506	3.701	3.895	4.090	4.284	4.478	4.673	4.867
30.0	0.163	0.812	1.623	2.432	2.917	3.079	3.240	3.401	3.563	3.724	3.885	4.046
35.0	0.139	0.696	1.391	2.084	2.499	2.637	2.775	2.913	3.051	3.189	3.327	3.465
40.0	0.122	0.609	1.217	1.823	2.166	2.307	2.428	2.548	2.669	2.790	2.911	3.031
45.0	0.108	0.541	1.081	1.620	1.943	2.051	2.158	2.265	2.373	2.480	2.587	2.694
50.0	0.098	0.487	0.973	1.458	1.749	1.846	1.942	2.039	2.136	2.232	2.329	2.425
60.0	0.081	0.406	0.811	1.216	1.458	1.539	1.619	1.700	1.780	1.861	1.941	2.022
80.0	0.061	0.305	0.609	0.912	1.094	1.155	1.215	1.276	1.336	1.397	1.457	1.518
100.0	0.049	0.244	0.487	0.730	0.876	0.924	0.973	1.021	1.070	1.118	1.167	1.215
120.0	0.041	0.203	0.406	0.609	0.730	0.771	0.811	0.851	0.892	0.932	0.973	1.013
140.0	0.035	0.174	0.348	0.522	0.626	0.661	0.695	0.730	0.765	0.799	0.834	0.869
160.0	0.030	0.152	0.305	0.457	0.548	0.578	0.609	0.639	0.669	0.700	0.730	0.760
180.0	0.027	0.135	0.271	0.406	0.487	0.514	0.541	0.568	0.595	0.622	0.649	0.676
200.0	0.024	0.122	0.244	0.365	0.438	0.463	0.487	0.511	0.536	0.560	0.584	0.609
220.0	0.022	0.111	0.222	0.332	0.399	0.421	0.443	0.465	0.487	0.509	0.531	0.553
240.0	0.020	0.102	0.203	0.305	0.365	0.386	0.406	0.426	0.447	0.467	0.487	0.507
260.0	0.019	0.094	0.188	0.281	0.337	0.356	0.375	0.394	0.412	0.431	0.450	0.468
280.0	0.017	0.087	0.174	0.261	0.313	0.331	0.348	0.365	0.383	0.400	0.418	0.435
300.0	0.016	0.081	0.163	0.244	0.292	0.309	0.325	0.341	0.357	0.374	0.390	0.406

Table 4.2.3 Helium⁴ density, ρ , mg/cm³. (continued).

PRES MM/H ² ATM	0.263 2.600	0.274 2.700	0.284 2.800	0.294 2.900	0.304 3.000	0.355 3.500	0.405 4.000	0.456 4.500	0.507 5.000	0.557 5.500	0.608 6.000	0.659 6.500
TEMP, K												
3.0	147.128	147.343	147.556	147.766	147.974	148.983	149.944	150.863	151.744	152.591	153.407	154.194
3.5	142.813	143.074	143.332	143.587	143.838	145.046	146.183	147.260	148.283	149.259	150.192	151.087
4.0	136.766	137.107	137.442	137.771	138.094	139.627	141.043	142.363	143.600	144.766	145.870	146.919
4.2	133.692	134.083	134.467	134.841	135.208	136.937	138.517	139.974	141.329	142.599	143.794	144.925
4.4	130.102	130.564	131.014	131.452	131.879	133.870	135.660	137.291	138.794	140.190	141.496	142.725
4.6	125.811	126.380	126.929	127.459	127.973	130.330	132.403	134.262	135.953	137.507	138.949	140.295
4.8	120.468	121.144	121.824	122.503	123.179	126.160	128.834	131.803	135.174	138.498	141.111	143.603
5.0	113.270	114.076	114.881	115.685	116.488	120.886	124.174	127.866	131.053	134.091	136.924	139.602
5.1	108.364	109.242	110.117	110.983	111.840	116.072	119.604	123.517	127.015	130.212	133.182	135.971
5.2	101.626	102.586	103.544	104.499	105.450	110.620	114.647	118.747	122.840	126.806	130.631	134.248
5.3	92.443	93.524	94.599	95.668	96.731	102.812	107.340	111.940	116.642	121.385	125.971	130.414
5.4	70.938	72.177	73.411	74.640	75.864	82.510	87.531	92.640	97.840	103.140	108.440	113.640
5.5	51.715	53.001	54.281	55.556	56.826	63.140	68.810	74.640	80.640	86.810	93.140	99.640
5.6	44.247	45.677	47.101	48.520	49.934	56.810	62.940	69.240	75.810	82.540	89.440	96.640
5.7	39.901	41.461	43.016	44.566	46.111	53.410	59.940	66.640	73.540	80.640	87.940	95.440
5.8	36.863	38.563	40.258	41.948	43.633	51.410	58.340	65.540	72.940	80.540	88.340	96.340
5.9	34.537	36.337	38.131	39.920	41.704	49.810	56.940	64.340	71.940	79.740	87.740	95.940
6.0	32.657	34.557	36.451	38.340	40.224	48.610	55.940	63.540	71.340	79.340	87.540	95.940
6.2	29.731	31.731	33.724	35.711	37.692	46.410	53.940	61.740	69.740	77.940	86.340	94.940
6.4	27.501	29.601	31.694	33.781	35.862	44.910	52.640	60.640	68.840	77.240	85.840	94.640
6.6	25.707	27.907	30.101	32.288	34.469	43.410	51.340	59.540	67.940	76.540	85.340	94.340
6.8	24.212	26.512	28.801	31.088	33.369	42.010	50.140	58.540	67.140	75.940	84.940	94.140
7.0	22.936	25.336	27.724	30.111	32.492	40.710	49.040	57.640	66.440	75.440	84.640	94.040
7.5	20.400	22.900	25.394	27.881	30.362	39.110	47.740	56.640	65.740	75.040	84.540	94.240
8.0	18.475	21.075	23.669	26.256	28.837	37.810	46.740	55.940	65.340	74.940	84.740	94.740
8.5	16.942	19.642	22.336	25.024	27.707	36.510	45.740	55.140	64.740	74.540	84.540	94.740
9.0	15.681	18.481	21.274	24.061	26.842	35.310	44.740	54.340	64.140	74.140	84.340	94.740
9.5	14.613	17.513	20.407	23.294	26.175	34.210	43.840	53.640	63.740	73.940	84.340	94.740
10.0	13.707	16.707	19.694	22.671	25.642	33.210	43.040	53.140	63.440	73.840	84.340	94.740
11.0	12.223	15.323	18.407	21.476	24.536	31.410	41.440	51.740	62.240	72.840	83.540	94.440
12.0	11.049	14.249	17.424	20.584	23.734	29.810	40.040	50.540	61.240	72.040	82.840	93.840
13.0	10.094	13.394	16.669	19.929	23.184	28.410	38.740	49.440	60.240	71.140	82.140	93.240
14.0	9.298	12.698	16.073	19.443	22.804	27.110	37.640	48.540	59.540	70.640	81.840	93.140
15.0	8.625	12.125	15.500	18.875	22.250	25.910	36.640	47.740	58.940	70.140	81.540	93.040
16.0	8.046	11.646	15.021	18.401	21.821	24.810	35.840	47.040	58.440	69.840	81.440	93.040
17.0	7.544	11.244	14.619	18.004	21.424	23.810	35.140	46.440	58.040	69.640	81.440	93.040
18.0	7.103	10.903	14.278	17.653	21.073	22.910	34.540	45.940	57.640	69.440	81.340	93.040
19.0	6.712	10.612	13.933	17.308	20.728	22.110	34.040	45.540	57.340	69.340	81.340	93.040
20.0	6.364	10.364	13.638	17.013	20.433	21.410	33.640	45.240	57.140	69.240	81.340	93.040
25.0	5.061	9.255	12.449	15.643	18.837	20.010	32.240	43.840	55.840	68.040	80.440	92.840
30.0	4.208	8.369	11.530	14.690	17.851	18.655	31.040	42.640	54.840	67.140	79.640	92.640
35.0	3.603	7.741	10.878	14.016	17.154	17.840	30.040	41.640	53.940	66.340	78.940	92.540
40.0	3.152	7.272	10.393	13.513	16.633	17.234	29.240	40.840	53.340	65.840	78.540	92.540
45.0	2.801	6.909	10.016	13.123	16.229	16.763	28.540	40.240	52.840	65.440	78.240	92.540
50.0	2.522	6.618	9.714	12.811	15.907	16.388	27.940	39.740	52.440	65.140	78.040	92.540
60.0	2.102	6.183	9.263	12.343	15.424	15.825	26.640	38.640	51.440	64.240	77.240	92.540
80.0	1.579	5.639	8.699	11.759	14.820	15.221	24.222	37.222	50.222	63.222	76.222	92.540
100.0	1.263	5.312	8.360	11.409	14.457	14.899	22.181	35.281	48.281	61.281	74.281	92.540
120.0	1.053	5.094	8.134	11.175	14.215	14.617	20.618	33.818	46.818	60.818	73.818	92.540
140.0	0.903	4.934	8.073	11.007	14.042	14.415	19.388	32.568	45.568	59.568	72.568	92.540
160.0	0.791	4.821	8.051	10.882	13.912	14.264	18.366	31.566	44.566	58.566	71.566	92.540
180.0	0.703	4.730	8.057	10.784	13.811	14.160	17.466	30.666	43.666	57.666	70.666	92.540
200.0	0.633	4.657	8.061	10.706	13.730	14.051	16.673	29.873	42.873	56.873	69.873	92.540
220.0	0.575	4.598	8.060	10.642	13.664	13.944	15.984	29.184	42.184	56.184	69.184	92.540
240.0	0.528	4.548	8.058	10.588	13.609	13.840	15.391	28.591	41.591	55.591	68.591	92.540
260.0	0.487	4.506	8.054	10.543	13.562	13.735	14.804	28.004	41.004	55.004	68.004	92.540
280.0	0.452	4.470	8.047	10.504	13.522	13.629	14.218	27.418	40.418	54.418	67.418	92.540
300.0	0.422	4.438	8.035	10.471	13.487	13.526	13.649	26.838	39.838	53.838	66.838	92.540

Table 4.2.3 Helium ⁴ density, ρ , mg/cm³. (continued).

PRES MM/H ATM	0.608 6.000	0.769 7.000	0.811 8.000	0.912 9.000	1.013 10.000	1.520 15.000	2.026 20.000	2.533 25.000	3.040 30.000	3.546 35.000	4.053 40.000	4.560 45.000
TEMP, K												
3.0	153.407	154.955	156.409	157.781	159.082	164.783	169.558	173.729	177.470	180.890	184.061	187.033
3.5	150.192	151.948	153.578	155.103	156.539	162.719	167.784	172.139	175.997	179.487	182.691	185.666
4.0	145.870	147.920	149.796	151.530	153.146	159.959	165.406	170.015	174.050	177.664	180.956	183.991
4.2	143.794	145.999	148.002	149.842	151.547	158.668	164.298	169.029	173.151	176.829	180.169	183.248
4.4	141.496	143.885	146.036	147.998	149.807	157.275	163.107	167.973	172.190	175.940	179.333	182.446
4.6	138.949	141.560	143.886	145.990	147.918	155.778	161.835	166.848	171.170	174.998	178.452	181.612
4.8	136.111	138.995	141.531	143.804	145.870	154.174	160.479	165.654	170.092	174.006	177.526	180.739
5.0	132.924	136.152	138.944	141.417	143.646	152.458	159.040	164.393	168.956	172.964	176.557	179.827
5.1	131.182	134.615	137.557	140.145	142.466	151.559	158.289	163.738	168.368	172.425	176.057	179.350
5.2	129.331	132.997	136.106	138.821	141.241	150.634	157.521	163.068	167.767	171.876	175.548	178.881
5.3	127.571	131.466	134.736	137.571	140.086	149.762	156.795	162.434	167.198	171.356	175.065	178.429
5.4	125.728	129.877	133.321	136.286	138.902	148.873	156.058	161.793	166.623	170.838	174.577	177.972
5.5	123.790	128.221	131.857	134.962	137.685	147.968	155.309	161.141	166.048	170.297	174.044	177.510
5.6	121.747	126.496	130.341	133.596	136.435	147.045	154.548	160.481	165.449	169.759	173.586	177.044
5.7	119.590	124.694	128.769	132.188	135.149	146.104	153.775	159.812	164.852	169.214	173.082	176.573
5.8	117.307	122.812	127.140	130.735	133.828	145.145	152.991	159.134	164.247	168.663	172.573	176.098
5.9	114.885	120.844	125.450	129.236	132.470	144.169	152.194	158.447	163.635	168.106	172.059	175.618
6.0	112.311	118.782	123.695	127.688	131.073	143.174	151.386	157.751	163.016	167.544	171.544	175.134
6.2	106.658	114.357	119.979	124.440	128.160	141.129	149.735	156.333	161.757	166.402	170.488	174.154
6.4	100.270	109.490	115.965	120.974	125.078	139.010	148.036	154.881	160.471	165.237	169.417	173.157
6.6	93.195	104.156	111.634	117.277	121.819	136.815	146.290	153.395	159.158	164.050	168.327	172.144
6.8	85.739	98.384	106.979	113.341	118.375	134.543	144.498	151.876	157.820	162.842	167.219	171.115
7.0	78.457	92.299	102.024	109.167	114.745	132.193	142.659	150.323	156.455	161.613	166.093	170.071
7.5	63.852	77.403	88.905	97.889	104.923	125.976	137.858	146.299	152.935	158.452	163.203	167.395
8.0	54.101	65.679	76.616	86.339	94.478	119.298	132.776	142.079	149.264	155.167	160.209	164.629
8.5	47.243	57.247	66.852	75.998	84.363	112.245	127.435	137.674	145.450	151.767	157.117	161.779
9.0	42.179	50.900	59.484	67.650	75.498	104.993	121.878	133.102	141.587	148.261	153.935	158.849
9.5	38.271	45.979	53.674	61.136	68.219	97.798	116.172	128.392	137.448	144.658	150.671	155.847
10.0	35.145	42.052	49.000	55.823	62.396	90.937	110.411	123.581	133.295	140.972	147.333	152.781
11.0	30.440	36.185	41.993	47.775	53.450	79.002	99.070	113.707	124.672	133.305	140.297	146.416
12.0	26.985	31.929	36.927	41.932	46.893	69.810	89.070	104.264	116.115	125.574	133.356	139.941
13.0	24.309	28.665	33.062	37.474	41.869	62.705	80.711	95.737	107.985	118.011	126.359	133.445
14.0	22.162	26.064	29.997	33.944	37.885	56.897	73.790	88.310	100.555	110.853	119.580	127.067
15.0	20.392	23.934	27.497	31.070	34.642	52.066	67.973	81.911	93.931	104.265	113.179	120.926
16.0	18.906	22.155	25.418	28.688	31.956	47.981	62.869	76.193	87.917	98.176	107.161	115.063
17.0	17.639	20.645	23.659	26.677	29.692	44.522	58.474	71.168	82.523	92.611	101.863	109.526
18.0	16.544	19.344	22.148	24.953	27.755	41.559	54.661	66.740	77.691	87.545	96.392	104.341
19.0	15.586	18.209	20.834	23.457	26.076	38.991	51.329	62.821	73.358	82.942	91.633	99.514
20.0	14.740	17.209	19.678	22.144	24.604	36.744	48.395	59.337	69.464	78.760	87.263	95.034
25.0	11.639	13.563	15.481	17.393	19.298	28.693	37.804	46.550	54.875	62.749	70.165	77.135
30.0	9.648	11.235	12.815	14.368	15.955	23.674	31.183	38.451	45.453	52.172	58.601	64.736
35.0	8.253	9.607	10.955	12.297	13.633	20.214	26.625	32.855	38.894	44.733	50.369	55.801
40.0	7.216	8.400	9.578	10.750	11.917	17.668	23.277	28.742	34.057	39.220	44.230	49.085
45.0	6.415	7.466	8.514	9.556	10.593	15.709	20.704	25.579	30.333	34.965	39.475	43.866
50.0	5.775	6.722	7.666	8.605	9.539	14.151	18.660	23.066	27.371	31.574	35.677	39.681
60.0	4.817	5.608	6.396	7.181	7.963	11.823	15.605	19.310	22.940	26.496	29.978	33.386
80.0	3.621	4.217	4.811	5.403	5.993	8.913	11.785	14.809	17.386	20.118	22.806	25.445
100.0	2.901	3.380	3.857	4.333	4.808	7.161	9.480	11.768	14.023	16.248	18.443	20.601
120.0	2.421	2.821	3.220	3.618	4.015	5.986	7.934	9.858	11.759	13.639	15.496	17.337
140.0	2.077	2.421	2.764	3.106	3.447	5.144	6.822	8.484	10.128	11.756	13.367	14.966
160.0	1.819	2.120	2.421	2.721	3.020	4.509	5.985	7.447	8.896	10.332	11.755	13.165
180.0	1.618	1.886	2.154	2.421	2.687	4.015	5.331	6.637	7.932	9.217	10.491	11.756
200.0	1.457	1.698	1.940	2.180	2.421	3.618	4.806	5.986	7.157	8.319	9.473	10.615
220.0	1.325	1.545	1.764	1.983	2.202	3.292	4.375	5.451	6.520	7.581	8.636	9.684
240.0	1.215	1.417	1.618	1.819	2.020	3.021	4.015	5.004	5.987	6.964	7.935	8.901
260.0	1.122	1.308	1.494	1.680	1.866	2.790	3.710	4.625	5.535	6.439	7.339	8.234
280.0	1.042	1.215	1.388	1.561	1.733	2.593	3.448	4.299	5.146	5.988	6.826	7.661
300.0	0.973	1.134	1.296	1.457	1.618	2.421	3.221	4.016	4.808	5.596	6.381	7.161

Table 4.2.3 Helium⁴ Density, ρ , mg/cm³ (continued).

PRES MN/M	5.066	5.573	6.079	6.586	7.093	7.599	8.106	8.613	9.119	9.626	10.133	10.639
ATM	50.000	55.000	60.000	65.000	70.000	75.000	80.000	85.000	90.000	95.000	100.000	105.000
TEMP, K												
3.0	189.843	192.519	195.082	197.551	199.939	202.260						
3.5	188.454	191.086	193.585	195.971	198.259	200.460	202.585	204.643	206.641	208.585	210.480	
4.0	186.817	189.469	191.973	194.350	196.617	198.787	200.872	202.880	204.820	206.697	208.519	210.289
4.2	186.093	188.764	191.282	193.668	195.940	198.111	200.193	202.196	204.128	205.996	207.805	209.561
4.4	185.331	188.028	190.565	192.965	195.247	197.424	199.510	201.514	203.444	205.307	207.110	208.858
4.6	184.535	187.261	189.822	192.241	194.537	196.726	198.819	200.828	202.761	204.625	206.427	208.172
4.8	183.704	186.465	189.053	191.495	193.810	196.013	198.119	200.137	202.076	203.945	205.750	207.496
5.0	182.839	185.638	188.259	190.727	193.063	195.285	197.406	199.436	201.386	203.263	205.074	206.825
5.1	182.395	185.215	187.852	190.335	192.684	194.916	197.045	199.083	201.039	202.921	204.736	206.490
5.2	181.944	184.785	187.441	189.939	192.300	194.543	196.682	198.728	200.690	202.578	204.398	206.156
5.3	181.516	184.377	187.050	189.562	191.936	194.189	196.337	198.390	200.360	202.253	204.078	205.840
5.4	181.084	183.966	186.656	189.183	191.570	193.835	195.991	198.053	200.029	201.929	203.758	205.525
5.5	180.648	183.552	186.260	188.802	191.202	193.478	195.645	197.715	199.699	201.604	203.448	205.211
5.6	180.208	183.134	185.861	188.419	190.832	193.120	195.297	197.376	199.368	201.280	203.122	204.898
5.7	179.764	182.713	185.458	188.033	190.460	192.760	194.944	197.036	199.036	200.956	202.804	204.586
5.8	179.317	182.288	185.053	187.644	190.086	192.399	194.598	196.696	198.704	200.631	202.486	204.274
5.9	178.865	181.860	184.645	187.254	189.710	192.036	194.246	196.354	198.371	200.306	202.168	203.962
6.0	178.410	181.429	184.234	186.860	189.332	191.671	193.893	196.011	198.037	199.981	201.849	203.650
6.2	177.489	180.537	183.404	186.066	188.570	190.936	193.182	195.322	197.367	199.328	201.212	203.026
6.4	176.553	179.672	182.563	185.263	187.799	190.193	192.465	194.627	196.693	198.671	200.572	202.481
6.6	175.603	178.775	181.711	184.449	187.019	189.443	191.741	193.927	196.013	198.011	199.928	201.773
6.8	174.639	177.866	180.848	183.626	186.230	188.685	191.010	193.228	195.329	197.346	199.281	201.142
7.0	173.662	176.944	179.974	182.793	185.433	187.928	190.272	192.508	194.638	196.676	198.630	200.508
7.5	171.161	174.589	177.742	180.668	183.402	185.978	188.396	190.697	192.887	194.978	196.988	198.983
8.0	168.568	172.162	175.446	178.484	181.316	183.971	186.473	188.843	191.095	193.242	195.296	197.266
8.5	165.924	169.667	173.088	176.243	179.177	181.922	184.505	186.946	189.262	191.468	193.576	195.594
9.0	163.198	167.109	170.671	173.948	176.988	179.826	182.491	185.086	187.389	189.656	191.818	193.887
9.5	160.407	164.492	168.200	171.603	174.751	177.684	180.434	183.025	185.477	187.805	190.024	192.145
10.0	157.557	161.821	165.680	169.211	172.478	175.582	178.338	181.087	183.528	185.920	188.196	190.370
11.0	151.651	156.242	160.466	164.264	167.755	170.988	174.003	176.829	179.442	182.012	184.405	186.684
12.0	145.641	150.667	155.167	159.243	162.974	166.416	169.614	172.664	175.413	178.065	180.577	182.981
13.0	139.587	144.990	149.812	154.168	158.141	161.796	165.183	168.340	171.299	174.085	176.719	179.218
14.0	133.500	139.323	144.448	149.072	153.283	157.150	160.724	164.050	167.180	170.083	172.841	175.455
15.0	127.722	133.745	139.135	144.002	148.435	152.502	156.259	159.749	163.009	166.068	168.951	171.677
16.0	122.056	128.291	133.893	138.966	143.592	147.838	151.761	155.405	158.806	161.995	164.997	167.834
17.0	116.637	123.022	128.788	134.027	138.817	143.222	147.294	151.078	154.611	157.922	161.039	163.982
18.0	111.502	117.978	123.859	129.226	134.150	138.687	142.889	146.798	150.449	153.874	157.096	160.139
19.0	106.670	113.185	119.137	124.594	129.619	134.263	138.573	142.589	146.345	149.871	153.190	156.325
20.0	102.142	108.656	114.639	120.152	125.247	129.972	134.369	138.474	142.319	145.932	149.337	152.555
25.0	83.679	89.823	95.593	101.017	106.123	110.934	115.474	119.766	123.829	127.681	131.340	134.821
30.0	70.590	76.105	81.476	86.535	91.357	95.956	100.345	104.536	108.543	112.377	116.048	119.567
35.0	61.027	66.054	70.888	75.534	80.000	84.295	88.426	92.401	96.228	99.915	103.469	106.897
40.0	53.788	58.339	62.741	67.000	71.118	75.102	78.955	82.684	86.293	89.787	93.172	96.452
45.0	48.124	52.277	56.307	60.222	64.025	67.720	71.309	74.796	78.185	81.479	84.682	87.796
50.0	43.585	47.392	51.103	54.720	58.245	61.681	65.029	68.293	71.474	74.576	77.601	80.551
60.0	36.729	40.000	43.202	46.336	49.405	52.409	55.351	58.231	61.050	63.811	66.516	69.164
70.0	28.050	30.608	33.125	35.602	38.039	40.437	42.797	45.119	47.405	49.655	51.869	54.045
80.0	22.744	24.851	26.931	28.982	31.007	33.006	34.978	36.924	38.846	40.743	42.616	44.465
100.0	19.147	20.941	22.715	24.469	26.204	27.919	29.615	31.292	32.951	34.592	36.215	37.821
150.0	16.541	18.105	19.653	21.186	22.704	24.207	25.696	27.171	28.631	30.078	31.511	32.931
200.0	14.564	15.949	17.323	18.685	20.036	21.374	22.702	24.018	25.323	26.617	27.901	29.174
300.0	13.010	14.255	15.490	16.716	17.932	19.139	20.337	21.526	22.706	23.877	25.039	26.194
400.0	11.757	12.887	14.009	15.124	16.230	17.329	18.421	19.505	20.581	21.651	22.713	23.768
500.0	10.725	11.760	12.788	13.809	14.824	15.833	16.836	17.832	18.822	19.806	20.784	21.756
600.0	9.860	10.814	11.762	12.706	13.643	14.575	15.502	16.424	17.341	18.252	19.158	20.060
700.0	9.124	10.009	10.890	11.765	12.637	13.503	14.365	15.223	16.076	16.925	17.769	18.608
800.0	8.490	9.316	10.137	10.955	11.769	12.578	13.384	14.186	14.984	15.778	16.568	17.355
900.0	7.949	8.712	9.463	10.249	11.012	11.772	12.528	13.281	14.030	14.776	15.519	16.259

Table 4.2.4 Helium⁴ specific heat at constant pressure, c_p , J/g-K.

PRES MN/M ² ATM	0.010 0.100	0.051 0.500	0.101 1.000	0.152 1.500	0.182 1.800	0.193 1.900	0.203 2.000	0.213 2.100	0.223 2.200	0.233 2.300	0.243 2.400	0.253 2.500
TEMP, K												
3.0	5.55	2.40	2.35	2.32	2.30	2.29	2.28	2.28	2.27	2.26	2.26	2.25
3.5	5.42	3.10	3.00	2.91	2.87	2.86	2.85	2.83	2.82	2.81	2.80	2.79
4.0	5.35	6.42	4.07	3.84	3.73	3.69	3.66	3.63	3.60	3.58	3.55	3.53
4.2	5.33	6.21	4.86	4.43	4.25	4.19	4.15	4.10	4.06	4.01	3.98	3.94
4.4	5.32	6.05	6.46	5.33	4.99	4.89	4.81	4.73	4.66	4.59	4.53	4.47
4.6	5.30	5.93	7.65	7.03	6.21	6.01	5.84	5.69	5.55	5.43	5.32	5.22
4.8	5.29	5.83	7.14	11.79	9.03	8.37	7.86	7.46	7.12	6.84	6.60	6.39
5.0	5.28	5.76	6.80	9.47	15.94	25.82	15.93	12.99	11.28	10.14	9.32	8.75
5.1	5.28	5.72	6.67	8.83	12.69	15.95	24.07	32.35	19.29	14.87	12.55	11.69
5.2	5.27	5.69	6.55	8.36	11.03	12.78	15.76	22.20	51.17	39.78	21.06	15.81
5.3	5.27	5.67	6.45	7.99	9.99	11.12	12.78	15.43	20.44	33.76	111.69	38.46
5.4	5.27	5.64	6.36	7.70	9.27	10.08	11.17	12.69	15.00	18.90	26.66	45.30
5.5	5.27	5.62	6.29	7.46	8.73	9.35	10.14	11.16	12.54	14.53	17.57	22.60
5.6	5.26	5.60	6.22	7.26	8.32	8.81	9.41	10.15	11.10	12.34	14.04	16.43
5.7	5.26	5.58	6.16	7.09	7.99	8.40	8.87	9.44	10.14	11.01	12.12	13.55
5.8	5.26	5.56	6.10	6.94	7.73	8.06	8.45	8.91	9.45	10.10	10.90	11.87
5.9	5.25	5.55	6.05	6.82	7.50	7.79	8.12	8.50	8.93	9.44	10.04	10.75
6.0	5.25	5.53	6.00	6.70	7.31	7.56	7.84	8.16	8.52	8.93	9.41	9.97
6.2	5.25	5.50	5.92	6.52	7.01	7.20	7.42	7.65	7.92	8.21	8.53	8.90
6.4	5.24	5.48	5.86	6.37	6.78	6.93	7.10	7.29	7.49	7.71	7.95	8.21
6.6	5.24	5.46	5.80	6.25	6.59	6.72	6.86	7.01	7.17	7.34	7.53	7.73
6.8	5.24	5.44	5.75	6.15	6.44	6.55	6.67	6.79	6.93	7.07	7.22	7.38
7.0	5.24	5.42	5.71	6.06	6.32	6.41	6.51	6.62	6.73	6.85	6.97	7.11
7.5	5.23	5.39	5.62	5.90	6.09	6.16	6.23	6.31	6.38	6.47	6.55	6.64
8.0	5.23	5.36	5.56	5.78	5.93	5.99	6.04	6.10	6.16	6.22	6.28	6.34
8.5	5.22	5.34	5.51	5.70	5.82	5.86	5.91	5.95	6.00	6.04	6.09	6.14
9.0	5.22	5.33	5.47	5.63	5.73	5.77	5.80	5.84	5.88	5.92	5.95	5.99
9.5	5.22	5.31	5.44	5.58	5.66	5.69	5.72	5.76	5.79	5.82	5.85	5.88
10.0	5.21	5.30	5.41	5.53	5.61	5.64	5.66	5.69	5.71	5.74	5.77	5.80
11.0	5.21	5.28	5.38	5.47	5.53	5.55	5.57	5.59	5.61	5.64	5.66	5.68
12.0	5.21	5.27	5.35	5.43	5.48	5.49	5.51	5.53	5.54	5.56	5.58	5.60
13.0	5.21	5.26	5.32	5.39	5.43	5.45	5.46	5.48	5.49	5.51	5.52	5.53
14.0	5.20	5.25	5.31	5.37	5.40	5.41	5.43	5.44	5.45	5.46	5.47	5.49
15.0	5.20	5.24	5.29	5.34	5.38	5.39	5.40	5.41	5.42	5.43	5.44	5.45
16.0	5.20	5.24	5.28	5.33	5.35	5.36	5.37	5.38	5.39	5.40	5.41	5.42
17.0	5.20	5.23	5.27	5.31	5.33	5.34	5.35	5.36	5.37	5.37	5.38	5.39
18.0	5.20	5.23	5.26	5.30	5.32	5.33	5.33	5.34	5.35	5.35	5.36	5.37
19.0	5.20	5.22	5.25	5.29	5.31	5.32	5.32	5.32	5.33	5.34	5.34	5.35
20.0	5.20	5.22	5.25	5.28	5.29	5.30	5.31	5.31	5.32	5.32	5.33	5.33
25.0	5.20	5.21	5.23	5.25	5.26	5.26	5.26	5.27	5.27	5.27	5.28	5.28
30.0	5.20	5.21	5.22	5.23	5.24	5.24	5.24	5.24	5.25	5.25	5.25	5.25
35.0	5.19	5.20	5.21	5.22	5.22	5.23	5.23	5.23	5.23	5.23	5.24	5.24
40.0	5.19	5.20	5.21	5.21	5.22	5.22	5.22	5.22	5.22	5.22	5.22	5.23
45.0	5.19	5.20	5.20	5.21	5.21	5.21	5.21	5.21	5.22	5.22	5.22	5.22
50.0	5.19	5.20	5.20	5.21	5.21	5.21	5.21	5.21	5.21	5.21	5.21	5.21
60.0	5.19	5.20	5.20	5.20	5.20	5.20	5.20	5.20	5.21	5.21	5.21	5.21
80.0	5.19	5.19	5.20	5.20	5.20	5.20	5.20	5.20	5.20	5.20	5.20	5.20
100.0	5.19	5.19	5.19	5.20	5.20	5.20	5.20	5.20	5.20	5.20	5.20	5.20
120.0	5.19	5.19	5.19	5.19	5.19	5.20	5.20	5.20	5.20	5.20	5.20	5.20
140.0	5.19	5.19	5.19	5.19	5.19	5.19	5.19	5.19	5.19	5.19	5.19	5.19
160.0	5.19	5.19	5.19	5.19	5.19	5.19	5.19	5.19	5.19	5.19	5.19	5.19
180.0	5.19	5.19	5.19	5.19	5.19	5.19	5.19	5.19	5.19	5.19	5.19	5.19
200.0	5.19	5.19	5.19	5.19	5.19	5.19	5.19	5.19	5.19	5.19	5.19	5.19
220.0	5.19	5.19	5.19	5.19	5.19	5.19	5.19	5.19	5.19	5.19	5.19	5.19
240.0	5.19	5.19	5.19	5.19	5.19	5.19	5.19	5.19	5.19	5.19	5.19	5.19
260.0	5.19	5.19	5.19	5.19	5.19	5.19	5.19	5.19	5.19	5.19	5.19	5.19
280.0	5.19	5.19	5.19	5.19	5.19	5.19	5.19	5.19	5.19	5.19	5.19	5.19
300.0	5.19	5.19	5.19	5.19	5.19	5.19	5.19	5.19	5.19	5.19	5.19	5.19

Table 4.2.4 Helium⁴ specific heat at constant pressure, c_p , J/g-K
(continued).

PRES MN/M ² ATM TEMP, K	0.263 2.600	0.274 2.700	0.284 2.800	0.294 2.900	0.304 3.000	0.355 3.500	0.405 4.000	0.456 4.500	0.507 5.000	0.557 5.500	0.608 6.000	0.659 6.500
3.0	2.24	2.24	2.23	2.23	2.22	2.20	2.17	2.15	2.12	2.10	2.08	2.06
3.5	2.78	2.77	2.75	2.74	2.73	2.69	2.65	2.61	2.57	2.54	2.51	2.48
4.0	3.50	3.48	3.46	3.44	3.41	3.32	3.24	3.17	3.11	3.06	3.01	2.96
4.2	3.90	3.87	3.84	3.81	3.78	3.65	3.54	3.45	3.37	3.30	3.24	3.19
4.4	4.42	4.37	4.32	4.27	4.23	4.05	3.90	3.78	3.67	3.58	3.50	3.43
4.6	5.12	5.04	4.96	4.89	4.82	4.54	4.32	4.15	4.02	3.90	3.80	3.71
4.8	6.20	6.04	5.89	5.76	5.64	5.18	4.85	4.61	4.42	4.26	4.13	4.02
5.0	8.20	7.80	7.46	7.17	6.92	6.06	5.53	5.16	4.89	4.67	4.50	4.36
5.1	10.08	9.32	8.74	8.27	7.88	6.63	5.93	5.48	5.15	4.90	4.70	4.53
5.2	13.19	11.58	10.48	9.66	9.04	7.23	6.33	5.77	5.38	5.09	4.87	4.68
5.3	22.08	16.64	13.85	12.12	10.93	8.03	6.80	6.09	5.62	5.28	5.02	4.82
5.4	64.28	34.77	22.54	17.35	14.50	9.19	7.43	6.52	5.94	5.53	5.23	4.99
5.5	31.23	42.26	43.09	30.46	22.18	10.88	8.25	7.03	6.30	5.81	5.46	5.18
5.6	19.92	24.92	30.89	34.87	33.24	13.46	9.31	7.64	6.72	6.13	5.71	5.39
5.7	15.46	18.00	21.25	24.92	27.96	17.32	10.72	8.40	7.22	6.50	6.00	5.63
5.8	13.09	14.63	16.54	18.82	21.28	21.49	12.57	9.34	7.81	6.91	6.31	5.89
5.9	11.62	12.66	13.91	15.39	17.06	22.23	14.82	10.49	8.50	7.39	6.67	6.17
6.0	10.61	11.37	12.25	13.28	14.45	19.92	16.89	11.83	9.31	7.93	7.07	6.48
6.2	9.31	9.77	10.29	10.88	11.53	15.41	17.19	14.46	11.22	9.23	8.01	7.21
6.4	8.50	8.82	9.17	9.55	9.97	12.54	14.78	15.00	12.93	10.70	9.12	8.06
6.6	7.95	8.19	8.44	8.71	9.01	10.79	12.69	13.70	13.40	11.88	10.26	9.00
6.8	7.55	7.73	7.93	8.14	8.36	9.67	11.15	12.29	12.68	12.24	11.10	9.89
7.0	7.24	7.39	7.55	7.71	7.89	8.89	10.05	11.10	11.72	11.83	11.38	10.51
7.5	6.73	6.82	6.92	7.03	7.13	7.73	8.41	9.12	9.74	10.16	10.36	10.37
8.0	6.41	6.48	6.55	6.62	6.69	7.10	7.55	8.02	8.49	8.89	9.18	9.36
8.5	6.19	6.24	6.30	6.35	6.41	6.70	7.02	7.37	7.71	8.03	8.31	8.52
9.0	6.03	6.08	6.12	6.16	6.20	6.43	6.68	6.93	7.20	7.45	7.69	7.89
9.5	5.92	5.95	5.98	6.02	6.05	6.24	6.43	6.64	6.84	7.05	7.24	7.42
10.0	5.83	5.85	5.88	5.91	5.94	6.09	6.25	6.42	6.58	6.75	6.91	7.06
11.0	5.70	5.72	5.74	5.77	5.79	5.98	6.02	6.13	6.25	6.37	6.49	6.60
12.0	5.61	5.63	5.65	5.67	5.68	5.77	5.86	5.95	6.05	6.14	6.23	6.31
13.0	5.55	5.56	5.58	5.59	5.61	5.68	5.75	5.83	5.90	5.98	6.05	6.12
14.0	5.50	5.51	5.52	5.54	5.55	5.61	5.67	5.74	5.80	5.86	5.92	5.98
15.0	5.46	5.47	5.48	5.49	5.50	5.56	5.61	5.67	5.72	5.77	5.82	5.88
16.0	5.43	5.44	5.44	5.45	5.46	5.51	5.56	5.60	5.65	5.69	5.74	5.78
17.0	5.40	5.41	5.41	5.42	5.43	5.47	5.51	5.55	5.59	5.63	5.67	5.71
18.0	5.37	5.38	5.39	5.40	5.40	5.44	5.47	5.51	5.55	5.58	5.62	5.65
19.0	5.36	5.36	5.37	5.37	5.38	5.41	5.44	5.48	5.51	5.54	5.57	5.60
20.0	5.34	5.35	5.35	5.36	5.36	5.39	5.42	5.45	5.47	5.50	5.53	5.56
25.0	5.29	5.29	5.29	5.30	5.30	5.32	5.33	5.35	5.37	5.39	5.40	5.42
30.0	5.26	5.26	5.26	5.26	5.27	5.28	5.29	5.30	5.31	5.33	5.34	5.35
35.0	5.24	5.24	5.24	5.24	5.25	5.25	5.26	5.27	5.28	5.29	5.30	5.31
40.0	5.23	5.23	5.23	5.23	5.23	5.24	5.25	5.25	5.26	5.27	5.27	5.28
45.0	5.22	5.22	5.22	5.22	5.22	5.23	5.23	5.24	5.24	5.25	5.25	5.26
50.0	5.21	5.22	5.22	5.22	5.22	5.22	5.23	5.23	5.23	5.24	5.24	5.25
60.0	5.21	5.21	5.21	5.21	5.21	5.21	5.21	5.22	5.22	5.22	5.23	5.23
80.0	5.20	5.20	5.20	5.20	5.20	5.20	5.20	5.21	5.21	5.21	5.21	5.21
100.0	5.20	5.20	5.20	5.20	5.20	5.20	5.20	5.20	5.20	5.20	5.20	5.20
120.0	5.20	5.20	5.20	5.20	5.20	5.20	5.20	5.20	5.20	5.20	5.20	5.20
140.0	5.19	5.19	5.19	5.20	5.20	5.20	5.20	5.20	5.20	5.20	5.20	5.20
160.0	5.19	5.19	5.19	5.19	5.19	5.19	5.19	5.20	5.20	5.20	5.20	5.20
180.0	5.19	5.19	5.19	5.19	5.19	5.19	5.19	5.19	5.19	5.19	5.19	5.20
200.0	5.19	5.19	5.19	5.19	5.19	5.19	5.19	5.19	5.19	5.19	5.19	5.19
220.0	5.19	5.19	5.19	5.19	5.19	5.19	5.19	5.19	5.19	5.19	5.19	5.19
240.0	5.19	5.19	5.19	5.19	5.19	5.19	5.19	5.19	5.19	5.19	5.19	5.19
260.0	5.19	5.19	5.19	5.19	5.19	5.19	5.19	5.19	5.19	5.19	5.19	5.19
280.0	5.19	5.19	5.19	5.19	5.19	5.19	5.19	5.19	5.19	5.19	5.19	5.19
300.0	5.19	5.19	5.19	5.19	5.19	5.19	5.19	5.19	5.19	5.19	5.19	5.19

Table 4.2.4 Helium⁴ specific heat at constant pressure, c_p , J/g-K
(continued).

PRES MM/HG ATM TEMP, K	0.600 6.000	0.709 7.000	0.811 8.000	0.912 9.000	1.013 10.000	1.520 15.000	2.026 20.000	2.533 25.000	3.040 30.000	3.546 35.000	4.053 40.000	4.560 45.000
3.0	2.00	2.05	2.01	1.98	1.95	1.82	1.71	1.62	1.54	1.48	1.44	1.41
3.5	2.51	2.45	2.40	2.36	2.32	2.15	2.01	1.90	1.81	1.73	1.67	1.62
4.0	3.01	2.92	2.84	2.78	2.72	2.49	2.34	2.21	2.11	2.03	1.96	1.90
4.2	3.24	3.13	3.04	2.97	2.90	2.65	2.48	2.35	2.25	2.16	2.09	2.03
4.4	3.50	3.37	3.26	3.17	3.10	2.81	2.63	2.49	2.39	2.30	2.22	2.16
4.6	3.80	3.63	3.50	3.40	3.30	2.99	2.79	2.64	2.53	2.44	2.37	2.30
4.8	4.13	3.92	3.76	3.63	3.52	3.17	2.95	2.79	2.68	2.58	2.51	2.44
5.0	4.50	4.24	4.04	3.88	3.76	3.35	3.11	2.95	2.82	2.73	2.65	2.58
5.1	4.70	4.40	4.18	4.01	3.87	3.44	3.19	3.02	2.90	2.80	2.72	2.65
5.2	4.87	4.53	4.29	4.11	3.96	3.50	3.25	3.07	2.94	2.84	2.76	2.70
5.3	5.02	4.64	4.38	4.18	4.02	3.53	3.27	3.09	2.96	2.85	2.77	2.70
5.4	5.23	4.80	4.50	4.28	4.11	3.59	3.31	3.13	2.99	2.89	2.80	2.73
5.5	5.46	4.96	4.63	4.39	4.20	3.65	3.36	3.17	3.03	2.92	2.84	2.77
5.6	5.71	5.15	4.77	4.51	4.30	3.71	3.41	3.21	3.07	2.96	2.87	2.80
5.7	6.00	5.34	4.93	4.63	4.41	3.78	3.46	3.26	3.11	3.00	2.91	2.84
5.8	6.31	5.56	5.09	4.76	4.52	3.85	3.51	3.30	3.15	3.04	2.95	2.87
5.9	6.67	5.79	5.26	4.90	4.64	3.92	3.57	3.35	3.20	3.08	2.99	2.91
6.0	7.07	6.05	5.45	5.05	4.76	3.99	3.63	3.40	3.24	3.12	3.02	2.95
6.2	8.01	6.63	5.87	5.38	5.03	4.14	3.74	3.50	3.33	3.20	3.10	3.02
6.4	9.12	7.31	6.34	5.74	5.32	4.31	3.86	3.60	3.42	3.29	3.18	3.10
6.6	10.26	8.08	6.87	6.14	5.64	4.47	3.99	3.71	3.51	3.37	3.26	3.17
6.8	11.10	8.87	7.45	6.58	5.99	4.65	4.12	3.81	3.61	3.46	3.34	3.25
7.0	11.38	9.56	8.04	7.04	6.36	4.84	4.25	3.92	3.70	3.55	3.43	3.33
7.5	10.36	10.15	9.20	8.16	7.33	5.33	4.59	4.20	3.95	3.77	3.63	3.52
8.0	9.18	9.44	9.33	8.88	8.11	5.85	4.95	4.49	4.19	3.99	3.83	3.71
8.5	8.31	8.67	8.79	8.73	8.43	5.32	4.32	4.78	4.44	4.20	4.03	3.90
9.0	7.69	8.05	8.25	8.31	8.29	6.02	5.69	5.07	4.68	4.42	4.23	4.08
9.5	7.24	7.57	7.79	7.91	7.95	7.14	6.83	5.35	4.93	4.63	4.42	4.26
10.0	6.91	7.20	7.42	7.56	7.63	7.31	6.33	5.62	5.16	4.84	4.61	4.43
11.0	6.49	6.70	6.88	7.02	7.11	7.18	6.69	6.07	5.59	5.24	4.97	4.76
12.0	6.23	6.39	6.54	6.66	6.76	6.89	6.73	6.33	5.91	5.56	5.28	5.06
13.0	6.05	6.19	6.31	6.42	6.51	6.63	6.63	6.40	6.10	5.80	5.54	5.31
14.0	5.92	6.04	6.14	6.24	6.32	6.53	6.51	6.38	6.17	5.94	5.72	5.51
15.0	5.82	5.92	6.02	6.11	6.18	6.41	6.42	6.32	6.17	6.00	5.82	5.65
16.0	5.74	5.83	5.91	5.99	6.06	6.29	6.34	6.29	6.19	6.05	5.91	5.76
17.0	5.67	5.75	5.82	5.89	5.95	6.18	6.26	6.25	6.18	6.06	5.96	5.84
18.0	5.62	5.68	5.75	5.81	5.87	6.09	6.19	6.20	6.15	6.08	5.99	5.89
19.0	5.57	5.63	5.69	5.74	5.80	6.00	6.11	6.14	6.12	6.07	6.00	5.92
20.0	5.53	5.58	5.64	5.69	5.73	5.93	6.04	6.09	6.09	6.05	6.00	5.94
25.0	5.40	5.44	5.47	5.50	5.53	5.67	5.78	5.85	5.89	5.91	5.91	5.90
30.0	5.34	5.36	5.38	5.41	5.43	5.53	5.61	5.68	5.73	5.77	5.79	5.80
35.0	5.30	5.31	5.33	5.35	5.36	5.44	5.51	5.56	5.61	5.65	5.68	5.70
40.0	5.27	5.28	5.30	5.31	5.32	5.38	5.43	5.48	5.52	5.56	5.59	5.61
45.0	5.25	5.26	5.27	5.28	5.29	5.34	5.38	5.42	5.46	5.49	5.52	5.54
50.0	5.24	5.25	5.26	5.27	5.27	5.31	5.35	5.38	5.41	5.44	5.46	5.48
60.0	5.23	5.23	5.24	5.24	5.25	5.27	5.30	5.32	5.34	5.36	5.38	5.40
80.0	5.21	5.21	5.22	5.22	5.22	5.23	5.25	5.26	5.27	5.29	5.30	5.31
100.0	5.20	5.20	5.21	5.21	5.21	5.22	5.23	5.23	5.24	5.25	5.26	5.26
120.0	5.20	5.20	5.20	5.20	5.20	5.21	5.21	5.22	5.22	5.23	5.23	5.24
140.0	5.20	5.20	5.20	5.20	5.20	5.20	5.21	5.21	5.21	5.22	5.22	5.22
160.0	5.20	5.20	5.20	5.20	5.20	5.20	5.20	5.20	5.21	5.21	5.21	5.21
180.0	5.19	5.20	5.20	5.20	5.20	5.20	5.20	5.20	5.20	5.20	5.21	5.21
200.0	5.19	5.19	5.19	5.20	5.20	5.20	5.20	5.20	5.20	5.20	5.20	5.20
220.0	5.19	5.19	5.19	5.19	5.19	5.20	5.20	5.20	5.20	5.20	5.20	5.20
240.0	5.19	5.19	5.19	5.19	5.19	5.19	5.20	5.20	5.20	5.20	5.20	5.20
260.0	5.19	5.19	5.19	5.19	5.19	5.19	5.19	5.19	5.20	5.20	5.20	5.20
280.0	5.19	5.19	5.19	5.19	5.19	5.19	5.19	5.19	5.19	5.19	5.19	5.20
300.0	5.19	5.19	5.19	5.19	5.19	5.19	5.19	5.19	5.19	5.19	5.19	5.19

Table 4.2.4 Helium⁴ specific heat at constant pressure, c_p , J/g-K
(continued).

PRES MM/HG ATM	5.066 50.000	5.573 55.000	6.079 60.000	6.586 65.000	7.093 70.000	7.599 75.000	8.106 80.000	8.613 85.000	9.119 90.000	9.626 95.000	10.133 100.000	10.639 105.000
TEMP, K												
3.0	1.48	1.41	1.44	1.49	1.57	1.68						
3.5	1.57	1.54	1.53	1.52	1.53	1.55	1.58	1.63	1.69	1.77	1.86	
4.0	1.85	1.81	1.78	1.76	1.75	1.74	1.74	1.75	1.77	1.80	1.84	1.88
4.2	1.98	1.94	1.91	1.88	1.86	1.85	1.85	1.85	1.87	1.88	1.91	1.94
4.4	2.11	2.07	2.04	2.01	1.99	1.98	1.97	1.97	1.97	1.98	2.00	2.02
4.6	2.25	2.21	2.17	2.14	2.12	2.10	2.09	2.09	2.09	2.09	2.11	2.12
4.8	2.39	2.35	2.31	2.28	2.25	2.24	2.22	2.21	2.21	2.21	2.22	2.23
5.0	2.53	2.48	2.44	2.41	2.39	2.37	2.35	2.34	2.33	2.33	2.33	2.34
5.1	2.59	2.55	2.51	2.48	2.45	2.43	2.41	2.40	2.39	2.39	2.39	2.39
5.2	2.64	2.59	2.55	2.52	2.49	2.47	2.45	2.44	2.43	2.42	2.42	2.42
5.3	2.64	2.60	2.56	2.52	2.49	2.47	2.45	2.44	2.43	2.42	2.41	2.41
5.4	2.68	2.63	2.59	2.55	2.52	2.50	2.48	2.46	2.45	2.44	2.44	2.43
5.5	2.71	2.66	2.62	2.58	2.55	2.53	2.50	2.49	2.47	2.46	2.46	2.46
5.6	2.74	2.69	2.65	2.61	2.58	2.55	2.53	2.51	2.50	2.49	2.48	2.48
5.7	2.78	2.72	2.68	2.64	2.61	2.58	2.56	2.54	2.53	2.52	2.51	2.50
5.8	2.81	2.76	2.71	2.67	2.64	2.61	2.59	2.57	2.55	2.54	2.53	2.52
5.9	2.85	2.79	2.75	2.71	2.67	2.64	2.62	2.60	2.58	2.57	2.56	2.55
6.0	2.88	2.83	2.78	2.74	2.71	2.68	2.65	2.63	2.61	2.59	2.58	2.57
6.2	2.95	2.90	2.85	2.81	2.77	2.74	2.71	2.69	2.67	2.65	2.63	2.62
6.4	3.03	2.97	2.92	2.87	2.83	2.80	2.77	2.75	2.72	2.70	2.69	2.67
6.6	3.10	3.04	2.98	2.94	2.90	2.86	2.83	2.80	2.78	2.76	2.74	2.72
6.8	3.17	3.11	3.05	3.01	2.96	2.93	2.89	2.86	2.84	2.81	2.79	2.78
7.0	3.25	3.18	3.12	3.07	3.03	2.99	2.95	2.92	2.89	2.87	2.85	2.83
7.5	3.43	3.35	3.29	3.23	3.18	3.14	3.10	3.07	3.03	3.01	2.98	2.96
8.0	3.61	3.53	3.46	3.39	3.34	3.29	3.25	3.21	3.17	3.14	3.11	3.08
8.5	3.79	3.70	3.62	3.55	3.49	3.44	3.39	3.35	3.31	3.27	3.24	3.21
9.0	3.96	3.86	3.77	3.70	3.64	3.58	3.53	3.48	3.44	3.40	3.36	3.33
9.5	4.13	4.02	3.93	3.85	3.78	3.72	3.66	3.61	3.57	3.53	3.49	3.45
10.0	4.29	4.18	4.08	3.99	3.92	3.85	3.80	3.74	3.69	3.65	3.61	3.57
11.0	4.60	4.47	4.35	4.26	4.17	4.10	4.03	3.97	3.92	3.87	3.83	3.78
12.0	4.88	4.73	4.61	4.50	4.40	4.32	4.25	4.19	4.13	4.07	4.02	3.98
13.0	5.13	4.97	4.84	4.72	4.62	4.53	4.45	4.38	4.32	4.26	4.21	4.16
14.0	5.33	5.16	5.04	4.92	4.81	4.72	4.64	4.56	4.49	4.43	4.38	4.33
15.0	5.49	5.34	5.21	5.09	4.98	4.89	4.80	4.72	4.65	4.59	4.53	4.48
16.0	5.62	5.49	5.36	5.25	5.14	5.05	4.96	4.88	4.81	4.74	4.68	4.63
17.0	5.72	5.60	5.49	5.38	5.28	5.19	5.10	5.02	4.95	4.88	4.82	4.77
18.0	5.79	5.69	5.58	5.49	5.39	5.31	5.22	5.15	5.08	5.01	4.95	4.89
19.0	5.84	5.75	5.66	5.57	5.48	5.40	5.33	5.25	5.18	5.12	5.06	5.00
20.0	5.87	5.79	5.72	5.64	5.56	5.49	5.41	5.34	5.28	5.22	5.16	5.10
25.0	5.86	5.85	5.84	5.78	5.74	5.70	5.66	5.62	5.57	5.53	5.49	5.44
30.0	5.80	5.80	5.79	5.78	5.76	5.74	5.72	5.70	5.67	5.65	5.62	5.60
35.0	5.71	5.72	5.72	5.72	5.72	5.71	5.71	5.70	5.69	5.67	5.66	5.65
40.0	5.63	5.64	5.65	5.66	5.66	5.67	5.67	5.66	5.66	5.66	5.65	5.65
45.0	5.56	5.58	5.59	5.60	5.61	5.61	5.62	5.62	5.62	5.62	5.62	5.62
50.0	5.50	5.52	5.53	5.55	5.56	5.56	5.57	5.58	5.58	5.58	5.59	5.59
60.0	5.42	5.43	5.45	5.46	5.47	5.48	5.49	5.50	5.50	5.51	5.51	5.52
80.0	5.32	5.33	5.34	5.35	5.36	5.37	5.37	5.38	5.39	5.40	5.40	5.41
100.0	5.27	5.28	5.28	5.29	5.30	5.30	5.31	5.31	5.32	5.32	5.33	5.33
120.0	5.24	5.25	5.25	5.26	5.26	5.27	5.27	5.27	5.28	5.28	5.29	5.29
140.0	5.23	5.23	5.23	5.24	5.24	5.24	5.25	5.25	5.25	5.25	5.26	5.26
160.0	5.22	5.22	5.22	5.22	5.23	5.23	5.23	5.23	5.23	5.23	5.24	5.24
180.0	5.21	5.21	5.21	5.21	5.22	5.22	5.22	5.22	5.22	5.22	5.22	5.23
200.0	5.20	5.21	5.21	5.21	5.21	5.21	5.21	5.21	5.21	5.21	5.22	5.22
220.0	5.20	5.20	5.20	5.20	5.20	5.21	5.21	5.21	5.21	5.21	5.21	5.21
240.0	5.20	5.20	5.20	5.20	5.20	5.20	5.20	5.20	5.20	5.20	5.20	5.20
260.0	5.20	5.20	5.20	5.20	5.20	5.20	5.20	5.20	5.20	5.20	5.20	5.20
280.0	5.20	5.20	5.20	5.20	5.20	5.20	5.20	5.20	5.20	5.20	5.20	5.20
300.0	5.19	5.19	5.19	5.19	5.20	5.20	5.20	5.20	5.20	5.20	5.20	5.20

Table 4.2.5 Helium⁴ specific heat at constant volume, c_v , J/g-K.

PRES MN/M ² ATM	0.010 0.100	0.051 0.500	0.101 1.000	0.152 1.500	0.184 1.800	0.193 1.900	0.203 2.000	0.213 2.100	0.223 2.200	0.233 2.300	0.243 2.400	0.253 2.500
TEMP. K												
3.0	3.16	1.92	1.91	1.90	1.90	1.90	1.90	1.89	1.89	1.89	1.89	1.89
3.5	3.14	2.11	2.10	2.09	2.09	2.08	2.08	2.08	2.08	2.08	2.07	2.07
4.0	3.13	2.21	2.27	2.26	2.25	2.25	2.24	2.24	2.24	2.23	2.23	2.23
4.2	3.12	3.18	2.36	2.33	2.32	2.32	2.32	2.31	2.31	2.30	2.30	2.30
4.4	3.12	3.17	3.29	2.42	2.41	2.40	2.40	2.39	2.39	2.38	2.38	2.38
4.6	3.12	3.15	3.24	2.53	2.50	2.50	2.49	2.48	2.48	2.47	2.47	2.46
4.8	3.12	3.14	3.21	3.33	2.63	2.62	2.61	2.60	2.59	2.58	2.57	2.56
5.0	3.12	3.14	3.18	3.27	3.34	3.38	2.70	2.76	2.74	2.72	2.70	2.69
5.1	3.12	3.13	3.17	3.25	3.31	3.33	3.36	2.90	2.85	2.82	2.79	2.77
5.2	3.12	3.13	3.17	3.23	3.28	3.30	3.32	3.34	3.35	2.99	2.90	2.86
5.3	3.12	3.13	3.16	3.21	3.25	3.27	3.29	3.30	3.32	3.33	3.26	2.99
5.4	3.12	3.13	3.15	3.20	3.23	3.25	3.26	3.28	3.29	3.30	3.31	3.29
5.5	3.12	3.12	3.15	3.19	3.22	3.23	3.24	3.25	3.26	3.28	3.28	3.29
5.6	3.12	3.12	3.14	3.18	3.20	3.21	3.22	3.23	3.24	3.25	3.26	3.27
5.7	3.12	3.12	3.14	3.17	3.19	3.20	3.21	3.22	3.22	3.23	3.24	3.25
5.8	3.12	3.12	3.13	3.16	3.18	3.19	3.19	3.20	3.21	3.22	3.22	3.23
5.9	3.12	3.12	3.13	3.15	3.17	3.18	3.18	3.19	3.20	3.20	3.21	3.22
6.0	3.12	3.12	3.13	3.15	3.16	3.17	3.17	3.18	3.18	3.19	3.20	3.20
6.2	3.12	3.12	3.12	3.14	3.15	3.15	3.16	3.16	3.17	3.17	3.18	3.18
6.4	3.12	3.11	3.12	3.13	3.14	3.14	3.15	3.15	3.15	3.16	3.16	3.16
6.6	3.12	3.11	3.12	3.12	3.13	3.13	3.14	3.14	3.14	3.14	3.15	3.15
6.8	3.12	3.11	3.12	3.12	3.13	3.13	3.13	3.13	3.13	3.13	3.14	3.14
7.0	3.12	3.11	3.11	3.12	3.12	3.12	3.12	3.12	3.13	3.13	3.13	3.13
7.5	3.12	3.11	3.11	3.11	3.11	3.11	3.11	3.11	3.12	3.12	3.12	3.12
8.0	3.12	3.11	3.11	3.11	3.11	3.11	3.11	3.11	3.11	3.11	3.11	3.11
8.5	3.12	3.11	3.11	3.11	3.11	3.11	3.11	3.11	3.11	3.11	3.11	3.11
9.0	3.12	3.11	3.11	3.11	3.11	3.11	3.11	3.11	3.11	3.11	3.11	3.11
9.5	3.12	3.11	3.11	3.11	3.11	3.11	3.11	3.11	3.11	3.11	3.11	3.11
10.0	3.12	3.11	3.11	3.11	3.11	3.11	3.11	3.11	3.11	3.11	3.11	3.11
11.0	3.12	3.11	3.11	3.11	3.11	3.11	3.11	3.11	3.11	3.11	3.11	3.11
12.0	3.12	3.12	3.11	3.11	3.11	3.11	3.11	3.11	3.11	3.11	3.11	3.11
13.0	3.12	3.12	3.12	3.12	3.12	3.12	3.12	3.12	3.12	3.12	3.12	3.12
14.0	3.12	3.12	3.12	3.12	3.12	3.12	3.12	3.12	3.12	3.12	3.12	3.12
15.0	3.12	3.12	3.12	3.12	3.12	3.12	3.12	3.12	3.12	3.12	3.12	3.12
16.0	3.12	3.12	3.12	3.12	3.12	3.12	3.12	3.12	3.12	3.12	3.12	3.12
17.0	3.12	3.12	3.12	3.12	3.12	3.12	3.12	3.12	3.12	3.12	3.12	3.12
18.0	3.12	3.12	3.12	3.12	3.12	3.12	3.12	3.12	3.12	3.12	3.12	3.12
19.0	3.12	3.12	3.12	3.12	3.12	3.12	3.12	3.12	3.12	3.12	3.12	3.12
20.0	3.12	3.12	3.12	3.12	3.12	3.12	3.12	3.12	3.12	3.12	3.12	3.12
25.0	3.12	3.12	3.12	3.12	3.12	3.12	3.12	3.12	3.12	3.12	3.12	3.12
30.0	3.12	3.12	3.12	3.12	3.12	3.12	3.12	3.12	3.12	3.12	3.12	3.12
35.0	3.12	3.12	3.12	3.12	3.12	3.12	3.12	3.12	3.12	3.12	3.12	3.12
40.0	3.12	3.12	3.12	3.12	3.12	3.12	3.12	3.12	3.12	3.12	3.12	3.12
45.0	3.12	3.12	3.12	3.12	3.12	3.12	3.12	3.12	3.12	3.12	3.12	3.12
50.0	3.12	3.12	3.12	3.12	3.12	3.12	3.12	3.12	3.12	3.12	3.12	3.12
60.0	3.12	3.12	3.12	3.12	3.12	3.12	3.12	3.12	3.12	3.12	3.12	3.12
80.0	3.12	3.12	3.12	3.12	3.12	3.12	3.12	3.12	3.12	3.12	3.12	3.12
100.0	3.12	3.12	3.12	3.12	3.12	3.12	3.12	3.12	3.12	3.12	3.12	3.12
120.0	3.12	3.12	3.12	3.12	3.12	3.12	3.12	3.12	3.12	3.12	3.12	3.12
140.0	3.12	3.12	3.12	3.12	3.12	3.12	3.12	3.12	3.12	3.12	3.12	3.12
160.0	3.12	3.12	3.12	3.12	3.12	3.12	3.12	3.12	3.12	3.12	3.12	3.12
180.0	3.12	3.12	3.12	3.12	3.12	3.12	3.12	3.12	3.12	3.12	3.12	3.12
200.0	3.12	3.12	3.12	3.12	3.12	3.12	3.12	3.12	3.12	3.12	3.12	3.12
220.0	3.12	3.12	3.12	3.12	3.12	3.12	3.12	3.12	3.12	3.12	3.12	3.12
240.0	3.12	3.12	3.12	3.12	3.12	3.12	3.12	3.12	3.12	3.12	3.12	3.12
260.0	3.12	3.12	3.12	3.12	3.12	3.12	3.12	3.12	3.12	3.12	3.12	3.12
280.0	3.12	3.12	3.12	3.12	3.12	3.12	3.12	3.12	3.12	3.12	3.12	3.12
300.0	3.12	3.12	3.12	3.12	3.12	3.12	3.12	3.12	3.12	3.12	3.12	3.12

Table 4.2.5 Helium⁴ specific heat at constant volume, c_v , J/g-K
(continued).

PNES MN/M ³ ATM TEMP, K	0.263 2.600	0.274 2.700	0.284 2.800	0.294 2.900	0.304 3.000	0.355 3.500	0.405 4.000	0.456 4.500	0.507 5.000	0.557 5.500	0.608 6.000	0.659 6.500
3.0	1.89	1.88	1.88	1.88	1.88	1.87	1.86	1.86	1.85	1.84	1.83	1.82
3.5	2.07	2.07	2.07	2.07	2.06	2.05	2.05	2.04	2.03	2.02	2.01	2.00
4.0	2.23	2.22	2.22	2.22	2.22	2.20	2.19	2.18	2.17	2.16	2.15	2.14
4.2	2.30	2.29	2.29	2.29	2.28	2.27	2.26	2.24	2.23	2.22	2.21	2.20
4.4	2.37	2.37	2.36	2.36	2.36	2.34	2.33	2.31	2.30	2.29	2.28	2.27
4.6	2.46	2.45	2.45	2.44	2.44	2.42	2.40	2.39	2.37	2.36	2.35	2.34
4.8	2.56	2.55	2.54	2.54	2.53	2.51	2.49	2.47	2.45	2.44	2.43	2.41
5.0	2.68	2.67	2.66	2.65	2.64	2.60	2.58	2.56	2.54	2.52	2.51	2.49
5.1	2.75	2.74	2.72	2.71	2.70	2.66	2.62	2.60	2.58	2.56	2.55	2.53
5.2	2.83	2.80	2.78	2.76	2.75	2.69	2.65	2.63	2.60	2.58	2.56	2.55
5.3	2.90	2.85	2.81	2.79	2.77	2.69	2.65	2.61	2.59	2.56	2.55	2.53
5.4	3.17	3.00	2.92	2.86	2.83	2.72	2.67	2.63	2.60	2.57	2.55	2.54
5.5	3.28	3.23	3.13	3.00	2.93	2.76	2.69	2.65	2.61	2.59	2.56	2.55
5.6	3.27	3.27	3.24	3.19	3.10	2.82	2.73	2.67	2.63	2.60	2.58	2.56
5.7	3.25	3.26	3.25	3.24	3.20	2.90	2.77	2.70	2.65	2.62	2.59	2.57
5.8	3.24	3.24	3.24	3.24	3.23	3.00	2.82	2.73	2.68	2.64	2.61	2.59
5.9	3.22	3.23	3.23	3.23	3.23	3.11	2.88	2.77	2.71	2.66	2.63	2.60
6.0	3.21	3.21	3.22	3.22	3.22	3.15	2.96	2.82	2.74	2.69	2.65	2.62
6.2	3.18	3.19	3.19	3.19	3.20	3.18	3.09	2.93	2.82	2.75	2.70	2.67
6.4	3.17	3.17	3.17	3.17	3.18	3.17	3.14	3.04	2.91	2.82	2.76	2.72
6.6	3.15	3.15	3.16	3.16	3.16	3.16	3.14	3.10	3.00	2.90	2.83	2.77
6.8	3.14	3.14	3.14	3.15	3.15	3.15	3.14	3.11	3.07	2.98	2.90	2.83
7.0	3.13	3.13	3.13	3.14	3.14	3.14	3.14	3.12	3.09	3.04	2.96	2.90
7.5	3.12	3.12	3.12	3.12	3.12	3.12	3.12	3.12	3.10	3.08	3.06	3.02
8.0	3.11	3.11	3.11	3.11	3.11	3.11	3.11	3.11	3.10	3.09	3.08	3.06
8.5	3.11	3.11	3.11	3.11	3.11	3.11	3.11	3.11	3.10	3.10	3.09	3.08
9.0	3.11	3.11	3.11	3.11	3.11	3.11	3.11	3.10	3.10	3.10	3.09	3.09
9.5	3.11	3.11	3.11	3.11	3.11	3.11	3.11	3.10	3.10	3.10	3.09	3.09
10.0	3.11	3.11	3.11	3.11	3.11	3.11	3.10	3.10	3.10	3.10	3.10	3.09
11.0	3.11	3.11	3.11	3.11	3.11	3.11	3.11	3.10	3.10	3.10	3.10	3.10
12.0	3.11	3.11	3.11	3.11	3.11	3.11	3.11	3.11	3.11	3.11	3.10	3.10
13.0	3.12	3.12	3.12	3.12	3.11	3.11	3.11	3.11	3.11	3.11	3.11	3.11
14.0	3.12	3.12	3.12	3.12	3.12	3.12	3.12	3.12	3.12	3.12	3.12	3.11
15.0	3.12	3.12	3.12	3.12	3.12	3.12	3.12	3.12	3.12	3.12	3.12	3.12
16.0	3.12	3.12	3.12	3.12	3.12	3.12	3.12	3.12	3.12	3.12	3.12	3.12
17.0	3.12	3.12	3.12	3.12	3.12	3.12	3.12	3.12	3.12	3.12	3.13	3.13
18.0	3.12	3.12	3.12	3.12	3.12	3.12	3.12	3.12	3.12	3.12	3.13	3.13
19.0	3.12	3.12	3.12	3.12	3.12	3.12	3.12	3.12	3.12	3.12	3.13	3.13
20.0	3.12	3.12	3.12	3.12	3.12	3.12	3.12	3.12	3.12	3.12	3.13	3.13
25.0	3.12	3.12	3.12	3.12	3.12	3.12	3.12	3.12	3.12	3.12	3.13	3.13
30.0	3.12	3.12	3.12	3.12	3.12	3.12	3.12	3.12	3.12	3.12	3.13	3.13
35.0	3.12	3.12	3.12	3.12	3.12	3.12	3.12	3.12	3.12	3.12	3.13	3.13
40.0	3.12	3.12	3.12	3.12	3.12	3.12	3.12	3.12	3.12	3.12	3.13	3.13
45.0	3.12	3.12	3.12	3.12	3.12	3.12	3.12	3.12	3.12	3.12	3.13	3.13
50.0	3.12	3.12	3.12	3.12	3.12	3.12	3.12	3.12	3.12	3.12	3.13	3.13
60.0	3.12	3.12	3.12	3.12	3.12	3.12	3.12	3.12	3.12	3.12	3.12	3.12
80.0	3.12	3.12	3.12	3.12	3.12	3.12	3.12	3.12	3.12	3.12	3.12	3.12
100.0	3.12	3.12	3.12	3.12	3.12	3.12	3.12	3.12	3.12	3.12	3.12	3.12
120.0	3.12	3.12	3.12	3.12	3.12	3.12	3.12	3.12	3.12	3.12	3.12	3.12
140.0	3.12	3.12	3.12	3.12	3.12	3.12	3.12	3.12	3.12	3.12	3.12	3.12
160.0	3.12	3.12	3.12	3.12	3.12	3.12	3.12	3.12	3.12	3.12	3.12	3.12
180.0	3.12	3.12	3.12	3.12	3.12	3.12	3.12	3.12	3.12	3.12	3.12	3.12
200.0	3.12	3.12	3.12	3.12	3.12	3.12	3.12	3.12	3.12	3.12	3.12	3.12
220.0	3.12	3.12	3.12	3.12	3.12	3.12	3.12	3.12	3.12	3.12	3.12	3.12
240.0	3.12	3.12	3.12	3.12	3.12	3.12	3.12	3.12	3.12	3.12	3.12	3.12
260.0	3.12	3.12	3.12	3.12	3.12	3.12	3.12	3.12	3.12	3.12	3.12	3.12
280.0	3.12	3.12	3.12	3.12	3.12	3.12	3.12	3.12	3.12	3.12	3.12	3.12
300.0	3.12	3.12	3.12	3.12	3.12	3.12	3.12	3.12	3.12	3.12	3.12	3.12

Table 4.2.5 Helium⁴ specific heat at constant volume, c_v , J/g-K
(continued).

PRES MM/HG ATM TEMP, K	0.600 6.000	0.709 7.000	0.811 8.000	0.912 9.000	1.013 10.000	1.520 15.000	2.026 20.000	2.533 25.000	3.040 30.000	3.546 35.000	4.053 40.000	4.560 45.000
3.0	1.83	1.81	1.80	1.78	1.76	1.68	1.60	1.52	1.45	1.40	1.35	1.31
3.5	2.01	1.99	1.97	1.96	1.94	1.85	1.77	1.69	1.62	1.55	1.49	1.44
4.0	2.15	2.13	2.11	2.09	2.08	1.99	1.92	1.85	1.78	1.73	1.67	1.63
4.2	2.21	2.19	2.17	2.15	2.14	2.06	1.98	1.92	1.86	1.81	1.76	1.72
4.4	2.28	2.26	2.24	2.22	2.20	2.12	2.05	1.99	1.94	1.89	1.85	1.81
4.6	2.35	2.33	2.31	2.29	2.27	2.19	2.13	2.07	2.02	1.98	1.94	1.90
4.8	2.43	2.40	2.38	2.36	2.34	2.27	2.21	2.16	2.11	2.07	2.04	2.00
5.0	2.51	2.48	2.46	2.44	2.42	2.35	2.29	2.24	2.20	2.16	2.13	2.10
5.1	2.55	2.52	2.50	2.48	2.46	2.39	2.33	2.28	2.24	2.21	2.18	2.15
5.2	2.56	2.54	2.51	2.49	2.47	2.40	2.35	2.30	2.26	2.23	2.20	2.17
5.3	2.55	2.52	2.49	2.47	2.45	2.38	2.33	2.28	2.25	2.21	2.18	2.16
5.4	2.55	2.52	2.50	2.47	2.45	2.38	2.33	2.29	2.25	2.22	2.20	2.17
5.5	2.56	2.53	2.50	2.48	2.46	2.39	2.34	2.30	2.26	2.23	2.21	2.19
5.6	2.58	2.54	2.51	2.49	2.47	2.40	2.35	2.31	2.28	2.25	2.22	2.20
5.7	2.59	2.55	2.52	2.50	2.48	2.41	2.36	2.32	2.29	2.26	2.24	2.21
5.8	2.61	2.57	2.53	2.51	2.49	2.41	2.37	2.33	2.30	2.27	2.25	2.23
5.9	2.63	2.59	2.55	2.52	2.50	2.43	2.38	2.34	2.31	2.29	2.27	2.25
6.0	2.65	2.60	2.56	2.53	2.51	2.44	2.39	2.36	2.33	2.30	2.28	2.26
6.2	2.70	2.64	2.59	2.56	2.54	2.46	2.42	2.38	2.36	2.33	2.31	2.30
6.4	2.76	2.68	2.63	2.60	2.57	2.49	2.44	2.41	2.39	2.36	2.35	2.33
6.6	2.83	2.73	2.67	2.63	2.60	2.52	2.47	2.44	2.42	2.40	2.38	2.36
6.8	2.90	2.78	2.72	2.67	2.64	2.54	2.50	2.47	2.45	2.43	2.41	2.40
7.0	2.96	2.84	2.76	2.71	2.67	2.57	2.53	2.50	2.48	2.46	2.44	2.43
7.5	3.06	2.97	2.88	2.81	2.76	2.65	2.60	2.57	2.55	2.53	2.52	2.51
8.0	3.08	3.04	2.98	2.91	2.86	2.72	2.67	2.64	2.62	2.60	2.59	2.58
8.5	3.09	3.07	3.04	2.99	2.94	2.79	2.73	2.70	2.68	2.67	2.65	2.65
9.0	3.09	3.08	3.06	3.04	3.00	2.85	2.79	2.76	2.74	2.72	2.71	2.70
9.5	3.09	3.08	3.07	3.06	3.04	2.91	2.84	2.81	2.79	2.78	2.77	2.76
10.0	3.10	3.09	3.08	3.07	3.06	2.96	2.89	2.86	2.84	2.82	2.81	2.81
11.0	3.10	3.09	3.09	3.08	3.07	3.02	2.97	2.94	2.92	2.91	2.90	2.89
12.0	3.10	3.10	3.10	3.09	3.08	3.06	3.02	2.99	2.98	2.97	2.96	2.96
13.0	3.11	3.11	3.10	3.10	3.10	3.07	3.05	3.03	3.01	3.01	3.00	3.00
14.0	3.12	3.11	3.11	3.11	3.11	3.09	3.07	3.05	3.04	3.04	3.03	3.03
15.0	3.12	3.12	3.12	3.12	3.11	3.10	3.08	3.07	3.06	3.06	3.06	3.06
16.0	3.12	3.12	3.12	3.12	3.12	3.11	3.10	3.09	3.08	3.08	3.08	3.08
17.0	3.13	3.13	3.13	3.13	3.13	3.12	3.12	3.11	3.10	3.10	3.10	3.09
18.0	3.13	3.13	3.13	3.13	3.13	3.13	3.13	3.12	3.12	3.11	3.11	3.11
19.0	3.13	3.13	3.13	3.13	3.13	3.13	3.14	3.13	3.13	3.12	3.12	3.12
20.0	3.13	3.13	3.13	3.13	3.14	3.14	3.14	3.14	3.14	3.14	3.13	3.13
25.0	3.13	3.13	3.14	3.14	3.14	3.15	3.15	3.16	3.16	3.16	3.16	3.17
30.0	3.13	3.13	3.13	3.14	3.14	3.15	3.15	3.16	3.17	3.17	3.17	3.18
35.0	3.13	3.13	3.13	3.13	3.14	3.15	3.15	3.16	3.17	3.17	3.18	3.18
40.0	3.13	3.13	3.13	3.13	3.13	3.14	3.15	3.16	3.16	3.17	3.17	3.18
45.0	3.13	3.13	3.13	3.13	3.13	3.14	3.15	3.16	3.16	3.17	3.17	3.18
50.0	3.13	3.13	3.13	3.13	3.13	3.14	3.14	3.15	3.16	3.16	3.17	3.17
60.0	3.12	3.12	3.13	3.13	3.13	3.13	3.14	3.15	3.15	3.16	3.16	3.17
80.0	3.12	3.12	3.12	3.12	3.13	3.13	3.13	3.14	3.14	3.15	3.15	3.16
100.0	3.12	3.12	3.12	3.12	3.12	3.13	3.13	3.13	3.14	3.14	3.14	3.15
120.0	3.12	3.12	3.12	3.12	3.12	3.12	3.12	3.13	3.13	3.13	3.14	3.14
140.0	3.12	3.12	3.12	3.12	3.12	3.12	3.12	3.13	3.13	3.13	3.13	3.14
160.0	3.12	3.12	3.12	3.12	3.12	3.12	3.12	3.13	3.13	3.13	3.13	3.14
180.0	3.12	3.12	3.12	3.12	3.12	3.12	3.12	3.12	3.13	3.13	3.13	3.13
200.0	3.12	3.12	3.12	3.12	3.12	3.12	3.12	3.12	3.13	3.13	3.13	3.13
220.0	3.12	3.12	3.12	3.12	3.12	3.12	3.12	3.12	3.13	3.13	3.13	3.13
240.0	3.12	3.12	3.12	3.12	3.12	3.12	3.12	3.12	3.12	3.13	3.13	3.13
260.0	3.12	3.12	3.12	3.12	3.12	3.12	3.12	3.12	3.12	3.13	3.13	3.13
280.0	3.12	3.12	3.12	3.12	3.12	3.12	3.12	3.12	3.12	3.13	3.13	3.13
300.0	3.12	3.12	3.12	3.12	3.12	3.12	3.12	3.12	3.12	3.12	3.13	3.13

Table 4.2.5 Helium⁴ specific heat at constant volume, c_v , J/g-K
(continued).

PRES MM/HG ATM	5.066 50.000	5.573 55.000	6.079 60.000	6.586 65.000	7.093 70.000	7.599 75.000	8.106 80.000	8.613 85.000	9.119 90.000	9.626 95.000	10.133 100.000	10.639 105.000
TEMP. K												
3.0	1.29	1.28	1.29	1.31	1.35	1.40						
3.5	1.40	1.37	1.34	1.32	1.31	1.31	1.32	1.34	1.37	1.40	1.45	
4.0	1.59	1.55	1.52	1.50	1.48	1.47	1.46	1.46	1.47	1.48	1.50	1.52
4.2	1.68	1.64	1.62	1.59	1.58	1.56	1.56	1.55	1.55	1.56	1.57	1.59
4.4	1.77	1.74	1.72	1.70	1.68	1.67	1.66	1.65	1.65	1.66	1.66	1.68
4.6	1.87	1.85	1.82	1.80	1.79	1.77	1.76	1.76	1.76	1.76	1.77	1.77
4.8	1.97	1.95	1.93	1.91	1.89	1.88	1.87	1.87	1.87	1.87	1.87	1.88
5.0	2.08	2.05	2.03	2.02	2.00	1.99	1.98	1.98	1.98	1.98	1.98	1.98
5.1	2.12	2.10	2.08	2.07	2.05	2.04	2.03	2.03	2.03	2.03	2.03	2.03
5.2	2.15	2.13	2.11	2.10	2.08	2.07	2.06	2.06	2.06	2.06	2.06	2.06
5.3	2.14	2.12	2.10	2.09	2.07	2.06	2.06	2.05	2.05	2.05	2.05	2.05
5.4	2.15	2.13	2.12	2.10	2.09	2.08	2.07	2.07	2.06	2.06	2.06	2.07
5.5	2.16	2.15	2.13	2.12	2.11	2.10	2.09	2.08	2.08	2.08	2.08	2.08
5.6	2.18	2.16	2.15	2.13	2.12	2.11	2.11	2.10	2.10	2.10	2.10	2.10
5.7	2.20	2.18	2.16	2.15	2.14	2.13	2.13	2.12	2.12	2.12	2.11	2.12
5.8	2.21	2.20	2.18	2.17	2.16	2.15	2.14	2.14	2.14	2.13	2.13	2.13
5.9	2.23	2.21	2.20	2.19	2.18	2.17	2.16	2.16	2.15	2.15	2.15	2.15
6.0	2.25	2.23	2.22	2.21	2.20	2.19	2.18	2.18	2.17	2.17	2.17	2.17
6.2	2.28	2.27	2.25	2.24	2.24	2.23	2.22	2.22	2.21	2.21	2.21	2.21
6.4	2.32	2.30	2.29	2.28	2.27	2.27	2.26	2.25	2.25	2.25	2.24	2.24
6.6	2.35	2.34	2.33	2.32	2.31	2.30	2.30	2.29	2.28	2.28	2.28	2.28
6.8	2.38	2.37	2.36	2.35	2.35	2.34	2.33	2.33	2.32	2.32	2.31	2.31
7.0	2.42	2.41	2.40	2.39	2.38	2.37	2.37	2.36	2.35	2.35	2.35	2.34
7.5	2.50	2.49	2.48	2.47	2.46	2.46	2.45	2.44	2.44	2.43	2.43	2.42
8.0	2.57	2.56	2.55	2.54	2.54	2.53	2.52	2.52	2.51	2.50	2.50	2.49
8.5	2.64	2.63	2.62	2.61	2.61	2.60	2.59	2.58	2.58	2.57	2.57	2.56
9.0	2.70	2.69	2.68	2.67	2.67	2.66	2.65	2.65	2.64	2.63	2.63	2.62
9.5	2.75	2.74	2.74	2.73	2.72	2.72	2.71	2.70	2.70	2.69	2.68	2.68
10.0	2.80	2.79	2.79	2.78	2.77	2.77	2.76	2.76	2.75	2.74	2.74	2.73
11.0	2.89	2.88	2.88	2.87	2.87	2.86	2.86	2.85	2.84	2.84	2.83	2.82
12.0	2.95	2.95	2.94	2.94	2.94	2.93	2.93	2.92	2.92	2.91	2.91	2.90
13.0	3.00	3.00	2.99	2.99	2.99	2.99	2.98	2.98	2.98	2.97	2.97	2.97
14.0	3.03	3.03	3.03	3.03	3.03	3.03	3.03	3.02	3.02	3.02	3.02	3.01
15.0	3.06	3.06	3.06	3.06	3.06	3.06	3.06	3.06	3.06	3.05	3.05	3.05
16.0	3.08	3.08	3.08	3.08	3.08	3.08	3.08	3.08	3.08	3.08	3.08	3.08
17.0	3.10	3.10	3.10	3.10	3.10	3.10	3.11	3.11	3.11	3.11	3.11	3.11
18.0	3.11	3.11	3.11	3.12	3.12	3.12	3.12	3.12	3.12	3.13	3.13	3.13
19.0	3.12	3.12	3.13	3.13	3.13	3.13	3.13	3.14	3.14	3.14	3.14	3.14
20.0	3.13	3.13	3.14	3.14	3.14	3.14	3.15	3.15	3.15	3.15	3.15	3.15
25.0	3.17	3.17	3.17	3.17	3.17	3.18	3.18	3.18	3.18	3.18	3.19	3.19
30.0	3.18	3.18	3.19	3.19	3.19	3.19	3.19	3.20	3.20	3.20	3.20	3.20
35.0	3.18	3.19	3.19	3.19	3.20	3.20	3.20	3.20	3.21	3.21	3.21	3.21
40.0	3.18	3.19	3.19	3.19	3.20	3.20	3.21	3.21	3.21	3.21	3.22	3.22
45.0	3.18	3.19	3.19	3.19	3.20	3.20	3.21	3.21	3.21	3.22	3.22	3.22
50.0	3.18	3.18	3.19	3.19	3.20	3.20	3.20	3.21	3.21	3.22	3.22	3.22
60.0	3.17	3.19	3.18	3.19	3.19	3.19	3.20	3.20	3.21	3.21	3.21	3.22
80.0	3.16	3.16	3.17	3.17	3.18	3.18	3.18	3.19	3.19	3.20	3.20	3.20
100.0	3.15	3.16	3.16	3.16	3.17	3.17	3.17	3.18	3.18	3.18	3.19	3.19
120.0	3.15	3.15	3.15	3.16	3.16	3.16	3.16	3.17	3.17	3.17	3.18	3.18
140.0	3.14	3.14	3.15	3.15	3.15	3.15	3.16	3.16	3.16	3.17	3.17	3.17
160.0	3.14	3.14	3.14	3.15	3.15	3.15	3.15	3.15	3.16	3.16	3.16	3.16
180.0	3.14	3.14	3.14	3.14	3.14	3.15	3.15	3.15	3.15	3.15	3.16	3.16
200.0	3.13	3.14	3.14	3.14	3.14	3.14	3.15	3.15	3.15	3.15	3.15	3.16
220.0	3.13	3.13	3.14	3.14	3.14	3.14	3.14	3.14	3.15	3.15	3.15	3.15
240.0	3.13	3.13	3.13	3.14	3.14	3.14	3.14	3.14	3.14	3.15	3.15	3.15
260.0	3.13	3.13	3.13	3.13	3.14	3.14	3.14	3.14	3.14	3.14	3.14	3.15
280.0	3.13	3.13	3.13	3.13	3.13	3.14	3.14	3.14	3.14	3.14	3.14	3.14
300.0	3.13	3.13	3.13	3.13	3.13	3.13	3.14	3.14	3.14	3.14	3.14	3.14

Table 4.2.6 $(P/T) (\partial T / \partial P)_h$ This is the dimensionless quantity,
Joule Thomson coefficient times pressure divided
by temperature.

PRES MM/H ² ATM	0.010 0.100	0.051 0.500	0.101 1.000	0.152 1.500	0.182 1.800	0.193 1.900	0.203 2.000	0.213 2.100	0.223 2.200	0.233 2.300	0.243 2.400	0.253 2.500
TEMP, K												
3.0	0.047	-0.040	-0.082	-0.126	-0.152	-0.162	-0.171	-0.180	-0.189	-0.198	-0.206	-0.217
3.5	0.032	-0.022	-0.047	-0.075	-0.093	-0.099	-0.105	-0.111	-0.117	-0.123	-0.130	-0.136
4.0	0.024	0.133	-0.019	-0.035	-0.047	-0.050	-0.054	-0.059	-0.063	-0.067	-0.071	-0.076
4.2	0.021	0.117	-0.006	-0.019	-0.029	-0.032	-0.036	-0.039	-0.043	-0.046	-0.050	-0.054
4.4	0.019	0.104	0.231	-0.002	-0.010	-0.013	-0.016	-0.019	-0.022	-0.026	-0.029	-0.032
4.6	0.017	0.093	0.203	0.021	0.013	0.010	0.007	0.003	0.000	-0.003	-0.006	-0.009
4.8	0.016	0.084	0.180	0.293	0.045	0.041	0.036	0.032	0.029	0.025	0.021	0.018
5.0	0.015	0.076	0.161	0.257	0.321	0.339	0.391	0.381	0.373	0.366	0.359	0.354
5.1	0.014	0.073	0.153	0.242	0.300	0.319	0.335	0.334	0.312	0.298	0.288	0.279
5.2	0.013	0.069	0.145	0.229	0.283	0.300	0.317	0.330	0.326	0.313	0.302	0.294
5.3	0.013	0.066	0.138	0.217	0.267	0.283	0.299	0.314	0.325	0.324	0.311	0.300
5.4	0.012	0.063	0.132	0.206	0.252	0.268	0.283	0.298	0.310	0.319	0.320	0.300
5.5	0.012	0.061	0.126	0.196	0.239	0.254	0.268	0.282	0.295	0.307	0.314	0.310
5.6	0.011	0.058	0.120	0.186	0.227	0.241	0.255	0.268	0.281	0.293	0.303	0.309
5.7	0.011	0.056	0.115	0.178	0.216	0.229	0.242	0.255	0.267	0.275	0.290	0.296
5.8	0.011	0.054	0.110	0.170	0.206	0.219	0.231	0.243	0.255	0.266	0.277	0.286
5.9	0.010	0.052	0.106	0.162	0.197	0.209	0.220	0.232	0.243	0.254	0.264	0.274
6.0	0.010	0.050	0.102	0.155	0.188	0.200	0.211	0.222	0.232	0.243	0.253	0.262
6.2	0.009	0.046	0.094	0.143	0.173	0.183	0.193	0.203	0.213	0.222	0.232	0.241
6.4	0.009	0.043	0.087	0.132	0.159	0.169	0.178	0.187	0.196	0.205	0.213	0.222
6.6	0.008	0.040	0.081	0.122	0.148	0.156	0.164	0.173	0.181	0.189	0.197	0.205
6.8	0.007	0.038	0.075	0.114	0.137	0.145	0.152	0.160	0.168	0.175	0.183	0.190
7.0	0.007	0.035	0.071	0.106	0.128	0.135	0.142	0.149	0.156	0.163	0.170	0.177
7.5	0.006	0.030	0.060	0.090	0.108	0.114	0.120	0.126	0.132	0.137	0.143	0.149
8.0	0.005	0.026	0.052	0.077	0.093	0.098	0.103	0.108	0.113	0.118	0.122	0.127
8.5	0.005	0.023	0.045	0.067	0.080	0.085	0.089	0.093	0.097	0.102	0.106	0.110
9.0	0.004	0.020	0.040	0.059	0.070	0.074	0.078	0.082	0.085	0.089	0.093	0.096
9.5	0.004	0.018	0.035	0.052	0.062	0.065	0.069	0.072	0.075	0.078	0.082	0.085
10.0	0.003	0.016	0.031	0.046	0.055	0.058	0.061	0.064	0.067	0.070	0.072	0.075
11.0	0.003	0.013	0.025	0.037	0.045	0.047	0.049	0.052	0.054	0.056	0.059	0.061
12.0	0.002	0.010	0.021	0.031	0.037	0.039	0.041	0.042	0.044	0.046	0.048	0.050
13.0	0.002	0.009	0.017	0.026	0.030	0.032	0.034	0.035	0.037	0.039	0.040	0.042
14.0	0.001	0.007	0.014	0.021	0.026	0.027	0.028	0.030	0.031	0.032	0.034	0.035
15.0	0.001	0.006	0.012	0.018	0.022	0.023	0.024	0.025	0.026	0.027	0.029	0.030
16.0	0.001	0.005	0.010	0.015	0.018	0.019	0.020	0.021	0.022	0.023	0.024	0.025
17.0	0.001	0.004	0.009	0.013	0.016	0.016	0.017	0.018	0.019	0.020	0.021	0.021
18.0	0.001	0.004	0.007	0.011	0.013	0.014	0.015	0.016	0.016	0.017	0.018	0.018
19.0	0.001	0.003	0.006	0.010	0.012	0.012	0.013	0.013	0.014	0.015	0.015	0.016
20.0	0.001	0.003	0.006	0.008	0.010	0.010	0.011	0.012	0.012	0.013	0.013	0.014
25.0	0.000	0.001	0.003	0.004	0.005	0.005	0.005	0.006	0.006	0.006	0.007	0.007
30.0	0.000	0.001	0.001	0.002	0.002	0.003	0.003	0.003	0.003	0.003	0.003	0.003
35.0	0.000	0.000	0.001	0.001	0.001	0.001	0.001	0.001	0.001	0.001	0.001	0.001
40.0	0.000	0.000	0.000	0.000	0.000	0.000	0.000	0.000	0.000	0.000	0.000	0.000
45.0	-0.000	-0.000	-0.000	-0.000	-0.000	-0.000	-0.000	-0.000	-0.000	-0.000	-0.000	-0.000
50.0	-0.000	-0.000	-0.000	-0.000	-0.000	-0.000	-0.001	-0.001	-0.001	-0.001	-0.001	-0.001
60.0	-0.000	-0.000	-0.000	-0.001	-0.001	-0.001	-0.001	-0.001	-0.001	-0.001	-0.001	-0.001
80.0	-0.000	-0.000	-0.001	-0.001	-0.001	-0.001	-0.001	-0.001	-0.001	-0.001	-0.001	-0.001
100.0	-0.000	-0.000	-0.000	-0.001	-0.001	-0.001	-0.001	-0.001	-0.001	-0.001	-0.001	-0.001
120.0	-0.000	-0.000	-0.000	-0.001	-0.001	-0.001	-0.001	-0.001	-0.001	-0.001	-0.001	-0.001
140.0	-0.000	-0.000	-0.000	-0.001	-0.001	-0.001	-0.001	-0.001	-0.001	-0.001	-0.001	-0.001
160.0	-0.000	-0.000	-0.000	-0.001	-0.001	-0.001	-0.001	-0.001	-0.001	-0.001	-0.001	-0.001
180.0	-0.000	-0.000	-0.000	-0.001	-0.001	-0.001	-0.001	-0.001	-0.001	-0.001	-0.001	-0.001
200.0	-0.000	-0.000	-0.000	-0.000	-0.001	-0.001	-0.001	-0.001	-0.001	-0.001	-0.001	-0.001
220.0	-0.000	-0.000	-0.000	-0.000	-0.001	-0.001	-0.001	-0.001	-0.001	-0.001	-0.001	-0.001
240.0	-0.000	-0.000	-0.000	-0.000	-0.000	-0.001	-0.001	-0.001	-0.001	-0.001	-0.001	-0.001
260.0	-0.000	-0.000	-0.000	-0.000	-0.000	-0.000	-0.001	-0.001	-0.001	-0.001	-0.001	-0.001
280.0	-0.000	-0.000	-0.000	-0.000	-0.000	-0.000	-0.000	-0.001	-0.001	-0.001	-0.001	-0.001
300.0	-0.000	-0.000	-0.000	-0.000	-0.000	-0.000	-0.000	-0.000	-0.000	-0.000	-0.001	-0.001

Table 4.2.6 $(P/T)(\partial T/\partial P)_h$ This is the dimensionless quantity,
Joule Thomson coefficient times pressure divided
by temperature
(continued).

PRES MM/H ² ATM	0.263 2.600	0.274 2.700	0.284 2.800	0.294 2.900	0.304 3.000	0.355 3.500	0.405 4.000	0.456 4.500	0.507 5.000	0.557 5.500	0.608 6.000	0.659 6.500
TEMP.K												
3.0	-0.226	-0.236	-0.245	-0.255	-0.264	-0.313	-0.362	-0.412	-0.462	-0.514	-0.566	-0.618
3.5	-0.142	-0.149	-0.155	-0.162	-0.168	-0.202	-0.236	-0.271	-0.306	-0.343	-0.380	-0.417
4.0	-0.080	-0.085	-0.089	-0.094	-0.098	-0.122	-0.147	-0.173	-0.199	-0.226	-0.253	-0.281
4.2	-0.058	-0.062	-0.066	-0.070	-0.074	-0.095	-0.117	-0.140	-0.164	-0.188	-0.212	-0.237
4.4	-0.036	-0.039	-0.043	-0.047	-0.050	-0.063	-0.089	-0.110	-0.131	-0.153	-0.176	-0.196
4.6	-0.013	-0.016	-0.019	-0.023	-0.026	-0.044	-0.063	-0.082	-0.101	-0.121	-0.142	-0.163
4.8	0.014	0.010	0.007	0.003	-0.000	-0.018	-0.036	-0.054	-0.073	-0.092	-0.111	-0.131
5.0	0.049	0.044	0.039	0.035	0.030	0.010	-0.009	-0.027	-0.046	-0.064	-0.082	-0.101
5.1	0.072	0.065	0.059	0.053	0.048	0.025	0.005	-0.014	-0.032	-0.051	-0.069	-0.087
5.2	0.101	0.090	0.082	0.074	0.067	0.040	0.018	-0.002	-0.021	-0.039	-0.058	-0.076
5.3	0.147	0.127	0.113	0.102	0.092	0.058	0.033	0.012	-0.008	-0.027	-0.045	-0.063
5.4	0.244	0.191	0.161	0.141	0.126	0.079	0.050	0.027	0.006	-0.014	-0.032	-0.051
5.5	0.305	0.276	0.236	0.199	0.172	0.105	0.069	0.043	0.020	0.000	-0.019	-0.038
5.6	0.311	0.305	0.287	0.261	0.232	0.135	0.090	0.060	0.036	0.014	-0.006	-0.025
5.7	0.304	0.306	0.302	0.291	0.274	0.171	0.114	0.079	0.052	0.025	0.008	-0.011
5.8	0.294	0.299	0.302	0.299	0.292	0.210	0.141	0.100	0.069	0.038	0.023	0.002
5.9	0.283	0.290	0.295	0.297	0.295	0.242	0.170	0.122	0.088	0.061	0.037	0.016
6.0	0.271	0.279	0.285	0.290	0.292	0.261	0.199	0.145	0.107	0.077	0.052	0.030
6.2	0.250	0.258	0.265	0.272	0.277	0.278	0.241	0.192	0.148	0.113	0.084	0.060
6.4	0.230	0.238	0.245	0.252	0.259	0.275	0.259	0.226	0.187	0.149	0.117	0.090
6.6	0.213	0.220	0.227	0.234	0.241	0.263	0.263	0.242	0.215	0.182	0.149	0.120
6.8	0.197	0.204	0.211	0.218	0.224	0.249	0.258	0.249	0.229	0.205	0.177	0.149
7.0	0.183	0.190	0.196	0.203	0.209	0.234	0.249	0.248	0.236	0.218	0.197	0.173
7.5	0.154	0.160	0.166	0.171	0.176	0.201	0.219	0.230	0.231	0.226	0.215	0.202
8.0	0.132	0.137	0.142	0.146	0.151	0.172	0.191	0.205	0.213	0.215	0.212	0.206
8.5	0.114	0.118	0.122	0.126	0.130	0.149	0.166	0.181	0.191	0.197	0.200	0.198
9.0	0.100	0.103	0.107	0.110	0.114	0.131	0.146	0.159	0.170	0.178	0.184	0.186
9.5	0.088	0.091	0.094	0.097	0.100	0.115	0.129	0.141	0.152	0.161	0.167	0.171
10.0	0.078	0.081	0.084	0.086	0.089	0.102	0.114	0.126	0.136	0.144	0.151	0.156
11.0	0.063	0.065	0.068	0.070	0.072	0.083	0.093	0.102	0.111	0.118	0.125	0.130
12.0	0.052	0.054	0.056	0.057	0.059	0.068	0.077	0.084	0.092	0.098	0.104	0.110
13.0	0.043	0.045	0.046	0.048	0.049	0.057	0.064	0.071	0.077	0.083	0.088	0.093
14.0	0.036	0.038	0.039	0.040	0.042	0.048	0.054	0.060	0.065	0.070	0.075	0.079
15.0	0.031	0.032	0.033	0.034	0.035	0.041	0.046	0.051	0.056	0.060	0.064	0.068
16.0	0.026	0.027	0.028	0.029	0.030	0.035	0.039	0.043	0.047	0.051	0.055	0.058
17.0	0.022	0.023	0.024	0.025	0.026	0.029	0.033	0.037	0.041	0.044	0.047	0.050
18.0	0.019	0.020	0.020	0.021	0.022	0.025	0.029	0.032	0.035	0.038	0.041	0.043
19.0	0.016	0.017	0.018	0.018	0.019	0.022	0.025	0.027	0.030	0.033	0.035	0.037
20.0	0.014	0.015	0.015	0.016	0.016	0.019	0.021	0.024	0.026	0.028	0.030	0.032
25.0	0.007	0.007	0.008	0.008	0.008	0.009	0.011	0.012	0.013	0.014	0.015	0.016
30.0	0.003	0.004	0.004	0.004	0.004	0.005	0.005	0.006	0.006	0.007	0.008	0.008
35.0	0.002	0.002	0.002	0.002	0.002	0.002	0.002	0.003	0.003	0.003	0.003	0.004
40.0	0.000	0.000	0.000	0.000	0.000	0.001	0.001	0.001	0.001	0.001	0.001	0.001
45.0	-0.000	-0.000	-0.000	-0.000	-0.000	-0.000	-0.000	-0.000	-0.001	-0.001	-0.001	-0.001
50.0	-0.001	-0.001	-0.001	-0.001	-0.001	-0.001	-0.001	-0.001	-0.001	-0.002	-0.002	-0.002
60.0	-0.001	-0.001	-0.001	-0.001	-0.001	-0.002	-0.002	-0.002	-0.002	-0.002	-0.003	-0.003
80.0	-0.001	-0.001	-0.001	-0.002	-0.002	-0.002	-0.002	-0.002	-0.003	-0.003	-0.003	-0.003
100.0	-0.001	-0.001	-0.001	-0.001	-0.001	-0.002	-0.002	-0.002	-0.002	-0.003	-0.003	-0.003
120.0	-0.001	-0.001	-0.001	-0.001	-0.001	-0.002	-0.002	-0.002	-0.002	-0.003	-0.003	-0.003
140.0	-0.001	-0.001	-0.001	-0.001	-0.001	-0.002	-0.002	-0.002	-0.002	-0.002	-0.002	-0.003
160.0	-0.001	-0.001	-0.001	-0.001	-0.001	-0.001	-0.001	-0.002	-0.002	-0.002	-0.002	-0.002
180.0	-0.001	-0.001	-0.001	-0.001	-0.001	-0.001	-0.001	-0.002	-0.002	-0.002	-0.002	-0.002
200.0	-0.001	-0.001	-0.001	-0.001	-0.001	-0.001	-0.001	-0.001	-0.002	-0.002	-0.002	-0.002
220.0	-0.001	-0.001	-0.001	-0.001	-0.001	-0.001	-0.001	-0.001	-0.001	-0.002	-0.002	-0.002
240.0	-0.001	-0.001	-0.001	-0.001	-0.001	-0.001	-0.001	-0.001	-0.001	-0.001	-0.002	-0.002
260.0	-0.001	-0.001	-0.001	-0.001	-0.001	-0.001	-0.001	-0.001	-0.001	-0.001	-0.001	-0.002
280.0	-0.001	-0.001	-0.001	-0.001	-0.001	-0.001	-0.001	-0.001	-0.001	-0.001	-0.001	-0.001
300.0	-0.001	-0.001	-0.001	-0.001	-0.001	-0.001	-0.001	-0.001	-0.001	-0.001	-0.001	-0.001

Table 4.2.6 $(P/T)(\partial T/\partial P)_h$ This is the dimensionless quantity,
Joule Thomson coefficient times pressure divided
by temperature
(continued).

PRES MM/H ATM	3.600	0.709	1.811	0.912	1.013	1.520	2.026	2.533	3.040	3.546	4.053	4.560
TEMP, K	6.000	7.000	8.000	9.000	10.000	15.000	20.000	25.000	30.000	35.000	40.000	45.000
3.0	-0.566	-0.671	-0.779	-0.889	-1.000	-1.505	-2.209	-2.865	-3.543	-4.226	-4.894	-5.521
3.5	-0.380	-0.455	-0.532	-0.611	-0.691	-1.113	-1.564	-2.040	-2.537	-3.049	-3.571	-4.092
4.0	-0.253	-0.310	-0.367	-0.427	-0.487	-0.805	-1.143	-1.496	-1.862	-2.238	-2.620	-3.005
4.2	-0.212	-0.263	-0.315	-0.369	-0.423	-0.709	-1.012	-1.328	-1.653	-1.986	-2.325	-2.665
4.4	-0.176	-0.221	-0.269	-0.317	-0.367	-0.625	-0.898	-1.182	-1.473	-1.770	-2.070	-2.372
4.6	-0.142	-0.184	-0.227	-0.272	-0.317	-0.552	-0.800	-1.055	-1.317	-1.583	-1.851	-2.121
4.8	-0.111	-0.150	-0.190	-0.231	-0.273	-0.469	-0.714	-0.946	-1.182	-1.422	-1.664	-1.906
5.0	-0.082	-0.119	-0.157	-0.195	-0.234	-0.433	-0.640	-0.852	-1.067	-1.285	-1.504	-1.723
5.1	-0.069	-0.105	-0.142	-0.179	-0.217	-0.409	-0.607	-0.818	-1.016	-1.224	-1.433	-1.643
5.2	-0.058	-0.094	-0.130	-0.166	-0.202	-0.389	-0.581	-0.777	-0.975	-1.177	-1.379	-1.581
5.3	-0.045	-0.082	-0.117	-0.153	-0.190	-0.373	-0.562	-0.755	-0.950	-1.148	-1.346	-1.544
5.4	-0.032	-0.069	-0.104	-0.140	-0.175	-0.355	-0.540	-0.727	-0.917	-1.109	-1.301	-1.494
5.5	-0.019	-0.056	-0.091	-0.127	-0.162	-0.338	-0.517	-0.700	-0.885	-1.071	-1.258	-1.445
5.6	-0.006	-0.043	-0.078	-0.113	-0.148	-0.321	-0.496	-0.674	-0.854	-1.035	-1.217	-1.398
5.7	0.008	-0.030	-0.066	-0.100	-0.134	-0.304	-0.475	-0.649	-0.824	-1.000	-1.177	-1.353
5.8	0.023	-0.017	-0.053	-0.087	-0.121	-0.288	-0.455	-0.624	-0.795	-0.966	-1.138	-1.310
5.9	0.037	-0.003	-0.040	-0.075	-0.108	-0.272	-0.436	-0.601	-0.767	-0.934	-1.101	-1.268
6.0	0.052	0.010	-0.027	-0.062	-0.095	-0.257	-0.417	-0.578	-0.740	-0.902	-1.065	-1.228
6.2	0.084	0.038	-0.001	-0.037	-0.070	-0.228	-0.381	-0.535	-0.689	-0.843	-0.998	-1.152
6.4	0.117	0.066	0.025	-0.012	-0.046	-0.200	-0.348	-0.495	-0.641	-0.788	-0.935	-1.082
6.6	0.149	0.095	0.051	0.013	-0.022	-0.174	-0.317	-0.457	-0.598	-0.738	-0.878	-1.017
6.8	0.177	0.123	0.076	0.037	0.002	-0.149	-0.288	-0.423	-0.557	-0.691	-0.824	-0.958
7.0	0.197	0.140	0.081	0.061	0.025	-0.126	-0.260	-0.390	-0.519	-0.647	-0.775	-0.902
7.5	0.215	0.188	0.152	0.114	0.078	-0.072	-0.198	-0.318	-0.435	-0.551	-0.666	-0.781
8.0	0.212	0.197	0.177	0.151	0.120	-0.024	-0.145	-0.257	-0.365	-0.471	-0.575	-0.679
8.5	0.200	0.194	0.181	0.166	0.146	0.018	-0.098	-0.204	-0.304	-0.402	-0.498	-0.593
9.0	0.184	0.185	0.178	0.166	0.155	0.052	-0.058	-0.158	-0.252	-0.343	-0.432	-0.526
9.5	0.167	0.173	0.170	0.163	0.153	0.078	-0.023	-0.117	-0.207	-0.292	-0.375	-0.457
10.0	0.151	0.159	0.161	0.157	0.149	0.095	0.006	-0.082	-0.167	-0.247	-0.326	-0.402
11.0	0.125	0.135	0.139	0.140	0.137	0.104	0.045	-0.028	-0.102	-0.174	-0.244	-0.312
12.0	0.104	0.114	0.120	0.123	0.123	0.099	0.062	0.007	-0.055	-0.118	-0.180	-0.241
13.0	0.088	0.097	0.104	0.108	0.110	0.096	0.066	0.025	-0.024	-0.077	-0.132	-0.186
14.0	0.075	0.083	0.090	0.094	0.097	0.091	0.066	0.034	-0.006	-0.050	-0.097	-0.144
15.0	0.064	0.072	0.078	0.083	0.086	0.086	0.067	0.038	0.004	-0.033	-0.072	-0.113
16.0	0.055	0.061	0.067	0.072	0.075	0.079	0.064	0.041	0.013	-0.019	-0.053	-0.089
17.0	0.047	0.053	0.058	0.062	0.066	0.071	0.061	0.042	0.018	-0.009	-0.039	-0.070
18.0	0.041	0.046	0.050	0.054	0.057	0.064	0.057	0.042	0.021	-0.003	-0.029	-0.056
19.0	0.035	0.040	0.044	0.047	0.050	0.057	0.053	0.040	0.022	0.002	-0.021	-0.046
20.0	0.030	0.034	0.038	0.041	0.044	0.051	0.048	0.038	0.023	0.005	-0.016	-0.037
25.0	0.015	0.017	0.019	0.021	0.023	0.028	0.028	0.024	0.017	0.007	-0.005	-0.018
30.0	0.008	0.009	0.010	0.011	0.011	0.014	0.015	0.012	0.008	0.002	-0.006	-0.014
35.0	0.003	0.004	0.004	0.005	0.005	0.006	0.006	0.004	0.001	-0.004	-0.009	-0.015
40.0	0.001	0.001	0.001	0.001	0.001	0.001	-0.000	-0.002	-0.005	-0.008	-0.013	-0.018
45.0	-0.001	-0.001	-0.001	-0.001	-0.001	-0.002	-0.004	-0.006	-0.009	-0.012	-0.016	-0.020
50.0	-0.002	-0.002	-0.002	-0.003	-0.003	-0.004	-0.006	-0.009	-0.011	-0.014	-0.018	-0.021
60.0	-0.003	-0.003	-0.004	-0.004	-0.004	-0.007	-0.009	-0.012	-0.014	-0.017	-0.020	-0.023
80.0	-0.003	-0.004	-0.004	-0.005	-0.005	-0.008	-0.010	-0.013	-0.015	-0.018	-0.021	-0.024
100.0	-0.003	-0.003	-0.004	-0.004	-0.005	-0.007	-0.010	-0.012	-0.015	-0.017	-0.020	-0.022
120.0	-0.003	-0.003	-0.004	-0.004	-0.005	-0.007	-0.009	-0.011	-0.013	-0.016	-0.018	-0.020
140.0	-0.002	-0.003	-0.003	-0.004	-0.004	-0.006	-0.008	-0.010	-0.012	-0.014	-0.016	-0.018
160.0	-0.002	-0.003	-0.003	-0.003	-0.004	-0.006	-0.007	-0.009	-0.011	-0.013	-0.015	-0.017
180.0	-0.002	-0.002	-0.003	-0.003	-0.003	-0.005	-0.007	-0.008	-0.010	-0.012	-0.014	-0.015
200.0	-0.002	-0.002	-0.003	-0.003	-0.003	-0.005	-0.006	-0.008	-0.009	-0.011	-0.012	-0.014
220.0	-0.002	-0.002	-0.002	-0.003	-0.003	-0.004	-0.006	-0.007	-0.009	-0.010	-0.011	-0.013
240.0	-0.002	-0.002	-0.002	-0.002	-0.003	-0.004	-0.005	-0.007	-0.008	-0.009	-0.011	-0.012
260.0	-0.001	-0.002	-0.002	-0.002	-0.002	-0.004	-0.005	-0.006	-0.007	-0.009	-0.010	-0.011
280.0	-0.001	-0.002	-0.002	-0.002	-0.002	-0.003	-0.005	-0.006	-0.007	-0.008	-0.009	-0.010
300.0	-0.001	-0.002	-0.002	-0.002	-0.002	-0.003	-0.004	-0.005	-0.006	-0.007	-0.008	-0.010

Table 4.2.6 $(P/T) (\partial T/\partial P)_h$ This is the dimensionless quantity,
Joule Thomson coefficient times pressure divided
by temperature
(continued).

PRES MM/HG ATM	5.066 50.000	5.573 55.000	6.079 60.000	6.586 65.000	7.093 70.000	7.599 75.000	8.106 80.000	8.613 85.000	9.119 90.000	9.626 95.000	10.133 100.000	10.639 105.000
TEMP, K												
3.0	-6.079	-6.537	-6.873	-7.068	-7.117	-7.024						
3.5	-4.603	-5.092	-5.546	-5.953	-6.301	-6.582	-6.788	-6.916	-6.967	-6.944	-6.854	
4.0	-3.389	-3.766	-4.133	-4.484	-4.815	-5.120	-5.397	-5.640	-5.848	-6.019	-6.151	-6.245
4.2	-3.004	-3.339	-3.668	-3.985	-4.288	-4.575	-4.840	-5.083	-5.301	-5.492	-5.654	-5.788
4.4	-2.673	-2.972	-3.265	-3.551	-3.827	-4.090	-4.339	-4.572	-4.787	-4.983	-5.157	-5.311
4.6	-2.390	-2.657	-2.920	-3.177	-3.428	-3.669	-3.900	-4.119	-4.325	-4.517	-4.693	-4.854
4.8	-2.148	-2.388	-2.625	-2.858	-3.085	-3.306	-3.519	-3.723	-3.917	-4.102	-4.274	-4.435
5.0	-1.942	-2.159	-2.374	-2.585	-2.792	-2.995	-3.191	-3.381	-3.564	-3.739	-3.905	-4.062
5.1	-1.852	-2.059	-2.264	-2.466	-2.665	-2.859	-3.048	-3.232	-3.409	-3.579	-3.741	-3.896
5.2	-1.782	-1.983	-2.181	-2.376	-2.568	-2.757	-2.941	-3.119	-3.292	-3.459	-3.619	-3.772
5.3	-1.742	-1.938	-2.133	-2.325	-2.515	-2.701	-2.882	-3.059	-3.231	-3.397	-3.557	-3.711
5.4	-1.686	-1.877	-2.066	-2.254	-2.438	-2.620	-2.797	-2.971	-3.139	-3.303	-3.461	-3.613
5.5	-1.632	-1.818	-2.002	-2.184	-2.364	-2.541	-2.714	-2.884	-3.050	-3.211	-3.366	-3.517
5.6	-1.580	-1.761	-1.940	-2.117	-2.292	-2.465	-2.634	-2.801	-2.963	-3.121	-3.275	-3.423
5.7	-1.530	-1.705	-1.880	-2.053	-2.223	-2.392	-2.557	-2.720	-2.879	-3.034	-3.185	-3.332
5.8	-1.481	-1.652	-1.822	-1.990	-2.157	-2.321	-2.483	-2.642	-2.797	-2.950	-3.099	-3.243
5.9	-1.435	-1.601	-1.767	-1.930	-2.093	-2.253	-2.411	-2.566	-2.719	-2.869	-3.015	-3.158
6.0	-1.390	-1.552	-1.713	-1.873	-2.031	-2.187	-2.342	-2.494	-2.643	-2.790	-2.934	-3.074
6.2	-1.306	-1.460	-1.613	-1.764	-1.915	-2.064	-2.211	-2.357	-2.500	-2.641	-2.780	-2.916
6.4	-1.228	-1.374	-1.520	-1.664	-1.808	-1.953	-2.091	-2.230	-2.367	-2.503	-2.637	-2.768
6.6	-1.157	-1.296	-1.434	-1.572	-1.709	-1.844	-1.979	-2.112	-2.244	-2.375	-2.504	-2.631
6.8	-1.090	-1.223	-1.355	-1.486	-1.617	-1.747	-1.876	-2.004	-2.130	-2.256	-2.380	-2.503
7.0	-1.029	-1.156	-1.282	-1.407	-1.532	-1.657	-1.780	-1.903	-2.025	-2.145	-2.265	-2.383
7.5	-0.895	-1.008	-1.122	-1.234	-1.347	-1.459	-1.570	-1.681	-1.791	-1.901	-2.010	-2.119
8.0	-0.783	-0.885	-0.988	-1.090	-1.192	-1.293	-1.394	-1.495	-1.595	-1.695	-1.795	-1.894
8.5	-0.688	-0.782	-0.875	-0.968	-1.061	-1.153	-1.246	-1.338	-1.429	-1.521	-1.612	-1.703
9.0	-0.607	-0.693	-0.779	-0.864	-0.949	-1.034	-1.119	-1.203	-1.287	-1.371	-1.454	-1.538
9.5	-0.538	-0.617	-0.697	-0.775	-0.854	-0.932	-1.009	-1.087	-1.164	-1.241	-1.318	-1.395
10.0	-0.477	-0.561	-0.625	-0.698	-0.771	-0.843	-0.915	-0.986	-1.058	-1.129	-1.200	-1.271
11.0	-0.379	-0.445	-0.510	-0.574	-0.638	-0.701	-0.764	-0.827	-0.889	-0.951	-1.013	-1.075
12.0	-0.301	-0.361	-0.419	-0.476	-0.533	-0.590	-0.646	-0.702	-0.757	-0.812	-0.866	-0.921
13.0	-0.240	-0.293	-0.346	-0.398	-0.449	-0.500	-0.551	-0.601	-0.651	-0.700	-0.749	-0.798
14.0	-0.192	-0.240	-0.287	-0.334	-0.381	-0.427	-0.473	-0.519	-0.564	-0.609	-0.653	-0.697
15.0	-0.155	-0.198	-0.240	-0.283	-0.325	-0.367	-0.409	-0.451	-0.492	-0.533	-0.574	-0.614
16.0	-0.126	-0.163	-0.202	-0.240	-0.276	-0.316	-0.355	-0.392	-0.430	-0.468	-0.505	-0.542
17.0	-0.103	-0.136	-0.171	-0.205	-0.240	-0.275	-0.309	-0.344	-0.379	-0.413	-0.447	-0.481
18.0	-0.085	-0.115	-0.146	-0.177	-0.208	-0.240	-0.272	-0.303	-0.335	-0.367	-0.398	-0.430
19.0	-0.071	-0.098	-0.126	-0.154	-0.182	-0.211	-0.240	-0.269	-0.298	-0.328	-0.357	-0.386
20.0	-0.060	-0.084	-0.109	-0.135	-0.161	-0.187	-0.214	-0.240	-0.267	-0.294	-0.321	-0.348
25.0	-0.033	-0.048	-0.063	-0.080	-0.097	-0.114	-0.131	-0.149	-0.168	-0.186	-0.205	-0.223
30.0	-0.024	-0.035	-0.046	-0.057	-0.069	-0.081	-0.094	-0.107	-0.120	-0.133	-0.146	-0.160
35.0	-0.022	-0.030	-0.038	-0.047	-0.056	-0.065	-0.075	-0.084	-0.094	-0.104	-0.115	-0.125
40.0	-0.023	-0.029	-0.035	-0.042	-0.049	-0.057	-0.064	-0.072	-0.080	-0.088	-0.096	-0.104
45.0	-0.024	-0.029	-0.034	-0.040	-0.046	-0.052	-0.058	-0.065	-0.071	-0.078	-0.085	-0.091
50.0	-0.025	-0.030	-0.034	-0.039	-0.044	-0.049	-0.054	-0.060	-0.065	-0.071	-0.077	-0.083
60.0	-0.027	-0.030	-0.034	-0.038	-0.041	-0.045	-0.050	-0.054	-0.058	-0.063	-0.067	-0.072
80.0	-0.026	-0.029	-0.032	-0.035	-0.038	-0.041	-0.044	-0.047	-0.051	-0.054	-0.057	-0.060
100.0	-0.025	-0.027	-0.030	-0.032	-0.035	-0.037	-0.040	-0.042	-0.045	-0.048	-0.050	-0.053
120.0	-0.022	-0.025	-0.027	-0.029	-0.031	-0.034	-0.036	-0.038	-0.040	-0.043	-0.045	-0.047
140.0	-0.020	-0.022	-0.024	-0.026	-0.028	-0.030	-0.032	-0.034	-0.036	-0.038	-0.041	-0.043
160.0	-0.018	-0.020	-0.022	-0.024	-0.026	-0.028	-0.029	-0.031	-0.033	-0.035	-0.037	-0.039
180.0	-0.017	-0.019	-0.020	-0.022	-0.024	-0.025	-0.027	-0.028	-0.030	-0.032	-0.033	-0.035
200.0	-0.015	-0.017	-0.018	-0.020	-0.022	-0.023	-0.025	-0.026	-0.028	-0.029	-0.031	-0.032
220.0	-0.014	-0.016	-0.017	-0.018	-0.020	-0.021	-0.023	-0.024	-0.025	-0.027	-0.028	-0.030
240.0	-0.013	-0.014	-0.016	-0.017	-0.018	-0.020	-0.021	-0.022	-0.023	-0.025	-0.026	-0.027
260.0	-0.012	-0.013	-0.015	-0.016	-0.017	-0.018	-0.019	-0.021	-0.022	-0.023	-0.024	-0.025
280.0	-0.011	-0.013	-0.014	-0.015	-0.016	-0.017	-0.018	-0.019	-0.020	-0.021	-0.022	-0.023
300.0	-0.011	-0.012	-0.013	-0.014	-0.015	-0.016	-0.017	-0.018	-0.019	-0.020	-0.021	-0.022

Table 4.2.7 Helium⁴ Prandtl number, $c_p \mu / K$.

PRES MN/M ² ATM	0.010	0.051	0.101	0.152	0.182	0.193	0.203	0.213	0.223	0.233	0.243	0.253
TEMP, K	0.100	0.500	1.000	1.500	1.900	1.900	2.000	2.100	2.200	2.300	2.400	2.500
3.0	0.667	0.500	0.500	0.501	0.501	0.502	0.502	0.502	0.512	0.502	0.503	0.503
3.5	0.659	0.579	0.571	0.565	0.562	0.562	0.561	0.560	0.550	0.559	0.550	0.550
4.0	0.654	0.754	0.692	0.664	0.652	0.649	0.645	0.641	0.630	0.636	0.633	0.630
4.2	0.652	0.748	0.708	0.733	0.714	0.704	0.698	0.692	0.697	0.682	0.678	0.674
4.4	0.652	0.736	0.961	0.843	0.738	0.706	0.775	0.765	0.750	0.747	0.740	0.733
4.6	0.651	0.726	0.900	1.033	0.352	0.925	0.902	0.881	0.853	0.847	0.832	0.819
4.8	0.651	0.718	0.859	1.238	1.230	1.163	1.110	1.007	1.051	1.000	0.973	0.949
5.0	0.651	0.711	0.810	1.079	1.512	1.929	1.793	1.571	1.427	1.323	1.245	1.182
5.1	0.651	0.708	0.818	1.031	1.328	1.527	1.894	2.682	2.000	1.707	1.526	1.401
5.2	0.651	0.706	0.808	0.992	1.218	1.344	1.530	1.844	2.594	2.786	2.062	1.760
5.3	0.651	0.703	0.798	0.961	1.141	1.233	1.354	1.524	1.738	2.267	3.351	2.730
5.4	0.651	0.701	0.790	0.936	1.085	1.155	1.243	1.357	1.511	1.731	2.072	2.610
5.5	0.651	0.699	0.783	0.914	1.040	1.097	1.166	1.249	1.355	1.492	1.676	1.931
5.6	0.651	0.698	0.776	0.895	1.005	1.052	1.108	1.173	1.252	1.349	1.470	1.624
5.7	0.651	0.696	0.770	0.879	0.975	1.016	1.062	1.115	1.178	1.251	1.339	1.446
5.8	0.651	0.694	0.765	0.865	0.951	0.986	1.025	1.070	1.121	1.179	1.248	1.327
5.9	0.652	0.693	0.760	0.853	0.929	0.960	0.994	1.033	1.076	1.124	1.179	1.242
6.0	0.652	0.692	0.757	0.841	0.911	0.936	0.969	1.002	1.039	1.080	1.125	1.177
6.2	0.653	0.690	0.747	0.823	0.881	0.903	0.927	0.953	0.992	1.013	1.046	1.083
6.4	0.653	0.688	0.740	0.807	0.857	0.876	0.896	0.917	0.940	0.964	0.991	1.019
6.6	0.654	0.686	0.735	0.794	0.836	0.854	0.871	0.889	0.907	0.926	0.949	0.971
6.8	0.655	0.685	0.730	0.784	0.822	0.836	0.850	0.866	0.882	0.899	0.916	0.935
7.0	0.655	0.684	0.725	0.774	0.808	0.821	0.834	0.847	0.861	0.875	0.891	0.906
7.5	0.657	0.682	0.717	0.757	0.783	0.793	0.802	0.812	0.822	0.833	0.844	0.855
8.0	0.650	0.681	0.711	0.744	0.766	0.773	0.781	0.789	0.797	0.805	0.813	0.822
8.5	0.662	0.681	0.707	0.735	0.753	0.759	0.765	0.772	0.778	0.785	0.791	0.798
9.0	0.664	0.681	0.704	0.728	0.743	0.748	0.754	0.759	0.764	0.770	0.775	0.781
9.5	0.666	0.682	0.702	0.723	0.736	0.740	0.745	0.750	0.754	0.759	0.763	0.768
10.0	0.668	0.682	0.700	0.719	0.730	0.734	0.738	0.742	0.746	0.750	0.754	0.758
11.0	0.672	0.684	0.699	0.714	0.723	0.726	0.729	0.732	0.735	0.739	0.742	0.745
12.0	0.676	0.686	0.698	0.710	0.718	0.721	0.723	0.726	0.728	0.731	0.733	0.736
13.0	0.679	0.688	0.698	0.708	0.715	0.717	0.719	0.721	0.723	0.725	0.727	0.730
14.0	0.683	0.690	0.698	0.707	0.713	0.714	0.716	0.718	0.720	0.722	0.723	0.725
15.0	0.685	0.691	0.699	0.707	0.711	0.713	0.714	0.716	0.717	0.719	0.720	0.722
16.0	0.688	0.693	0.700	0.706	0.710	0.712	0.713	0.714	0.716	0.717	0.718	0.719
17.0	0.690	0.695	0.701	0.706	0.710	0.711	0.712	0.713	0.714	0.715	0.717	0.718
18.0	0.693	0.697	0.702	0.707	0.709	0.710	0.711	0.712	0.713	0.714	0.715	0.716
19.0	0.695	0.698	0.702	0.707	0.709	0.710	0.711	0.712	0.713	0.714	0.715	0.715
20.0	0.696	0.699	0.703	0.707	0.709	0.710	0.711	0.712	0.713	0.714	0.715	0.715
25.0	0.703	0.704	0.707	0.709	0.710	0.711	0.711	0.712	0.712	0.712	0.713	0.713
30.0	0.706	0.707	0.709	0.710	0.711	0.711	0.711	0.712	0.712	0.712	0.713	0.713
35.0	0.708	0.709	0.709	0.710	0.711	0.711	0.711	0.712	0.712	0.712	0.712	0.712
40.0	0.708	0.709	0.709	0.710	0.710	0.711	0.711	0.711	0.711	0.711	0.711	0.711
45.0	0.708	0.708	0.709	0.709	0.709	0.709	0.709	0.710	0.710	0.710	0.710	0.710
50.0	0.707	0.707	0.707	0.708	0.708	0.708	0.708	0.708	0.708	0.708	0.708	0.708
60.0	0.704	0.704	0.704	0.704	0.705	0.705	0.705	0.705	0.705	0.705	0.705	0.705
80.0	0.697	0.697	0.697	0.697	0.697	0.697	0.697	0.697	0.697	0.697	0.697	0.697
100.0	0.691	0.691	0.691	0.691	0.691	0.691	0.691	0.691	0.691	0.691	0.691	0.691
120.0	0.685	0.685	0.685	0.685	0.685	0.685	0.685	0.685	0.685	0.685	0.685	0.685
140.0	0.681	0.681	0.681	0.681	0.681	0.681	0.681	0.681	0.681	0.681	0.681	0.681
160.0	0.679	0.679	0.679	0.679	0.679	0.679	0.679	0.679	0.679	0.679	0.679	0.679
180.0	0.677	0.677	0.677	0.677	0.677	0.677	0.677	0.677	0.677	0.677	0.677	0.677
200.0	0.677	0.677	0.677	0.677	0.677	0.677	0.677	0.677	0.677	0.677	0.677	0.677
220.0	0.677	0.677	0.677	0.677	0.677	0.677	0.677	0.677	0.677	0.677	0.677	0.677
240.0	0.678	0.678	0.678	0.678	0.678	0.678	0.678	0.678	0.678	0.678	0.678	0.678
260.0	0.680	0.680	0.680	0.680	0.680	0.680	0.680	0.680	0.680	0.680	0.680	0.680
280.0	0.683	0.683	0.682	0.682	0.682	0.682	0.682	0.682	0.682	0.682	0.682	0.682
300.0	0.686	0.686	0.686	0.685	0.685	0.685	0.685	0.685	0.685	0.685	0.685	0.685

Table 4.2.7 Helium⁴ Prandtl number, $c_p \mu / K$ (continued).

PRES MN/H ² ATM	0.263	0.274	0.284	0.294	0.304	0.355	0.405	0.455	0.517	0.557	0.608	0.659
TEMP, K	2.600	2.700	2.800	2.900	3.000	3.500	4.000	4.500	5.000	5.500	6.000	6.500
3.0	0.503	0.503	0.504	0.504	0.504	0.506	0.507	0.509	0.511	0.512	0.514	0.516
3.5	0.557	0.557	0.557	0.556	0.556	0.554	0.553	0.552	0.552	0.552	0.552	0.552
4.0	0.628	0.626	0.623	0.621	0.619	0.611	0.604	0.593	0.584	0.581	0.580	0.585
4.2	0.670	0.666	0.662	0.659	0.656	0.642	0.632	0.623	0.616	0.610	0.606	0.602
4.4	0.726	0.720	0.714	0.708	0.703	0.682	0.665	0.653	0.642	0.634	0.627	0.621
4.6	0.807	0.796	0.786	0.777	0.768	0.734	0.708	0.683	0.674	0.661	0.651	0.643
4.8	0.939	0.917	0.898	0.880	0.865	0.805	0.764	0.735	0.712	0.695	0.680	0.669
5.0	1.132	1.070	1.054	1.023	0.996	0.908	0.839	0.793	0.759	0.734	0.714	0.698
5.1	1.309	1.237	1.179	1.132	1.092	0.958	0.885	0.826	0.786	0.756	0.732	0.714
5.2	1.567	1.434	1.337	1.261	1.200	1.015	0.916	0.856	0.807	0.772	0.745	0.724
5.3	2.126	1.810	1.612	1.474	1.371	1.092	0.962	0.884	0.831	0.789	0.757	0.733
5.4	3.085	2.609	2.162	1.856	1.654	1.203	1.025	0.925	0.865	0.814	0.777	0.748
5.5	2.273	2.632	2.750	2.456	2.116	1.556	1.104	0.975	0.896	0.843	0.799	0.766
5.6	1.821	2.062	2.313	2.493	2.505	1.565	1.204	1.035	0.937	0.872	0.825	0.786
5.7	1.576	1.712	1.912	2.096	2.248	1.831	1.331	1.103	0.956	0.907	0.852	0.810
5.8	1.421	1.531	1.658	1.797	1.938	2.054	1.486	1.197	1.043	0.947	0.882	0.837
5.9	1.314	1.336	1.430	1.594	1.706	2.060	1.653	1.301	1.109	0.994	0.916	0.861
6.0	1.234	1.293	1.372	1.452	1.539	1.918	1.787	1.416	1.195	1.046	0.955	0.891
6.2	1.124	1.168	1.216	1.268	1.325	1.631	1.780	1.615	1.355	1.173	1.046	0.961
6.4	1.049	1.082	1.117	1.154	1.195	1.422	1.606	1.641	1.433	1.302	1.152	1.044
6.6	0.996	1.021	1.048	1.077	1.107	1.279	1.447	1.537	1.523	1.402	1.256	1.133
6.8	0.955	0.970	0.997	1.020	1.044	1.178	1.320	1.423	1.451	1.428	1.330	1.216
7.0	0.923	0.940	0.958	0.977	0.997	1.105	1.222	1.322	1.379	1.391	1.352	1.272
7.5	0.867	0.879	0.891	0.904	0.917	0.987	1.064	1.139	1.201	1.241	1.259	1.258
8.0	0.830	0.839	0.848	0.858	0.867	0.918	0.972	1.027	1.077	1.119	1.148	1.164
8.5	0.805	0.812	0.819	0.827	0.834	0.873	0.913	0.955	0.995	1.030	1.060	1.081
9.0	0.787	0.793	0.798	0.804	0.810	0.841	0.873	0.905	0.937	0.967	0.994	1.015
9.5	0.773	0.778	0.783	0.788	0.793	0.818	0.844	0.870	0.896	0.921	0.944	0.964
10.0	0.762	0.756	0.771	0.775	0.779	0.800	0.822	0.844	0.856	0.887	0.906	0.924
11.0	0.748	0.751	0.754	0.758	0.761	0.777	0.793	0.810	0.826	0.841	0.856	0.869
12.0	0.739	0.741	0.744	0.746	0.749	0.762	0.775	0.787	0.800	0.812	0.824	0.834
13.0	0.732	0.734	0.736	0.738	0.740	0.751	0.761	0.771	0.782	0.791	0.801	0.809
14.0	0.727	0.729	0.730	0.732	0.734	0.743	0.752	0.760	0.769	0.777	0.784	0.792
15.0	0.724	0.725	0.727	0.728	0.730	0.737	0.745	0.752	0.759	0.766	0.773	0.779
16.0	0.721	0.722	0.723	0.725	0.726	0.732	0.739	0.745	0.751	0.757	0.762	0.768
17.0	0.719	0.720	0.721	0.722	0.723	0.729	0.734	0.739	0.745	0.750	0.755	0.759
18.0	0.717	0.718	0.719	0.720	0.721	0.726	0.731	0.735	0.740	0.744	0.748	0.753
19.0	0.716	0.717	0.718	0.719	0.720	0.724	0.728	0.732	0.736	0.740	0.743	0.747
20.0	0.715	0.716	0.717	0.718	0.719	0.722	0.726	0.729	0.733	0.736	0.739	0.743
25.0	0.714	0.714	0.715	0.715	0.715	0.718	0.720	0.722	0.724	0.726	0.728	0.729
30.0	0.713	0.713	0.714	0.714	0.714	0.716	0.717	0.718	0.719	0.721	0.722	0.723
35.0	0.712	0.713	0.713	0.713	0.713	0.714	0.715	0.716	0.717	0.717	0.718	0.719
40.0	0.711	0.712	0.712	0.712	0.712	0.712	0.713	0.714	0.714	0.715	0.715	0.716
45.0	0.710	0.710	0.710	0.710	0.710	0.711	0.711	0.712	0.712	0.713	0.713	0.713
50.0	0.708	0.709	0.709	0.709	0.709	0.709	0.709	0.710	0.710	0.710	0.711	0.711
60.0	0.705	0.705	0.705	0.705	0.705	0.705	0.705	0.706	0.706	0.706	0.706	0.706
80.0	0.697	0.697	0.697	0.697	0.697	0.697	0.698	0.698	0.698	0.698	0.698	0.698
100.0	0.691	0.691	0.691	0.691	0.691	0.691	0.691	0.691	0.691	0.691	0.691	0.691
120.0	0.685	0.685	0.685	0.685	0.685	0.685	0.685	0.685	0.685	0.685	0.685	0.685
140.0	0.681	0.681	0.681	0.681	0.681	0.681	0.681	0.681	0.681	0.681	0.681	0.681
160.0	0.679	0.679	0.679	0.679	0.679	0.679	0.679	0.678	0.678	0.678	0.678	0.678
180.0	0.677	0.677	0.677	0.677	0.677	0.677	0.677	0.677	0.677	0.677	0.677	0.677
200.0	0.676	0.676	0.676	0.676	0.676	0.676	0.676	0.676	0.676	0.676	0.676	0.676
220.0	0.677	0.677	0.677	0.677	0.677	0.677	0.677	0.677	0.677	0.677	0.677	0.677
240.0	0.678	0.678	0.678	0.678	0.678	0.678	0.678	0.678	0.678	0.678	0.678	0.678
260.0	0.680	0.680	0.680	0.680	0.680	0.680	0.680	0.680	0.680	0.680	0.680	0.679
280.0	0.682	0.682	0.682	0.682	0.682	0.682	0.682	0.682	0.682	0.682	0.682	0.682
300.0	0.685	0.685	0.685	0.685	0.685	0.685	0.685	0.685	0.685	0.685	0.685	0.685

Table 4.2.7 Helium⁴ Prandtl number, $c_p \mu/K$ (continued).

PRES MM/HG ATM	0.600 0.000	0.709 7.000	0.811 8.000	0.912 9.000	1.013 10.000	1.520 15.000	2.026 20.000	2.533 25.000	3.040 30.000	3.546 35.000	4.053 40.000	4.560 45.000
TEMP, K												
3.0	0.514	0.510	0.522	0.525	0.529	0.547	0.566	0.586	0.607	0.633	0.664	0.703
3.5	0.552	0.552	0.553	0.555	0.557	0.567	0.580	0.594	0.609	0.627	0.646	0.670
4.0	0.588	0.583	0.580	0.578	0.577	0.578	0.586	0.597	0.610	0.625	0.642	0.661
4.2	0.606	0.598	0.593	0.590	0.587	0.584	0.590	0.599	0.611	0.626	0.643	0.661
4.4	0.627	0.616	0.608	0.602	0.598	0.591	0.594	0.602	0.614	0.628	0.644	0.662
4.6	0.651	0.636	0.625	0.617	0.611	0.598	0.599	0.606	0.616	0.629	0.645	0.662
4.8	0.680	0.659	0.644	0.633	0.625	0.606	0.604	0.609	0.619	0.631	0.646	0.663
5.0	0.714	0.685	0.665	0.651	0.640	0.614	0.609	0.613	0.621	0.633	0.647	0.663
5.1	0.732	0.699	0.676	0.659	0.647	0.618	0.611	0.614	0.621	0.633	0.646	0.662
5.2	0.745	0.707	0.682	0.663	0.650	0.617	0.609	0.610	0.617	0.628	0.641	0.655
5.3	0.757	0.713	0.684	0.663	0.648	0.611	0.600	0.600	0.606	0.615	0.627	0.641
5.4	0.777	0.726	0.692	0.669	0.652	0.610	0.597	0.596	0.600	0.609	0.620	0.633
5.5	0.799	0.740	0.702	0.676	0.656	0.609	0.594	0.592	0.596	0.603	0.613	0.625
5.6	0.825	0.756	0.713	0.683	0.662	0.609	0.593	0.589	0.591	0.598	0.607	0.619
5.7	0.852	0.775	0.726	0.692	0.668	0.610	0.591	0.586	0.587	0.593	0.602	0.612
5.8	0.882	0.796	0.740	0.703	0.676	0.612	0.590	0.583	0.584	0.589	0.597	0.607
5.9	0.916	0.820	0.756	0.714	0.684	0.614	0.590	0.582	0.581	0.585	0.592	0.602
6.0	0.955	0.843	0.774	0.727	0.694	0.616	0.590	0.580	0.579	0.582	0.588	0.597
6.2	1.046	0.899	0.814	0.756	0.716	0.623	0.591	0.578	0.575	0.576	0.581	0.589
6.4	1.152	0.964	0.858	0.792	0.742	0.631	0.593	0.578	0.572	0.572	0.576	0.582
6.6	1.256	1.038	0.909	0.828	0.772	0.641	0.597	0.578	0.570	0.569	0.571	0.576
6.8	1.330	1.114	0.965	0.869	0.804	0.653	0.602	0.579	0.570	0.566	0.567	0.571
7.0	1.352	1.100	1.023	0.914	0.839	0.666	0.608	0.582	0.570	0.565	0.564	0.567
7.5	1.259	1.235	1.135	1.024	0.932	0.706	0.627	0.591	0.573	0.564	0.560	0.559
8.0	1.148	1.160	1.150	1.089	1.011	0.753	0.652	0.605	0.580	0.567	0.559	0.556
8.5	1.060	1.094	1.099	1.085	1.046	0.801	0.681	0.622	0.591	0.573	0.562	0.556
9.0	0.994	1.031	1.046	1.046	1.035	0.846	0.713	0.643	0.604	0.581	0.567	0.558
9.5	0.944	0.980	1.000	1.007	1.003	0.801	0.744	0.665	0.620	0.592	0.574	0.562
10.0	0.906	0.939	0.961	0.971	0.973	0.902	0.774	0.689	0.637	0.604	0.583	0.568
11.0	0.858	0.885	0.905	0.919	0.925	0.902	0.817	0.733	0.673	0.632	0.604	0.584
12.0	0.824	0.844	0.862	0.874	0.882	0.871	0.827	0.762	0.704	0.660	0.627	0.603
13.0	0.801	0.818	0.832	0.844	0.852	0.852	0.821	0.774	0.726	0.684	0.650	0.623
14.0	0.784	0.799	0.811	0.822	0.830	0.837	0.812	0.777	0.737	0.700	0.668	0.641
15.0	0.773	0.785	0.796	0.806	0.813	0.826	0.807	0.776	0.742	0.710	0.680	0.656
16.0	0.762	0.773	0.783	0.791	0.798	0.814	0.803	0.778	0.750	0.721	0.695	0.671
17.0	0.755	0.764	0.772	0.780	0.787	0.803	0.798	0.779	0.755	0.730	0.706	0.683
18.0	0.748	0.757	0.764	0.771	0.777	0.794	0.792	0.778	0.758	0.736	0.714	0.694
19.0	0.743	0.751	0.757	0.763	0.769	0.786	0.787	0.776	0.760	0.741	0.721	0.702
20.0	0.739	0.746	0.752	0.757	0.762	0.778	0.781	0.774	0.760	0.744	0.727	0.709
25.0	0.728	0.731	0.735	0.738	0.741	0.753	0.759	0.759	0.755	0.748	0.739	0.729
30.0	0.722	0.724	0.726	0.729	0.731	0.739	0.744	0.747	0.746	0.744	0.739	0.734
35.0	0.718	0.720	0.721	0.723	0.724	0.730	0.735	0.737	0.738	0.737	0.735	0.732
40.0	0.715	0.717	0.718	0.719	0.720	0.724	0.727	0.730	0.731	0.731	0.730	0.729
45.0	0.713	0.714	0.715	0.715	0.716	0.719	0.722	0.724	0.725	0.725	0.725	0.725
50.0	0.711	0.711	0.712	0.712	0.713	0.715	0.717	0.719	0.720	0.721	0.721	0.720
60.0	0.706	0.706	0.707	0.707	0.707	0.709	0.710	0.711	0.712	0.712	0.713	0.713
80.0	0.698	0.698	0.698	0.698	0.698	0.699	0.699	0.700	0.700	0.700	0.700	0.700
100.0	0.691	0.691	0.691	0.691	0.691	0.691	0.691	0.691	0.691	0.691	0.691	0.691
120.0	0.685	0.685	0.685	0.685	0.685	0.685	0.685	0.685	0.685	0.685	0.684	0.684
140.0	0.681	0.681	0.681	0.681	0.681	0.681	0.681	0.680	0.680	0.680	0.680	0.679
160.0	0.678	0.678	0.678	0.678	0.678	0.678	0.678	0.677	0.677	0.677	0.676	0.676
180.0	0.677	0.677	0.677	0.677	0.677	0.677	0.676	0.676	0.675	0.675	0.674	0.674
200.0	0.676	0.676	0.676	0.676	0.676	0.676	0.675	0.675	0.674	0.674	0.674	0.673
220.0	0.677	0.676	0.676	0.676	0.676	0.676	0.675	0.675	0.675	0.674	0.674	0.673
240.0	0.678	0.678	0.678	0.677	0.677	0.677	0.676	0.676	0.676	0.675	0.675	0.674
260.0	0.680	0.679	0.679	0.679	0.679	0.679	0.678	0.678	0.677	0.677	0.676	0.676
280.0	0.682	0.682	0.682	0.682	0.682	0.681	0.681	0.680	0.680	0.679	0.679	0.678
300.0	0.685	0.685	0.685	0.685	0.685	0.684	0.684	0.683	0.683	0.682	0.681	0.681

Table 4.2.7 Helium⁴ Prandtl number, $c_p \mu / K$ (continued).

PRES MM/HG ATM	5.066 50.000	5.573 55.000	6.079 60.000	6.586 65.000	7.093 70.000	7.599 75.000	8.106 80.000	8.613 85.000	9.119 90.000	9.626 95.000	10.133 100.000	10.639 105.000
TEMP. K												
3.0	0.751	0.814	0.893	0.994	1.123	1.288						
3.5	0.697	0.729	0.766	0.814	0.870	0.937	1.016	1.111	1.225	1.360	1.520	
4.0	0.684	0.709	0.737	0.770	0.807	0.849	0.896	0.951	1.013	1.083	1.163	1.254
4.2	0.683	0.706	0.733	0.763	0.796	0.834	0.876	0.923	0.975	1.034	1.101	1.174
4.4	0.682	0.705	0.730	0.759	0.789	0.823	0.861	0.902	0.948	0.999	1.056	1.118
4.6	0.682	0.704	0.728	0.754	0.782	0.814	0.848	0.886	0.927	0.972	1.022	1.075
4.8	0.682	0.702	0.725	0.750	0.776	0.806	0.837	0.872	0.909	0.949	0.993	1.041
5.0	0.680	0.700	0.722	0.745	0.770	0.797	0.827	0.858	0.892	0.929	0.968	1.010
5.1	0.679	0.698	0.719	0.742	0.766	0.792	0.820	0.851	0.883	0.918	0.955	0.995
5.2	0.672	0.690	0.710	0.732	0.755	0.780	0.807	0.836	0.867	0.900	0.935	0.973
5.3	0.656	0.673	0.692	0.712	0.734	0.758	0.783	0.810	0.839	0.869	0.902	0.937
5.4	0.647	0.664	0.681	0.701	0.722	0.744	0.768	0.793	0.820	0.850	0.880	0.913
5.5	0.639	0.655	0.672	0.690	0.710	0.731	0.754	0.778	0.804	0.831	0.860	0.891
5.6	0.632	0.646	0.663	0.680	0.699	0.719	0.741	0.764	0.788	0.814	0.842	0.871
5.7	0.625	0.639	0.654	0.671	0.689	0.708	0.729	0.751	0.774	0.798	0.824	0.852
5.8	0.619	0.632	0.647	0.662	0.680	0.699	0.717	0.738	0.760	0.784	0.808	0.834
5.9	0.613	0.625	0.639	0.654	0.671	0.688	0.707	0.727	0.748	0.770	0.793	0.818
6.0	0.607	0.619	0.633	0.647	0.662	0.679	0.697	0.716	0.736	0.757	0.779	0.802
6.2	0.598	0.608	0.620	0.633	0.646	0.663	0.679	0.696	0.714	0.733	0.753	0.774
6.4	0.590	0.599	0.610	0.621	0.634	0.648	0.663	0.678	0.695	0.712	0.730	0.749
6.6	0.582	0.591	0.600	0.611	0.622	0.635	0.648	0.662	0.677	0.693	0.710	0.727
6.8	0.576	0.584	0.592	0.601	0.612	0.623	0.635	0.648	0.662	0.676	0.691	0.707
7.0	0.571	0.577	0.585	0.593	0.603	0.613	0.624	0.636	0.648	0.661	0.675	0.689
7.5	0.561	0.565	0.570	0.576	0.583	0.591	0.600	0.609	0.619	0.629	0.640	0.652
8.0	0.555	0.557	0.560	0.564	0.569	0.575	0.581	0.589	0.596	0.605	0.613	0.622
8.5	0.553	0.552	0.553	0.555	0.558	0.563	0.567	0.573	0.579	0.585	0.592	0.600
9.0	0.553	0.550	0.549	0.549	0.551	0.554	0.557	0.561	0.566	0.571	0.576	0.582
9.5	0.555	0.550	0.547	0.546	0.547	0.548	0.550	0.553	0.556	0.560	0.564	0.568
10.0	0.558	0.552	0.548	0.545	0.544	0.544	0.545	0.546	0.549	0.551	0.555	0.558
11.0	0.570	0.559	0.552	0.546	0.543	0.540	0.539	0.538	0.538	0.539	0.540	0.542
12.0	0.585	0.571	0.560	0.552	0.546	0.542	0.538	0.536	0.534	0.533	0.533	0.533
13.0	0.602	0.585	0.572	0.562	0.554	0.547	0.542	0.538	0.535	0.532	0.531	0.530
14.0	0.619	0.601	0.586	0.573	0.563	0.555	0.548	0.543	0.538	0.535	0.532	0.530
15.0	0.634	0.615	0.599	0.586	0.574	0.565	0.557	0.550	0.544	0.540	0.536	0.532
16.0	0.649	0.630	0.614	0.600	0.587	0.577	0.568	0.560	0.553	0.548	0.543	0.539
17.0	0.663	0.644	0.628	0.613	0.600	0.589	0.579	0.571	0.563	0.557	0.551	0.546
18.0	0.674	0.656	0.640	0.626	0.613	0.601	0.591	0.582	0.573	0.566	0.560	0.554
19.0	0.684	0.667	0.652	0.637	0.624	0.613	0.602	0.592	0.584	0.576	0.569	0.563
20.0	0.693	0.677	0.662	0.646	0.633	0.623	0.613	0.603	0.594	0.586	0.579	0.572
25.0	0.718	0.707	0.696	0.686	0.676	0.666	0.656	0.647	0.639	0.631	0.623	0.616
30.0	0.727	0.720	0.713	0.705	0.698	0.690	0.683	0.676	0.669	0.662	0.656	0.649
35.0	0.729	0.724	0.720	0.714	0.709	0.704	0.698	0.693	0.687	0.682	0.677	0.671
40.0	0.727	0.724	0.721	0.718	0.714	0.710	0.706	0.702	0.698	0.694	0.689	0.685
45.0	0.723	0.722	0.720	0.718	0.715	0.712	0.709	0.706	0.703	0.700	0.697	0.693
50.0	0.720	0.719	0.717	0.716	0.714	0.712	0.710	0.708	0.705	0.703	0.700	0.698
60.0	0.712	0.712	0.711	0.711	0.710	0.708	0.707	0.706	0.704	0.703	0.701	0.700
80.0	0.700	0.700	0.700	0.699	0.699	0.698	0.698	0.697	0.696	0.696	0.695	0.694
100.0	0.691	0.690	0.690	0.690	0.690	0.689	0.689	0.688	0.688	0.687	0.687	0.686
120.0	0.684	0.684	0.683	0.683	0.683	0.682	0.682	0.681	0.681	0.680	0.680	0.679
140.0	0.679	0.679	0.678	0.678	0.678	0.677	0.677	0.676	0.676	0.675	0.675	0.674
160.0	0.676	0.675	0.675	0.674	0.674	0.674	0.673	0.673	0.672	0.672	0.671	0.671
180.0	0.674	0.673	0.673	0.672	0.672	0.672	0.671	0.671	0.670	0.670	0.669	0.669
200.0	0.673	0.672	0.672	0.671	0.671	0.671	0.670	0.670	0.669	0.669	0.668	0.668
220.0	0.673	0.672	0.672	0.671	0.671	0.671	0.670	0.670	0.669	0.669	0.668	0.668
240.0	0.674	0.673	0.673	0.672	0.672	0.671	0.671	0.670	0.670	0.669	0.669	0.668
260.0	0.675	0.675	0.674	0.674	0.673	0.673	0.672	0.672	0.671	0.671	0.670	0.670
280.0	0.676	0.677	0.677	0.676	0.676	0.675	0.675	0.674	0.674	0.673	0.673	0.672
300.0	0.680	0.680	0.679	0.679	0.678	0.678	0.677	0.677	0.676	0.676	0.675	0.675

Table 4.2.8 $(P/\rho)(\partial\rho/\partial P)_T$. This is the dimensionless quantity, pressure times isothermal compressibility

PRES MM/H ² ATM	0.010	0.051	0.101	0.152	0.182	0.193	0.203	0.213	0.223	0.233	0.243	0.253
TEMP, K	0.100	0.500	1.000	1.500	1.800	1.900	2.000	2.100	2.200	2.300	2.400	2.500
3.0	1.059	0.010	0.010	0.024	0.020	0.029	0.030	0.032	0.033	0.034	0.035	0.036
3.5	1.039	0.014	0.024	0.033	0.037	0.039	0.040	0.041	0.042	0.044	0.045	0.046
4.0	1.028	1.208	0.041	0.051	0.056	0.057	0.059	0.060	0.061	0.062	0.064	0.065
4.2	1.025	1.173	0.055	0.065	0.070	0.071	0.072	0.073	0.074	0.075	0.076	0.077
4.4	1.022	1.140	1.536	0.090	0.092	0.093	0.093	0.094	0.095	0.095	0.096	0.096
4.6	1.020	1.127	1.406	0.146	0.136	0.134	0.132	0.130	0.129	0.128	0.127	0.126
4.8	1.018	1.112	1.325	2.051	0.256	0.236	0.221	0.210	0.201	0.193	0.187	0.182
5.0	1.016	1.099	1.269	1.686	2.657	4.079	0.659	0.512	0.429	0.376	0.339	0.311
5.1	1.016	1.093	1.247	1.586	2.168	2.643	3.786	1.757	0.942	0.679	0.546	0.466
5.2	1.015	1.088	1.220	1.511	1.914	2.172	2.599	3.483	7.155	2.621	1.192	0.820
5.3	1.014	1.083	1.212	1.453	1.755	1.923	2.161	2.533	3.205	4.857	12.296	2.809
5.4	1.014	1.079	1.197	1.407	1.644	1.764	1.922	2.138	2.454	2.963	3.980	5.799
5.5	1.013	1.075	1.184	1.368	1.561	1.653	1.767	1.912	2.105	2.370	2.757	3.346
5.6	1.013	1.071	1.172	1.336	1.497	1.570	1.657	1.764	1.896	2.065	2.286	2.581
5.7	1.012	1.068	1.162	1.308	1.445	1.505	1.575	1.657	1.755	1.875	2.021	2.204
5.8	1.012	1.064	1.152	1.285	1.403	1.453	1.510	1.576	1.653	1.743	1.849	1.976
5.9	1.011	1.061	1.144	1.264	1.368	1.410	1.459	1.513	1.575	1.646	1.727	1.821
6.0	1.011	1.059	1.136	1.246	1.338	1.375	1.416	1.462	1.513	1.571	1.636	1.709
6.2	1.010	1.054	1.122	1.215	1.289	1.318	1.349	1.383	1.421	1.462	1.506	1.555
6.4	1.009	1.049	1.110	1.190	1.251	1.275	1.299	1.326	1.355	1.386	1.419	1.455
6.6	1.008	1.045	1.100	1.170	1.221	1.241	1.261	1.282	1.305	1.330	1.356	1.383
6.8	1.008	1.042	1.092	1.153	1.197	1.213	1.230	1.248	1.267	1.287	1.307	1.329
7.0	1.007	1.039	1.084	1.138	1.177	1.190	1.205	1.220	1.236	1.252	1.270	1.287
7.5	1.006	1.032	1.068	1.110	1.138	1.150	1.169	1.180	1.191	1.191	1.203	1.214
8.0	1.005	1.027	1.057	1.090	1.111	1.119	1.126	1.134	1.142	1.151	1.159	1.167
8.5	1.004	1.023	1.047	1.074	1.091	1.097	1.103	1.109	1.116	1.122	1.128	1.135
9.0	1.004	1.020	1.040	1.062	1.076	1.081	1.086	1.091	1.096	1.101	1.106	1.111
9.5	1.003	1.017	1.034	1.053	1.064	1.068	1.072	1.076	1.080	1.084	1.088	1.092
10.0	1.003	1.014	1.030	1.045	1.055	1.058	1.061	1.065	1.068	1.071	1.075	1.078
11.0	1.002	1.011	1.022	1.034	1.041	1.043	1.046	1.048	1.051	1.053	1.055	1.058
12.0	1.002	1.008	1.017	1.026	1.031	1.033	1.035	1.036	1.038	1.040	1.042	1.044
13.0	1.001	1.006	1.013	1.020	1.024	1.025	1.026	1.028	1.029	1.030	1.032	1.033
14.0	1.001	1.005	1.010	1.015	1.018	1.019	1.020	1.021	1.022	1.023	1.024	1.025
15.0	1.001	1.004	1.008	1.012	1.014	1.015	1.015	1.016	1.017	1.018	1.018	1.019
16.0	1.001	1.003	1.006	1.009	1.010	1.011	1.012	1.012	1.013	1.013	1.014	1.014
17.0	1.000	1.002	1.004	1.006	1.008	1.008	1.009	1.009	1.009	1.010	1.010	1.011
18.0	1.000	1.002	1.003	1.005	1.006	1.006	1.006	1.006	1.007	1.007	1.007	1.008
19.0	1.000	1.001	1.002	1.003	1.004	1.004	1.004	1.004	1.005	1.005	1.005	1.005
20.0	1.000	1.001	1.001	1.002	1.002	1.003	1.003	1.003	1.003	1.003	1.003	1.003
25.0	1.000	1.000	0.999	0.999	0.998	0.998	0.998	0.998	0.998	0.998	0.998	0.998
30.0	1.000	0.999	0.998	0.997	0.997	0.997	0.996	0.996	0.996	0.996	0.996	0.995
35.0	1.000	0.999	0.998	0.997	0.996	0.996	0.996	0.995	0.995	0.995	0.995	0.995
40.0	1.000	0.999	0.998	0.997	0.996	0.996	0.995	0.995	0.995	0.995	0.994	0.994
45.0	1.000	0.999	0.998	0.997	0.996	0.996	0.995	0.995	0.995	0.995	0.994	0.994
50.0	1.000	0.999	0.998	0.997	0.996	0.996	0.995	0.995	0.995	0.995	0.995	0.994
60.0	1.000	0.999	0.998	0.997	0.996	0.996	0.996	0.996	0.996	0.995	0.995	0.995
80.0	1.000	0.999	0.998	0.997	0.997	0.997	0.997	0.996	0.996	0.996	0.996	0.996
100.0	1.000	0.999	0.999	0.998	0.997	0.997	0.997	0.997	0.997	0.997	0.997	0.996
120.0	1.000	0.999	0.999	0.998	0.998	0.998	0.998	0.997	0.997	0.997	0.997	0.997
140.0	1.000	0.999	0.999	0.998	0.998	0.998	0.998	0.998	0.998	0.998	0.997	0.997
160.0	1.000	1.000	0.999	0.999	0.998	0.998	0.998	0.998	0.998	0.998	0.998	0.998
180.0	1.000	1.000	0.999	0.999	0.998	0.998	0.998	0.998	0.998	0.998	0.998	0.998
200.0	1.000	1.000	0.999	0.999	0.999	0.999	0.999	0.998	0.998	0.998	0.998	0.998
220.0	1.000	1.000	0.999	0.999	0.999	0.999	0.999	0.999	0.999	0.999	0.998	0.998
240.0	1.000	1.000	0.999	0.999	0.999	0.999	0.999	0.999	0.999	0.999	0.999	0.998
260.0	1.000	1.000	0.999	0.999	0.999	0.999	0.999	0.999	0.999	0.999	0.999	0.999
280.0	1.000	1.000	0.999	0.999	0.999	0.999	0.999	0.999	0.999	0.999	0.999	0.999
300.0	1.000	1.000	1.000	0.999	0.999	0.999	0.999	0.999	0.999	0.999	0.999	0.999

Table 4.2.8 $(P/\rho)(\partial\rho/\partial P)_T$. This is the dimensionless quantity, pressure times isothermal compressibility (continued).

PRES MM/H ² ATM	0.263 2.600	0.274 2.700	0.284 2.800	0.294 2.900	0.304 3.000	0.355 3.500	0.405 4.000	0.456 4.500	0.507 5.000	0.557 5.500	0.608 6.000	0.659 6.500
TEMP, K												
3.0	0.037	0.038	0.039	0.039	0.040	0.045	0.046	0.052	0.055	0.058	0.061	0.063
3.5	0.047	0.048	0.049	0.050	0.051	0.055	0.059	0.063	0.066	0.069	0.072	0.074
4.0	0.066	0.067	0.068	0.069	0.070	0.074	0.078	0.081	0.084	0.086	0.089	0.091
4.2	0.078	0.079	0.080	0.081	0.082	0.085	0.089	0.091	0.094	0.096	0.098	0.100
4.4	0.097	0.097	0.098	0.098	0.099	0.101	0.103	0.105	0.106	0.108	0.109	0.110
4.6	0.126	0.125	0.125	0.124	0.124	0.123	0.122	0.122	0.122	0.123	0.123	0.123
4.8	0.177	0.173	0.170	0.167	0.164	0.155	0.150	0.146	0.143	0.142	0.140	0.140
5.0	0.290	0.273	0.260	0.248	0.239	0.207	0.190	0.179	0.172	0.166	0.162	0.159
5.1	0.412	0.373	0.343	0.320	0.301	0.245	0.217	0.200	0.189	0.181	0.175	0.171
5.2	0.644	0.541	0.473	0.424	0.388	0.290	0.246	0.221	0.206	0.195	0.187	0.181
5.3	1.369	0.957	0.747	0.623	0.541	0.356	0.286	0.250	0.228	0.213	0.202	0.195
5.4	6.381	2.733	1.550	1.091	0.855	0.455	0.340	0.286	0.255	0.235	0.220	0.210
5.5	4.215	4.932	4.195	2.526	1.640	0.611	0.413	0.332	0.287	0.260	0.241	0.227
5.6	2.977	3.468	3.890	3.073	3.237	0.874	0.516	0.390	0.327	0.290	0.265	0.247
5.7	2.432	2.710	3.020	3.282	3.357	1.330	0.664	0.467	0.376	0.325	0.292	0.269
5.8	2.127	2.305	2.507	2.716	2.890	1.971	0.881	0.569	0.438	0.368	0.324	0.295
5.9	1.930	2.055	2.195	2.345	2.493	2.376	1.183	0.704	0.515	0.419	0.362	0.324
6.0	1.792	1.885	1.988	2.099	2.214	2.395	1.536	0.888	0.612	0.481	0.407	0.359
6.2	1.609	1.668	1.731	1.799	1.870	2.153	1.932	1.324	0.877	0.647	0.521	0.443
6.4	1.493	1.534	1.577	1.623	1.672	1.982	1.916	1.631	1.199	0.872	0.675	0.559
6.6	1.412	1.442	1.475	1.508	1.543	1.720	1.805	1.688	1.433	1.117	0.866	0.697
6.8	1.352	1.376	1.401	1.427	1.453	1.591	1.686	1.668	1.512	1.308	1.059	0.860
7.0	1.306	1.325	1.345	1.366	1.387	1.496	1.585	1.601	1.521	1.379	1.205	1.016
7.5	1.227	1.239	1.252	1.265	1.278	1.346	1.408	1.448	1.447	1.399	1.319	1.223
8.0	1.176	1.185	1.194	1.203	1.212	1.259	1.303	1.338	1.354	1.346	1.312	1.258
8.5	1.141	1.148	1.155	1.161	1.168	1.202	1.235	1.262	1.281	1.285	1.274	1.247
9.0	1.116	1.121	1.126	1.131	1.137	1.163	1.188	1.210	1.226	1.234	1.233	1.228
9.5	1.097	1.101	1.105	1.109	1.113	1.134	1.153	1.171	1.185	1.194	1.196	1.191
10.0	1.081	1.085	1.088	1.092	1.095	1.112	1.128	1.142	1.154	1.162	1.166	1.165
11.0	1.068	1.063	1.065	1.067	1.070	1.081	1.092	1.102	1.110	1.117	1.121	1.122
12.0	1.045	1.047	1.049	1.050	1.052	1.061	1.068	1.075	1.082	1.086	1.090	1.092
13.0	1.034	1.036	1.037	1.038	1.040	1.046	1.051	1.057	1.061	1.065	1.068	1.069
14.0	1.026	1.027	1.028	1.029	1.030	1.035	1.039	1.043	1.046	1.049	1.051	1.052
15.0	1.020	1.021	1.021	1.022	1.023	1.026	1.029	1.032	1.034	1.036	1.038	1.039
16.0	1.015	1.015	1.016	1.016	1.017	1.019	1.022	1.024	1.026	1.027	1.028	1.029
17.0	1.011	1.011	1.012	1.012	1.012	1.014	1.016	1.017	1.019	1.020	1.020	1.021
18.0	1.008	1.008	1.008	1.009	1.009	1.010	1.011	1.012	1.013	1.014	1.014	1.014
19.0	1.005	1.006	1.006	1.006	1.006	1.007	1.008	1.008	1.009	1.009	1.009	1.009
20.0	1.003	1.003	1.004	1.004	1.004	1.004	1.005	1.005	1.005	1.005	1.005	1.005
25.0	0.998	0.997	0.997	0.997	0.997	0.997	0.996	0.995	0.995	0.994	0.993	0.992
30.0	0.995	0.995	0.995	0.995	0.994	0.994	0.993	0.992	0.991	0.990	0.989	0.988
35.0	0.994	0.994	0.994	0.994	0.993	0.993	0.992	0.991	0.990	0.989	0.988	0.987
40.0	0.994	0.994	0.994	0.993	0.993	0.992	0.991	0.990	0.989	0.988	0.987	0.986
45.0	0.994	0.994	0.994	0.993	0.993	0.992	0.991	0.990	0.989	0.988	0.987	0.986
50.0	0.994	0.994	0.994	0.993	0.993	0.992	0.991	0.990	0.989	0.988	0.987	0.986
60.0	0.995	0.994	0.994	0.994	0.994	0.993	0.992	0.991	0.990	0.989	0.988	0.987
80.0	0.995	0.995	0.995	0.995	0.995	0.994	0.993	0.992	0.991	0.991	0.990	0.989
100.0	0.996	0.996	0.996	0.996	0.996	0.995	0.994	0.993	0.993	0.992	0.991	0.991
120.0	0.997	0.997	0.997	0.996	0.996	0.995	0.994	0.993	0.994	0.993	0.993	0.992
140.0	0.997	0.997	0.997	0.997	0.997	0.996	0.995	0.994	0.995	0.994	0.994	0.993
160.0	0.998	0.997	0.997	0.997	0.997	0.997	0.996	0.995	0.995	0.995	0.994	0.994
180.0	0.998	0.998	0.998	0.998	0.997	0.997	0.997	0.996	0.996	0.995	0.995	0.995
200.0	0.998	0.998	0.998	0.998	0.998	0.997	0.997	0.997	0.996	0.996	0.996	0.995
220.0	0.998	0.998	0.998	0.998	0.998	0.998	0.997	0.997	0.997	0.996	0.996	0.996
240.0	0.998	0.998	0.998	0.998	0.998	0.998	0.998	0.997	0.997	0.997	0.996	0.996
260.0	0.999	0.998	0.998	0.998	0.998	0.998	0.998	0.997	0.997	0.997	0.997	0.996
280.0	0.999	0.999	0.999	0.998	0.998	0.998	0.998	0.997	0.997	0.997	0.997	0.997
300.0	0.999	0.999	0.999	0.999	0.999	0.998	0.998	0.998	0.998	0.997	0.997	0.997

Table 4.2.8 $(P/\rho)(\partial\rho/\partial P)_T$. This is the dimensionless quantity, pressure times isothermal compressibility (continued).

PRES MM/HG ATM TEMP, K	6.600 6.000	0.709 7.000	0.811 8.000	0.912 9.000	1.013 10.000	1.520 15.000	2.026 20.000	2.533 25.000	3.040 30.000	3.546 35.000	4.053 40.000	4.560 45.000
3.0	0.061	0.066	0.070	0.074	0.078	0.092	0.103	0.111	0.119	0.126	0.132	0.137
3.5	0.072	0.077	0.081	0.085	0.088	0.101	0.110	0.118	0.124	0.129	0.134	0.139
4.0	0.089	0.093	0.096	0.099	0.102	0.113	0.120	0.126	0.131	0.136	0.140	0.143
4.2	0.098	0.101	0.104	0.107	0.109	0.119	0.125	0.130	0.135	0.139	0.142	0.146
4.4	0.109	0.112	0.114	0.116	0.118	0.125	0.130	0.135	0.139	0.142	0.145	0.148
4.6	0.123	0.124	0.125	0.126	0.127	0.132	0.136	0.140	0.143	0.146	0.149	0.151
4.8	0.140	0.139	0.138	0.138	0.138	0.140	0.142	0.145	0.147	0.150	0.152	0.154
5.0	0.162	0.157	0.154	0.152	0.150	0.148	0.149	0.150	0.152	0.154	0.156	0.158
5.1	0.175	0.167	0.162	0.159	0.157	0.152	0.152	0.153	0.154	0.156	0.158	0.159
5.2	0.187	0.177	0.170	0.166	0.163	0.156	0.155	0.155	0.156	0.158	0.159	0.160
5.3	0.202	0.189	0.180	0.174	0.170	0.161	0.159	0.158	0.159	0.160	0.161	0.162
5.4	0.220	0.202	0.191	0.183	0.178	0.166	0.162	0.161	0.161	0.162	0.163	0.164
5.5	0.241	0.217	0.202	0.193	0.186	0.171	0.166	0.164	0.164	0.164	0.165	0.166
5.6	0.265	0.234	0.216	0.204	0.195	0.176	0.170	0.168	0.167	0.167	0.167	0.168
5.7	0.292	0.253	0.230	0.215	0.205	0.182	0.174	0.171	0.170	0.169	0.169	0.170
5.8	0.324	0.274	0.246	0.228	0.216	0.188	0.179	0.174	0.173	0.172	0.172	0.172
5.9	0.362	0.298	0.263	0.242	0.227	0.194	0.183	0.178	0.175	0.174	0.174	0.174
6.0	0.407	0.325	0.283	0.257	0.240	0.201	0.188	0.182	0.179	0.177	0.176	0.176
6.2	0.521	0.392	0.328	0.291	0.267	0.215	0.197	0.189	0.185	0.182	0.181	0.180
6.4	0.675	0.478	0.385	0.333	0.299	0.231	0.208	0.197	0.191	0.188	0.186	0.185
6.6	0.866	0.586	0.454	0.382	0.337	0.248	0.219	0.206	0.198	0.194	0.191	0.189
6.8	1.059	0.715	0.537	0.440	0.381	0.267	0.231	0.215	0.206	0.200	0.197	0.194
7.0	1.205	0.854	0.634	0.508	0.432	0.287	0.244	0.225	0.214	0.207	0.202	0.199
7.5	1.319	1.118	0.891	0.711	0.587	0.349	0.281	0.251	0.235	0.224	0.217	0.213
8.0	1.312	1.194	1.056	0.902	0.761	0.424	0.325	0.282	0.258	0.244	0.234	0.227
8.5	1.274	1.208	1.110	1.010	0.900	0.511	0.375	0.316	0.284	0.265	0.252	0.243
9.0	1.233	1.198	1.131	1.050	0.976	0.604	0.432	0.355	0.314	0.288	0.272	0.260
9.5	1.196	1.179	1.134	1.073	1.006	0.694	0.494	0.398	0.346	0.314	0.293	0.278
10.0	1.166	1.158	1.128	1.083	1.029	0.768	0.558	0.444	0.380	0.341	0.316	0.297
11.0	1.121	1.120	1.107	1.082	1.047	0.857	0.677	0.543	0.459	0.404	0.368	0.341
12.0	1.090	1.092	1.085	1.071	1.050	0.897	0.760	0.633	0.538	0.472	0.424	0.390
13.0	1.068	1.070	1.067	1.059	1.045	0.931	0.812	0.702	0.609	0.537	0.483	0.441
14.0	1.051	1.053	1.052	1.047	1.038	0.954	0.848	0.752	0.667	0.595	0.538	0.492
15.0	1.038	1.040	1.039	1.035	1.030	0.968	0.879	0.790	0.711	0.643	0.586	0.539
16.0	1.028	1.029	1.028	1.026	1.022	0.974	0.899	0.821	0.748	0.684	0.628	0.580
17.0	1.020	1.021	1.020	1.018	1.014	0.976	0.914	0.845	0.778	0.718	0.664	0.618
18.0	1.014	1.014	1.013	1.011	1.008	0.976	0.924	0.863	0.802	0.746	0.695	0.650
19.0	1.009	1.009	1.008	1.006	1.003	0.976	0.931	0.877	0.822	0.770	0.722	0.679
20.0	1.005	1.004	1.003	1.001	0.999	0.975	0.936	0.888	0.839	0.790	0.745	0.703
25.0	0.993	0.992	0.990	0.988	0.985	0.969	0.946	0.918	0.886	0.853	0.820	0.788
30.0	0.989	0.986	0.984	0.982	0.980	0.966	0.948	0.928	0.906	0.882	0.858	0.833
35.0	0.987	0.984	0.982	0.980	0.977	0.964	0.950	0.934	0.916	0.898	0.879	0.859
40.0	0.986	0.984	0.982	0.979	0.977	0.965	0.952	0.938	0.923	0.908	0.892	0.876
45.0	0.986	0.984	0.982	0.979	0.977	0.965	0.953	0.941	0.928	0.915	0.902	0.888
50.0	0.987	0.984	0.982	0.980	0.978	0.967	0.956	0.944	0.933	0.921	0.909	0.897
60.0	0.988	0.986	0.984	0.981	0.979	0.969	0.960	0.950	0.940	0.930	0.920	0.910
80.0	0.990	0.988	0.986	0.985	0.983	0.975	0.967	0.958	0.951	0.943	0.935	0.927
100.0	0.991	0.990	0.988	0.987	0.986	0.979	0.972	0.965	0.959	0.952	0.945	0.939
120.0	0.993	0.991	0.990	0.989	0.988	0.982	0.976	0.970	0.965	0.959	0.953	0.948
140.0	0.994	0.993	0.992	0.990	0.989	0.984	0.979	0.974	0.969	0.964	0.959	0.955
160.0	0.994	0.993	0.993	0.992	0.991	0.986	0.982	0.977	0.973	0.968	0.964	0.960
180.0	0.995	0.994	0.993	0.993	0.992	0.988	0.984	0.980	0.976	0.972	0.968	0.964
200.0	0.996	0.995	0.994	0.993	0.993	0.989	0.985	0.982	0.978	0.975	0.971	0.968
220.0	0.996	0.995	0.995	0.994	0.993	0.990	0.987	0.983	0.980	0.977	0.974	0.971
240.0	0.996	0.996	0.995	0.994	0.994	0.991	0.988	0.985	0.982	0.979	0.976	0.973
260.0	0.997	0.996	0.995	0.995	0.994	0.992	0.989	0.986	0.983	0.981	0.978	0.975
280.0	0.997	0.996	0.996	0.995	0.995	0.992	0.990	0.987	0.985	0.982	0.980	0.977
300.0	0.997	0.997	0.996	0.996	0.995	0.993	0.990	0.988	0.986	0.984	0.981	0.979

Table 4.2.8 $(P/\rho) (\partial \rho / \partial P)_T$. This is the dimensionless quantity, pressure times isothermal compressibility (continued).

PRES MM/HG ATM	5.066 50.000	5.573 55.000	6.079 60.000	6.586 65.000	7.093 70.000	7.599 75.000	8.106 80.000	8.613 85.000	9.119 90.000	9.626 95.000	10.133 100.000	10.639 105.000
TEMP, K												
3.0	0.143	0.140	0.153	0.158	0.163	0.168						
3.5	0.143	0.147	0.151	0.154	0.158	0.161	0.164	0.168	0.171	0.174	0.177	
4.0	0.146	0.150	0.152	0.155	0.158	0.160	0.163	0.165	0.168	0.170	0.172	0.174
4.2	0.148	0.151	0.154	0.156	0.159	0.161	0.163	0.166	0.168	0.170	0.172	0.174
4.4	0.151	0.153	0.156	0.158	0.160	0.162	0.164	0.166	0.168	0.170	0.172	0.174
4.6	0.153	0.156	0.158	0.160	0.162	0.164	0.166	0.167	0.169	0.171	0.172	0.174
4.8	0.156	0.158	0.160	0.162	0.164	0.165	0.167	0.169	0.170	0.172	0.173	0.174
5.0	0.159	0.161	0.163	0.164	0.166	0.167	0.169	0.170	0.171	0.173	0.174	0.175
5.1	0.161	0.162	0.164	0.165	0.167	0.168	0.169	0.171	0.172	0.173	0.175	0.176
5.2	0.162	0.163	0.165	0.166	0.167	0.169	0.170	0.171	0.173	0.174	0.175	0.176
5.3	0.163	0.165	0.166	0.167	0.169	0.170	0.171	0.172	0.173	0.175	0.176	0.177
5.4	0.165	0.166	0.167	0.169	0.170	0.171	0.172	0.173	0.174	0.175	0.176	0.177
5.5	0.167	0.168	0.169	0.170	0.171	0.172	0.173	0.174	0.175	0.176	0.177	0.178
5.6	0.169	0.169	0.170	0.171	0.172	0.173	0.174	0.175	0.176	0.177	0.178	0.179
5.7	0.170	0.171	0.172	0.173	0.174	0.175	0.176	0.177	0.178	0.179	0.180	0.181
5.8	0.172	0.173	0.173	0.174	0.175	0.176	0.177	0.178	0.179	0.180	0.181	0.182
5.9	0.174	0.174	0.175	0.176	0.177	0.178	0.179	0.180	0.181	0.182	0.183	0.184
6.0	0.176	0.176	0.177	0.178	0.179	0.180	0.181	0.182	0.183	0.184	0.185	0.186
6.2	0.180	0.180	0.180	0.180	0.181	0.181	0.181	0.182	0.182	0.183	0.184	0.185
6.4	0.184	0.183	0.183	0.183	0.184	0.184	0.184	0.184	0.185	0.185	0.186	0.186
6.6	0.188	0.187	0.187	0.187	0.187	0.187	0.187	0.187	0.187	0.188	0.188	0.188
6.8	0.192	0.191	0.191	0.190	0.190	0.190	0.190	0.190	0.190	0.190	0.190	0.191
7.0	0.197	0.195	0.194	0.194	0.193	0.193	0.193	0.192	0.192	0.193	0.193	0.193
7.5	0.209	0.206	0.204	0.203	0.202	0.201	0.200	0.200	0.199	0.199	0.199	0.199
8.0	0.222	0.218	0.215	0.213	0.211	0.210	0.208	0.207	0.206	0.206	0.206	0.205
8.5	0.236	0.231	0.227	0.224	0.221	0.219	0.217	0.216	0.214	0.213	0.213	0.212
9.0	0.251	0.244	0.239	0.235	0.231	0.229	0.226	0.224	0.223	0.221	0.220	0.219
9.5	0.267	0.259	0.252	0.247	0.242	0.239	0.236	0.233	0.231	0.229	0.228	0.226
10.0	0.284	0.274	0.266	0.259	0.254	0.249	0.246	0.243	0.240	0.238	0.236	0.234
11.0	0.322	0.307	0.296	0.287	0.279	0.273	0.267	0.263	0.259	0.255	0.253	0.250
12.0	0.365	0.345	0.329	0.317	0.306	0.298	0.291	0.284	0.279	0.275	0.271	0.267
13.0	0.410	0.385	0.365	0.349	0.336	0.325	0.316	0.308	0.301	0.295	0.290	0.285
14.0	0.456	0.427	0.403	0.384	0.368	0.354	0.342	0.333	0.324	0.317	0.310	0.304
15.0	0.500	0.468	0.441	0.419	0.400	0.384	0.370	0.359	0.348	0.339	0.332	0.325
16.0	0.540	0.506	0.477	0.452	0.432	0.414	0.398	0.385	0.373	0.363	0.354	0.345
17.0	0.577	0.542	0.511	0.485	0.463	0.443	0.426	0.411	0.398	0.386	0.376	0.367
18.0	0.610	0.575	0.544	0.517	0.493	0.472	0.453	0.437	0.423	0.410	0.398	0.388
19.0	0.640	0.605	0.574	0.546	0.521	0.499	0.480	0.463	0.447	0.433	0.421	0.410
20.0	0.666	0.632	0.601	0.573	0.548	0.526	0.505	0.487	0.471	0.456	0.443	0.431
25.0	0.758	0.729	0.702	0.677	0.654	0.632	0.611	0.592	0.575	0.558	0.543	0.529
30.0	0.809	0.786	0.763	0.742	0.722	0.702	0.684	0.666	0.650	0.634	0.619	0.605
35.0	0.840	0.821	0.802	0.784	0.766	0.749	0.733	0.718	0.703	0.688	0.675	0.661
40.0	0.860	0.844	0.828	0.813	0.797	0.782	0.768	0.754	0.741	0.728	0.715	0.703
45.0	0.874	0.860	0.847	0.833	0.820	0.807	0.794	0.781	0.769	0.757	0.746	0.735
50.0	0.885	0.872	0.860	0.848	0.836	0.825	0.813	0.802	0.791	0.780	0.770	0.760
60.0	0.900	0.890	0.880	0.870	0.860	0.851	0.841	0.832	0.823	0.814	0.805	0.796
80.0	0.920	0.912	0.905	0.897	0.890	0.882	0.875	0.868	0.861	0.854	0.847	0.840
100.0	0.933	0.927	0.920	0.914	0.908	0.902	0.896	0.890	0.885	0.879	0.873	0.868
120.0	0.942	0.937	0.932	0.927	0.921	0.916	0.911	0.906	0.901	0.896	0.892	0.887
140.0	0.950	0.945	0.941	0.936	0.932	0.927	0.923	0.918	0.914	0.910	0.905	0.901
160.0	0.956	0.952	0.948	0.943	0.939	0.936	0.932	0.928	0.924	0.920	0.916	0.912
180.0	0.961	0.957	0.953	0.950	0.946	0.942	0.939	0.935	0.932	0.928	0.925	0.922
200.0	0.964	0.961	0.958	0.954	0.951	0.948	0.945	0.942	0.938	0.935	0.932	0.929
220.0	0.968	0.965	0.962	0.959	0.956	0.953	0.950	0.947	0.944	0.941	0.938	0.935
240.0	0.970	0.968	0.965	0.962	0.959	0.957	0.954	0.951	0.949	0.946	0.943	0.941
260.0	0.973	0.970	0.968	0.965	0.963	0.960	0.958	0.955	0.953	0.950	0.948	0.946
280.0	0.975	0.973	0.970	0.968	0.965	0.963	0.961	0.959	0.956	0.954	0.952	0.950
300.0	0.977	0.974	0.972	0.970	0.968	0.966	0.964	0.961	0.959	0.957	0.955	0.953

THIS PAGE IS BEST QUALITY PRACTICABLE
FROM COPY FURNISHED TO DDC

Table 4.2.9 $-(T/\rho) (\partial \rho / \partial T)_P$. This is the dimensionless quantity, temperature times bulk expansivity.

PRES MM/H ² ATM TEMP, K	0.010 0.100	0.051 0.500	0.101 1.000	0.152 1.500	0.162 1.800	0.193 1.900	0.203 2.000	0.213 2.100	0.223 2.200	0.233 2.300	0.243 2.400	0.253 2.500
3.0	1.132	0.197	0.103	0.170	0.163	0.161	0.159	0.157	0.155	0.154	0.152	0.150
3.5	1.088	0.359	0.323	0.295	0.281	0.277	0.273	0.269	0.265	0.261	0.257	0.254
4.0	1.063	1.483	0.612	0.529	0.492	0.480	0.470	0.460	0.451	0.442	0.433	0.425
4.2	1.056	1.402	0.847	0.696	0.633	0.615	0.599	0.583	0.569	0.555	0.542	0.530
4.4	1.050	1.342	2.294	0.969	0.849	0.817	0.780	0.762	0.737	0.714	0.694	0.674
4.6	1.046	1.296	1.975	1.530	1.236	1.166	1.105	1.052	1.004	0.962	0.924	0.889
4.8	1.041	1.260	1.779	1.639	2.203	1.964	1.780	1.633	1.514	1.413	1.320	1.255
5.0	1.038	1.230	1.645	2.705	5.310	9.336	4.696	3.606	2.975	2.559	2.260	2.034
5.1	1.036	1.217	1.593	2.452	4.802	5.319	8.609	10.864	5.936	4.281	3.422	2.885
5.2	1.034	1.206	1.548	2.265	3.331	4.037	5.238	7.633	19.487	13.807	6.631	4.640
5.3	1.033	1.195	1.508	2.120	2.914	3.370	4.032	5.096	7.109	12.438	43.000	13.368
5.4	1.032	1.185	1.474	2.004	2.626	2.950	3.384	3.994	4.917	6.473	9.558	16.872
5.5	1.030	1.176	1.443	1.908	2.413	2.660	2.971	3.377	3.929	4.719	5.926	7.914
5.6	1.029	1.168	1.416	1.829	2.250	2.445	2.682	2.977	3.352	3.846	4.516	5.460
5.7	1.028	1.160	1.391	1.761	2.119	2.278	2.467	2.693	2.959	3.313	3.750	4.316
5.8	1.027	1.153	1.369	1.703	2.012	2.146	2.300	2.481	2.694	2.951	3.263	3.647
5.9	1.026	1.146	1.349	1.652	1.923	2.037	2.166	2.315	2.487	2.687	2.924	3.205
6.0	1.025	1.140	1.330	1.608	1.848	1.946	2.057	2.182	2.323	2.486	2.673	2.889
6.2	1.023	1.129	1.298	1.534	1.727	1.803	1.887	1.980	2.083	2.197	2.324	2.467
6.4	1.022	1.119	1.271	1.474	1.634	1.695	1.762	1.835	1.913	1.999	2.093	2.195
6.6	1.020	1.110	1.247	1.425	1.560	1.611	1.666	1.724	1.787	1.854	1.927	2.005
6.8	1.019	1.102	1.227	1.384	1.500	1.544	1.589	1.638	1.689	1.744	1.802	1.864
7.0	1.018	1.095	1.209	1.350	1.451	1.488	1.527	1.568	1.611	1.657	1.705	1.756
7.5	1.015	1.081	1.174	1.283	1.358	1.385	1.412	1.441	1.471	1.503	1.535	1.569
8.0	1.013	1.069	1.147	1.234	1.293	1.313	1.335	1.356	1.379	1.402	1.425	1.450
8.5	1.012	1.060	1.125	1.198	1.245	1.261	1.278	1.295	1.313	1.331	1.349	1.368
9.0	1.010	1.052	1.109	1.170	1.209	1.222	1.236	1.250	1.264	1.278	1.293	1.308
9.5	1.009	1.046	1.095	1.147	1.180	1.191	1.203	1.214	1.226	1.238	1.250	1.262
10.0	1.008	1.041	1.084	1.129	1.157	1.166	1.176	1.186	1.196	1.206	1.216	1.226
11.0	1.006	1.033	1.067	1.102	1.124	1.131	1.138	1.146	1.153	1.161	1.168	1.176
12.0	1.005	1.027	1.054	1.082	1.100	1.105	1.111	1.117	1.123	1.129	1.135	1.141
13.0	1.004	1.022	1.045	1.068	1.082	1.086	1.091	1.096	1.101	1.105	1.110	1.115
14.0	1.004	1.018	1.037	1.056	1.068	1.072	1.075	1.079	1.083	1.087	1.091	1.095
15.0	1.003	1.015	1.031	1.047	1.057	1.060	1.063	1.066	1.070	1.073	1.076	1.079
16.0	1.003	1.013	1.026	1.040	1.048	1.050	1.053	1.056	1.058	1.061	1.064	1.067
17.0	1.002	1.011	1.022	1.034	1.040	1.043	1.045	1.047	1.049	1.052	1.054	1.056
18.0	1.002	1.009	1.019	1.029	1.034	1.036	1.038	1.040	1.042	1.044	1.046	1.048
19.0	1.002	1.008	1.016	1.025	1.030	1.031	1.033	1.034	1.036	1.038	1.039	1.041
20.0	1.001	1.007	1.014	1.021	1.025	1.027	1.028	1.030	1.031	1.032	1.034	1.035
25.0	1.001	1.003	1.007	1.010	1.012	1.013	1.014	1.015	1.015	1.016	1.017	1.017
30.0	1.000	1.002	1.003	1.005	1.006	1.006	1.007	1.007	1.007	1.008	1.008	1.008
35.0	1.000	1.001	1.002	1.002	1.003	1.003	1.003	1.003	1.003	1.003	1.004	1.004
40.0	1.000	1.000	1.000	1.001	1.001	1.001	1.001	1.001	1.001	1.001	1.001	1.001
45.0	1.000	1.000	1.000	1.000	1.000	0.999	0.999	0.999	0.999	0.999	0.999	0.999
50.0	1.000	1.000	0.999	0.999	0.999	0.999	0.999	0.999	0.999	0.999	0.998	0.998
60.0	1.000	0.999	0.999	0.998	0.998	0.998	0.998	0.998	0.998	0.997	0.997	0.997
80.0	1.000	0.999	0.999	0.998	0.998	0.998	0.997	0.997	0.997	0.997	0.997	0.997
100.0	1.000	0.999	0.999	0.998	0.998	0.998	0.998	0.997	0.997	0.997	0.997	0.997
120.0	1.000	0.999	0.999	0.998	0.998	0.998	0.998	0.998	0.997	0.997	0.997	0.997
140.0	1.000	0.999	0.999	0.998	0.998	0.998	0.998	0.998	0.998	0.998	0.998	0.997
160.0	1.000	1.000	0.999	0.998	0.998	0.998	0.998	0.998	0.998	0.998	0.998	0.998
180.0	1.000	1.000	0.999	0.999	0.998	0.998	0.998	0.998	0.998	0.998	0.998	0.998
200.0	1.000	1.000	0.999	0.999	0.999	0.999	0.999	0.998	0.998	0.998	0.998	0.998
220.0	1.000	1.000	0.999	0.999	0.999	0.999	0.999	0.998	0.998	0.998	0.998	0.998
240.0	1.000	1.000	0.999	0.999	0.999	0.999	0.999	0.999	0.999	0.998	0.998	0.998
260.0	1.000	1.000	0.999	0.999	0.999	0.999	0.999	0.999	0.999	0.999	0.999	0.998
280.0	1.000	1.000	0.999	0.999	0.999	0.999	0.999	0.999	0.999	0.999	0.999	0.999
300.0	1.000	1.000	0.999	0.999	0.999	0.999	0.999	0.999	0.999	0.999	0.999	0.999

Table 4.2.9 $-(T/\rho)(\partial\rho/\partial T)_P$. This is the dimensionless quantity, temperature times bulk expansivity (continued).

PRES MM/H ² ATM TEMP, K	0.263 2.600	0.274 2.700	0.284 2.800	0.294 2.900	0.304 3.000	0.355 3.500	0.405 4.000	0.456 4.500	0.507 5.000	0.557 5.500	0.608 6.000	0.659 6.500
3.0	0.148	0.147	0.145	0.143	0.142	0.135	0.128	0.122	0.117	0.112	0.108	0.104
3.5	0.250	0.247	0.244	0.241	0.238	0.224	0.212	0.202	0.192	0.184	0.176	0.169
4.0	0.417	0.410	0.403	0.396	0.390	0.361	0.337	0.316	0.299	0.283	0.270	0.258
4.2	0.518	0.508	0.497	0.488	0.478	0.437	0.404	0.377	0.354	0.334	0.316	0.301
4.4	0.656	0.639	0.623	0.608	0.594	0.534	0.488	0.450	0.419	0.393	0.370	0.351
4.6	0.858	0.829	0.802	0.778	0.755	0.663	0.594	0.541	0.498	0.463	0.433	0.408
4.8	1.191	1.134	1.084	1.038	0.998	0.841	0.734	0.655	0.595	0.547	0.507	0.474
5.0	1.856	1.712	1.592	1.491	1.405	1.106	0.926	0.806	0.717	0.649	0.595	0.551
5.1	2.515	2.242	2.031	1.862	1.724	1.286	1.047	0.895	0.787	0.707	0.644	0.593
5.2	3.659	3.062	2.656	2.359	2.132	1.486	1.173	0.984	0.856	0.762	0.690	0.633
5.3	7.038	4.967	3.916	3.271	2.831	1.775	1.343	1.100	0.943	0.831	0.747	0.681
5.4	23.812	11.900	7.226	5.236	4.157	2.190	1.562	1.242	1.045	0.910	0.811	0.735
5.5	11.277	15.439	15.426	10.339	7.100	2.806	1.846	1.415	1.155	1.001	0.883	0.794
5.6	6.828	8.763	11.016	12.386	11.551	3.765	2.225	1.628	1.307	1.105	0.964	0.860
5.7	5.063	6.049	7.299	8.674	9.753	5.242	2.738	1.894	1.476	1.225	1.056	0.933
5.8	4.125	4.722	5.458	6.326	7.243	6.908	3.429	2.229	1.679	1.364	1.159	1.015
5.9	3.541	3.945	4.428	4.993	5.627	7.301	4.289	2.647	1.921	1.526	1.277	1.106
6.0	3.141	3.435	3.778	4.172	4.617	6.529	5.115	3.149	2.210	1.714	1.411	1.208
6.2	2.626	2.806	3.007	3.231	3.480	4.897	5.356	4.174	2.914	2.175	1.735	1.449
6.4	2.307	2.430	2.565	2.712	2.871	3.821	4.551	4.462	3.580	2.718	2.130	1.743
6.6	2.089	2.180	2.277	2.382	2.494	3.158	3.809	4.062	3.824	3.184	2.552	2.078
6.8	1.930	2.000	2.075	2.154	2.239	2.726	3.249	3.592	3.622	3.366	2.887	2.409
7.0	1.809	1.866	1.925	1.988	2.053	2.428	2.842	3.173	3.320	3.261	3.027	2.658
7.5	1.604	1.640	1.678	1.717	1.757	1.979	2.225	2.465	2.652	2.749	2.754	2.690
8.0	1.475	1.501	1.527	1.554	1.582	1.732	1.894	2.059	2.208	2.322	2.387	2.403
8.5	1.387	1.406	1.426	1.446	1.467	1.576	1.692	1.811	1.924	2.022	2.096	2.148
9.0	1.323	1.338	1.354	1.369	1.385	1.469	1.557	1.647	1.734	1.814	1.881	1.931
9.5	1.274	1.287	1.299	1.312	1.325	1.392	1.461	1.531	1.600	1.665	1.723	1.778
10.0	1.236	1.247	1.257	1.268	1.278	1.333	1.389	1.446	1.502	1.555	1.604	1.646
11.0	1.184	1.191	1.199	1.207	1.215	1.254	1.294	1.334	1.373	1.411	1.446	1.478
12.0	1.147	1.153	1.159	1.165	1.171	1.201	1.231	1.262	1.291	1.319	1.346	1.371
13.0	1.120	1.124	1.129	1.134	1.139	1.163	1.187	1.211	1.234	1.256	1.277	1.297
14.0	1.099	1.103	1.107	1.111	1.115	1.134	1.154	1.173	1.191	1.209	1.227	1.243
15.0	1.083	1.086	1.089	1.093	1.096	1.112	1.128	1.144	1.159	1.174	1.188	1.202
16.0	1.069	1.072	1.075	1.077	1.080	1.093	1.107	1.120	1.132	1.145	1.157	1.168
17.0	1.059	1.061	1.063	1.065	1.068	1.079	1.090	1.101	1.111	1.122	1.132	1.141
18.0	1.050	1.052	1.054	1.056	1.057	1.067	1.076	1.085	1.094	1.103	1.112	1.120
19.0	1.043	1.044	1.046	1.047	1.049	1.057	1.065	1.073	1.081	1.088	1.095	1.102
20.0	1.037	1.038	1.039	1.041	1.042	1.049	1.056	1.063	1.069	1.075	1.082	1.088
25.0	1.018	1.019	1.019	1.020	1.021	1.024	1.027	1.030	1.034	1.037	1.040	1.043
30.0	1.009	1.009	1.009	1.010	1.010	1.012	1.013	1.015	1.016	1.018	1.019	1.021
35.0	1.004	1.004	1.004	1.004	1.004	1.005	1.006	1.007	1.007	1.008	1.008	1.009
40.0	1.001	1.001	1.001	1.001	1.001	1.001	1.002	1.002	1.002	1.002	1.002	1.002
45.0	0.999	0.999	0.999	0.999	0.999	0.999	0.999	0.999	0.999	0.999	0.998	0.998
50.0	0.998	0.998	0.998	0.998	0.998	0.998	0.997	0.997	0.997	0.997	0.996	0.996
60.0	0.997	0.997	0.997	0.997	0.997	0.996	0.996	0.996	0.995	0.994	0.993	0.993
80.0	0.997	0.997	0.996	0.996	0.996	0.995	0.995	0.994	0.994	0.993	0.992	0.992
100.0	0.997	0.997	0.997	0.996	0.996	0.996	0.995	0.994	0.994	0.993	0.993	0.992
120.0	0.997	0.997	0.997	0.997	0.997	0.996	0.995	0.995	0.994	0.994	0.993	0.993
140.0	0.997	0.997	0.997	0.997	0.997	0.996	0.996	0.995	0.995	0.994	0.994	0.993
160.0	0.998	0.997	0.997	0.997	0.997	0.997	0.996	0.996	0.995	0.995	0.994	0.994
180.0	0.998	0.998	0.998	0.998	0.997	0.997	0.997	0.996	0.996	0.995	0.995	0.994
200.0	0.998	0.998	0.998	0.998	0.998	0.997	0.997	0.996	0.996	0.996	0.996	0.995
220.0	0.998	0.998	0.998	0.998	0.998	0.997	0.997	0.997	0.996	0.996	0.996	0.996
240.0	0.998	0.998	0.998	0.998	0.998	0.998	0.997	0.997	0.997	0.996	0.996	0.996
260.0	0.998	0.998	0.998	0.998	0.998	0.998	0.998	0.997	0.997	0.997	0.996	0.996
280.0	0.999	0.998	0.998	0.998	0.998	0.998	0.998	0.997	0.997	0.997	0.997	0.996
300.0	0.999	0.999	0.998	0.998	0.998	0.998	0.998	0.998	0.997	0.997	0.997	0.997

Table 4.2.9 $-(T/\rho) (\partial \rho / \partial T)_P$. This is the dimensionless quantity, temperature times bulk expansivity (continued).

PRES MN/M ATM TEMP, K	0.608 6.000	0.709 7.000	0.811 8.000	0.912 9.000	1.013 10.000	1.120 15.000	1.226 20.000	1.333 25.000	1.440 30.000	1.546 35.000	1.653 40.000	1.760 45.000
3.0	0.108	0.100	0.093	0.087	0.082	0.064	0.053	0.047	0.043	0.041	0.040	0.041
3.5	0.176	0.163	0.152	0.142	0.134	0.105	0.088	0.077	0.069	0.064	0.061	0.058
4.0	0.270	0.247	0.228	0.212	0.199	0.154	0.128	0.111	0.099	0.091	0.084	0.079
4.2	0.316	0.287	0.264	0.245	0.229	0.176	0.145	0.126	0.112	0.101	0.094	0.088
4.4	0.370	0.333	0.304	0.281	0.262	0.198	0.163	0.140	0.124	0.112	0.103	0.096
4.6	0.433	0.386	0.349	0.321	0.297	0.222	0.181	0.155	0.137	0.123	0.113	0.105
4.8	0.507	0.446	0.400	0.364	0.335	0.247	0.200	0.170	0.150	0.134	0.123	0.114
5.0	0.595	0.514	0.456	0.412	0.377	0.273	0.219	0.185	0.162	0.146	0.133	0.122
5.1	0.644	0.551	0.486	0.437	0.399	0.286	0.228	0.193	0.169	0.151	0.137	0.127
5.2	0.690	0.586	0.514	0.461	0.419	0.298	0.237	0.200	0.175	0.156	0.142	0.131
5.3	0.747	0.628	0.547	0.488	0.442	0.311	0.247	0.208	0.181	0.162	0.147	0.135
5.4	0.811	0.674	0.583	0.517	0.467	0.325	0.257	0.216	0.188	0.167	0.152	0.139
5.5	0.883	0.724	0.621	0.548	0.493	0.340	0.267	0.224	0.194	0.173	0.157	0.144
5.6	0.964	0.780	0.663	0.581	0.520	0.355	0.278	0.232	0.201	0.179	0.162	0.148
5.7	1.056	0.840	0.707	0.616	0.549	0.370	0.289	0.240	0.208	0.184	0.167	0.153
5.8	1.159	0.907	0.756	0.654	0.580	0.386	0.300	0.249	0.215	0.190	0.172	0.157
5.9	1.277	0.981	0.808	0.694	0.613	0.403	0.311	0.257	0.222	0.196	0.177	0.162
6.0	1.411	1.062	0.865	0.737	0.647	0.420	0.322	0.266	0.229	0.202	0.182	0.166
6.2	1.735	1.251	0.993	0.833	0.723	0.456	0.346	0.284	0.244	0.215	0.193	0.176
6.4	2.130	1.478	1.144	0.942	0.807	0.495	0.372	0.303	0.259	0.227	0.204	0.186
6.6	2.552	1.742	1.317	1.066	0.903	0.537	0.398	0.323	0.274	0.241	0.215	0.196
6.8	2.887	2.025	1.511	1.206	1.008	0.582	0.426	0.343	0.291	0.254	0.227	0.206
7.0	3.027	2.287	1.717	1.358	1.124	0.629	0.455	0.364	0.307	0.268	0.239	0.216
7.5	2.754	2.563	2.152	1.749	1.443	0.762	0.535	0.421	0.352	0.304	0.270	0.243
8.0	2.387	2.379	2.251	2.005	1.727	0.913	0.624	0.483	0.399	0.343	0.303	0.272
8.5	2.096	2.155	2.116	2.028	1.870	1.071	0.721	0.551	0.451	0.385	0.338	0.303
9.0	1.881	1.961	1.969	1.923	1.860	1.220	0.823	0.622	0.506	0.429	0.375	0.335
9.5	1.723	1.804	1.835	1.821	1.777	1.339	0.926	0.698	0.563	0.476	0.414	0.368
10.0	1.684	1.688	1.728	1.725	1.702	1.413	1.022	0.774	0.623	0.524	0.454	0.403
11.0	1.446	1.506	1.547	1.567	1.567	1.428	1.163	0.917	0.743	0.624	0.538	0.475
12.0	1.346	1.394	1.430	1.453	1.463	1.376	1.220	1.021	0.851	0.721	0.624	0.550
13.0	1.277	1.316	1.347	1.370	1.384	1.343	1.220	1.079	0.932	0.806	0.704	0.623
14.0	1.227	1.259	1.286	1.307	1.322	1.312	1.220	1.105	0.983	0.870	0.772	0.690
15.0	1.188	1.215	1.238	1.258	1.273	1.283	1.215	1.117	1.013	0.914	0.824	0.746
16.0	1.157	1.179	1.199	1.216	1.230	1.249	1.203	1.124	1.036	0.949	0.868	0.793
17.0	1.132	1.151	1.168	1.182	1.195	1.219	1.188	1.125	1.051	0.975	0.901	0.832
18.0	1.112	1.128	1.142	1.155	1.166	1.192	1.171	1.122	1.059	0.993	0.926	0.864
19.0	1.095	1.109	1.121	1.133	1.143	1.168	1.155	1.116	1.063	1.005	0.945	0.888
20.0	1.082	1.093	1.104	1.114	1.123	1.147	1.139	1.108	1.064	1.012	0.960	0.907
25.0	1.040	1.045	1.051	1.056	1.060	1.075	1.076	1.066	1.045	1.018	0.987	0.955
30.0	1.019	1.022	1.025	1.027	1.029	1.037	1.038	1.032	1.021	1.005	0.986	0.964
35.0	1.008	1.010	1.011	1.012	1.013	1.015	1.014	1.010	1.002	0.991	0.978	0.962
40.0	1.002	1.002	1.003	1.003	1.003	1.002	0.999	0.995	0.988	0.979	0.969	0.958
45.0	0.998	0.998	0.998	0.997	0.997	0.994	0.990	0.985	0.979	0.971	0.962	0.953
50.0	0.996	0.995	0.994	0.994	0.993	0.989	0.984	0.979	0.972	0.965	0.958	0.949
60.0	0.993	0.992	0.991	0.990	0.989	0.984	0.978	0.972	0.966	0.959	0.952	0.945
80.0	0.992	0.991	0.990	0.989	0.987	0.981	0.975	0.969	0.963	0.957	0.950	0.944
100.0	0.993	0.991	0.990	0.989	0.988	0.982	0.976	0.970	0.964	0.959	0.953	0.947
120.0	0.993	0.992	0.991	0.990	0.989	0.983	0.978	0.973	0.967	0.962	0.957	0.952
140.0	0.994	0.993	0.992	0.991	0.990	0.985	0.980	0.975	0.970	0.965	0.961	0.956
160.0	0.994	0.993	0.993	0.992	0.991	0.986	0.982	0.977	0.973	0.968	0.964	0.960
180.0	0.995	0.994	0.993	0.992	0.992	0.987	0.983	0.979	0.975	0.971	0.967	0.963
200.0	0.995	0.995	0.994	0.993	0.992	0.988	0.985	0.981	0.977	0.974	0.970	0.966
220.0	0.996	0.995	0.994	0.994	0.993	0.989	0.986	0.982	0.979	0.976	0.972	0.969
240.0	0.996	0.995	0.995	0.994	0.993	0.990	0.987	0.984	0.981	0.977	0.974	0.971
260.0	0.996	0.996	0.995	0.994	0.994	0.991	0.988	0.985	0.982	0.979	0.976	0.973
280.0	0.997	0.996	0.995	0.995	0.994	0.991	0.989	0.986	0.983	0.980	0.978	0.975
300.0	0.997	0.996	0.996	0.995	0.995	0.992	0.989	0.987	0.984	0.982	0.979	0.977

Table 4.2.9 $-(T/\rho) (\partial \rho / \partial T)_P$. This is the dimensionless quantity,
temperature times bulk expansivity (continued).

PRES MM/H ATM TEMP, K	5.066 50.000	5.573 55.000	6.079 60.000	6.586 65.000	7.093 70.000	7.599 75.000	8.106 80.000	8.613 85.000	9.119 90.000	9.626 95.000	10.133 100.000	10.639 105.000
3.0	0.042	0.044	0.047	0.051	0.055	0.061						
3.5	0.057	0.056	0.056	0.057	0.058	0.059	0.061	0.064	0.066	0.069	0.073	
4.0	0.075	0.073	0.070	0.069	0.068	0.067	0.067	0.068	0.068	0.069	0.070	0.071
4.2	0.083	0.079	0.077	0.074	0.073	0.072	0.071	0.070	0.070	0.070	0.071	0.071
4.4	0.091	0.086	0.083	0.080	0.078	0.076	0.075	0.074	0.073	0.072	0.072	0.072
4.6	0.099	0.093	0.089	0.086	0.083	0.080	0.079	0.077	0.076	0.075	0.074	0.074
4.8	0.106	0.100	0.095	0.091	0.088	0.085	0.083	0.081	0.079	0.077	0.076	0.075
5.0	0.114	0.107	0.102	0.097	0.093	0.090	0.087	0.084	0.082	0.080	0.079	0.078
5.1	0.118	0.111	0.105	0.100	0.096	0.092	0.089	0.086	0.084	0.082	0.080	0.079
5.2	0.122	0.114	0.108	0.103	0.098	0.094	0.091	0.088	0.086	0.083	0.082	0.080
5.3	0.126	0.118	0.111	0.106	0.101	0.097	0.093	0.090	0.087	0.085	0.083	0.081
5.4	0.129	0.121	0.114	0.108	0.103	0.099	0.095	0.092	0.089	0.087	0.085	0.083
5.5	0.133	0.125	0.117	0.111	0.106	0.102	0.098	0.094	0.091	0.088	0.086	0.084
5.6	0.137	0.128	0.121	0.114	0.109	0.104	0.100	0.096	0.093	0.090	0.088	0.085
5.7	0.141	0.132	0.124	0.117	0.112	0.107	0.102	0.098	0.095	0.092	0.089	0.087
5.8	0.145	0.136	0.127	0.120	0.114	0.109	0.105	0.101	0.097	0.094	0.091	0.089
5.9	0.149	0.139	0.131	0.124	0.117	0.112	0.107	0.103	0.099	0.096	0.093	0.090
6.0	0.154	0.143	0.134	0.127	0.120	0.114	0.109	0.105	0.101	0.098	0.095	0.092
6.2	0.162	0.151	0.141	0.133	0.126	0.120	0.115	0.110	0.106	0.102	0.098	0.095
6.4	0.171	0.159	0.148	0.140	0.132	0.125	0.120	0.115	0.110	0.106	0.102	0.099
6.6	0.180	0.167	0.156	0.146	0.138	0.131	0.125	0.120	0.115	0.110	0.106	0.103
6.8	0.189	0.175	0.163	0.153	0.145	0.137	0.131	0.125	0.120	0.115	0.111	0.107
7.0	0.198	0.183	0.171	0.160	0.151	0.143	0.136	0.130	0.125	0.120	0.115	0.111
7.5	0.222	0.205	0.191	0.179	0.168	0.159	0.151	0.144	0.138	0.132	0.127	0.122
8.0	0.248	0.228	0.212	0.198	0.186	0.176	0.167	0.159	0.151	0.145	0.139	0.134
8.5	0.275	0.252	0.234	0.218	0.205	0.193	0.183	0.174	0.166	0.159	0.152	0.147
9.0	0.303	0.278	0.257	0.239	0.224	0.212	0.200	0.190	0.181	0.173	0.166	0.160
9.5	0.333	0.304	0.281	0.261	0.245	0.231	0.218	0.207	0.197	0.189	0.181	0.174
10.0	0.363	0.332	0.306	0.284	0.266	0.250	0.236	0.224	0.214	0.204	0.195	0.188
11.0	0.426	0.387	0.356	0.330	0.308	0.289	0.272	0.258	0.245	0.234	0.224	0.215
12.0	0.492	0.447	0.409	0.378	0.352	0.330	0.311	0.294	0.279	0.266	0.254	0.244
13.0	0.559	0.507	0.464	0.428	0.398	0.373	0.350	0.331	0.314	0.299	0.285	0.273
14.0	0.622	0.566	0.519	0.479	0.445	0.416	0.391	0.369	0.350	0.333	0.317	0.304
15.0	0.678	0.620	0.571	0.528	0.492	0.460	0.432	0.408	0.386	0.367	0.350	0.335
16.0	0.728	0.670	0.619	0.575	0.537	0.503	0.473	0.447	0.424	0.403	0.384	0.367
17.0	0.770	0.713	0.663	0.618	0.579	0.544	0.513	0.485	0.460	0.438	0.417	0.399
18.0	0.805	0.751	0.702	0.658	0.618	0.582	0.550	0.521	0.495	0.471	0.450	0.431
19.0	0.834	0.783	0.736	0.692	0.653	0.617	0.585	0.555	0.528	0.504	0.482	0.461
20.0	0.857	0.809	0.764	0.723	0.684	0.649	0.617	0.587	0.560	0.535	0.512	0.491
25.0	0.921	0.888	0.855	0.823	0.792	0.763	0.735	0.708	0.683	0.659	0.636	0.615
30.0	0.941	0.918	0.894	0.870	0.846	0.823	0.801	0.779	0.758	0.737	0.718	0.699
35.0	0.946	0.928	0.910	0.892	0.874	0.855	0.837	0.819	0.802	0.785	0.768	0.752
40.0	0.945	0.931	0.917	0.903	0.888	0.873	0.858	0.843	0.829	0.814	0.800	0.786
45.0	0.942	0.931	0.920	0.908	0.896	0.883	0.871	0.858	0.846	0.833	0.821	0.809
50.0	0.940	0.931	0.921	0.911	0.900	0.889	0.879	0.868	0.857	0.846	0.836	0.825
60.0	0.937	0.930	0.922	0.914	0.905	0.897	0.888	0.880	0.871	0.863	0.854	0.845
80.0	0.938	0.932	0.925	0.919	0.912	0.906	0.900	0.893	0.887	0.880	0.874	0.868
100.0	0.942	0.936	0.931	0.925	0.920	0.914	0.909	0.903	0.898	0.893	0.887	0.882
120.0	0.947	0.942	0.937	0.932	0.927	0.922	0.917	0.912	0.907	0.903	0.898	0.893
140.0	0.951	0.947	0.942	0.938	0.933	0.929	0.925	0.920	0.916	0.912	0.907	0.903
160.0	0.956	0.951	0.947	0.943	0.939	0.935	0.931	0.927	0.923	0.919	0.915	0.911
180.0	0.959	0.956	0.952	0.948	0.944	0.940	0.937	0.933	0.929	0.926	0.922	0.919
200.0	0.963	0.959	0.956	0.952	0.949	0.945	0.942	0.938	0.935	0.932	0.928	0.925
220.0	0.966	0.962	0.959	0.956	0.953	0.949	0.946	0.943	0.940	0.937	0.934	0.931
240.0	0.968	0.965	0.962	0.959	0.956	0.953	0.950	0.947	0.944	0.941	0.938	0.936
260.0	0.970	0.967	0.965	0.962	0.959	0.956	0.953	0.951	0.948	0.945	0.943	0.940
280.0	0.972	0.970	0.967	0.964	0.962	0.959	0.956	0.954	0.951	0.949	0.946	0.944
300.0	0.974	0.971	0.969	0.967	0.964	0.962	0.959	0.957	0.954	0.952	0.950	0.947

NBS TECHNICAL PUBLICATIONS

PERIODICALS

JOURNAL OF RESEARCH reports National Bureau of Standards research and development in physics, mathematics, and chemistry. Comprehensive scientific papers give complete details of the work, including laboratory data, experimental procedures, and theoretical and mathematical analyses. Illustrated with photographs, drawings, and charts. Includes listings of other NBS papers as issued.

Published in two sections, available separately:

- **Physics and Chemistry**

Papers of interest primarily to scientists working in these fields. This section covers a broad range of physical and chemical research, with major emphasis on standards of physical measurement, fundamental constants, and properties of matter. Issued six times a year. Annual subscription: Domestic, \$9.50; \$2.25 additional for foreign mailing.

- **Mathematical Sciences**

Studies and compilations designed mainly for the mathematician and theoretical physicist. Topics in mathematical statistics, theory of experiment design, numerical analysis, theoretical physics and chemistry, logical design and programming of computers and computer systems. Short numerical tables. Issued quarterly. Annual subscription: Domestic, \$5.00; \$1.25 additional for foreign mailing.

TECHNICAL NEWS BULLETIN

The best single source of information concerning the Bureau's measurement, research, developmental, cooperative, and publication activities, this monthly publication is designed for the industry-oriented individual whose daily work involves intimate contact with science and technology—for engineers, chemists, physicists, research managers, product-development managers, and company executives. Includes listing of all NBS papers as issued. Annual subscription: Domestic, \$3.00; \$1.00 additional for foreign mailing.

Bibliographic Subscription Services

The following current-awareness and literature-survey bibliographies are issued periodically by the Bureau: Cryogenic Data Center Current Awareness Service (weekly), Liquefied Natural Gas (quarterly), Superconducting Devices and Materials (quarterly), and Electromagnetic Metrology Current Awareness Service (monthly). Available only from NBS Boulder Laboratories. Ordering and cost information may be obtained from the Program Information Office, National Bureau of Standards, Boulder, Colorado 80302.

NONPERIODICALS

Applied Mathematics Series. Mathematical tables, manuals, and studies.

Building Science Series. Research results, test methods, and performance criteria of building materials, components, systems, and structures.

Handbooks. Recommended codes of engineering and industrial practice (including safety codes) developed in cooperation with interested industries, professional organizations, and regulatory bodies.

Special Publications. Proceedings of NBS conferences, bibliographies, annual reports, wall charts, pamphlets, etc.

Monographs. Major contributions to the technical literature on various subjects related to the Bureau's scientific and technical activities.

National Standard Reference Data Series. NSRDS provides quantitative data on the physical and chemical properties of materials, compiled from the world's literature and critically evaluated.

Product Standards. Provide requirements for sizes, types, quality, and methods for testing various industrial products. These standards are developed cooperatively with interested Government and industry groups and provide the basis for common understanding of product characteristics for both buyers and sellers. Their use is voluntary.

Technical Notes. This series consists of communications and reports (covering both other-agency and NBS-sponsored work) of limited or transitory interest.

Federal Information Processing Standards Publications. This series is the official publication within the Federal Government for information on standards adopted and promulgated under the Public Law 89-306, and Bureau of the Budget Circular A-86 entitled, Standardization of Data Elements and Codes in Data Systems.

Consumer Information Series. Practical information, based on NBS research and experience, covering areas of interest to the consumer. Easily understandable language and illustrations provide useful background knowledge for shopping in today's technological marketplace.

CATALOGS OF NBS PUBLICATIONS

NBS Special Publication 305, Publications of the NBS, 1966-1967. When ordering, include Catalog No. C13.10:305. Price \$2.00; 50 cents additional for foreign mailing.

NBS Special Publication 305, Supplement 1, Publications of the NBS, 1968-1969. When ordering, include Catalog No. C13.10:305/Suppl. 1. Price \$4.50; \$1.25 additional for foreign mailing.

NBS Special Publication 305, Supplement 2, Publications of the NBS, 1970. When ordering, include Catalog No. C13.10:305/Suppl. 2. Price \$3.25; 85 cents additional for foreign mailing.

Order NBS publications (except Bibliographic Subscription Services) from: Superintendent of Documents, Government Printing Office, Washington, D.C. 20402.